

ADVANCES IN POLYMERIC BIOMATERIALS SERIES

Absorbable and Biodegradable Polymers

Shalaby W. Shalaby
Karen J.L. Burg

 CRC PRESS

Also available as a printed book
see title verso for ISBN details

Absorbable and Biodegradable Polymers

ADVANCES IN POLYMERIC BIOMATERIALS SERIES

Absorbable and Biodegradable Polymers

Shalaby W. Shalaby
Karen J.L. Burg



CRC PRESS

Boca Raton London New York Washington, D.C.

This edition published in the Taylor & Francis e-Library, 2005.

“To purchase your own copy of this or any of Taylor & Francis or Routledge’s collection of thousands of eBooks please go to www.eBookstore.tandf.co.uk.”

Library of Congress Cataloging-in-Publication Data

Absorbable biodegradable polymers / Shalaby W. Shalaby, Karen

J.L. Burg [editors]

p. cm. (Advances in polymeric biomaterials)

Includes bibliographical references and index.

ISBN 0-8493-1484-4 (alk. paper)

1. Polymers in medicine. 2. Biodegradable plastics. 3. Polymers--Absorption and adsorption. 4. Polymers--Biodegradation. I. Shalaby, Shalaby W. II. Burg, Karen J.L. III Series.

R857.P6A276 2003

610'.28'4—dc21

2003055093

This book contains information obtained from authentic and highly regarded sources. Reprinted material is quoted with permission, and sources are indicated. A wide variety of references are listed. Reasonable efforts have been made to publish reliable data and information, but the author and the publisher cannot assume responsibility for the validity of all materials or for the consequences of their use.

Neither this book nor any part may be reproduced or transmitted in any form or by any means, electronic or mechanical, including photocopying, microfilming, and recording, or by any information storage or retrieval system, without prior permission in writing from the publisher.

All rights reserved. Authorization to photocopy items for internal or personal use, or the personal or internal use of specific clients, may be granted by CRC Press LLC, provided that \$1.50 per page photocopied is paid directly to Copyright Clearance Center, 222 Rosewood Drive, Danvers, MA 01923 USA. The fee code for users of the Transactional Reporting Service is ISBN 0-8493-1484-4/04/\$0.00+\$1.50. The fee is subject to change without notice. For organizations that have been granted a photocopy license by the CCC, a separate system of payment has been arranged.

The consent of CRC Press LLC does not extend to copying for general distribution, for promotion, for creating new works, or for resale. Specific permission must be obtained in writing from CRC Press LLC for such copying.

Direct all inquiries to CRC Press LLC, 2000 N.W. Corporate Blvd., Boca Raton, Florida 33431.

Trademark Notice: Product or corporate names may be trademarks or registered trademarks, and are used only for identification and explanation, without intent to infringe.

Visit the CRC Press Web site at www.crcpress.com

© 2004 by CRC Press LLC

No claim to original U.S. Government works
International Standard Book Number 0-8493-1484-4
Library of Congress Card Number 2003055093

ISBN 0-203-49301-X Master e-book ISBN

ISBN 0-203-58651-4 (Adobe eReader Format)

Preface

For the past two decades, the fast-growing interest in synthetic absorbable polymers has lured most authors to focus on this family of polymers while practically ignoring biodegradable materials of natural origin. Revival of interest in natural polymers by contemporary investigators compelled the editors of this volume to develop it in a form that provides integrated accounts of most of the recent developments not only in synthetic absorbable polymers but also in biodegradable polymers of natural origin. Hence, the theme of this volume is based on the fact that technology of absorbable/biodegradable polymers (A/BP) has evolved in two independent areas which need to be treated in an integrated manner because of their common end use in clinical applications.

The evolution of natural polymers takes place through chain modification of existing materials, mostly by using chemical means to impart certain physical and/or functional properties. Meanwhile, the evolution of synthetic A/BP has been achieved through modulating their chemical composition using different polymerization schemes and, to a lesser extent, chemical modification of presynthesized polymers. In concert with this theme, the book begins with an introduction (Section A) to prepare the reader for the three main sections (B, C, and D) comprising 15 chapters which are based mostly on evolutionary materials developments, processing methods, and characterization/evaluation methods, as well as clinical and newly sought applications that have become available over the past decade. Section B deals with development and applications of new systems. Section C pertains to development in preparative, processing, and evaluation methods. Section D addresses growing and newly sought applications.

It is to be emphasized that the diverse topics presented in this book are integrated in such a fashion as to yield a coherent source of diverse but interrelated information for use by scientists, engineers, and clinicians who are interested in the use of A/BP in pharmaceutical and biomedical applications. The clinical components of the book are prepared by clinicians who are also well-versed scientists to maximize the effectiveness of integrating clinical with preclinical information.

The editors express gratitude to all contributors for their highly informative chapters on cutting-edge technologies and their enthusiastic response to making contributions to the book. The comprehensive nature of the chapters and their extensive biographies will make this volume a valuable source well-suited for use by students, industrialists, and educators with interest in development and/or investigation of A/BP for use in pharmaceutical and biomedical applications.

Acknowledgment

The editors express their gratitude to Dr. Joanne E. Shalaby of Poly-Med, Inc., for her guidance and valuable contributions during the compilation and integration of the diverse segments of the book.

The Editors

Shalaby W. Shalaby is currently president and director of R&D at Poly-Med, Inc., Anderson, South Carolina. After completing his undergraduate training in chemistry and botany as well as pharmacy in Egypt at Ain Shams University and Cairo University, he enrolled at the University of Massachusetts at Lowell to complete his graduate studies toward an M.S. degree in textiles, a Ph.D. in chemistry, and a second Ph.D. in polymer science. Following the completion of his graduate training, 2 years of teaching, and a postdoctoral assignment, Dr. Shalaby spent four years as a senior research chemist at Allied Signal, Polymer Research Group. Subsequently, he joined Ethicon/Johnson & Johnson to start an exploratory group on polymers for biomedical applications, with some focus on new absorbable and radiation-sterilizable polymers. Before joining Clemson University in the summer of 1990, Dr. Shalaby headed the Johnson & Johnson Polymer Technology Center. Dr. Shalaby's previous research activities pertained to the molecular design of polymeric systems with a major focus on biomedical and pharmaceutical applications. At Clemson University, Dr. Shalaby's research activities addressed primarily the molecular and engineering design of bioabsorbable systems, high performance composites, radio-stabilization of polymers, and new aspects of radiation processing. He has supervised or cosupervised 30 M.S. and Ph.D. thesis projects. After joining United States Surgical Corporation in 1993 as a corporate research scientist/senior director, Dr. Shalaby directed his efforts toward the establishment of new R&D programs pertinent to surgical and allied products and assessment of new product opportunities through technology acquisition. In late 1994, Shalaby directed his industrial efforts, as president of Poly-Med, Inc., toward focused R&D of polymeric materials for biomedical and pharmaceutical applications. Since 1994, he has been an adjunct or visiting professor at four universities. He has over 100 patents and 250 publications, including eight books.

Karen J. L. Burg earned a B.S. in chemical engineering with a minor in biochemical engineering from North Carolina State University in 1990, an M.S. in bioengineering from Clemson University in 1992, and a Ph.D. in bioengineering with a minor in experimental statistics from Clemson University in 1996. She completed a tissue engineering postdoctoral research fellowship in 1998 at Carolinas Medical Center in Charlotte, North Carolina, and is currently associate professor of bioengineering at Clemson University and an adjunct research faculty member at Carolinas Medical Center.

Professional affiliations include membership in Sigma Xi, Society for Biomaterials, Tissue Engineering Society, and American Institute of Chemical

Engineers; she also serves on the ASTM Tissue Engineering Standards Development Committee.

Awards include the 2001 National Science Foundation Faculty Early Career Award, 2001 Clemson University Board of Trustees Award for Faculty Excellence, 2001 Presidential Early Career Award for Scientists and Engineers, and 2003 Clemson University Outstanding Woman Faculty Award.

Among her research interests are the optimization of absorbable biomaterials processing for tissue engineering applications, application of magnetic resonance imaging in tissue engineering, development of absorbable composites for orthopedic and soft tissue applications, surface modulation of absorbable implants to enhance biocompatibility, and evaluation of physicochemical changes in absorbing systems.

Contributors

Shalaby W. Shalaby, Ph.D. Poly-Med, Inc., Anderson, South Carolina

Karen J. L. Burg, Ph.D. Department of Bioengineering, Clemson University, Clemson, South Carolina

Sasa Andjelic, Ph. D. Ethicon, Inc., Somerville, New Jersey

Griet G. Atkins, M.S. Southern BioSystems, Inc., Birmingham, Alabama

Bruce L. Anneaux, M.S. Poly-Med, Inc., Anderson, South Carolina

Kimberly A. Carpenter, B.S. Poly-Med, Inc., Anderson, South Carolina

John A. DuBose, B.S. Poly-Med, Inc., Anderson, South Carolina

Benjamin D. Fitz, Ph.D. Ethicon, Inc., Somerville, New Jersey

Dennis D. Jamiolkowski, M.S. Ethicon, Inc., Somerville, New Jersey

Marc Shalaby, M.D. Department of Medicine, Lehigh Valley Hospital, Allentown, Pennsylvania

Waleed S.W. Shalaby, M.D., Ph.D. Division of Gynecologic Oncology, University of Pennsylvania Medical Center, Philadelphia, Pennsylvania

Chuck B. Thomas, B.S. Department of Bioengineering, Clemson University, Clemson, South Carolina

Contents

Section A Introduction Notes

- 1 Absorbable/Biodegradable Polymers: Technology Evolution..... 3**
Shalaby W. Shalaby and Karen J.L. Burg

Section B Development and Application of New Systems

- 2 Segmented Copolyesters with Prolonged Strength Retention Profiles..... 15**
Shalaby W. Shalaby
- 3 Polyaxial Crystalline Fiber-Forming Copolyester..... 25**
Shalaby W. Shalaby
- 4 Polyethylene Glycol-Based Copolyesters 39**
Shalaby W. Shalaby and Marc Shalaby
- 5 Cyanoacrylate-Based Systems as Tissue Adhesives 59**
Shalaby W. Shalaby and Waleed S. W. Shalaby
- 6 Chitosan-Based Systems 77**
Shalaby W. Shalaby, John A. DuBose, and Marc Shalaby
- 7 Hyaluronic Acid-Based Systems 91**
Shalaby W. Shalaby and Waleed S. W. Shalaby

Section C Developments in Preparative, Processing, and Evaluation Methods

- 8 New Approaches to the Synthesis of Crystalline Fiber-Forming Aliphatic Copolyesters 103**
Shalaby W. Shalaby, Kimberly A. Carpenter, and Bruce L. Anneaux

9	Advances in Morphological Development to Tailor the Performance of Medical Absorbable Devices	113
	<i>Sasa Andjelic, Benjamin D. Fitz, and Dennis D. Jamiolkowski</i>	
10	Polymer Biocompatibility and Toxicity	143
	<i>Karen J.L. Burg, Shalaby W. Shalaby, and Griet G. Atkins</i>	

Section D Growing and Newly Sought Applications

11	Tissue Engineering Systems	159
	<i>Chuck B. Thomas and Karen J.L. Burg</i>	
12	Synthetic Vascular Constructs	175
	<i>Shalaby W. Shalaby and Waleed S.W. Shalaby</i>	
13	Postoperative Adhesion Prevention	191
	<i>Waleed S.W. Shalaby and Shalaby W. Shalaby</i>	
14	Implantable Insulin Controlled Release Systems for Treating Diabetes Mellitus	205
	<i>Marc Shalaby and Shalaby W. Shalaby</i>	
15	Absorbable Delivery Systems for Cancer Therapy	227
	<i>Waleed S.W. Shalaby</i>	
16	Tumor Immunotherapeutic Systems	257
	<i>Waleed S.W. Shalaby and Shalaby W. Shalaby</i>	
	Index	275

Section A

Introduction Notes

1

Absorbable/Biodegradable Polymers: Technology Evolution

Shalaby W. Shalaby and Karen J.L. Burg

CONTENTS

1.1	Introduction	3
1.2	Technology Evolution of Absorbable/Biodegradable Polymers as Materials	4
1.2.1	Evolution of Natural Absorbable/Biodegradable Polymers	4
1.2.2	Evolution of Synthetic Absorbable/Biodegradable Polymers	5
1.2.2.1	Heterochain Ester-Based Absorbable Synthetic Polymers	6
1.2.2.2	Homochain Ester-Based Absorbable Synthetic Polymers	7
1.3	Evolving Applications and Pertinent Processing Methods of Absorbable/Biodegradable Polymers	7
1.3.1	Extrudable Gel-Forming Implants	8
1.3.2	Scaffolds for Tissue Engineering	8
1.3.3	Polyester/Peptide Ionic Conjugates	8
1.3.4	Enabling New Processing Methods	9
1.4	Conclusion and Perspective on the Future	10
	References	10

1.1 Introduction

Egyptians sutured wounds as early as 3500 B.C. using a variety of natural polymers including treated intestines, which are the early versions of collagen-based surgical gut sutures.¹ Synthetic, absorbable polyesters based on

2-hydroxyacetic acids were developed for preparing less tissue reactive alternatives to surgical gut sutures in the early 1970s. In addition to collagen-based polymers, other natural, absorbable polymers, such as albumin, chitosan, and hyaluronic acid and derivatives thereof have been used for many pharmaceutical and biomedical applications for several decades.² Of these polymers, the application of chitosan and hyaluronic acid-based polymers has received a great deal of attention in the past 15 years for use in controlled drug delivery systems, tissue repair, tissue engineering, and controlling certain biological events.

1.2 Technology Evolution of Absorbable/Biodegradable Polymers as Materials

Technology of absorbable/biodegradable polymers (A/BP) has evolved in two independent areas. The evolution of natural polymers took place through chain modification of existing materials using chemical means or modulating the biosynthetic process for fermentation to impart certain physical and/or functional properties. On the other hand, the evolution of synthetic A/BP has been achieved through modulating their chemical composition using several polymerization techniques and, to a lesser extent, chemical modification of presynthesized polymers.

1.2.1 Evolution of Natural Absorbable/Biodegradable Polymers

Evolution and development of absorbable/biodegradable polysaccharides was associated mostly with chitosan and hyaluronic acid. Chitosan is among the most important members of the absorbable/biodegradable polymer family. It is a partially deacetylated chitin where 70 to 90% of the monosaccharide sequences carry free amino groups and the balance is retained with its original acetamido side groups. Most of the research to develop novel A/BP products was directed to reaction of the chain amine and/or hydroxyl groups.² In an interesting approach to developing absorbable drug delivery systems, Shalaby and co-workers acylated chitosan with mono- and dicarboxylic acids, anhydrides and conjugated the carboxylated products with bioactive amine-bearing oligopeptides.^{3,4}

Hyaluronic acid is a naturally occurring polysaccharide comprising monosaccharide sequences with carboxylic or acetamido side groups. Early production of hyaluronic acid, a biodegradable polymer similar to chitosan, was achieved through extraction of natural tissues, and the evolution of hyaluronic acid technology was made possible after its successful production in sufficient quantities as a fermentation product.² The key evolution of

hyaluronic acid technology commenced with its chemical modification and crosslinking.² These entailed:

- Esterification with monohydric alcohol to improve its film-forming properties and lower its solubility
- Reaction with basic drugs to control their release profiles
- Crosslinking to produce water-swellaable systems as surgical implants

Evolution in the development of proteins for novel pharmaceutical and biomedical applications was directed towards the modification of:

- Collagen to decrease its hydrophilicity by acylation with long chain alkyl-substituted succinic anhydrides
- Insulin to increase its iontophoretic mobility and bioavailability as part of a transdermal delivery system by acylation with succinic anhydride, or to improve its enzymatic stability by acylation with certain fatty acid anhydrides
- Epidermal growth factor (EGF) to improve its enzymatic stability and hence bioavailability by acylation with fatty acid anhydrides⁵⁻¹¹

Bacterial polyhydroxyalkanoates (PHA) are among the most important biodegradable polymers produced via biosynthesis.¹² Initial production of the PHA was focused on poly(2-hydroxybutyrate) (PHB). However, the high melting temperature and crystallinity of PHB prompted the evolutionary development of copolymers having about 15 to 20% of the chain sequences as 2-hydroxyvalerate through controlling the composition of the feed during the fermentation process. The resulting copolyesters (PHBV) were suggested to have more suitable properties for conversion by traditional processing techniques into biomedical devices.

1.2.2 Evolution of Synthetic Absorbable/Biodegradable Polymers

Interest in synthetic absorbable polymers has grown considerably over the past three decades, principally because of their transient nature when used as biomedical implants or drug carriers. The genesis of absorbable polymers was driven by the need to replace the highly tissue-reactive, absorbable, collagen-based sutures with synthetic polymers, which elicit milder tissue response. This led to the early development of polyglycolide as an absorbable polyester suture. In spite of the many polymeric systems investigated as candidates for absorbable implants and drug carriers, ester-based polymers maintain an almost absolute dominance among clinically used systems and others that are under investigation.

In addition to ester-based polyesters, a great deal of research activity has been directed to other types of absorbable polymers, but the clinical relevance of their properties practically halted their evolution beyond the exploratory phase. Typical examples of these polymers have been covered in a review by Shalaby and include those based on polyanhydrides, polyorthoesters, polyphosphazenes, and certain polyamidoesters.¹³

With the development of absorbable cyanoacrylate systems, the classification of synthetic, absorbable polymers into the traditional heterochain polymers (e.g., polyesters and polyanhydrides) and less-conventional homochain polymers (e.g., cyanoacrylate polymers) became inevitable.^{14–16} Meanwhile, since ester-based systems are most important among both the heterochain- and homochain-type synthetic, absorbable polymers, they are given special attention in this chapter.

1.2.2.1 Heterochain Ester-Based Absorbable Synthetic Polymers

Detailed accounts of this class of absorbable polymers were a subject of a review by Shalaby and Johnson.¹⁷ The review dealt with:

- Polymerization of lactones such as glycolide (G), *l*-lactide (LL), *dl*-lactide (DL-L), *p*-dioxanone (PD), trimethylene carbonate (TMC), ϵ -caprolactone (CL), 1,5 dioxepan-2-one (DOX), glycosalicylate (GS), morpholine-2,5-dione (MD)
- Polyalkylene oxalates and their isomorphous copolymers
- Polyoxamates
- Partially aromatic, segmented glycolide copolymers

The authors discussed briefly what were then considered as new trends. These included:

- Segmented copolymers as low modulus materials comprising polymeric CL or TMC soft segments
- Fast-absorbing polylactones containing MD-based sequences
- Segmented copolyester as hydrophilic substrates based on end-grafted polyethylene glycol (PEG)
- Polymeric prodrugs including those containing GS-based sequences
- Radiation-sterilizable, segmented copolyester made by end-grafting radiostable aromatic prepolymers with glycolide
- The early use of polyglycolide and 90/10 G/LL copolymer in braided forms as scaffolds for tissue engineering

Over the past 8 years, impressive advances have been made toward the development of new absorbable systems for novel or improved applications

as absorbable implants or carriers for the controlled delivery of bioactive agents. These include:

- Gel-forming (GF) absorbable copolyesters made by end-grafting one or more cyclic monomer onto a polyalkylene glycol, such as polyethylene glycol for use in tissue repair and controlled delivery of bioactive agents
- Segmented high-lactide copolymers for use in implants with prolonged *in vivo* strength retention
- Crystalline fiber-forming copolyesters based on amorphous polyaxial initiators
- Fiber-forming, segmented copolyesters based on polyalkylene succinate prepolymers with minimized hydrolytic instability as compliant materials^{18–21}

1.2.2.2 Homochain Ester-Based Absorbable Synthetic Polymers

Early demonstration that the absorption of poly(methoxypropyl cyanoacrylate) can be accelerated in the presence of liquid absorbable oxalate polymers led Shalaby to develop a new family of methoxypropyl cyanoacrylate (MPC)/polyester formulations as tissue adhesives with a broad range of properties.^{22,23} These formulations were tailored to produce absorbable tissue adhesives with a range of adhesive properties and compositionally controlled compliance depending on the type and content of the absorbable polyester component in the formulation.

1.3 Evolving Applications and Pertinent Processing Methods of Absorbable/Biodegradable Polymers

While playing a significant role as implants for wound repair in extruded and molded solid forms, absorbable polymers are:

- Being used in several forms of orthopedic devices
- Making inroads in a number of new vascular applications
- Providing the foundation for the fast-growing area of tissue engineering
- Rightfully acknowledged as the premium carrier for the controlled release of bioactive agents for maximized efficacy in local and systemic therapies, as well as directing key post-surgical events

1.3.1 Extrudable Gel-Forming Implants

A novel family of copolyesters was developed as a unique form of extrudable or injectable absorbable liquids that undergo physical transformation to gels or semi-solids upon contacting water at the application site.¹⁸ Typical gel-formers (GFs) are made by grafting one or two cyclic monomers onto polyethylene glycol (PEG) to produce an amphiphilic copolymer with a hydrophilic PEG segment and hydrophobic copolyester or copolyester-carbonate segments, which are comiscible in the dry state. In the presence of water, the PEG segments absorb the water, forcing the hydrophobic segments to associate forming quasi-crosslinks and leading to physical gelation. Among the main applications of these GFs are their use as:

- Carriers of antibiotics such as doxycycline for treating periodontitis and vancomycin for management of osteomyelitis
- Suture or staple adjuvants to aid in wound healing and allow a reduction of the traditional number per unit length of such mechanical devices at the specific surgical site
- Carriers of bioactive agents to reduce incidence of postoperative surgical adhesion
- Covers to accelerate the healing of burn wounds and possibly ulcers²⁴⁻²⁸

1.3.2 Scaffolds for Tissue Engineering

The fast-growing field of tissue engineering or tissue regeneration can be considered an outgrowth of the absorbable polymer technology. This is because tissue engineering relies, for the most part, on the use of an absorbable scaffold that undergoes mass loss in tandem with tissue formation to replace the absorbing scaffold. In spite of the availability of a broad range of absorbable polymers, their conversion to an easily sterilizable scaffold having the proper microporosity that optimally allows cell propagation and removal of metabolic by-products is yet to be realized. However, the prospect of developing such a scaffold is now more feasible with the availability of the crystallization-induced microphase separation (CIMS) process for forming continuous cell, microporous, absorbable constructs of any desirable dimension and porosity and the highly effective radiochemical sterilization process discussed in the next section.^{29,30}

1.3.3 Polyester/Peptide Ionic Conjugates

Shalaby and co-workers pioneered the evolutionary development of absorbable copolyester/peptide ionic conjugates for the controlled release of highly potent bioactive peptides.^{31,32} Copolyesters made typically of glycolide and

l-lactide and malic acid as initiators are prepared by ring-opening polymerization. The carboxyl-bearing polyesters are then allowed to form ionic conjugates with oligopeptides to allow for the sustained release of these peptides over several weeks. Similarly, ionic conjugates of oligopeptides and cyclodextrin derivatives were prepared as fast-releasing (few to several days), controlled delivery systems.^{33,34} The carboxyl-bearing cyclodextrin derivative was prepared following the steps of:

- Mixed acylation with fatty acid and succinic (or glutaric) acid anhydride
- Grafting a mixture of glycolide and *l*-lactide onto unacylated hydroxyl groups on the cyclodextrin molecule^{33,34}

1.3.4 Enabling New Processing Methods

With growing interest in polymers for the development of high modulus orthopedic implants, Shalaby and co-workers developed:

- A solid-state orientation process for uniaxial orientation of polymers using compressive forces to increase the modulus of crystalline polymers toward those of typical bones
- A process for surface phosphonylation to create covalently bonded phosphonate groups which encourage osseointegration with bone tissue
- A surface-microtexturing process using the solvent-induced microphase separation (CIMS) technique to maximize bone implant interlocking, which is aided by surface phosphonylation³⁵⁻⁴¹

To supplement the growing area of tissue engineering, Shalaby and co-workers developed a process for producing continuous cell microporous foam, or highly oriented implants with microtextured microporous surfaces, which entails the use of the CIMS technology described above.³⁹⁻⁴² This allows preparation of foam preforms by traditional polymer processing methods, followed by generation of the microporous architecture by removal of a diluent used in processing.

To minimize or eliminate reliance on ethylene oxide and exploit reliability of assured sterility using radiation for absorbable polymers and particularly those used in tissue engineering, Shalaby and co-workers developed the radiochemical sterilization (RC-S) process.^{30,43} The RC-S process represents a novel approach to the sterilization of certain mechanical devices, such as those made of absorbable polyesters, that are sensitive to high-energy radiation delivered at the traditional dose of 25 kGy.³⁰ RC-S is a hybrid process encompassing the attributes of chemical high-energy radiation sterilization without the drawbacks associated with the use of the parent processes. RC-

S entails the use of about 5 to 7.5 kGy of gamma radiation and a polyformaldehyde package insert capable of a radiolytic, controlled release of formaldehyde in a hermetically sealed package under dry nitrogen. The process has been applied successfully to absorbable sutures without compromising their clinically relevant properties, such as their *in vivo* breaking strength retention. Typical BSR data of radiochemically sterilized suture braids and controls are reported by Anneaux and co-workers.⁴³

1.4 Conclusion and Perspective on the Future

For naturally derived polymers, chitosan commands the lead as a fast-growing material for use in pharmaceutical and biomedical applications. The development of novel chitosan-based systems and new applications can be accelerated through improved processing and purification methods.

Although the use of synthetic, absorbable implants for wound repair has grown substantially over the past three decades, such growth is expected to continue for at least the next decade. The modest present uses of absorbable implants in orthopedic and vascular systems are expected to grow at a considerably high rate over the next two decades. Successful application of absorbable scaffolds in tissue engineering is expected to continue at a modest rate until an ideal scaffold is developed and more efforts are directed to *in situ* tissue engineering; then the growth rate of this technology will accelerate phenomenally.

References

1. Shalaby, S. W. and Pearce, E. M., The role of polymers in medicine and surgery, *Chemistry*, 51(5), 17, 1978.
2. Shalaby, S. W. and Shah, K. R., Chemical Modifications of Natural Polymers and Their Technological Relevance, in *Water Soluble Polymers*, Vol. 467, ACS Symposium Series, American Chemical Society, Washington, DC, 1991, chap. 4.
3. Shalaby, S. W. and Ignatious, F., Ionic Molecular Conjugates of Biodegradable Fully N-Acylated Derivatives of Poly(2-Amino-2-Deoxy-D-Glucose) and Bioactive Polypeptides, U.S. Patent (to Biomeasure, Inc.) 5,665,702, 1997.
4. Shalaby, S. W., Jackson, S. A., Ignatious, F. S. and Moreau, J.-P., Ionic Molecular Conjugates of N-acylated Derivatives of Poly(2-Amino-2-Deoxy-D-Glucose) and Polypeptides, U.S. Patent (to Biomeasure, Inc.) 6,479,457, 2002.
5. Shalaby, S. W., Allan, J. M. and Corbett, J. T., Peracylated Proteins and Synthetic Polypeptides and Process for Making the Same, U.S. Patent (to Poly-Med, Inc.) 5,986,050, 1999.

6. Corbett, J. T., Dooley, R. L., Michniak, B. B., Zimmerman, J. K. and Shalaby, S. W., Iontophoretic Controlled Delivery of Modified Insulin, *Proc. Fifth World Biomater. Congr.*, Toronto, Canada, 1, 28, 1996.
7. Corbett, J. T., Dooley, R. L., Michniak, B. B., Zimmerman, J. K. and Shalaby, S. W., Succinylation of Insulin for Accelerated Iontophoretic Delivery, *Proc. Fifth World Biomater. Congr.*, Toronto, Canada, 2, 157, 1996.
8. Njieha, F. K. and Shalaby, S. W., Dynamic and physico-chemical properties of modified insulin, *Polym. Prepr.*, 33(3), 536, 1992.
9. Njieha, F. K. and Shalaby, S. W., Modification of Epidermal Growth Factor, *Polym. Prepr.* 32(2), 233, 1991.
10. Njieha, F. K. and Shalaby, S. W., Acylated Epidermal Growth Factor, U.S. Patent (to Ethicon, Inc.) 5,070,188, 1991.
11. Njieha, F. K. and Shalaby, S. W., Stabilization of Epidermal Growth Factor, *J. Bioact. Biocomp. Polym.*, 7, 288, 1992.
12. Gross, R. A., in *Biomedical Polymers: Designed-to-Degrade Systems*, Shalaby, S. W., Ed., Hanser Publishers, New York, 1994, chap. 7.
13. Shalaby, S. W., Ed., *Biomedical Polymers: Designed-to-Degrade Systems*, Hanser Publishers, New York, 1994.
14. Linden, C. L., Jr. and Shalaby, S. W., Absorbable Tissue Adhesive, U.S. Patent (to U.S. Army) 5,350,798, 1994.
15. Linden, C. L., Jr. and Shalaby, S. W., Modified Cyanoacrylate Composition as Absorbable Adhesives for Soft Tissue, *Proc. Fifth World Biomater. Congr.*, Toronto, Canada, 2, 352, 1996.
16. Shalaby, S. W., Polyester/Cyanoacrylate Tissue Adhesive Formulations, U.S. Patent (to Poly-Med, Inc.) 6,299,631, 2001.
17. Shalaby, S. W. and Johnson, R. A., *Biomedical Polymers: Designed-to-Degrade Systems*, Shalaby, S. W., Ed., Hanser Publishers, New York, 1994, 1.
18. Shalaby, S. W., Hydrogel-forming, Self-solvating Absorbable Polyester Copolymers, and Methods for Use Thereof, U.S. Patent (to Poly-Med, Inc.) 6,413,539, 2002.
19. Shalaby, S. W., High Strength Fibers of *l*-Lactide Copolymers, ϵ -Caprolactone, and Trimethylene Carbonate and Absorbable Medical Constructs Thereof, U.S. Patent (to Poly-Med, Inc.) 6,342,065, 2002.
20. Shalaby, S. W., Amorphous Polymeric Polyaxial Initiators and Compliant Crystalline Copolymers Thereof, U.S. Patent (to Poly-Med, Inc.), 6,462,169, 2002.
21. Shalaby, S. W., Copolyesters with Minimized Hydrolytic Instability and Crystalline Absorbable Copolymers Thereof, U.S. Patent (to Poly-Med, Inc.) 6,255,408 B1, 2001.
22. Linden, C. L., Jr. and Shalaby, S. W., Absorbable Tissue Adhesive, U.S. Patent (to US Army) 5,350,798, 1994.
23. Shalaby, S. W., Polyester/Cyanoacrylate Tissue Adhesive Formulations, U.S. Patent (to Poly-Med, Inc.) 6,299,631, 2002.
24. Salz, U., Bolis, C., Radl, A., Rheinberger, V. M., Carpenter, K. A. and Shalaby, S.W., Absorbable gel-forming doxycycline controlled system for non-surgical periodontal therapy, *Trans. Soc. Biomater.*, 24, 294, 2001.
25. Corbett, J. T., Kelly, J. W., Dooley, R. L., Fulton, L. K. and Shalaby, S. W., Development of an animal model for evaluation of antibiotic controlled release systems for the management of osteomyelitis, *Trans. Soc. Biomater.*, 24, 292, 2001.

26. Allan, J. M., Kline, J. D., Wrana, J. S., Flagle, J. A., Corbett, J. T. and Shalaby, S. W., Absorbable gel forming sealants/adhesives as a staple adjuvant in wound repair, *Trans. Soc. Biomater.*, 22, 374, 1999.
27. Corbett, J. T., Anneaux, B. L., Quirk, J. R., Fulton, L. K., Shalaby, M., Linden, D. E., Woods, D. W. and Shalaby, S. W., Comparative Study of absorbable and non-absorbable tissue adhesives: A preliminary report, *Trans. Soc. Biomater.*, 25, 636, 2002.
28. Kline, J. D., Gerdes, G. A., Allan, J. M., Lake, R. A., Corbett, J. T., Fulton, L. K. and Shalaby, S. W., Effect of Gel Formers on Burn Wounds Using an Optimized Animal Model, *Sixth World Biomaterials Congress, Trans. Soc. Biomater.*, III, 1092, 2000.
29. Shalaby, S. W. and Roweton, S. L., Microporous Polymeric Foams and Microtextured Surfaces, U.S. Patent (to Poly-Med, Inc.) 5,898,040, 1999.
30. Shalaby, S. W. and Linden, C. L., Jr., Radiochemical Sterilization, U.S. Patent 5,422,068, 1995.
31. Shalaby, S. W., Jackson, S. A. and Moreau, J.-P., Ionic Molecular Conjugates of Biodegradable Polyesters and Bioactive Polypeptides, U.S. Patent (to Biomeasure, Inc.) 5,672,659, 1997.
32. Shalaby, S. W., Jackson, S. A. and Moreau, J.-P., Ionic Molecular Conjugates of Biodegradable Polyesters and Bioactive Polypeptides, U.S. Patent (to Biomeasure, Inc.) 6,221,958, 2001.
33. Shalaby, S. W. and Corbett, J. T., Acylated Cyclodextrin Derivatives, U.S. Patent (to Poly-Med, Inc.) 5,916,883, 1999.
34. Shalaby, S. W. and Corbett, J. T., Acylated Cyclodextrin Derivatives, U.S. Patent (to Poly-Med, Inc.) 6,204,256, 2001.
35. Shalaby, S. W. and McCaig, S., Surface Phosphorylation of Polymers, U.S. Patent (to Clemson University) 5,491,198, 1996.
36. Shalaby, S. W. and Rogers, K. R., Polymeric Prosthesis Having a Phosphorylated Surface, U.S. Patent (to Clemson University) 5,558,517, 1996.
37. Shalaby, S. W., Johnson, R. A. and Deng, M., Process of Making a Bone Healing Device, U.S. Patent (to Clemson University) 5,529,736, 1996.
38. Allan, J. M., Wrana, J. S., Linden, D. L., Dooley, R. L., Farris, H., Budsberg, S. and Shalaby, S. W., Osseointegration of morphologically and chemically modified polymeric dental implants, *Trans. Soc. Biomater.*, 22, 37, 1999.
39. Shalaby, S. W. and Roweton, S. L., Continuous Open Cell Polymeric Foam Containing Living Cells, U.S. Patent 5,677,355, 1997.
40. Shalaby, S. W. and Roweton, S. L., Microporous Polymeric Foams and Microtextured Surfaces, U.S. Patent (to Poly-Med, Inc.) 5,969,020, 1999.
41. Roweton, S. L. and Shalaby, S. W., Microcellular Foams, in *Polymers of Biological and Biomedical Significance*, Shalaby, S. W., Ikada, Y., Langer, R. and Williams, J. Eds., Vol. 520, ACS Symposium Series, American Chemical Society, Washington, DC, 1993.
42. Mukherjee, D. P., Rogers, S., Smith, D. and Shalaby, S. W., A comparison of chondrocyte cell growth in a biodegradable scaffold with and without mixing, *Trans. Soc. Biomater.*, 22, 528, 1999.
43. Anneaux, B. L., Atkins, G. G., Linden, D. E., Corbett, J. T., Fulton, L. K. and Shalaby, S. W., *In vivo* breaking strength retention of radiochemically sterilized absorbable braided sutures, *Trans. Soc. Biomater.*, 24, 157, 2001.

Section B

Development and Application of New Systems

2

Segmented Copolyesters with Prolonged Strength Retention Profiles

Shalaby W. Shalaby

CONTENTS

2.1	Introduction	15
2.2	Molecular Chain Design for Tailored Properties	16
2.3	Composition and Properties of Typical Copolymers and Sutures Thereof	17
2.3.1	Copolymers for Monofilament Sutures	18
2.3.2	Copolymers for Braided Sutures	19
2.3.3	Effect of Composition on Properties of Segmented Polymers and Their Braided Sutures.....	21
2.4	Conclusion and Perspective on the Future	23
	References	23

2.1 Introduction

Since the first development of polyglycolide as an absorbable suture, the majority of the absorbable products pertained to soft tissue repair and were based primarily on polymers with short to moderate strength retention profiles in the biological environment. However, interest in using absorbable systems in orthopedics justified the search for absorbable polymers that can be used in the production of devices with prolonged strength retention, due to the slow healing rate of bones as compared to soft tissues. Meanwhile, a special need for sutures with prolonged breaking strength retention (BSR) profiles for soft tissue repair has been voiced by a number of surgeons, particularly those who repair slow-healing soft tissues, as in the case of geriatric patients or patients with compromised wounds. For investigators, including the author, who are interested in fibers with prolonged BSR, it is

well recognized that absorbable fibers suitable for constructing biomedical constructs, as in certain surgical sutures and meshes as well as prosthetic tendons and ligaments, must be based on polymers that meet certain requirements. In effect, these polymers are expected to have:

- High molecular weight
- A high degree of crystallinity
- Minimum or no monomeric species

These requirements were claimed to have been fulfilled by the *L*-lactide/glycolide copolymers described by Benicewicz et al. as well as Kennedy and Liu.¹⁻³ However, in certain high load-bearing applications where a prosthetic fibrous construct experiences cyclic stresses and is expected to maintain a substantial fraction of its initial strength for several weeks postoperatively, additional requirements are imposed. Typical examples of such constructs are surgical meshes for hernia repair and prosthetic tendons and ligaments. These additional requirements are expected to be associated with having a high degree of toughness, as measured in terms of the work-to-break, without compromising significantly their high tensile strength, high Young's modulus, low stretchability, and high yield strength. Such requirements also are expected to be associated with a polymeric chain exhibiting higher hydrolytic stability than those containing primarily glycolate sequences. Unfortunately, until recently, the available literature on absorbable polymers provided conflicting teachings that may be applied towards meeting the aforementioned additional requirements. To increase toughness, more flexible ϵ -caprolactone-based sequences in polyglycolide chain have been introduced successfully in the production of low modulus sutures, but with compromised strength.^{4,5} A similar situation is encountered in the copolymer of glycolide and trimethylene carbonate.⁶ Interestingly, fibers made of these two types of copolymers do display a lower propensity to hydrolysis than polyglycolide, but their strength loss profiles remain unsuitable for long-term, load-bearing applications. This provided the incentive to develop the high lactide copolymer discussed in the rest of this chapter.

2.2 Molecular Chain Design for Tailored Properties

The basic design of a chain molecule to achieve the sought properties for a device with prolonged breaking strength retention (BSR) profile was based on copolymeric ϵ -caprolactone and trimethylene carbonate derived compositions, which meet the above-noted stringent requirement for fibers suited for the construction of biomedical devices. Particularly, surgical ligatures or sutures are expected to:

- Support high loads
- Experience cyclic stresses
- Display minimum or average stretchability
- Display a high degree of toughness
- Display optimum hydrolytic stability
- Possess a prolonged strength profile, especially during the initial postoperative period, as braided multifilament or monofilament sutures

Following the tenets of this design, it was possible to prepare a model system that is a crystalline copolymer made of *l*-lactide and at least one cyclic monomer that is a liquid at or melts above about 40°C. In this model system the *l*-lactide-derived sequences of the polymer chain comprise from about 60 to about 90% of all sequences, and the copolymer has a T_m of at least 150°C, exhibits a crystallinity of at least about 20%, and has an inherent viscosity of at least about 1.1 dl/g. In typical compositions for preparing representative copolymers, the cyclic monomer, other than *l*-lactide, was ϵ -caprolactone, trimethylene carbonate, or both. Useful molar ratios of *l*-lactide to cyclic monomers were 60:40, 62:38, 65:35, 68:32, 72:28, 76:24, 80:20, 84:16, 85:15, 86:14, 90:10, and 94:6.

The copolymer chain was designed to have the *l*-lactide-based repeat units constitute about 95% of the crystallizable chain segments. These were expected to be randomly linked to one or two types of repeat units based on trimethylene carbonate and/or ϵ -caprolactone. For many useful copolymers, the chain design dealt with *l*-lactide-based repeat units comprising about 65 to 94% of the total copolymeric chain; such units were expected to be present as crystallizable segments or blocks. A monofilament suture made from the copolymers based on the subject design was expected to have an elastic modulus greater than about 400,000 psi, a tensile strength greater than about 40,000 psi, and a percent elongation less than about 50%. A molecular chain having a relatively lower fraction of *l*-lactide-based segments was intended for producing monofilaments having an elastic modulus of greater than about 100,000 psi, a tensile strength greater than about 40,000 psi, and percent elongation less than 80%. Copolymers made with a relatively high fraction of the *l*-lactide-based sequences were intended for the production of multifilaments. These were multifilament yarns intended for use in preparing surgical sutures and allied surgical devices such as meshes, prosthetic tendons, ligaments, or vascular grafts.

2.3 Composition and Properties of Typical Copolymers and Sutures Thereof

Outlined in this section are (1) preliminary data on segmented copolymers containing between 71.2 and 76% of lactide-based repeat units and properties

of monofilament sutures therefrom; (2) preliminary data on segmented copolymers based on 86 to 88% lactide and properties of braided sutures therefrom; and (3) results of a study on the effect of copolymer composition on its properties and those of braided sutures therefrom.

2.3.1 Copolymers for Monofilament Sutures

A group of segmented copolymers described by Shalaby were studied by Carpenter and co-workers for conversion into monofilament sutures.^{7,8} These were crystalline copolymers based on *l*-lactide (L), ϵ -caprolactone (CL) and trimethylene carbonate (TMC). Polymerization was conducted in two stages. In the first stage, an amorphous copolymer of CL and/or TMC was prepared. In the second stage, the prepolymer was allowed to react with an *l*-lactide or a mixture of *l*-lactide and CL or TMC in the solid state. Polymerization was conducted as described by Shalaby using stannous octanoate and 1,3-propanediol as catalyst and initiator, respectively.⁷ At the conclusion of polymerization, the solid polymer was isolated, ground, and trace amounts of unreacted monomer were removed by heating under reduced pressure. The dry polymer granules were characterized for composition by nuclear magnetic resonance (NMR) and infrared (IR), for molecular dimensions using gel permeation chromatography, and for inherent viscosity (I.V.) measurement and thermal properties using differential scanning calorimetry (DSC). The dry polymer granules were extruded into monofilaments using a 1/2 in. single screw extruder at a temperature that was at least 10°C above the polymer melting temperature (T_m). The undrawn extrudate was oriented by drawing using a two-stage process. The composition of typical polymers (I to IV) and their properties, as well as the resulting monofilaments (M-I to M-IV), are summarized in Tables 2.1 and 2.2, respectively.

To simulate the *in vivo* performance of the drawn monofilaments, a study of their BSR at 37°C was conducted in a phosphate buffered solution at pH 7.4. Typical BSR data are noted in Table 2.2. The tensile properties of the

TABLE 2.1

Chemical Composition and Physical Properties of Typical Polymers

Polymer Number	Polymer Composition L/TMC/CL ^a	I.V. (CHCl ₃) (dL/g)	DSC Data	
			T_m (°C)	ΔH_f (J/g)
I	74/16/10	1.25	177	47
II	76/14/10	2.04	175	34
III	74/15/11	1.52	168	52
IV	71.2/16/3/12.5	1.26	173	55

^a Ratio of contributing components to the segmented chain: L = *l*-lactide; CL = ϵ -caprolactone; TMC = trimethylene carbonate.

TABLE 2.2Physical Properties and *In Vitro* BSR of Typical Monofilaments

Monofilament Number ^a	Fiber Properties					% <i>In Vitro</i> BSR ^b	
	Diameter (mm)	Linear	Knot	Modulus (Kpsi)	Elongation (%)	At 37°C	At 50°C
		Strength (Kpsi)	Strength (N)			at 6 Weeks	at 4 Weeks
M-I	0.20	64	7.4	316	57	78 ^c	52
M-II	0.20	82	—	486	52	74	—
M-III	0.22	83	12.3	479	57	—	44
M-IV	0.20	98	7.5	544	59	84	53

^a M-I to M-IV were produced from Polymers I to IV, respectively.^b BSR = breaking strength retention in a phosphate buffer at pH 7.4.^c 52% at 12 weeks.

monofilaments were measured using an MTS Minibionix Universal Testing Unit (Model 858).

The results in Table 2.1 demonstrate that a highly crystalline (in terms of ΔH_f) segmented copolymer of *L*-lactide can be produced using the solid-state polymerization approach. The data in Table 2.2 indicate that segmented *L*-lactide copolymers are excellent fiber formers and are promising candidates for the production of monofilament sutures with comparable modulus (or compliance) to the most commonly used nonabsorbable monofilament suture, polypropylene. In addition, at this stage of development, the intrinsic modulus of the present monofilament suture is slightly higher than those of poly-*p*-dioxanone (PDS-II®). Its perceived compliance and resilience are competitive with those of PDS-II and other commercial, absorbable monofilament sutures.^{9,10} Most importantly, the BSR data in Table 2.2 verify the ability of the present monofilament suture to retain at least 50% of its initial strength at 12 weeks. This far exceeds known BSR values for PDS-II and other absorbable monofilament sutures. The results of this report demonstrated the feasibility of designing a segmented, high-lactide copolymer chain needed for the production of crystalline monofilament sutures with a breaking strength profile that can be prolonged to 12 weeks, which is about double that known for PDS-II.

2.3.2 Copolymers for Braided Sutures

Since the disclosure and recent commercialization of the 95/5 *L*-lactide/glycolide random copolymer as a braided suture for limited orthopedic application (Panacryl®) the surgical community has called for a new family of long-lasting braided sutures for broad use in different surgical procedures associated with slow-healing tissues.^{1,2} The recognized need for a new braid and the reported success in converting the segmented high-lactide copolymers as discussed in Section 2.3.1 provided Anneaux and co-workers with an incentive to explore the use of similar polymers with relatively higher

TABLE 2.3Chemical Composition and Physical Properties^a of Typical High Lactide-Based Polymers

Polymer Number	Polymer Composition ^b		DSC Data	
	L/TMC/CL	I.V. (dL/g)	T _m (°C)	ΔH _f (J/g)
V	88/12/0	3.27	183	62
VI	88/12/0	1.87	183	59
VII	88/8/4	2.46	180	50
VIII	86/15/0	2.97	170	53

^a All polymers were insoluble in hexafluoro-2-propanol for viscosity measurement.^b Ratio of contributing components to segmented chains: L = *l*-lactide; TMC = trimethylene carbonate; CL = ϵ -caprolactone.

lactide content for the production of multifilament yarn and braided sutures therefrom.¹¹ Accordingly, highly crystalline copolymers were prepared using 86 to 88 M% of *l*-lactide and 12 to 14 M% of TMC or a mixture of TMC and CL. The polymers were made as described for similar polymers in Section 2.3.1. The composition and properties of four typical examples of these polymers (V to VIII) are summarized in Table 2.3. Conversion of the polymer to spun-drawn multifilament yarn was accomplished using a 3/4 in. single-screw extruder equipped with a multihole die and integrated with a spin-finish applicator, a take-up roll, heated and unheated Godeys, and winder. The multifilament yarns were prepared for braiding using an 8- or 16-carrier braiding unit. Accordingly, braids BR-I to BR-IV based on polymers V to VIII were constructed into clinically relevant sizes for use in orthopedic applications. Prior to testing, the spin-finish was removed, braid dimensions were stabilized, and an absorbable coating was applied. For coating, a nitrogenous caprolactone copolymer was used.¹² The tensile properties of the yarn and braid were determined using an MTS Minibionix Universal Testing Unit (Model 858). The *in vitro* BSR was evaluated using a phosphate buffered solution at pH 7.4 and a temperature of 37°C or 50°C. Braid properties and *in vitro* BSR data are summarized in Table 2.4.

The results of polymers V to VIII in Table 2.3 demonstrate that highly crystalline segmented copolymers of *l*-lactide can be produced using a solid-state polymerization protocol. The data from Braids BR-I to BR-IV in Table 2.4 show that these polymers are promising precursors for strong, multifilament yarn that can be converted into high-strength braids with exceptionally high knot strength. The high knot strength of this suture, as compared to Panacryl®, is attributed to the inherent toughness of the yarn that, in turn, is associated with the unique segmented structure of the polymer chains. The results also reflect the promising properties of this braid for use not only in orthopedic applications but also for a broad range of surgical procedures.

Results in this study demonstrated the feasibility of designing segmented, high-lactide copolymer chains as crystalline fiber-forming polymers for the

TABLE 2.4Physical Properties and *In Vitro* BSR of Typical Suture Braids

Braid Number ^a	Fiber Properties				% <i>In Vitro</i> BSR ^b		
	Diameter (mm)	Linear	Knot	Elongation (%)	At 37°C at Week 12	At 50°C at Week	
		Strength (N)	Strength (N)			2	4
BR-I	0.41	63	43	38	91	96 ^c	—
BR-II	0.46	65	42	55	—	—	60
BR-III	0.68	118	62	40	—	—	—
BR-IV	0.61	76	48	34	—	—	—

^a BR-I to BR-IV were produced from Polymers V to VIII, respectively.^b BSR in a phosphate buffer at pH 7.4.^c 63% at 6 weeks.

production of long-lasting suture braids with exceptional knot strength and breaking strength retention.

2.3.3 Effect of Composition on Properties of Segmented Polymers and Their Braided Sutures

The demonstrated ability to use segmented high-lactide copolymers for repairing monofilament and braided sutures, with promising physicochemical and biological properties, spurred the initiation of a study on modulating the suture properties by controlling polymer composition.¹³ The study entails the preparation of five segmented lactide copolymers (IX to XIII). These were prepared using different amounts of *L*-lactide, ϵ -caprolactone, and trimethylene carbonate in the presence of stannous octanoate and 1,3-propanediol as the catalyst and initiator, respectively. The polymerization, conversion of the yarn to multifilament, and finally to coated braids and testing of the suture properties were conducted as described in Section 2.3.2. The *in vitro* BSR was determined using a phosphate buffer at pH 7.4 and 37°C or 50°C. The *in vivo* BSR was determined using the traditional rat model, which entails subcutaneous implantation of the test suture as described earlier.¹⁰

The composition as well as pertinent thermal data of Polymers IX to XIII used in preparing the braids, subject of the present study, are summarized in Table 2.5. They show that:

- The melting temperature, which is due to the hard segment, is practically the same for all polymers.
- The heat of fusion, in general, decreases slightly with the decrease in soft/hard segment ratio.
- Most polymers are suitable for producing one or more types of braid construction.

TABLE 2.5

Physical Properties of Typical Compositions of Segmented Copoly lactides Used for Braid Construction

Polymer Number	Polymer Composition (M)		DSC Data		Number of Resulting Braids
	S/H ^a	LL/TMC/CL	T _m (°C)	ΔH _f (J/g)	
IX	8/92	88/12/0	183	52	B-I-7a
X	8/92	88/12/0	180	49	B-I-9b
XI	8/92	86/14/0	180	59	B-III-2
XII	10/90	84/11/5	179	56	B-IV-1
XIII	10/90	84/11/5	181	43	B-IV-5a

^a Ratio of soft/hard segments.

TABLE 2.6

Typical *In Vitro* and *In Vivo* BSR Profiles of Braided Sutures of Different Polymer Compositions

Braid ^a Number	Diameter (mm)	Initial Linear Strength (N)	% <i>In Vitro</i> BSR			% <i>In Vivo</i> BSR	
			At 37°C on Week		At 50°C on Week	at Week	
			12	26	6	12	26
BR-V	0.38	62	75	—	64	54	37
BR-VI	0.64	47	70	—	57	—	—
BR-VII	0.58	84	74	37	70	67	—
BR-VIII	0.50	76	78	57	—	75	60
BR-IX	0.24	38	82	—	82	—	—

^a Braids V to IX were based on Polymers IX to XIII, respectively.

Braids BR-V to BR-IX were prepared using multifilament yarns of Polymers IX to XIII, respectively. The BSR data of these braids are summarized in Table 2.6 and indicate that:

- All braids have clinically acceptable initial strength at the specific sizes.
- There exists a good correlation between the *in vitro* BSR at 37°C and *in vivo* BSR.
- *In vitro* BSR data at 50°C can be used to obtain accelerated BSR profiles that are relevant to the *in vivo* BSR profiles.
- Not only the *l*-lactide component in the copolymer but also the soft/hard segment ratio does affect the BSR profiles.
- The examined braids are suitable for use as long-lasting sutures over a period of 12 to 26 weeks.

The results of the study demonstrated that different segmented, high-lactide copolymers can be used to prepare braided sutures with clinically

acceptable strength and a range of breaking strength retention to justify their use clinically as biocompatible, long-lasting sutures over a 12- to 26-week period depending on their composition.

2.4 Conclusion and Perspective on the Future

The feasibility of developing segmented high-lactide copolyesters with a broad range of physicochemical and biological properties has been demonstrated. This development represents a key milestone in absorbable polymer technology and in the ability to tailor-make novel, absorbable materials to fill the gap between the traditional absorbable polymers and those known to be nonabsorbable. Perspective on the future in this area is expected to pertain to development of (1) new scaffolds for engineering soft and hard tissue, (2) exceptionally compliant monofilament sutures with tailored compliance and/or breaking strength retention profiles, (3) a range of textile constructs with a broad range of properties for reconstructive surgical procedures, and (4) new forms of carriers for controlled drug delivery.

References

1. Benicewicz, B. C., Oser, Z., Clemow, A. J. and Shalaby, S. W., Artificial Absorbable Ligament or Tendon Prostheses Containing Lactide or Glycolide-Lactide Polymeric Fibers, European Patent Application (to J & J Orthopedic Co.) 302, 979, 1987.
2. Benicewicz, B. C., Shalaby, S. W., Clemow, A. J. and Oser, Z., *In vitro* and *in vivo* degradation of poly(*L*-lactide) braided multifilament yarns, in *Agriculture and Synthetic Polymers*, Glass, J. E. and Swift, G., Eds., American Chemical Society, Washington, DC, 1990, chap. 14.
3. Kennedy, J. and Liu, C.-K., Absorbable Melt Spun Fiber Based on Glycolide-containing Copolymer, U.S. Patent (to U.S. Surgical Corp.) 5,425,984, 1993.
4. Shalaby, S. W. and Jamiolkowski, D. D., Surgical Articles of Copolymers of Glycolide and ϵ -caprolactone and Methods of Producing the Same, U.S. Patent (to Ethicon, Inc.) 4,605,730, 1986.
5. Shalaby, S. W. and Jamiolkowski, D. D., Surgical Articles of Copolymers of Glycolide and ϵ -caprolactone and Methods of Producing the Same, U.S. Patent (to Ethicon, Inc.) 4,700,704, 1987.
6. Casey, D. J. and Roby, M. S., Synthetic Copolymer Surgical Articles and Methods of Manufacturing the Same., U.S. Patent (to U.S. Surgical Corp.) 4,429,900, 1984.
7. Shalaby, S. W., High Strength Fibers of *L*-lactide Copolymers, ϵ -caprolactone, and Trimethylene Carbonate and Absorbable Medical Constructs Thereof, U.S. Patent (to Poly-Med, Inc.) 6,342,065, 2002.

8. Carpenter, K. A., Anneaux, B. L., Shalaby, W. S., Pilgrim, J. A., Linden, D. E., Quirk, J. R. and Shalaby, S. W., Segmented lactide copolymers as monofilament sutures — A preliminary report, *Trans. Soc. Biomater.*, 25, 660, 2002.
9. Burg, K. J. L. and Shalaby, S. W., Absorbable materials and pertinent devices, in *Handbook of Biomaterials Evaluation: Scientific, Technical, and Clinical Testing of Implant Materials*, 2nd ed, von Recum, A. F., Ed., Taylor & Francis, Philadelphia, 2nd ed., 1999, 99.
10. Shalaby, S. W., Fibrous materials for biomedical applications, in *High Technology Fibers: Part A*, Lewin, M. and Preston, J., Eds., Marcel Dekker, New York, 1985, chap. 3.
11. Anneaux, B. L., Carpenter, K. A., Shalaby, W. S. W., Linden, D. E., Pilgrim, J. A., Quirk, J. R. and Shalaby, S. W., Segmented lactide copolymers as braided sutures — A preliminary report, *Trans. Soc. Biomater.*, 25, 659, 2002.
12. Shalaby, S. W., Absorbable ϵ -Caprolactone Polymers As Suture Coatings Displaying Autocatalyzed Hydrolysis-Coating, U.S. Patent (to Poly-Med, Inc.) 5,522,842, 1996.
13. Anneaux, B. L., Carpenter, K. A., Greene, D. D., Taylor, M. S., Shalaby, M., Linden, D. E. and Shalaby, S. W., Effect of composition on physical properties of segmented copoly lactides and BSR of suture braids therefrom, *Trans. Soc. Biomater.*, 26, 321, 2003.

3

Polyaxial Crystalline Fiber-Forming Copolyester

Shalaby W. Shalaby

CONTENTS

3.1	Introduction	25
3.2	Synthesis and Properties of Typical Polyaxial Polymers.....	26
3.2.1	Conceptual Designs of the Polyaxial Chain and General Examples of Polymers and Their Applications	26
3.2.2	Typical Examples of Polyaxial Copolyesters and Properties of Monofilament Sutures Therefrom	29
3.2.3	Polyaxial Copolyesters with Different Central Atoms and Monofilaments Thereof	29
3.2.4	Preparation and Processing of Selected Polyaxial Copolyesters as Synthetic Alternatives to Surgical Gut Suture	31
3.2.5	Effect of Composition on the Breaking Strength Retention (BSR) of Radiochemically Sterilized Sutures.....	32
3.2.6	Contributions of the Polyaxial Chain Configuration and Composition of Polymeric Initiators to Thermal and Hydrolytic Stability.....	34
3.3	Conclusion and Perspective on the Future	36
	References	37

3.1 Introduction

Since the successful development of crystalline thermoplastic polyglycolide as an absorbable fiber-forming material, there has been a great deal of effort directed to the development of new linear fiber-forming polyesters with modulated mechanical properties and absorption profiles. Such modulation

was made possible through the application of the concept of chain segmentation or block formation, where linear macromolecular chains comprise different chemical entities with a wide range of physicochemical properties, among which is the ability to crystallize or impart internal plasticization. Typical examples illustrating the use of this strategy have been discussed by a number of investigators, where difunctional initiators were used to produce linear crystallizable copolymeric chains having different microstructures.¹⁻³

On the other hand, controlled branching in crystalline, homochain polymers, such as polyethylene, has been used as a strategy to broaden the distribution in crystallite size, lower the overall degree in crystallinity, and increase compliance.⁴ A similar but more difficult to implement approach to achieving such an effect on crystallinity, as alluded to above, has been used specifically in the production of linear segmented and block heterochain copolymers such as:

- Nonabsorbable polyether-esters of polybutylene terephthalate and polytetramethylene oxide
- Block/segmented absorbable copolymers of high melting crystallizable polyesters such as polyglycolide with amorphous polyether-ester such as poly-1,5-dioxepane-2-one
- Block/segmented absorbable copolyesters of crystallizable and non-crystallizable components^{3,5-7}

However, until recently, the use of a combination of controlled branching (polyaxial chain geometry) and chain segmentation or block formation of the individual branches to produce absorbable polymers with tailored properties has been overlooked. Accordingly, for addressing this area, the synthesis and available properties of this new family of copolyesters and monofilament sutures therefrom are discussed in this chapter.

3.2 Synthesis and Properties of Typical Polyaxial Polymers

3.2.1 Conceptual Designs of the Polyaxial Chain and General Examples of Polymers and Their Applications

The chain design is intended to lead to absorbable, polyaxial, monocentric, crystallizable, polymeric molecules with noncrystallizable, flexible components of the chain at the core and rigid, crystallizable segments at the chain terminals. The basic design calls for amorphous, polymeric, polyaxial initiators with branches originating from one polyfunctional organic compound so as to extend along more than two coordinates, and for their copolymerization with cyclic monomers to produce compliant, crystalline film- and fiber-forming absorbable materials. Typical examples of absorbable copoly-

meric materials comprise at least 30 to 65%, by weight, of a crystallizable component which is made primarily of glycolide-derived or *l*-lactide-derived sequences, exhibit first and second order transitions below 222°C and below 42°C, respectively, and undergo complete dissociation into water-soluble by-products in less than 18 months when incubated in a phosphate buffer at 37°C and pH 7.4 or implanted in living tissues.

The amorphous polymeric, polyaxial initiators (PPIs) used in these systems to produce crystalline absorbable copolymeric materials can be made by reacting a cyclic monomer or a mixture of cyclic monomers such as trimethylene carbonate, caprolactone, and 1,5-dioxapane-2-one in the presence of an organometallic catalyst with one or more polyhydroxy, polyamino, or hydroxyamino compounds having three or more reactive amines and/or hydroxyl groups. Typical examples of the latter compounds are glycerol and ethane-trimethylol, propane-trimethylol, pentaerythritol, triethanolamine, and *N*-2-aminoethyl-1,3-propanediamine.

The crystalline copolymers of the system are so designed to:

- Have the PPI devoid of any discernible level of crystallinity
- Have the PPI component function as a flexible spacer of a terminally placed, rigid, crystallizable component derived primarily from glycolide so as to allow for facile molecular entanglement to create pseudo-crosslinks, which in turn maximize the interfacing of the amorphous and crystalline fractions of the copolymer, leading to high compliance without compromising tensile strength
- Maximize the incorporation of the hydrolytically labile glycolate linkage in the copolymer without compromising the sought high compliance (achieved by directing the polyglycolide segments to grow on multiple active sites of the polymeric initiator and, thus, limiting the length of the crystallizable chain segments)
- Have a broad crystallization window featuring maximum nucleation sites and slow crystallite growth that, in turn, assists in securing a highly controlled post-processing and development of mechanical properties (achieved by allowing the crystallizable components to entangle effectively with noncrystallizable components, leading to high affinity for nucleation, high precrystallization viscosity, slow chain motion, and low rate of crystallization)
- Force the polymer to form less perfect crystallites with broad size distribution and lower their melting temperature as compared to their homopolymeric crystalline analogs to aid melt-processing (achieved by limiting the length of the crystallizable segments of the copolymeric chain)
- Allow for incorporating basic moieties in the PPI which can affect autocatalytic hydrolysis of the entire system, which in turn accelerates the absorption rate

- Allow the polymer chain to associate so as to allow for endothermic thermal events to take place between 60 and 90°C that can be related to tensile toughness similar to that detected in PET relative to the so-called middle endothermic peak (MEP)⁸

As an example, the crystalline copolymeric materials of this family of polymers can be prepared as follows, although as noted above, other similar cyclic monomers can be used. The amorphous polymeric polyaxial initiator is formed by a preliminary polymerization of a mixture of ϵ -caprolactone and trimethylene carbonate in the presence of trimethylolpropane and a catalytic amount of stannous octanoate, using standard ring-opening polymerization conditions, which entail heating the stirred reactants in a nitrogen atmosphere at a temperature exceeding 110°C until substantial or complete conversion of the monomers is realized. This can be followed by adding a predetermined amount of glycolide. Following the dissolution of the glycolide in the reaction mixture, the temperature is raised above 150°C to allow the glycolide to copolymerize with the polyaxial initiator. When practically all the glycolide is allowed to react, the resulting copolymer is cooled to 25°C. After removing the polymer from the reaction kettle and grinding, trace amounts of unreacted monomer are removed by heating under reduced pressure. The ground polymer can then be extruded and pelletized prior to its conversion to fibers or films by conventional melt-processing methods. At the appropriate stage of polymerization and product purification, traditional analytical methods, such as gel-permeation chromatography (GPC), solution viscosity, differential scanning calorimetry (DSC), nuclear magnetic resonance (NMR), and infrared spectroscopy (IR) are used to monitor or determine (directly or indirectly) the extent of monomer conversion, molecular weight, thermal transitions (melting temperature, T_m , and glass transition temperature, T_g), chain microstructure, and chemical entity, respectively.

Another conceptual design deals with end-grafting a PPI with ϵ -caprolactone or *L*-lactide in the presence of a minor amount of a second monomer to produce absorbable crystalline polymers for use as bone sealants, barrier membranes, or films that can form a continuous cell microporous foam, respectively.

Other general applications of the crystalline axial copolyester include:

- The production of compliant absorbable films with modulated absorption and strength loss profiles to allow for their use in a wide range of applications as vascular devices or components — more specifically the use of these devices in sealing punctured blood vessels (Chapter 10)
- Compliant monofilament sutures

The latter application is illustrated in Section 3.2.2.

3.2.2 Typical Examples of Polyaxial Copolyesters and Properties of Monofilament Sutures Therefrom

Using the general method for preparing polyaxial copolyesters, several compositions were prepared and converted to monofilament sutures. The sutures were then evaluated for clinically relevant properties such as those discussed earlier by Shalaby.⁹ These include:

- Initial linear and knot breaking strength
- Elastic modulus and percent elongation to assess their compliance and stretchability, respectively
- *In vitro* breaking strength retention and mass loss during incubation in a phosphate buffer at 37°C and pH 7.4
- *In vivo* breaking strength retention using a rat model where the sutures are implanted subcutaneously for 1 to 4 weeks and individual lengths are explanted periodically to determine percent of retained breaking strength

Prior to *in vivo* evaluation of the suture breaking strength retention, some of the sutures were subjected to radiochemical sterilization using a 5-kGy dose.¹⁰ This sterilization process has been described briefly in Chapter 1 and can be used to achieve suture sterility without compromising its breaking strength. This is contrary to what is known to occur when absorbable sutures are radiation-sterilized using the traditional dose of about 25 kGy.

3.2.3 Polyaxial Copolyesters with Different Central Atoms and Monofilaments Thereof

In a study by Carpenter and co-workers, two types of copolyesters were made to determine the effect of a basic central group on the properties of the polymer.¹¹ Accordingly, triethanolamine (TEA) and trimethylolpropane (TMP) were used to prepare the polyaxial initiator with central amine and carbon atoms, respectively, using trimethylene carbonate (TMC) and caprolactone (CL) as comonomers.

In a typical experimental scheme for the preparation of the amorphous triaxial polymeric initiator, a mixture of CL and TMC (with and without less than 3% glycolide) was copolymerized, as described by Shalaby, in the presence of a suitable amount of TMP or TEA at 150 to 180°C with stannous octanoate as a catalyst to achieve a number average molecular weight (M_n) exceeding 10 kDa.¹² The reaction was monitored for M_n and conversion using gel-permeation chromatography (GPC). The end-grafting was typically achieved by dissolving the polyaxial initiator in an added amount of G (with and without less than 3% CL or TMC) at a temperature at or below 180°C. The end-grafting was completed by heating at 160 to 180°C for 2 to 6 h,

TABLE 3.1

Compositions and Thermal Properties of Typical Copolymers as Determined by DSC

Polymer Number	Composition CL/TMC/G	DSC Data	
		T _m (°C)	ΔH _f (J/g)
I ^a	13.5/17/69.5	224	90
II ^b	15/20/65	224	66
III ^b	15/25/60	221	53

^a Made using TEA.

^b Made using TMP.

depending on the end-grafted copolymer composition. The final copolymer was isolated, ground, and heated under reduced pressure to remove the residual monomer. The thermal properties of the copolymer were determined using differential scanning calorimetry (DSC). Representative copolymers were melt-spun into monofilaments using a 1/2 in. single screw extruder at temperatures that were at least 5°C above the DSC determined T_m. Inherent viscosity (I.V.) of the polymers or extruded monofilaments was measured in hexafluoro-2-propanol if their crystallinity allowed their solubility in such solvent. High-strength oriented monofilaments were obtained by orienting the extruded monofilaments using a two-stage drawing process. The tensile properties of the monofilaments were determined using an MTS MiniBionix Universal Tester (Model 858). Compositions and physical properties of typical copolymers are depicted in Table 3.1. Tensile properties of typical examples of oriented monofilaments are summarized in Table 3.2. The data in Table 3.1 demonstrated the feasibility of producing highly crystalline copolymers with polyglycolide (or high glycolide copolymer) terminal segments having T_m values that approach 225°C that is typical for polyglycolide. This, in turn, shows that during the end-grafting process, there is a minimum or no ester-ester interchange between the terminal polyglycolide segments and the triaxial polymeric initiator components at the core. The tensile properties data of the oriented monofilaments, outlined in Table 3.2, showed clearly that the triaxial chain conformation of the polymer does not compromise the ability of the chain to orient sufficiently to produce high-strength fibers. It was further postulated that the terminal

TABLE 3.2

Tensile Properties^a of Typical Oriented Monofilament

Polymer Number	Monofilament Number	Diameter (mm)	Tensile Strength (Kpsi)	Modulus (Kpsi)	Elongation (%)
I	M1	0.17	86	451	48
II	M2	0.28	78	335	42

^a Fibers were insoluble in HFIP for I.V. measurement.

polyglycolide segments can cluster in a three-dimensional manner and form physical, noncovalent crosslinks that increase the monofilament tensile strength and its resilience.

The available results allowed for the conclusion that:

- Amorphous polymeric triaxial initiators can be used to produce crystalline, highly oriented, strong monofilaments.
- Having a central nitrogen leads to longer crystallizable segments and, hence, higher T_m and tensile properties.

3.2.4 Preparation and Processing of Selected Polyaxial Copolyesters as Synthetic Alternatives to Surgical Gut Suture

In a study by Carpenter and co-workers, three polymers (I, III, and IV) were made using TMP to prepare the respective polymeric initiators, as described in Section 3.2.3.¹³ In an effort to produce compliant monofilaments, these polymers were extruded to monofilaments and processed under slightly different conditions from those used in preparing their counterparts in section 3.2.3. One of the polymers (I) was used to prepare a second set of monofilaments for studying the effect of radiation dose, under a typical radiochemical sterilization process (RC-S) on their *in vitro* breaking strength retention (BSR).

The composition and thermal data of typical polymers and tensile properties of their respective nonsterile monofilaments are summarized in Tables 3.3 and 3.4, respectively. The monofilaments were then radiochemically sterilized using 5 and 7.5 kGy gamma radiation and a polyformaldehyde package insert as described earlier by Correa et al.¹⁰ The tensile properties of typical sterile monofilament sutures and their BSR profiles were determined after incubation in a phosphate buffer at 37°C and pH 7.4 to simulate their *in vivo* profile. The tensile properties and BSR data of a typical radiochemically sterilized monofilament suture are summarized in Table 3.5.

The results in Tables 3.3 and 3.4 indicate that members of this new family of absorbable polymers can be used to produce compliant, high-strength

TABLE 3.3

Compositions and Thermal Properties
of Typical Polymers

Polymer Number	Composition CL/TMC/G	DSC Data	
		T_m (°C)	ΔH_f (J/g)
I ^a	13.5/17/69.5	228	73
III ^b	15/15/70	226	80
IV ^b	15/20/65	220	81

^a Made using TEA.

^b Made using TMP.

TABLE 3.4Tensile Properties^a of Monofilament Sutures

Polymer Number	Fiber Number	Diameter (mm)	Tensile Strength (Kpsi)	Modulus (Kpsi)	Elongation (%)
I	M3	0.30	67 ^a	262	46
III	M4	0.28	72 ^b	345	36
IV	M5	0.29	78	296	58

^a Knot strength = 47 Kpsi.^b Knot Strength = 56 Kpsi.**TABLE 3.5**Typical *In Vitro* BSR Data of a Radiochemically Sterilized Monofilament Suture^a

Radiation Dose	5 kGy	7.5 kGy
BSR, % at 1 week	82	72
BSR, % at 2 weeks	18	17

^a Having 10 mil. diameter and initial tensile strength = 7.1 Kpsi; modulus = 190 Kpsi; elongation = 20%; made from 13.5/17/69.5 CL/TM/G copolymer composition (Polymer I).

monofilament sutures with comparable or improved physical properties as compared with surgical plain and chrome surgical gut of comparable sizes.⁹ The data in Table 3.5 suggest that the candidate monofilament sutures can be radiochemically sterilized using a relatively high dose of 7.5 kGy to accelerate the BSR profile if so desired.

The results of this study led the authors to conclude that:

- Certain polyaxial copolymers can be converted to compliant monofilaments with comparable, or superior, initial strength relative to surgical gut sutures.
- The BSR of the monofilament can be modulated by controlling the sterilization dose to produce sutures that can be competitive with many types of surgical gut sutures.
- Polyaxial copolyesters may be well suited to preparing a synthetic alternative to surgical gut sutures.

3.2.5 Effect of Composition on the Breaking Strength Retention (BSR) of Radiochemically Sterilized Sutures

Having demonstrated that the radiation dose during RC-S can be used to modulate the BSR of monofilament sutures based on polyaxial copolyesters (Section 3.2.4), Anneaux and co-workers studied the effect of composition

TABLE 3.6

Copolyester Compositions and BSR Data of Their Respective Monofilament Sutures

Polymer Number	Monofilament	kGy	Overall Polymer Composition ^a C/T/G	Initial Suture Properties		% BSR of Aged Sutures			
				Diameter (mm)	Linear Strength	In Vitro at Week		In Vivo at Week	
						1	2	1	2
V	M6	0	15/20/65	0.27	36	66	48	75	52
		5				68	34	70	42
VI	M7	0	15/25/60	0.30	35	72	36	77	52
		5				63	37	65	35

^a C = Caprolactone; T = Trimethylene Carbonate; G = Glycolide.

on BSR at a 5-kGy dose.¹⁴ Accordingly, two crystalline copolymers (V and VI) were synthesized using TMP to prepare the polymeric initiators from CL, TMC, and G. The polymeric initiator was then grafted to the glycolide; the resulting copolyesters (V and VI) were converted to monofilaments (M6 and M7) as discussed in Sections 3.2.3 and 3.2.4. The composition of the copolymers (V and VI) and the initial strength of their respective monofilaments (M6 and M7) are shown in Table 3.6.

The *in vitro* BSR was evaluated by determining the breaking strength of the sutures after incubation in a phosphate buffered solution at pH 7.4 and 37°C for predetermined periods of time. The *in vivo* BSR was determined on explanted sutures that have been implanted subcutaneously in rats for predetermined periods according to the animal protocols described in a previous report.¹⁵ The linear breaking strength of the explanted sutures as well as those exposed to the phosphate buffer was determined using an MTS MiniBionix Universal Tester (Model 858).

The BSR data of the high glycolide segmented monofilament sutures are summarized in Table 3.6 and indicate that:

- The effect of the RC-S process at a 5-kGy dose is generally minimal for both sutures.
- The monofilament suture M6, having a slightly higher glycolide content than suture M7, was less sensitive to radiolytic degradation.
- The *in vivo* BSR values were generally higher than the corresponding *in vitro* values.

Results of the study led the authors to conclude that:

- RC-S using ~5 kGy of gamma rays is suitable for sterilizing segmented copolymers having high content of glycolide-derived sequences.
- BSR is affected by composition within a narrow range.

3.2.6 Contributions of the Polyaxial Chain Configuration and Composition of Polymeric Initiators to Thermal and Hydrolytic Stability

In a study by Carpenter and co-workers, the authors addressed the effect of:

- Using polyaxial polymeric initiators on the thermal properties of crystalline end-grafted products as compared with those having linear molecules
- Minor changes in the polymeric polyaxial initiator composition on the hydrolytic stability of the polyaxial end-grafted system¹⁶

A typical polyaxial initiator and its end-grafting with crystallizable segments was prepared as described by Shalaby.⁸ This entails the use of the trifunctional monomeric initiator, trimethylolpropane (TMP) and a mixture of caprolactone and methylene carbonate with a small amount of glycolide to prepare an amorphous, polyaxial polyester as the polymeric initiator, in the presence of a catalytic amount of stannous octanoate. The polyaxial polymeric initiator was then end-grafted with glycolide to form a crystallizable terminal segment. The crystalline polymer (VII) was isolated and purified to remove residual monomer and melt-extruded into monofilaments. Both the unextruded and extruded polymer were characterized for their thermal properties using a Perkin Elmer DSC-6D. In a second experiment, TMP was substituted by 1,3-propanediol in the proper stoichiometry to prepare a linear copolyester (VIII) having a comparable molecular mass to the VII. The former was treated and characterized under identical conditions as VII.

To study the effect of minor changes in composition of the polyaxial initiator on the hydrolytic and thermal properties of crystalline polymeric end-grafted copolyester, glycolide was substituted with a molecularly equivalent amount of *dl*-lactide to prepare the polyaxial polymeric initiator. The corresponding end-grafted crystalline copolyester (IX) was isolated, purified, and characterized under conditions identical to VII. Both polymers were similarly compression molded into microtensile specimens (using a Carver Press, Model 395) to study their hydrolytic stability in terms of BSR after incubation in a phosphate buffer at 37°C and pH 7.4, as well as in a constant humidity chamber having a relative humidity of 75% at 25°C. The physical testing was conducted using an MTS MiniBionix Universal Tester (Model 858).

Comparative thermal data of crystalline polyaxial and linear copolyester VII and VIII, respectively, are summarized in Table 3.7. The data in Table 3.7 show that the:

- Unextruded annealed polyaxial polymer exhibits a lower melting (T_m) and heat of fusion (ΔH_f) as compared to its linear counterpart.
- Difference in T_m of the two polymers becomes more pronounced after extrusion and subsequent heat treatment (or annealing).

TABLE 3.7

Thermal Properties of Compression Molded Films

Polymer Number	Type	Thermal Data			
		Before Extrusion		After Extrusion	
		T_m (°C)	ΔH_f (J/g)	T_m (°C)	ΔH_f (J/g)
VII	Polyaxial	217	24	208	23
VIII	Linear	229	44	215	36

TABLE 3.8

Hydrolytic Stability Data of Compression Molded Films

Sample Number	Inherent Viscosity (dL/g) (CHCl ₃)		Initial Breaking Strength (N/mm ²)	% BSR of Molded Specimens Incubated				
				In Phosphate Buffer at pH 7.4 and 37°C on Day			At 75% RH and 25°C on Day	
				4	7	10	7	14
	Before Molding	After Molding						
VII	0.93	0.64	12.29	75	60	43	87	86
IX	0.82	0.69	14.52	80	71	54	100	100

- Effect of extrusion on the difference in ΔH_f between both polymers is less pronounced.

The DSC thermal data of annealed polymer before extrusion are consistent with the expected lower tendency of the polyaxial system to crystallize and, to a lesser extent, its tendency to form smaller, relatively imperfect crystallites. Thermal data for unannealed extrudate demonstrate the limited effect of extrusion on formation of small crystallites in the polyaxial system. This is attributed to the higher frequency of nucleation sites in the polyaxial system as compared to its linear counterpart. The latter appears to have a lower tendency for immediate crystallization as compared to the polyaxial system. The thermal properties of the polyaxial system make it more suitable for construction of tougher, higher compliance devices as compared with its linear counterpart.

The hydrolytic stability data of films made from Polymers VII and IX was measured in terms of BSR, a traditional parameter for studying hydrolytic stability of absorbable polyesters, and are summarized in Table 3.8. The BSR data in Table 3.8 show that substitution of *dl*-lactide for glycolide at levels of less than 5 mol% of total chain composition led to a substantial improvement of the polyaxial polymer hydrolytic stability. Accordingly, glycolide-containing polymeric initiators will be more suitable for developing fast-absorbing devices as compared to their *dl*-lactide counterparts.

Results of the study led the authors to conclude that:

- Crystalline copolyesters made by end-grating crystallizable segments onto amorphous polyaxial initiators exhibit a lower overall degree of crystallinity but higher tendency to crystallize from the melt into smaller crystallites as compared to their linear counterparts.
 - The polyaxial polymers are more suitable than linear ones for developing high-impact, more compliant biomedical devices as compared with their linear counterparts.
 - Composition of the amorphous initiator for the polyaxial crystalline systems can be easily adjusted to provide biomaterials for constructing devices with a broad range of strength retention profiles.
-

3.3 Conclusion and Perspective on the Future

Studies discussed in this chapter demonstrate the feasibility of predictably modulating the properties of fiber-forming polymers by controlling their molecular architecture and composition. More specifically, it has been shown that amorphous, polyaxial copolyesters can be used as initiators for preparing high molecular weight, polyaxial, crystalline absorbable copolyesters by end-grafting short crystallizable terminal segments, leading to unique physical and biological properties. This created a new opportunity to apply traditional molecular engineering principles to the development of novel, absorbable, biomedical devices with tailored properties. Branched polymers were usually excluded as suitable precursors of high strength fibers partly because of the limited ability to optimally integrate their amorphous and crystalline components, a requirement for the production of strong fibers. However, formation of polyaxial chains with practically symmetrical geometry and properly spaced crystallizable chain segments rather than randomly branched systems allowed the conversion of typical polyaxial crystalline copolyesters into high-strength fibers. Additionally, the effect of using polyaxial polymeric initiators on the thermal properties of crystalline end-grafted products as compared to those having linear molecules has been illustrated. The report also describes the effect of minor changes in the polymeric polyaxial initiator composition on the hydrolytic stability of the polyaxial end-grafted system.

Successful development of crystalline, polyaxial, absorbable polyesters with modulated compliance and unique thermal properties and microtexture are expected to lead to new applications and more effective uses of absorbable polymers as biomaterial devices, which calls for highly compliant, resilient, and/or microporous forms of textile constructs, films, and foams.

References

1. Choi, S. H. and Park, T. G., Synthesis and Characterization of Elastic PGLA/PCL/PLGA Triblock Copolymers, *J. Biometer. Sci. Polymer Ed.*, 13, 1163, 2002.
2. Shalaby, S. W., Copolyesters with minimized hydrolytic instability and crystalline absorbable copolymers thereof, U.S. Patent (to Poly-Med, Inc.) 6,503,991, 2003.
3. Li, Y. and Kissel, T., Synthesis characteristics and *in vitro* degradation of star-block copolymers consisting of *L*-lactide, glycolide and branched multi-arm poly(ethylene oxide), *Polymer*, 39(18), 4421, 1998.
4. Mandelkern, L., *Crystallization of Polymers*, McGraw-Hill, New York, 1964, 105.
5. Shalaby, S. W. and Bair, H. E., Block copolymers and polyblends in *Thermal Characterization of Polymeric Materials*, Turi, E. A., Ed., Academic Press, New York, 1981, chap. 4.
6. Shalaby, S. W. and Koelmel, D. F., Flexible Copolymers of *p*-(Hydroxy-alkoxy) Benzoic Acid and Compliant Surgical Products, Particularly Sutures, U.S. Patent (to Ethicon, Inc.) 4,543,952, 1985.
7. Kafrawy, A., Mattei, F. V. and Shalaby, S. W., Copolymers of Lactide and/or Glycolide with 1,5-dioxepan-2-one), U.S. Patent (to Ethicon, Inc.) 4,470,416, 1984.
8. Shalaby, S. W., Thermoplastic copolymers, in *Thermal Characterization of Polymeric Materials*, Turi, E. A., Ed., Academic Press, New York, 1981, chap. 3.
9. Shalaby, S. W., Fibrous materials for biomedical applications in *High Technology Fibers: Part A*, Lewin, M. and Preston, J., Eds., Marcel Dekker, New York, 1985, chap. 3.
10. Correa, D. E., Kline, J. D., Barefoot, S. F., Corbett, J. T., Allan, J. M. and Shalaby, S. W., Radiochemical sterilization of polyglycolide sutures, *Sixth World Biomaterials Congress, Trans. Soc. Biomater.*, II, 992, 2000.
11. Carpenter, K. A., Anneaux, B. L., Shalaby, M., Bruce, T. F., Pilgrim, J. A., Schiretz, Jr., F. R. and Shalaby, S. W., A new family of absorbable crystalline copolyesters: An initial report, *Trans. Soc. Biomater.*, 25, 633, 2002.
12. Shalaby, S. W., Amorphous polymeric polyaxial initiators and compliant crystalline copolymers therefrom, U.S. Patent (to Poly-Med, Inc.) 6,462,169, 2002.
13. Carpenter, K. A., Schiretz, Jr., F. R., Anneaux, B. L., Shalaby, W. S. W., Bruce, T. G., Pilgrim, J. A., Linden, D. E. and Shalaby, S. W., Synthetic alternatives to surgical gut sutures: a preliminary report, *Trans. Soc. Biomater.*, 25, 663, 2002.
14. Anneaux, B. L., Carpenter, K. A., Schiretz, F. R., Fulton, L. K., Shalaby, W. S. W., and Shalaby, S. W., Effect of composition on the BSR of radiochemically sterilized sutures of segmented copolyesters, *Trans. Soc. Biomater.*, 26, 271, 2003.
15. Anneaux, B. L., Atkins, G. G., Linden, D. E., Corbett, J. T., Fulton, L. K. and Shalaby, S. W., *In vivo* breaking strength retention of radiochemically sterilized absorbable braided sutures, *Trans. Soc. Biomater.*, 24, 157, 2001.
16. Carpenter, K. A., Lindsey, J. M., III, Vaughn, M. A., Mathisen, T. L., and Shalaby, S. W., Thermal properties and hydrolytic stability of absorbable, polyaxial copolyesters: A preliminary report, *Trans. Soc. Biomater.*, 26, 328, 2003.

4

Polyethylene Glycol-Based Copolyesters

Shalaby W. Shalaby and Marc Shalaby

CONTENTS

4.1	Introduction	40
4.2	Novel Gel-Forming Liquid PEG-Based Copolyesters	40
4.2.1	Molecular Design and Attributes of Tailored Properties	40
4.2.2	Advances in Biomedical Applications and Clinical Relevance	43
4.2.3	Advances in the Applications of Controlled Delivery Systems and Clinical Relevance	45
4.2.3.1	Controlled Release Systems for Treating Osteomyelitis	45
4.2.3.2	Controlled Release of the Recombinant Protective Antigen Form of Anthrax Vaccine	46
4.2.3.3	PEG-Based Controlled Release System for Cervical Ripening	47
4.2.3.4	Absorbable Gel-forming Doxycycline Controlled Release System for Nonsurgical Periodontal Therapy	48
4.2.3.5	Gel-Forming Polyesters for Intravitreal Therapy for Cytomegalovirus (CMV) Retinitis	49
4.3	Advances in Solid PEG-Based Copolyesters	50
4.3.1	Alternating Multiblock Copolymers in Wound Healing Compositions	51
4.3.2	Nanospheres of PEG-Polycaprolactone A-B Block Copolymer as a Novel Drug Carrier	51
4.3.3	Copolyether-Ester Block Copolymers for Thermo-Responsive Controlled Delivery Systems	52
4.3.4	Radioisotope-Bearing Poly(Ethylene Glycol-b-Caprolactone) (PEG-PCL) for Bone Imaging	52
4.3.5	<i>In Situ</i> Crosslinkable PEG-Based Copolymers for Protein Controlled Delivery	53
4.4	Photopolymerizable PEG-Copolyesters	53

4.5 Conclusion and Perspective on the Future	54
References	54

4.1 Introduction

Over the past two decades, interest has grown in the development of absorbable pharmaceutical and surgical products which degrade in the biological environment to safe by-products leaving no residual mass at the application site. Such polymers are often described as absorbable or biodegradable. Their popularity in recent years has been amplified by the wide range of applications that these polymers possess. Their transient nature when used as biomedical implants such as surgical sutures has revolutionized modern surgical techniques. Their use as drug carriers for controlled delivery systems has permitted local drug delivery without the risks associated with permanent foreign bodies or with systemic therapy. On the other hand, with the exception of polyanhydrides, it is likely that all clinically useful absorbable polymers are polyesters or copolyesters. Perhaps the most important type of such polymers are those based on one or more of the following cyclic monomers — ϵ -caprolactone, glycolide, lactide, *p*-dioxanone, and trimethylene carbonate. Such polymers have been developed for use as surgical sutures, carriers for the controlled release of bioactive agents, and compliant absorbable tissue adhesives/sealants.

Polyethylene glycol (PEG) has been noted for being a biocompatible, non-toxic, nonimmunogenic, and water soluble material for use in pharmaceutical and biomedical applications.^{1,2} Block copolymers of PEG and polypropylene glycol have been used for coating absorbable suture braids to increase surface lubricity.³ Biocompatible, segmented polyurethanes containing PEG as the soft segment have been prepared and suggested for use as implant materials.⁴ Although PEGs do not degrade in the biological environment below certain molecular weight, they can be eliminated via excretion.¹ The many cited attributes of PEGs prompted Shalaby to copolymerize members of this class of polymers with cyclic lactones and carbonates to form liquid gel-formers.⁵ This led to the development of a novel family of absorbable copolyesters comprising liquid, hydrogel-forming, solid thermoplastic or photopolymerizable materials.

4.2 Novel Gel-Forming Liquid PEG-Based Copolyesters

4.2.1 Molecular Design and Attributes of Tailored Properties

Novel hydrogel-forming, self-solvating, absorbable copolyesters have been developed that are capable of selective, segmental association into a compli-

ant hydrogel mass when placed in an aqueous medium. Such systems are composed of a primary component that is made up of molecular chains having hydrophilic polyester blocks and relatively hydrophobic ones that are linked in alternating sequence and may be branched to maintain the same sequence. The hydrophobic block is a polyester formed by grafting glycolide, lactide, ϵ -caprolactone, *p*-dioxanone, trimethylene carbonate, or combinations thereof onto the hydroxylic or amino-end groups of a hydrophilic polymer precursor. The hydrophilic block comprises a polyoxyethylene, poly(oxyethylene-*b*-oxypropylene), or a liquid, high molecular weight polyether glycol interlinked with oxalate or succinate functionalities in linear or branched form.⁵

Copolyesters of PEG have been prepared in which ethylene glycol is pre-interlinked with succinate or oxalate bridges to increase the length of the hydrophilic block (and subsequently its molecular weight) without favoring its crystallization. This hydrophilic "prepolymer" with its terminal hydroxylic groups is typically end-grafted with a mixture of *dl*-lactide/glycolide to produce a block copolymer having a hydrophilic block fraction of about 25%. In order to make this copolyester more receptive to basic drugs, its end-groups can optionally be carboxylated.⁵

PEG-based copolymers can be present as liquids at room temperature which can be extruded through a die or administered through a syringe needle. The copolymer is introduced into a biological target site by conventional means and then undergoes selective-segmental segregation to form a flexible, compliant, reversible gel. This hydrogel mass adheres tenaciously to the surrounding tissues and acquires the configuration of the site. The hydrogel mass is stabilized by pseudo-crosslinks provided by the hydrophobic polyester component.⁵

Gel-forming copolyesters of PEG can be used as protective barriers, blocking agents of vascular defects caused by needle puncturing, sealants for damaged surfaces, or as a vehicle for the delivery of a host of therapeutic agents. When used as a controlled delivery system, such polymers are capable of local therapy with agents such as nonsteroidal antiinflammatory drugs (NSAIDs), anesthetic agents, antibiotics, antifungals, antimicrobial agents, immunosuppressive agents, immunostimulatory agents, and factors for regulating cellular events. Such therapeutic agents may be deposited directly in the copolymer, or alternatively, they may be deposited on a solid carrier that would then be dispersed in the polymer. Such a solid carrier would preferably be an absorbable, microporous, low molecular weight polyester which is highly crystalline and practically insoluble in the PEG-based copolymer. The addition of this additional solid carrier would then permit biologically active agents to be incorporated into the controlled-release system by a variety of means:

- A solute in the copolymer
- A dispersed solid in the copolymer

- A coating on the solid carrier
- Mechanically held agents within the pores of the solid carrier
- Ionically bound molecules on the copolymer

By varying the concentration of the solid carrier, the hydrogel formulation can be tailored to exhibit a broader range of properties and release profiles that allow its use in a variety of applications.⁵

An optional third component to the polymer system is a low molecular weight, absorbable, block copolyester that serves as a plasticizer. Such a copolymer has hydrophilic and hydrophobic components that are similar or identical to those of the base copolymer, with the exception of having a higher hydrophilic/hydrophobic ratio. This optional component can modulate the rheological properties, gel-formation time, and mechanical disposition of the primary copolymer at the site of application. In addition, this component can:

- Aid the dispersion of the solid carrier in the primary copolymer
- Reduce the overall system viscosity of the primary polymer/solid carrier formulation thereby facilitating the injectability of the solid carrier
- Increase the rate of hydration or gel formation

In short, this third optional component of the system is yet another means by which one may tailor the hydrogel forming system to meet the specific needs of an application.⁵

There are several advantages of the PEG-based copolyesters over earlier formulations that stem from the lack of organic solvents in the former. Hydrogel formers do not require the organic solvents commonly utilized in the formulations of solid polymers. Such solvents can compromise the copolymer's shelf-stability. For instance, propylene glycol can degrade polyester chains through alcoholysis, and trimethylene carbonate can copolymerize with polyester chains. Moreover, if radiation sterilization is employed, the presence of a solvent may lead to the generation of new chemical species. In addition, low molecular organic solvents can migrate from the application site and cause damage to living tissue, such as cell dehydration and necrosis. In sum, the presence of organic solvents can compromise the purity and efficacy of the polymer system and may damage local tissue.⁵

Another feature of PEG-based copolyesters that is a clear improvement on previous systems is that when these agents are administered to a biological site, the copolymers do not experience a discernible reduction in organic mass. Previous systems have been known to coagulate *in situ* by leaching out major water-soluble components. This leaching process can be associated with shrinkage and separation from the surrounding tissue and, in some cases, uncontrolled formation of a microporous mass.⁵

A further feature of PEG-based copolyesters is that since the copolymers comprised self-solvating molecules, their conversion to a hydrogel about a drug provides a uniform distribution of the therapeutic agent and thus a more predictable release profile. This is in contrast to conventional systems in which the presence of leachable solvents leads to complex physical events that can alter the kinetics of the system.⁵

4.2.2 Advances in Biomedical Applications and Clinical Relevance

Closure of skin wounds has traditionally been accomplished through the use of surgical sutures to achieve tissue approximation. Stapling has also gained wide acceptance as a quick method to close these same wounds.⁶ Both modalities offer good results at the expense of some degree of tissue trauma and the formation of scar tissue. In an effort to decrease the amount of tissue trauma (and subsequent scarring), novel absorbable gel-forming sealants/adhesives based on PEG have been developed. Such agents may serve as adhesives that obviate the need for sutures or staples to close wounds. Alternatively, these agents may serve as adjuvants to traditional mechanical devices for wound repair that would allow fewer staples or sutures to be used and hence minimize tissue trauma.^{7,8}

Earlier work in this field has shown that based on *in vitro* data, combinations of methoxypropyl cyanoacrylate (MPC) and poly(trioxyethylene glycol oxalate) (PTOX) can be used as absorbable tissue adhesive formulations.^{9,10} These combinations formed strong adhesive joints to animal skin from sacrificed goats and were absorbed in a buffered phosphate at pH 7.2 within about 6 months. The next step was to evaluate the effectiveness of these combinations compared to staples and sutures in an *in vivo* system. In a study by Flagle and co-workers, skin incisions were performed upon the dorsum of rats. These wounds were then closed with either sutures, staples, or the polymer adhesive. The tensile strengths of wounds healed after suture and staple closure (control groups) were compared to those of wounds healed after tissue approximation with the polymer adhesive (study group). No significant difference in tensile strength was observed between the study and control groups after a 2-week period.⁸

It must be noted that the biomechanics of certain wound sites may limit the use of PEG-based polymer adhesives as the sole modality for wound closure. In this instance, a combination of novel gel-forming adhesives with a fewer number of staples or stitches than traditionally practiced may achieve adequate skin closure and wound healing with less tissue trauma. In a study done by Allan and colleagues, skin incisions were performed upon the dorsum of rats. As a control, some of these wounds were closed with either sutures or staples in the traditional manner (two sutures/staples per centimeter of wound). The study group consisted of wounds closed with polymer adhesive plus half the number of staples/sutures (one suture/staple per centimeter). The tensile strengths of the wounds of the control and study

groups were measured after 2 weeks. No significant difference in tensile strength was observed between the study and control groups.⁷

In addition to serving as adhesives and sealants, gel-forming copolyesters of PEG can serve as promoters of vascular graft integration with surrounding tissues. Previous studies of small-diameter vascular grafts have shown unacceptable patency rates that significantly limit their widespread use. It has been postulated that transmural infiltration of microvessels through the interstices of graft materials could lead to improved endothelialization of the graft lumen.¹¹ This, in turn, could lead to improved healing, decreased thrombogenesis, and higher patency rates.

In a study by Trudel and co-workers, sample disks of vascular grafts made from expanded polytetrafluoroethylene (ePTFE) were impregnated with either a PEG-based gel-forming copolyester alone or with gel-former plus a microparticulate cation exchanger.¹² These samples as well as unmodified ePTFE disks (control group) were implanted subcutaneously and within the epididymal fat of rats. Four weeks after implantation, the sample disks were retrieved, fixed, stained, and assessed histologically. The number of microvessels present on the inside of the implants (neovascularization) was then quantified. Compared to the controls, the disks impregnated with gel-former alone or in conjunction with the microparticulate cation exchanger exhibited significantly greater neovascularization. The researchers postulate that this increase in neovascularization could promote higher patency rates in small-diameter vascular grafts.¹²

Recent studies have shown that antagonists of β_3 and α_v integrins can limit smooth muscle cell migration into the lumen of vascular grafts. This migration of smooth muscle cells is thought to play a significant role in restenosis of vascular grafts.¹³ It seems that gel-forming copolyesters of PEG would be an ideal system for study as they could serve as an absorbable synthetic carrier that would allow for local delivery of such integrin antagonists as well as promote the formation of microvessels around vascular grafts. Further study is currently being conducted.

The demonstrated desirable effects on wound healing that these absorbable gel-forming liquid polymers exhibited led to the exploration of these materials as adjuvants to assist the healing of burn wounds and ulcers.^{6,7} Kline and co-workers studied the effect of the gel-formers on burn wound healing in rats.¹⁴ Thus, CD hairless rats were premedicated, and a burning device (heated to 100°C), developed by the researchers, was used to achieve second or third degree burns. The burning device was applied to the skin 2 cm lateral to the dorsal midline of the rat and held in place for 20 sec (a time period which was shown in pilot studies to create a third degree, full thickness burn). Each rat received two such burns. One burn was left as an untreated control, and the other was treated by applying 250 μ L of a PEG-based gel-former. Three groups were designated for this study: group 1 received a single application of a low viscosity gel-former; group 2 received a single application of a high viscosity gel-former; and group 3 received weekly applications of a high viscosity gel-former. The healing wounds were

observed and evaluated on a weekly basis, and photographs were taken. Attention was paid to the area and width of the healing zone at the edge of the burn. Pictures were evaluated visually and using image analysis to quantify differences in healing rates. At 3 weeks the rats were euthanized, and the healed burn wounds were harvested and processed for histological examination. The researchers made several observations. For one, the tendency for granulation was found to be higher in the treated wounds compared to controls as early as within the first week. From week 2 to week 3, there was a noticeable decrease in the burn area, which was more noticeable with the treated sites as compared to the controls. At 3 weeks, signs of hypertrophy, noted in the control groups, were hardly detectable in treated sites. When comparing the low to high viscosity gel-formers, researchers found that the high viscosity gel-formers contribute to a faster rate of healing than the low viscosity ones. Furthermore, weekly administration of the high viscosity gel-former was the most effective therapy, achieving a higher rate of healing, a minimum degree of hypertrophy, and the largest reduction in wound area.¹⁴

4.2.3 Advances in the Applications of Controlled Delivery Systems and Clinical Relevance

PEG-based copolyesters possess the ability to serve as absorbable controlled release carriers for a whole host of bioactive agents.⁵ The ability to provide a means of local therapy with systemically toxic agents directly at the site of interest has heightened awareness of these PEG-based systems. In addition, since these copolymers are absorbable, they allow for local drug delivery without the inherent risks associated with permanent foreign bodies. Some applications of the PEG-based systems include, but are not limited to, antibiotic formulations for osteomyelitis, controlled release of vaccines, intravaginal delivery of misoprostol, periodontal application of antibiotics, and intraocular drug delivery.

4.2.3.1 Controlled Release Systems for Treating Osteomyelitis

Infection of bone, known as osteomyelitis, remains one of the most serious clinical complications associated with open reduction and internal fracture fixation. Conventional intravenous therapy with systemic antibiotics is the major modality of treatment employed by clinicians, but such therapy has inherent drawbacks. Long-term intravenous therapy often requires the use of indwelling intravenous lines which have the potential for serious morbidity including line infections and deep venous thromboses. In addition, dosing of the antibiotics may be as often as several times per day, which can lead to a decrease in patient compliance as well as increased risk of infection. Additionally, many systemic antibiotics have relatively narrow therapeutic windows, and their potential for toxicity requires close clinical monitoring. But even when drug toxicity and line-related complications are avoided, treatment of such infections has a less-than-impressive success record.^{15,16}

Increased recognition of the drawbacks of systemic therapy for osteomyelitis has led to a growing interest in controlled drug delivery systems aimed at specific pathological sites.^{17,18} Poly(methyl methacrylate) (PMMA) beads impregnated with antibiotics have been used clinically for several years to treat osteomyelitis.¹⁹ However, a number of investigators expressed concern regarding the nonbiodegradability of PMMA beads and the need for their surgical removal at the conclusion of their functional life.²⁰ This led others to explore the efficacy of controlled delivery systems based on absorbable polyesters in the form of solid microcapsules, which were later acknowledged to have their own clinical limitations. These limitations and the inherent risks to systemic therapy provided incentive to utilize novel, absorbable, hydrogel-forming carriers as a means for local drug delivery.⁵

In one study, gel-former formulations based on liquid, absorbable copolyesters described previously were loaded with vancomycin in one set and gentamicin in another.^{20,5} For the *in vivo* portion of the study, vancomycin-loaded formulations were implanted near an incised area of a healthy tibia in goats. The antibiotic formulation (typically 3.5 ml., 10% drug loading) was injected onto the surface of the incised periosteum. The subcutaneous tissue and outer layers were closed with continuous and interrupted sutures, respectively. Systemic drug levels were determined at various time periods, and drug levels in bone were measured at the time of euthanasia. Researchers found that large and moderate vancomycin doses did not lead to toxic drug levels in goat blood. In addition, discernible vancomycin levels were present in the bone itself for at least 2 weeks postoperatively and in the area about the tibial site for at least 4 weeks.

In vitro studies were carried out on both vancomycin and gentamicin using the same gel-forming system and a continuous flow system which simulated the biological environment. The release profiles of both antibiotics were strikingly different. While about 70% of vancomycin was released in 2 weeks, only about 10% gentamicin was released during this same period. More importantly, gentamicin continued to release slowly but steadily for at least 10 more days. This study concluded that PEG-based, injectable, gel-forming formulations can serve as vehicles for the controlled delivery of antibiotics, both for future treatment and prevention of osteomyelitis. Potentially, the release profiles of gentamicin and vancomycin justify the prediction of using a combination of the two antibiotics as a unique two-to-three-month controlled release system.²⁰

4.2.3.2 Controlled Release of the Recombinant Protective Antigen Form of Anthrax Vaccine

Anthrax is an acute bacterial infection caused by the bacteria *Bacillus anthracis*. The distribution of the disease is worldwide. And while all animals are susceptible to infection, the disease is most commonly encountered in domestic herbivores. In such animals, the disease tends to be severe with a high mortality rate. It is difficult to determine the actual worldwide preva-

lence of this disease in humans, but estimates as high as 100,000 cases per year have been made.²¹ Active immunization is accomplished through the use of killed vaccine derived from a component of the bacteria's exotoxin. The vaccine is administered by three injections during a 2-week period, followed by a three-booster inoculation.²²⁻²⁴ Availability of a relatively safe recombinant form of the vaccine, known as recombinant protective antigen (r-PA), and growing interest in one-shot immunization justified the search for novel injectable, absorbable, gel-forming copolyesters to serve as controlled delivery systems,^{5,25-27} the goal being the achievement of satisfactory anthrax immunization in a single- (or perhaps double-) shot controlled release system utilizing r-PA.

In a study by Corbett and colleagues, a series of polymeric gel-formers were evaluated to select an optimum gel-former to use as a carrier of different dosages of r-PA.²⁸ The liquid gel-formers were prepared by the copolymerization of polyethylene glycol 400 with a mixture of trimethylene carbonate and glycolide.^{5,27} Next, an absorbable cation exchanger was prepared by the polymerization of glycolide in the presence of a hydroxy acid initiator.⁵ A number of controlled release formulations were prepared composed of the gel-former with and without microencapsulated and/or immobilized r-PA on the absorbable cation-exchanger. Immunization of different sets of mice with the experimental controlled release systems was performed, and monitoring of the corresponding antibody titres was done and compared against titres from suitable vaccine controls. The researchers concluded that two doses of the microencapsulated r-PA in the gel-former (or conceivably a large single dose) was a viable system for securing prolonged immunity. The researchers postulated that a single large dose of r-PA may be deposited on two or three different carriers in order to provide two or three consecutive releases at two or three slightly overlapping intervals.²⁸

4.2.3.3 PEG-Based Controlled Release System for Cervical Ripening

Prolonged labor in the setting of an unfavorable cervix can lead to maternal and fetal complications. As such, pharmacological intervention is often employed in an effort to "ripen" the cervix and facilitate a vaginal delivery. The use of prostaglandins for labor induction through intracervical and intravaginal administration is well documented.²⁹ Recently, interest in misoprostol has grown considerably because of its superior clinical efficacy, its ease of administration, and its marginal cost.^{29,30} The most desirable effects of misoprostol are achieved using low dosages and frequent dosing intervals. This has obvious practical limitations in the laboring patient. As such, exploration into a single-dose, intravaginal, controlled release system for the delivery of misoprostol has been undertaken.³¹ Such a system is designed to optimize the safety and efficacy of misoprostol by providing a predictable release profile.

In a study by Allan and co-workers, pregnant Sprague-Dawley rats were selected for *in vivo* evaluation of PEG-based gel formulations containing

misoprostol at two different dosages.³¹ The effect of the gel-formers on cervical ripening was evaluated at 14 and 19 days of a 22-day gestation period. For both time periods, four groups were established with two rats per group: untreated control, placebo gel-former, gel-former containing 625 $\mu\text{g}/\text{mL}$ misoprostol, and gel-former containing 125 $\mu\text{g}/\text{mL}$ misoprostol. Of the formulations, 100 μL aliquots were administered to each rat intravaginally to the point where the vagina meets the cervix. Rats injected at 14 days of gestation were euthanized at 48 h after administration of the formulations. Rats injected at 19 days of gestation were euthanized at 24 h after administration. The cervix of each rat was harvested. One cervix per group was fixed and prepared for histological evaluation. The remaining cervix in each group was wrapped in saline-soaked gauze and immediately transported to the laboratory for mechanical testing. Cervical ripening involves a breakdown of collagen crosslinks which renders the tissue more compliant. Therefore, the modulus of elasticity was selected as the parameter most indicative of cervical ripening. Testing was accomplished using a method similar to that used for testing o-rings. Force vs. displacement curves were collected for each test cervix, and the strength, modulus, and elongation at break were calculated. In the group treated at 19 days, cervical tissue exposed to gel-formers containing misoprostol was found to exhibit a lower modulus of elasticity than those in the placebo and control groups. Additionally, the decrease in modulus was independent of the amount of misoprostol incorporated in the gel-former. Histological analysis of the cervical tissue corroborated the mechanical test results. More compliant tissue had a more loosely organized collagen structure as compared to the densely packed collagen of the untreated controls. The results of the groups treated at 14 days were not as decisively clear. Scattered results in this group were felt to be due to administration of the formulation too early in the gestation period or perhaps to testing at 48 h posttreatment instead of 24 h.³¹

4.2.3.4 Absorbable Gel-forming Doxycycline Controlled Release System for Nonsurgical Periodontal Therapy

The term periodontitis refers to a major inflammatory disease affecting the periodontal apparatus of the teeth. Most forms of periodontitis are believed to be the direct result of growth and accumulation of oral microorganisms.³² Periodontitis is known to destroy the tissues at the level of the periodontal attachment, which leads to the formation of a periodontal pocket. Therapy for this destructive process is aimed at halting the progression of the disease by reducing the etiologic factors below the threshold capable of producing damage. This allows the repair of the affected site and stabilization of periodontal attachments. Approaches to this end have included scaling and root planing, surgical therapy, pharmacological therapy, and periodontal regeneration.³²

Antibiotic therapy can play a primary or adjunctive role in the management of periodontitis.³³ A number of researchers have evaluated the use of

antibiotics in controlled delivery systems aimed at halting the progression of periodontitis.^{34–36} Such systems have utilized a host of antibiotics which have had variable success and several notable drawbacks. A doxycycline, solid-forming solution in *N*-methyl-pyrrolidone was shown to cause tissue irritation, tetracycline-loaded fiber inserts were found to be mechanically painful, and metronidazole formulations exhibited unacceptably fast release profiles.^{32,34,35,37}

The shortcomings of the current therapies prompted the study of PEG-based absorbable, gel-forming, controlled release systems for the administration of doxycycline for nonsurgical periodontal therapy.³² In one study, gel-forming polyesters were formulated as previously described.⁵ The liquid gel-former was then mixed with polyglycolic acid microparticles and doxycycline at about 15 to 20% and 12 to 17%, respectively. The release profile was monitored over 200 h using a continuous flow system designed to simulate conditions in the periodontal pocket. Researchers found that the cumulative release profile of this formulation demonstrated a sustained release over at least 200 h. Furthermore, the results also indicated that the antibiotic could be available at concentrations well above the expected therapeutic threshold.³² Clinical studies are currently being conducted and are very promising.

4.2.3.5 Gel-Forming Polyesters for Intravitreal Therapy for Cytomegalovirus (CMV) Retinitis

CMV, a member of the herpes virus family, is known to infect anywhere from 40 to 100% of the population, depending on geographics, age, socioeconomic class, and sexual orientation. The virus remains latent after the primary infection and becomes reactivated in immunocompromised hosts.³⁸ Reactivation of CMV disease in such patients can lead to end-organ damage such as retinitis, esophagitis, pneumonitis, adrenalitis, colitis, encephalitis, and radiculopathy.³⁹ Retinitis, however, is the most common clinical consequence of CMV disease.⁴⁰ Before the acquired immunodeficiency syndrome (AIDS) epidemic, the greatest number of cases of CMV retinitis was reported to have occurred in renal transplant patients receiving a host of immunosuppressive medications.^{41,42} Now, however, CMV retinitis occurs almost exclusively in AIDS patients whose CD4⁺ counts have fallen to less than 100 per μL .^{40,43}

For many years, intravenous antiviral therapy was the only means to combat CMV retinitis. Agents such as ganciclovir, foscarnet and, most recently, cidofovir work by decreasing viral replication by inhibiting CMV DNA polymerase.⁴³ Each of the agents has been shown to be efficacious in delaying the progression of CMV retinitis, but each is associated with its own significant toxicities and drug interactions that limit its use. Furthermore, the need for an indwelling catheter for intravenous therapy increases one's risk of catheter-related infection and complications. Because of these

drawbacks, there have been efforts to develop effective local therapy to combat CMV retinitis.

Local treatment modalities include intravitreal injections of antiviral agents, implantable, nonabsorbable systems, and absorbable sustained release preparations, including PEG-based systems. Intravitreal injections of antivirals have been employed by numerous researchers with very encouraging results, but because of the rapid drug clearance of many antiviral medications, single intravitreal injections often do not sustain intravitreal drug levels long enough to have a substantial therapeutic effect.⁴⁴⁻⁵⁶ Simply increasing the dose of medication may maintain higher drug levels in target tissues, but often at the expense of toxicity. As a result, multiple and frequent injections are required which increase the risk of complications and infection.

Nonabsorbable intraocular implants releasing ganciclovir have been the mainstay of therapy, but they require surgical procedures for both implantation and removal.³⁸ This prompted researchers to look for absorbable systems that could achieve sustained drug release but did not require extensive surgery to be employed. Absorbable, gel-forming PEG-based copolyesters described by Shalaby seemed the ideal system for such an application.⁵ These copolyesters are liquids at room temperature that can be injected into the intravitreal space with a simple syringe needle. When exposed to the aqueous environment of the intravitreal space, these polymers transform into soft, flexible gels. In a study by Shalaby and colleagues examining the effect of a ganciclovir-loaded gel-forming system in the rabbit vitreous space, neither the drug-free gel-formers nor their active formulations (which contained up to 10% ganciclovir) caused discernible adverse effects upon intravitreal space during the 4-week study period.⁵⁷ Furthermore, *in vitro* and *in vivo* release studies indicated that these carriers can be used for controlled drug release for at least 2 weeks. Ongoing activity is focusing on optimizing the composition of the gel-former to prolong the release profile beyond 2 months.

4.3 Advances in Solid PEG-Based Copolyesters

This group of copolyesters can be prepared by:

- Grafting high molecular weight solid PEG with relatively medium or large amounts of cyclic monomers, such as those used in preparing absorbable polyesters
- Grafting low molecular weight solid PEG with relatively large amounts of cyclic monomers, which are known precursors of absorbable polyesters

- Interlinking hydroxy-terminated, low molecular weight polyesters with polyethylene glycol using dicarboxylic acid anhydride and a carbodiimide. Almost all of the solid PEG-based copolyesters were developed for use as carriers for the controlled release of bioactive agents.

4.3.1 Alternating Multiblock Copolymers in Wound Healing Compositions

Alternating multiblock copolymers composed of short blocks of polyethylene-oxide (PEO) and poly- ϵ -caprolactone (PCL) or poly-*L*-lactic acid (PLLA) were synthesized by a coupling reaction.⁵⁸ The block copolymers of relatively high molecular weights ($M_n > 20,000$ Da) formed a physically crosslinked thermoplastic network, while low molecular weight polymers were water-soluble. The block copolymers demonstrated solubility in a variety of solvents including acetone, tetrahydrofuran, methylene chloride, dioxane, water/acetone mixtures, and water/ethanol mixtures. The degree of swelling, optical transparency, and mechanical property of the films, prepared by a solvent casting method, were affected by the nature of the hydrophobic block used, polymer composition, temperature, and thermal history. When PEO/PLLA multiblock copolymers were applied as a wound-healing material loaded with basic fibroblast-derived growth factor (bFGF), the data from a feasibility study showed improved wound healing when compared to copolymer placebo and no-treatment controls. This led to the suggestion that a certain degree of the bioactivity of bFGF is preserved.⁵⁸

4.3.2 Nanospheres of PEG-Polycaprolactone A-B Block Copolymer as a Novel Drug Carrier

Amphiphilic diblock polymeric nanospheres composed of methoxy polyethylene glycol (MePEG) and poly- ϵ -caprolactone (PCL) were prepared for application as a novel drug carrier.⁵⁹ MePEG/PCL nanospheres were obtained that exhibited an average diameter of less than 200 nm with narrow size distribution, a relatively high drug-loading efficiency of about 41.98 and 20.8% for indomethacin and paclitaxel, respectively. Cytotoxicity of the nanospheres was studied using the normal human fibroblast, the median lethal dose (LD_{50}), and various organ toxicities using male ICR mice. The indomethacin-loaded nanospheres showed higher cell viability than indomethacin in the cytotoxicity test using 3-(4,5-dimethylthiazol-2-yl)-2,5-diphenyl tetrazolium bromide (MTT) assay. The LD_{50} of MePEG/PCL nanospheres determined by the Litchfield-Wilcoxon method was 4.47 g/kg. After the mice were intraperitoneally injected with MePEG/PL nanospheres at a half-dose level of LD_{50} for 7 days, no significant histopathologic changes were observed in MePEG/PCL nanospheres-treated mice compared with

normal mice as per the light and electron microscopic observations of various critical organs such as the heart, lung, liver, and kidney.⁵⁹

4.3.3 Copolyether-Ester Block Copolymers for Thermo-Responsive Controlled Delivery Systems

Stimuli-sensitive polymeric systems can change their volume and shape reversibly according to various physicochemical factors, such as pH and temperature. Kim and co-workers prepared copolymeric thermoresponsive nanospheres of polyether-ester block copolymers comprising a central polyethylene glycol (PEG)/polypropylene glycol (PPG)/polyethylene glycol (PEG) block copolymer (PEG-PPG-PEG, or Pluronic) and poly- ϵ -caprolactone as the terminal blocks and demonstrated their effectiveness as a thermoresponsive vehicle for the controlled release of indomethacin.⁶⁰ These are amphiphilic block copolymers composed of relatively hydrophilic PEG-PPG-PEG block copolymer (Pluronic) and poly- ϵ -caprolactone with hydrophobic character. They were synthesized by ring-opening polymerization of ϵ -caprolactone in the presence of PEG-PPG-PEG block copolymer using stannous octanoate as a catalyst. Pluronic/PCL block copolymeric nanospheres with core-shell structure were prepared by a dialysis method. They were shown to have an average diameter of 116 to 196 nm, depending on the type of copolymer. The Pluronic/PCL block copolymeric nanospheres exhibited a reversible change of size depending on the temperature. The release profile of indomethacin from Pluronic/PCL block copolymeric nanospheres also showed temperature dependence and a sustained release pattern. In addition, cytotoxicity tests revealed that these indomethacin-loaded Pluronic/PCL nanospheres would remarkably reduce the cell damage compared to the unloaded free indomethacin.⁶⁰

4.3.4 Radioisotope-Bearing Poly(Ethylene Glycol-*b*-Caprolactone) (PEG-PCL) for Bone Imaging

Bone imaging has been a potential and useful tool for prompt diagnosis of osteomyelitis, septic arthritis, and myeloma. This led Park and co-workers to develop radioisotope-carrying PEG-PCL copolymeric micelles for targetable bone imaging without nonspecific phagocytosis.⁶¹ Thus, diamine-PEG, which has two terminal amino groups, was used to conjugate both PCL and ligands for specific radioisotopes. PCL was conjugated to one amino group of diamine-PEG by using dicyclohexylcarbodiimide (DCC) as a coupling agent. Hydroxyphenylpropionic acid (HPP), diethylenetriamine pentaacetic acid (DTPA), and mercaptoacetyl glycine glycidyl glycine (MAG3), as ligands for specific radioisotopes were coupled to the second amino group of diamine-PEG.⁶¹ Formation of ligand-conjugated block copolymers, critical micelle concentration (CMC) of the copolymers, hydrodynamic radii, and morphology of the micelles were investigated. The ¹²⁵I-labeling efficiency

and biodistribution of the micelles were examined. PEG-PCL block copolymer micelles demonstrated CMC of 25 mg/L and size of 60 nm, which may be adequate for blood vessel and bone imaging. ^{125}I -labeling efficiency was above 90% and was more stable in human serum for 24 h. ^{125}I -labeled polymeric micelles showed higher blood maintenance and bone uptake when compared to stannous colloid, used as a control. A noticeable decrease in liver or spleen uptake could be achieved by the micelles. Therefore, a radioisotope carrying the PEG-PCL micelle system was suggested as a useful tool for effective diagnostic bone targeting and imaging.⁶¹

4.3.5 *In Situ* Crosslinkable PEG-Based Copolymers for Protein Controlled Delivery

In contrast to the gel-forming liquids discussed in Section 4.2, Qiu and co-workers developed water-soluble solid PEG-based copolymers capable of *in situ* covalent crosslinking in an aqueous solution to form a novel hydrogel.⁶² Thus, a new polyethylene-based copolymer containing multiple thiol (-SH) groups was crosslinked *in situ* to form a polymer hydrogel under mild conditions. No organic solvent, elevated temperature, or harsh pH is required in the formulation or patient administration processes. This makes the gel precursor particularly useful for delivery of fragile therapeutics, such as proteins. The *in vitro* release of fluorescein-labeled bovine serum albumin and the *in vivo* release of the model proteins, erythropoietin, RANTES, and three PEG-conjugated RANTES derivatives showed sustained release for 2 to 4 weeks and demonstrated prolonged biological activity of the released proteins in animals.⁶²

4.4 Photopolymerizable PEG-Copolyesters

Sawhney and co-workers prepared a series of PEG-co-poly(α -hydroxy acid) diacrylate macromers and investigated their photopolymerization into crosslinked bioerodible hydrogels.⁶³ Certain types of these hydrogels were evaluated for use in preventing postsurgical adhesion and vascular restenosis.^{64,65}

Kim and colleagues copolymerized a number of PEGs with oligomers of *dl*-lactic acid and terminated the resulting copolymer with an acrylate group to form photopolymerizable macromers.⁶⁶ The resulting crosslinked polymers were evaluated as biodegradable lubricants for stainless steel needles and a potential substitute for the nonabsorbable silicones used presently.

4.5 Conclusion and Perspective on the Future

Traditional methods of macromolecular chain design can be used effectively to tailor-make novel copolymers with unique physicochemical and biological properties, using highly biocompatible polymers such as polyethylene glycol as a building block. Having absorbable, injectable gel-forming liquids represents a major milestone in the use of polymers for the development of minimally invasive, controlled-release devices for a broad range of bioactive agents. Equally important is the potential application of these liquids in the biomedical field as such, or as part of a traditional device. The photopolymerizable PEG-system does represent another class of copolymers with great potential in biomedical and pharmaceutical applications.

References

1. Harris, J. M., Introduction to biotechnical and biomedical applications of poly(ethylene glycol), in *Poly(ethylene glycol) Chemistry: Biotechnical & Biomedical Applications*, Harris, J. M., Ed., Plenum Press, New York, 1992, 1.
2. Merrill, E. W., Poly(ethylene oxide) and blood contact, a chronicle of one laboratory, in *Poly(ethylene glycol) Chemistry: Biotechnical & Biomedical Applications*, Harris, J. M., Ed., Plenum Press, New York, 1992, 199.
3. Perciaccante, V. A. and Landi, H. P., U.S. Patent No. 4,047,533, 1991.
4. Herbert, C. B., Hernandez, A. M. and Hubbel, J. A., Platelet adhesion to polyurethane blended with polytetramethylene oxide, *Biotechnol. Bioeng.*, 52, 81, 1996.
5. Shalaby, S. W., Self-Solvating Absorbable Polyester Copolymers, and Methods for Use Thereof, U.S. Patent (to Poly-Med, Inc.), U.S. Patent No. 5,612,052, 1997.
6. Shalaby, S. W., Fibrous materials for biomedical applications, in *High Technology Fibers: Part A*, Lewin, M. and Preston J., Eds., Marcel Dekker, New York, 1985, 87.
7. Allan, J. M., Kline, J. D., Wrana, J. S., Flagle, J. A., Corbett, J. T. and Shalaby, S. W., Absorbable gel forming sealants/adhesives as a staple adjuvant in wound repair, *Trans. Soc. Biomater.*, 22, 374, 1999.
8. Flagle, J., Kline, J. D., Allan, J. M., Dooley, R. L. and Shalaby, S. W., Absorbable tissue adhesives in skin wound repair, *Trans. Soc. Biomater.*, 22, 373, 1999.
9. Linden, C. L., Jr. and Shalaby, S. W., Absorbable Tissue Adhesive, U.S. Patent No. 5,350,798, 1994.
10. Linden, C. L., Jr. and Shalaby, S. W., Performance of modified tissue adhesives for soft and hard tissue, *J. Biomed. Mater. Res., Appl. Biomater.*, 38(4), 337, 1997.
11. Clowes, A. W., Kirkman, T. R. and Reidy, M. A., Mechanisms of arterial graft healing: rapid transmural capillary ingrowth provides a source of intimal endothelium and smooth muscle in porous PTFE prostheses, *Am. J. Pathol.*, 123(2), 220, 1986.

12. Trudel, J., LaBerge, M., Kleinert, L. B., Patula, V. B., Williams, S. K., Shalaby, S. W. and Massia, S. P., Absorbable gel-former modulates vascular profile around ePTFE implants, *Trans. Soc. Biomater.*, 24, 179, 2001.
13. Slepian, M. J., Massia, S. P., Dehdasht, B., Fritz, A. and Whitesell, L., Beta-3 integrins rather than beta-1 integrins dominate the integrin-matrix interactions involved in post-injury smooth muscle cell migration, *Circulation.*, 97(18), 1818, 1998.
14. Kline, J. D., Gerdes, G. A., Allan, J. M., Lake, R. A., Corbett, J. T., Fulton, L. K. and Shalaby, S. W., Effect of gel formers on burn wounds using an optimized animal model, *Trans. Sixth World Biomater. Congr.*, III, 1092, 2000.
15. Armstrong, E. P. and Rush, D. R., Treatment of osteomyelitis, *Clin. Pharmacol.*, 2(3), 213, 1983.
16. Gentry, L. O., Antibiotic therapy for osteomyelitis, *Infect. Dis. Clin.*, 4(3), 485, 1990.
17. Dunn, R. L., Polymeric matrices, in *Polymeric Drugs and Drug Delivery Systems*, Dunn, R. L. and Ottenbrite, R. M., Eds., ACS Symposium Series 467, American Chemical Society, Washington, DC, 1990.
18. Shalaby, S. W., Ed., *Biomedical Polymers: Designed to Degrade Systems*, Hanser Publishers, New York, 1994.
19. Calhoun, J. H. and Mader, J. T., Antibiotic beads in the management of surgical infections, *Am. J. Surg.*, 157(4), 443, 1989.
20. Corbett, J. T., Kelly, W., Farris, H., Fulton, L., Jerome, J. E., Kline, J. D., Allan, J. M. and Shalaby, S. W., Absorbable gel-forming system for controlled release of vancomycin for treating osteomyelitis, *Trans. Soc. Biomater.*, 21, 341, 1998.
21. Holmes, R. K., Diphtheria, Other corynebacterial infections, and anthrax, in *Harrison's Principles of Internal Medicine*, Isselbacher, K. J., Braunwald, E., Wilson, J. D., Martin, J. B., Fauci, A. S. and Kasper, D. L., Eds., McGraw-Hill, New York, 1994, 628.
22. Knudson, G. B., Treatment of anthrax in man: history and current concepts, *Mil. Med.*, 151(2), 71, 1986.
23. LaForce, F. M., Anthrax, *Clin. Infect. Dis.*, 19(6), 1009, 1994.
24. Turnbull, P. C., Anthrax vaccines: past, present, and future, *Vaccine*, 9(8), 533, 1991.
25. Corbett, J. T., Jerome, J. E., Allan, J. M., Kelley, W., Kline, J., Farris, H., Fulton, L. and Shalaby, S. W., *In vitro* and *in vivo* release of vancomycin and gentamicin from an injectable absorbable gel-forming matrix for treating osteomyelitis, *Mater. Res. Soc.*, 351, 1997.
26. Ivins, B. E., Welkos, S. L., Knudson, G. B. and Little, S. F., Immunization against anthrax with aromatic compound-dependent (aro-) mutants of *antracis subtilis* that produce anthrax protective antigen, *Infect. Immunol.*, 58(2), 303, 1990.
27. Shalaby, S. W., Final Report on National Institutes of Health Grant No. 1R43AI43128-01, entitled Controlled Delivery System for Anthrax Vaccine, April 23, 1999.
28. Corbett, J. T., Kende, M., Kline, J. D., Allan, J. M., Lake, R. A., Yan, C. and Shalaby, S. W., Controlled release of recombinant protective antigen (r-PA) form of anthrax vaccine, *Sixth World Biomaterials Congress, Trans Soc. Biomater.*, II, 766, 2000.
29. Bugalho, A., Bique, C., Machungo, F. and Faundes, A., Low dose vaginal misoprostol for induction of labor with a live fetus, *Int. J. Gynecol. Obstet.*, 49(2), 149, 1995.

30. Liggins, G. C., Controlled trial of induction of labor by vaginal suppositories containing prostaglandin E₂, *Prostaglandins*, 18(1), 167, 1979.
31. Allan, J. M., Shalaby, W. S., Corbett, J. T., Hamel, K. P., Gerdes, G. A., Anneaux, B. L., Fulton, L. K. and Shalaby, S. W., Preliminary study on controlled release system for cervical ripening, *Trans. Soc. Biomater.*, 23, 785, 2000.
32. Salz, U., Bolis, C., Radl, A., Rheinberger, V. M., Carpenter, K. A. and Shalaby, S. W., Absorbable gel-forming doxycycline controlled system for non-surgical periodontal therapy, *Trans. Soc. Biomater.*, 24, 294, 2001.
33. Slots, J. J., *Bacteroides gingivalis*, *bacteroides intermedius*, and *actinomycetemcomitans* in human periodontal disease, *Clin. Periodontol.*, 15(2), 85, 1988.
34. Dunn, R. L. et al. U.S. Patent No. 4,938,763, 1990.
35. Killoy, W. J. et al., Periodontal Disease Management, *American Academy of Periodontology*, Chicago, IL, 1993.
36. Okuda, K., Wolff, L., Oliver, R., Osborn, J., Stoltenberg, J., Bereuter, J., Anderson, L., Foster, P., Hardy, M., Aeppli, D., et al., Minocycline slow-release formulation effect on subgingival bacteria, *J. Periodontol.*, 63(2), 73, 1992.
37. Polson, A. M., Southard, G. L., Dunn, R. L., Yewey, G. L., Godowski, K. C., Polson, A. P., Fulfes, J. C. and Laster, L., Periodontal pocket treatment in beagle dogs using subgingival doxycycline from a biodegradable system. I. initial clinical responses, *J. Periodontol.*, 67, 1176, 1996.
38. Shalaby, M. and Shalaby, S. W., Intravitreal treatment of cytomegalovirus retinitis and need for controlled release systems, in *Tailored Polymeric Materials for Controlled Delivery Systems*, McCulloch, I. and Shalaby, S. W., Eds., ACS Symposium Series, American Chemical Society, Washington, DC, 1998.
39. Friedberg, D. N., Cytomegalovirus retinitis: diagnosis and status of systemic therapy, *J. AIDS Hum. Retrovirol.*, 14(1), S1, 1997.
40. Hardy, W. D., Management strategies for patients with cytomegalovirus retinitis, *J. AIDS Hum. Retrovirol.*, 14(1), S7, 1997.
41. McAuliffe, P. F., Hall, M. J., Castro-Malaspina, H. and Heinemann, M. H., Use of the ganciclovir implant for treating cytomegalovirus retinitis secondary to immunosuppression after bone marrow transplantation, *Am. J. Ophthalmol.*, 123, 702, 1997.
42. Current and future therapeutic modalities, *J. Am. Optometr. Assoc.*, 68(1), 11, 1997.
43. Spector, S. A., Current therapeutic challenges in the treatment of cytomegalovirus retinitis, *J. AIDS Hum. Retrovirol.*, 14(1), S32, 1997.
44. Kirsch, L. S., Arevalo, J. F., DeClercq, E., Chavez De La Paz, E., Munguia, D., Garcia, R. and Freeman, W. R., Phase I/II study of intravitreal cidofovir for the treatment of cytomegalovirus retinitis in patients with the acquired immunodeficiency syndrome, *Am. J. Ophthalmol.*, 119, 466, 1995.
45. Henry, K., Cantrill, H., Fletcher, C., Chinnock, B. J. and Balfour, H. H., Use of intravitreal ganciclovir (dihydroxy propoxymethyl guanine) for cytomegalovirus retinitis in a patient with AIDS, *Am. J. Ophthalmol.*, 103, 17, 1987.
46. Cantrill, H., Henry, K., Melroe, N. H., Knobloch, W. H., Ramsay, R. C. and Balfour, H. H., Treatment of cytomegalovirus retinitis with intravitreal ganciclovir, *Ophthalmology*, 96, 376, 1989.
47. Cochereau-Massin, I., Lehoang, P., Lautier-Frau, M., Zazoun, L., Marcel, P., Robinet, M., Matheron, S., Katlama, C., Gharakhanian, S., Rozenbaum, W., Ingrand, D. and Gentilini, M., Efficacy and tolerance of intravitreal ganciclovir in cytomegalovirus retinitis in acquired immune deficiency syndrome, *Ophthalmology*, 98, 1348, 1991.

48. Heinemann, M. H., Long-term intravitreal ganciclovir therapy for cytomegalovirus retinopathy, *Arch. of Ophthalmol.*, 107, 1767, 1989.
49. Ussery, F. M., Gibson, S. R., Conklin, R. H., Piot, D. F., Stool, E. W. and Conklin, A. J., Intravitreal ganciclovir in the treatment of aids-associated cytomegalovirus retinitis, *Ophthalmology*, 95(5), 640, 1988.
50. Daikos, G. L., Pulido, J., Kathalia, S. B. and Jackson, G. G., Intravenous and intraocular ganciclovir for CMV retinitis in patients with AIDS or chemotherapeutic immunosuppression, *Br. J. Ophthalmol.*, 72(7), 521, 1988.
51. Diaz-Llopis, M., Chipont, E., Sanchez, S., Espana, E., Navea, A. and Menezo, J. L., Intravitreal foscarnet for cytomegalovirus retinitis in a patient with acquired immunodeficiency syndrome, *Am. J. Ophthalmol.*, 114, 742, 1992.
52. Lieberman, R. M., Orellana, J. and Melton R. C., Efficacy of intravitreal foscarnet in a patient with AIDS, *N.Engl. J. Med.*, 330, 868, 1994.
53. Diaz-Llopis, M., Espana, E., Munoz, G., Navea, A., Chipont, E., Cano, J., Menezo, J. L. and Romero, F. J., High dose intravitreal foscarnet in the treatment of cytomegalovirus retinitis in AIDS, *Br. J. Ophthalmol.*, 78, 120, 1994.
54. Kirsch, L. S., Arevalo, J. F., Chavez De La Paz, E., Munguia, D., DeClercq, E. and Freeman, W. R., Intravitreal cidofovir (HPMPC) treatment of cytomegalovirus retinitis in patients with acquired immune deficiency syndrome, *Ophthalmology*, 102, 533, 1995.
55. Taskintuna, I., Rahhal, F. M., Arevalo, J. F., Munguia, D., Banker, A. S., De Clercq, E. and Freeman, W. R., Low-dose intravitreal cidofovir (HPMPC) therapy of cytomegalovirus retinitis in patients with acquired immune deficiency syndrome, *Ophthalmology*, 104, 1049, 1997.
56. Palestine, A. G., Cantrill, H. L., Luckie, A. P. and Ai, E., Intravitreal treatment of CMV retinitis with an antisense oligonucleotide, ISIS 2922 Abstracts, *Abstracts of the 10th International Conference on AIDS*, 332B, 1994.
57. Shalaby, S. W., Final Report on Department of Defense Phase I SBIR (DAMD17-97-C-7030) entitled, Injectable absorbable ocular inserts for controlled drug delivery, July 1997.
58. Bae, Y. H., Huh, K. M., Kim, Y. And Park, K-H., Biodegradable amphiphilic multiblock copolymers and their implications for biomedical applications, *J. Contr. Rel.*, 64, 3, 2000.
59. Kim, S. Y., Lee, Y. M., Baik, D. J. and Kang, J. S., Toxic characteristics of methoxy poly(ethylene glycol)/poly(ϵ -caprolactone nanospheres; *in vitro* and *in vivo* studies in the normal mice, *Biomaterials*, 24, 55, 2003.
60. Kim, S. Y, Ha, J. C. and Lee, Y. M., Poly(ethylene oxide)-poly(propylene oxide)-poly(ethylene oxide)/poly(ϵ -caprolactone) (PCL) amphiphilic block copolymeric nanospheres: II. Thermo-responsive drug release behaviors, *J. Contr. Rel.*, 65, 235, 2000.
61. Park, Y. J., Lee, J. Y., Chang, Y. S., Jeong, J. M., Chung, J. K., Lee, M. C., Park, K. B. and Lee, S. J., Radioisotope carrying polyethylene oxide-polycaprolactone copolymer micelles for targetable bone imaging, *Biomaterials*, 23, 873, 2002.
62. Qiu, B., Stefanos, S., Ma, J., Lallo, A., Perry, B. A., Leibowitz, M. J., Sinko, P. J. and Stein, S., A hydrogel prepared by *in situ* cross-linking of a thiol-containing poly(ethylene glycol)-based copolymer: a new biomaterial for protein drug delivery, *Biomaterials*, 24, 11, 2003).
63. Sawhney, A. S., Pathlak, C. P. and Hubbel, J. A., Bioerodible hydrogels based on photo-polymerized PEG-co-poly(x-hydroxy acid) diacrylate macromers, *Macromolecules*, 26, 581, 1993.

64. Hill-West, J. L., Chowdhury, S. M., Sawhney, A. S., Pathlak, C. P., Dunn, R. C. and Hubbel, J. A., Prevention of postoperative adhesions in the rat by *in situ* photopolymerization of bioresorbable hydrogel barriers, *Obstet. Gynecol.*, 83, 59, 1994.
65. Hill-West, J. L., Chowdhury, S. M., Slepian, M. J. and Hubbel, J. A., Inhibition of thrombosis and intimal thickening by *in situ* photo-polymerization of thin hydrogel barriers, *Proc. Natl. Acad. Sci., USA*, 91, 5967, 1994.
66. Kim, B. S., Hrkach, J. S. and Langer, R., Biodegradable photo-crosslinked poly(ester-ester) networks for lubricious coatings, *Biomaterials*, 21, 259, 2000.

5

Cyanoacrylate-Based Systems as Tissue Adhesives

Shalaby W. Shalaby and Waleed S. W. Shalaby

CONTENTS

5.1	Introduction	60
5.2	Rationale for and Genesis of Synthetic Absorbable Cyanoacrylate-Based Systems	61
5.3	Unique Properties of Absorbable Tissue Adhesives and Evolution of the Cyanoacrylate-Based Systems	62
5.4	Evolution of the Evaluation Methods for Synthetic Absorbable Tissue Adhesives	64
5.4.1	Characterization of Uncured Adhesive Formulations	64
5.4.2	Effect of pH on the Molecular Weight and Thermal Properties of Absorbable Tissue Adhesives	64
5.4.3	<i>In Vitro</i> Evaluation of the Adhesive Joint Strength and Pertinent Data	66
5.4.4	Evaluation of the <i>In Vitro</i> and <i>In Vivo</i> Absorption Profiles and Typical Results	69
5.4.4.1	<i>In Vitro</i> Absorption	69
5.4.4.2	Direct Evaluation of <i>In Vivo</i> Absorption	69
5.4.4.3	Indirect Evaluation of <i>In Vivo</i> Absorption Using Radiolabeled Tissue Adhesive	70
5.4.5	Evaluation of <i>In Vivo</i> Performance of Absorbable Tissue Adhesives	72
5.4.5.1	Comparative Evaluation of V-200 Tissue Adhesive Formulations against Suture and Staple Controls	72
5.4.5.2	Comparative Evaluation of Absorbable and Nonabsorbable Tissue Adhesive	74
5.5	Conclusion and Perspective on the Future	75
	References	75

5.1 Introduction

The exceptionally fast rate of anionic polymerization of cyanoacrylates in the presence of a base, including water, made this class of monomers unique among all acrylic and vinyl monomers. Of the alkyl cyanoacrylate family of monomers, the methyl- and ethyl-esters are used extensively in industrial and consumer-type adhesives. Meanwhile, the isobutyl, *n*-butyl, and *n*-octyl cyanoacrylate esters are used clinically as blocking agents, sealants, and/or tissue adhesives in different parts of the world due to their much lower toxicity as compared to their more reactive methyl counterpart.

The length of alkyl groups of the alkyl cyanoacrylate family of monomers has a profound effect on the rate of polymerization and properties of the corresponding polymer. Thus, as the length of the alkyl group increases as in the higher homologs of methyl cyanoacrylate:

- The rate of polymerization decreases.
- The tensile strength and modulus of the corresponding polymers decrease.
- The adhesive joint strength conferred by the polymerizing monomer decreases.
- Tissue response to the monomer decreases slightly.
- Stability toward hydrolytic degradation increases substantially.

Prior to the mid-1990s, the nonabsorbable, hydrolytically stable η -butyl and isobutyl cyanoacrylates were acknowledged as the most effective type of tissue adhesive in terms of adhesive strength. They have been used as hemostatic sealants as well as blocking agents for treating vascular aneurysms. In spite of the availability of other tissue adhesives, such as gelatin-resorcinol, those cyanoacrylates retained their competitive edge because of their fast-polymerization and strength of adhesive joint. The dominance of those cyanoacrylates was recently threatened by growing interest in biodegradable biomacromolecule-based systems, such as (1) fibrin glue; (2) mussel adhesive protein; (3) prolamine gel, a biodegradable protein; and (4) transforming growth factor beta (TGF- β).¹ However, none of those adhesives could provide the adhesive joint strength required in many applications, and hence remained mostly as tissue sealants or carriers of bioactive drugs. This and the growing interest in synthetic absorbable polymers prompted Shalaby and co-workers to explore the development of the absorbable cyanoacrylate-based systems, subject of this chapter.^{2,3}

5.2 Rationale for and Genesis of Synthetic Absorbable Cyanoacrylate-Based Systems

In the past few decades, there has been a great deal of interest in using tissue adhesives in many surgical procedures in favor of sutures and staples for a variety of reasons, including:

- Ease of application and reduced clinician time
- Location of repairable site as in contoured locations
- Biomechanical properties as in weak organs, such as liver and pancreas
- Minimized hypertrophy and scar formation as in plastic surgery

However, there have also been a number of concerns associated with the alkyl cyanoacrylates. These include:

- Their low viscosity and associated difficulties in precise delivery at the application site in nonmedical and medical applications
- Poor shear strength of the adhesive joint, particularly in aqueous environments in both medical and nonmedical applications
- High modulus or stiffness of cured polymers at soft tissue application sites and associated mechanical incompatibility, which can lead to adhesive joint failure and/or irritation of the surrounding tissue
- Excessive heat generation upon application of monomers to living tissue due to exceptionally fast rate of curing resulting in necrosis
- Site infection, among other pathological complications, associated with prolonged residence of the nonabsorbable tissue adhesives

In response to these concerns, and particularly the ones associated with the nonabsorbable cyanoacrylates that are used clinically, Linden and Shalaby disclosed a novel, absorbable tissue adhesive composition that addressed, to a practical extent, the drawbacks of the absorbable bioadhesive as well as nonabsorbable cyanoacrylates.² In effect, these absorbable tissue adhesive compositions were based (1) primarily on methoxyalkyl cyanoacrylates and preferably methoxypropyl cyanoacrylate as the precursor of an absorbable tissue adhesive polymer; and (2) on a polymeric, highly absorbable, liquid comprising an oxalate ester of triethylene glycol as a modifier to modulate the viscosity of the overall composition, lower the heat of polymerization, and increase the compliance and absorption rate of the cured adhesive joint. In a more recent disclosure by Shalaby, a number of other useful modifiers were described and the functional performance of the new adhesive compositions was reported.³

The rationale for developing the synthetic absorbable cyanoacrylate-based systems was consistent with certain minimum capabilities noted by Spotnitz for an ideal tissue adhesive.¹ Accordingly, the ideal tissue adhesive should be:

- Safe and biodegradable
- Effective in terms of adherence strength, internal sealant bonding strength, hemostatic potential, tissue healing and regeneration, and infection control
- Easily usable
- Affordable
- Approvable

Other desirable features cited were that the adhesive:

- May be used on moist tissues
- Distributes evenly over tissue surface
- Forms durable bond in a few seconds between tissues to be united
- Does not cause tissue damage locally or generally
- Is not carcinogenic
- Biodegrades in a relatively short period of time

5.3 Unique Properties of Absorbable Tissue Adhesives and Evolution of the Cyanoacrylate-Based Systems

The unique properties of absorbable tissue adhesives, and particularly those based on cyanoacrylates, include:

- Their finite life and temporary physical presence at the application site with eventual absorption following expected functional performance to minimize potential site infection
- If they absorb at a predictable rate, they can be used as vehicles for controlled drug delivery (e.g., anesthetics for relieving local pain).
- They can be used internally for several surgical procedures

The design criteria used in selecting the unique cyanoacrylate-based systems entail:

- Using a more hydrophilic cyanoacrylate than the *n*-butyl and *n*-octyl cyanoacrylates that are presently used as nonabsorbable tissue adhesives — for this, alkoxyalkyl cyanoacrylates such as methox-

propyl cyanoacrylate (MPC), which spreads readily at the biological application site, was selected as the main component of the adhesive systems.

- A more hydrolytically labile cyanoacrylate than the *n*-butyl, isobutyl, and *n*-octyl cyanoacrylates to yield polymers that, under facile hydrolysis of their ester group, produce water-soluble by-products and hence meet the minimum requirement for being an absorbable polymer — for this the alkoxyalkyl cyanoacrylates were chosen.
- A cyanoacrylate with a flexible side chain to yield a more pliable polymer than those of alkyl cyanoacrylate without compromising adhesive joint strength — for this, alkoxyalkyl cyanoacrylates were selected to meet the minimum compliance required for the resulting polymer.
- An absorbable polymeric modifier that is compatible with the chosen cyanoacrylate to achieve a moderate-to-high preuse viscosity for ease of application, and to increase the absorption rate and compliance of the cured adhesive for minimizing residence time at the application site and maximizing mechanical biocompatibility — for this, highly absorbable liquid oxalate polymers, such as poly(trioxethylene oxalate) (PTOEO) and amorphous or low-melting absorbable copolyesters such as those described in Chapter 3 — polyaxial copolyesters and other copolymers based on cyclic monomers — were selected.
- A stabilizer to prevent premature anionic polymerization to meet minimum shelf-life stability, such as those noted by Shalaby.^{2,4}

Based on the design criteria noted above, the evolution of the absorbable cyanoacrylate-based system commenced with methoxypropyl cyanoacrylate (MPC) and was followed by formulation of MPC with polyether oxalate or polyester carbonate. Figure 5.1 outlines a polymerization scheme and designation of the final polymer. Both V-100 and V-150 tissue adhesives contain the same components but in different proportions.

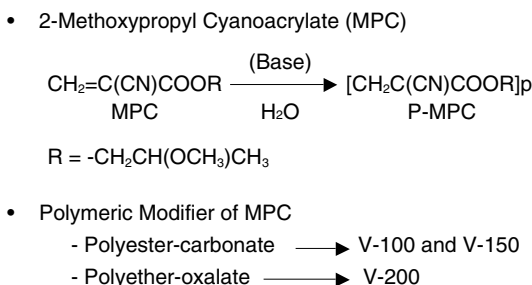


FIGURE 5.1

Chemistry of bioabsorbable tissue adhesives V-100, V-150 and V-200.

5.4 Evolution of the Evaluation Methods for Synthetic Absorbable Tissue Adhesives

As this is a new class of materials, there have been no specific methods available for their (1) characterization; (2) testing of *in vitro* adhesive strength; (3) *in vitro* and *in vivo* absorption profile; and (4) *in vivo* performance in wound repair. Accordingly, the required specific methods were developed through revising existing general ones or designing totally new ones.

5.4.1 Characterization of Uncured Adhesive Formulations

An infrared (IR) and spectroscopic proton-magnetic resonance (PMR) method was developed to determine the intact MPC content in the formulation using pure MPC as a reference. The double-bond vibrational frequency at about 1650 cm^{-1} of a liquid formulation in the IR method was used to ascertain its MPC content. Likewise, the chemical shifts of the $-\text{OCH}_3$ and $\text{C}=\text{CH}_2$ groups were used in the PMR method; CDCl_3 was used as a solvent. Rheological behavior of the liquid formulation was evaluated using a newly developed capillary method. For this, the efflux time of 1 mL of liquid through a polypropylene capillary was measured.

5.4.2 Effect of pH on the Molecular Weight and Thermal Properties of Absorbable Tissue Adhesives

In an effort to determine possible effect of pH at the application site in different clinical settings, the subject study was conducted by Bruce and co-workers using MPC as a model for absorbable tissue adhesives. Adjunct to this, the investigators compared the achievable molecular weight of polymeric MPC made under free-radical and anionic conditions. Accordingly, MPC was polymerized, in bulk, under typical free-radical polymerization conditions, as well as anionically by exposure to aqueous buffered solution at pH 6.5, 7.4, and 8.5. The anionic polymerization was intended to simulate MPC polymerization at different tissue sites. The GPC data of the resulting polymer after purification are summarized in Table 5.1. The data show that the free-radically prepared polymer has a higher M_n than the polymer formed under anionic conditions. Although the M_n of the free-radically polymerized monomer is higher than that of all of the polymers formed anionically, it is obvious that the highest M_n for the anionically polymerized monomer was achieved at the physiologic pH of 7.4. These results indicate that the pH of the application site should not be ignored in clinical usage. The M_w values for anionically polymerized monomer at pH levels of 7.4 and 6.5 were consistent with the observation of their corresponding M_n values.

TABLE 5.1

GPC Data for Free-Radically and Anionically Polymerized MPC

	GPC Data			
	M_n	M_w	M_p	PDI
Free Radical	60,600	130,200	112,800	2.15
Anionic (pH 7.4)	47,300	111,100	113,000	2.35
Anionic (pH 6.5)	36,400	72,100	93,800	1.98
Anionic (pH 8.5)	16,300	228,800	252,200	14.04

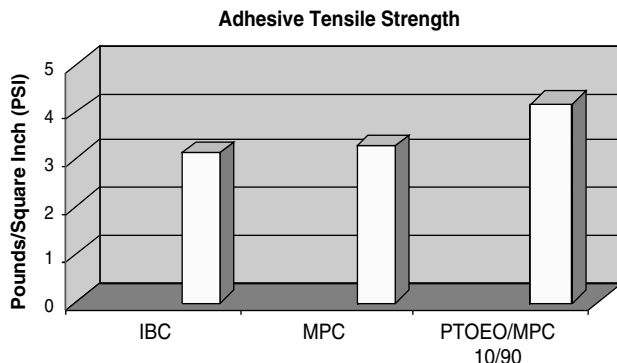
However, this was not the case for the monomer anionically polymerized at a pH of 8.5, where the M_w was found to be much higher than those at lower pH values. This could be a reflection of the propensity of the cyanoacrylate to undergo branching at high pH.

Thermal properties of the resulting polymers were determined using DSC. The resulting glass transition temperatures (T_g) and decomposition (or ceiling) temperatures (T_d) are summarized in Table 5.2 and clearly show that free-radically polymerized MPC has a higher ceiling temperature and higher stability than all of the anionically polymerized MPC samples. In addition, pH of the media appears to affect the ceiling temperature of anionically polymerized monomer. Lower ceiling temperatures were noted with polymers that were anionically formed at a pH value greater than 6.5. This may be related to low molecular weight recorded for anionically polymerized MPC samples as compared to those obtained by free-radical polymerization. This is not surprising since the concentration of end groups are higher in low molecular weight polymer and hence a higher cooperative chain motion displaying a lower T_g . Based on the preceding results, it was concluded that (1) anionically polymerized model cyanoacrylates such as MPC can produce, in general, lower molecular weight polymers than those produced by free-radical polymerization; and (2) the pH of the medium has substantial effect on average molecular weight of anionically polymerized polymers, and the pH of the application site in clinical use should be taken into consideration.⁵

TABLE 5.2

DSC Data for Free-Radically and Anionically Polymerized MPC

	GPC	
	T_g (°C)	T_d (°C)
Free Radical	54.7	246.1
Anionic (pH 7.4)	54.4	210.9
Anionic (pH 6.5)	74.6	230.2
Anionic (pH 8.5)	48.5	213.9

**FIGURE 5.2**

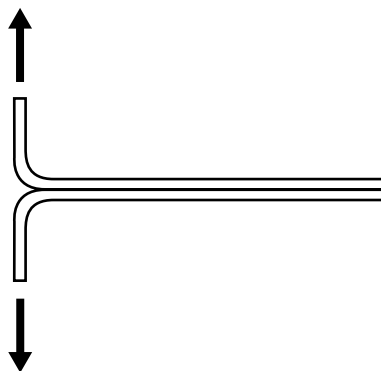
Tensile strength of adhesive joint of *in vitro* repaired goat skin.

5.4.3 *In Vitro* Evaluation of the Adhesive Joint Strength and Pertinent Data

In the first attempt in the development of absorbable tissue adhesives comprising a combination of methoxypropyl cyanoacrylate (MPC) and poly-(trioxyethylene oxalate) (PTOEO), a goatskin model was used to demonstrate *in vitro* superiority of this new tissue adhesive over the nonabsorbable adhesive isobutyl cyanoacrylate (IBC).^{2,6} Results for MPC, IBC, and a 10/90 poly(oxylineoxalate)(TOEO)/MPC are shown in Figure 5.2. The results suggest that the joint strength increases progressively for IBC and MPC to PTOEO/MPC. However, using this method for screening new candidates requires impractically large amounts of goatskin. This and the variability in the goatskin due to the location of the harvesting site on the animal, the animal's age, and storage conditions justified the need for developing new testing methods using more controllable substrates. Therefore, a study was pursued by Flagle et al. to address the development of new methods for evaluating tissue adhesives and comparison of the respective data with those obtained using the goatskin model.⁷

A brief description of the goatskin method and two new methods are noted below, followed by comparative analysis of respective results.

Goatskin Model: A layer of paraffin wax was molded into the bottom of polypropylene containers. The goatskin was dissected from the subcutaneous tissue, stretched to its original dimensions, and pinned onto the wax layer. The container was then filled with a saline solution (0.9% w/vol. NaCl and 0.05% w/vol. NaN_3) until the skin was totally submerged. The sample was stored in a freezer at -10°C . Prior to use, the sample was removed from the freezer and thawed at room temperature. The saline was poured from the container. A lint-free tissue was used to remove excess moisture. A 19-cm incision was made down the length of the sample. The skin around the incision was approximated and 400 μL of a cyanoacrylate tissue adhesive

**FIGURE 5.3**

Schematic depicting cotton fabric peel test.

was applied. After curing for 3 h, each incision was cut into test strips approximately 2 cm wide. The samples were tested in tension on an MTS Mini Bionix Universal Testing Unit (Model 858) at a strain rate of 2.5 cm/min. The tensile strength of the adhesive joint was calculated as the force required to separate the approximated edges of the skin, divided by the cross sectional area of the sample.

Nylon Peel Test: Nylon-6 films (10-mil thick) were pressed between Teflon-covered stainless steel plates on a 30-ton Carver hydraulic press at 235°C. The nylon film was then cut into 2×5 in panels, with care taken to ensure all sides were square. The panels were submerged in a phosphate buffer solution ($\text{pH} = 7.2$, $T = 25^\circ\text{C}$) for 1 h. Excess moisture was removed with lint-free tissue paper. The monomeric tissue adhesive, for example MPC, was applied to one panel, and another panel was placed on top. A $1/2 \times 5$ in portion of the panels was left unglued. The MPC was allowed to cure for 2 h. Each panel was then sectioned into smaller samples. The unglued portion was gripped into an MTS MiniBionix (Model 858) and the force required to separate the films at a displacement rate of 2.5 cm/min was measured. The average load after the initial peak was used to calculate the average peel force of the adhesive joint.

Fabric Peel Test: Samples were cut from a plain weave cotton fabric (306 g/m^2). Samples measuring $2.5 \times 8 \text{ cm}$ were cut, submerged in phosphate buffer ($\text{pH} = 7.2$), and allowed to air dry for 25 min. MPC measuring $350 \text{ }\mu\text{L}$ (used as a model for cyanoacrylate-based tissue adhesives) was spread over a $2.5 \times 6 \text{ cm}$ area of one fabric sample, and a mating sample was placed on top. A 1200-g weight was set on top of the specimen for 1 min. The specimen was then allowed to cure for 1 h. The unglued portion was gripped into an MTS MiniBionix (Model 858) and the force required to separate the films at a displacement rate of 5.0 cm/min was measured. The maximum load after the initial peak was used to calculate the peel force of the adhesive joint.⁷

TABLE 5.3

Results of Various Test Methods Using MPC as a Model
Tissue Adhesive

Test Method	Goat Tensile Test on Incision	Nylon T Type Peel Test	Fabric T Type Peel Test
Test Value	Adhesive Strength	Peel Force ^a	Peel Force ^a
Units	kN/M ²	N/m	N/m
Mean	151	1072	105
Standard Deviation	74	671	11

^a Maximum load-to-fail for 1-m sample width.

In comparing the results of the three tests, it was taken into account that the goatskin model is the closest test to the *in vivo* situation. However, there was variability in the skin and in the application of the adhesive. The nylon peel test uses a more controlled substrate. However, the force trace generated during testing was characterized by sharp peaks in the force-vs.-displacement curve instead of producing a steady peel load. This may be attributed to the stiffness of the substrate and nonuniform wetting of its surface by MPC. The fabric test provides a material which is able to absorb large quantities of the phosphate buffer and maintain a fairly constant load during testing. Results from the three tests are presented in Table 5.2. Each is a result of at least five separate data points.⁷

The results in Table 5.3 led to the conclusion that the fabric peel test (FPT) method is reproducible and provides lower variability as compared to the other two methods. Accordingly, this method was optimized in terms of curing time of V-200 (a PTOEO/MPC formulation) and adopted as an in-house standard test method. The peel force was recorded as the maximum load-to-fail in N for a sample width of 1 m. During optimization, a 15-min cure time was selected on the basis of data in Table 5.4. Typical results on absorbable and nonabsorbable formulations using the optimized FPT are summarized in Table 5.5. The peel force was recorded as the maximum load-to-fail in N, normalized to a sample width of 2.5 cm.

TABLE 5.4

Peel Force Data of V-200 Adhesive Formulation
as Measured by the Cotton Fabric Peel Test

Experiment No.	Peel Force ^a (N/m)	
	2-min Cure	60-min Cure
1	227 ± 73	93 ± 21
2	326 ± 80	842 ± 131
3	741 ± 277	801 ± 147
4	825 ± 244	1239 ± 64
5	480 ± 54	636 ± 135

^a Maximum load-to-fail for 1-m sample width.

TABLE 5.5Peel Force Data of Different Tissue Adhesives^a

Tissue Adhesive	Type	Maximum Force ^b (N)
<i>n</i> -Butyl cyanoacrylate	Nonabsorbable	37
V-100	MPC-based absorbable formulation	20
V-150	MPC-based absorbable formulation	40

^a Using the Fabric Peel Test.^b Maximum load-to-fail normalized for 2.5-cm sample width.

5.4.4 Evaluation of the *In Vitro* and *In Vivo* Absorption Profiles and Typical Results

5.4.4.1 *In Vitro* Absorption

For this study, 250 μ -thick circular discs, each having a diameter of 15 mm, were prepared by pouring the cured cyanoacrylate into a plastic template submerged in a phosphate buffer solution at pH = 7.4 and 37°C. The cured discs were dried and their dry weight was determined. Weight was determined periodically after incubating in a phosphate buffer at 37°C and pH = 7.4. Using this method, it was shown that MPC and V-200 lost $55 \pm 3\%$ and $80 \pm 4\%$ of their initial mass at 75 days. These results are consistent with the thesis that the oxalate polymer modifier accelerates the absorption rate of polymeric MPC.

5.4.4.2 *Direct Evaluation of In Vivo Absorption*

Direct and indirect methods for evaluating *in vivo* absorption were developed using the V-200 formulation.

The direct method entailed extruding the adhesive formulation into a 1.5 cm-long incision made along the fiber axis of the rat gluteal muscle. The amount of extruded liquid was adjusted to yield an implant having an average diameter of 1 mm. Standard surgical procedures were used in preparing the animal, surgical site, and in completing the procedure. At the conclusion of the predetermined period and using standard protocols, the gluteal muscle treated with the tissue adhesive was excised and prepared for histological evaluation. Reduction in the implant cross-sectional area was used as a measure of the extent of absorption. This method showed that the V-200 implant is practically absorbed in less than 56 weeks under the prevailing conditions.

The indirect method pertained to using a radiolabeled formulation and monitoring the degradation by-products as discussed in Section 5.4.4.3.

5.4.4.3 Indirect Evaluation of In Vivo Absorption Using Radiolabeled Tissue Adhesive

Prior to discussing the indirect method, a brief background and rationale is provided.

5.4.4.3.1 Background and Rationale

Absorption of polymethoxypropyl cyanoacrylate (P-MPC) modified with 5 to 10% of an oxalate polymer, in terms of mass loss in a phosphate buffer at 37°C and pH 7.4, was reported to occur between 3 and 12 months, depending on the surface-to-volume ratio of the polymer specimens.^{7,8} Although the mechanism by which P-MPC undergoes degradation is uncertain, the dependence of absorption, as measured in terms of mass loss on surface area, which takes place at unusually early periods and continues for prolonged periods, strongly suggests a continuous generation of water-soluble by-products at the specimen surface. This mode of degradation/mass loss is similar to that referred to by some authors as erosion, or delamination, as in the case of hydrophobic polyanhydride.⁹ The assumption of delaminating water-soluble by-products contradicts an early controversial claim that a polymer of the lowest member of the cyanoacrylate family of monomers, such as methyl cyanoacrylate, degrades into formaldehyde and methyl cyanoacetate.¹⁰ In an effort to shed some light on the degradation pathway of polycyanoacrylates, and, in particular P-MPC, the study to address this subject was pursued.¹¹ This entailed the preparation of ¹⁴C-labeled MPC with ¹⁴C incorporated in the terminal methylene group of the double bond, which was suggested earlier as the formaldehyde precursor.¹⁰

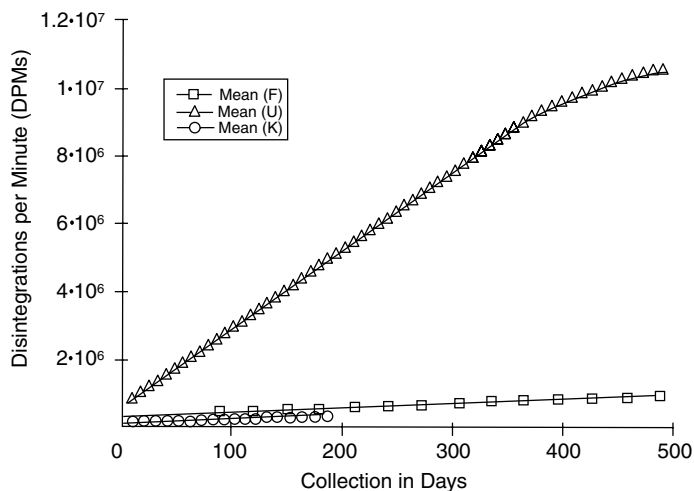
5.4.4.3.2 Outlines of the Materials and Methods Used

¹⁴Carbon-labeled MPC was prepared to have a specific activity of 1.8 μ Ci/mg.¹¹ This was mixed with pure, unlabeled methoxypropyl cyanoacrylate. The mixed MPC was mixed further with about 5%, by weight, of a liquid oxalate polymer (P-TOEO) made from diethyl oxalate and trimethylene glycol as described by Linden.⁸ Using Sprague–Dawley rats, aliquots of the MPC/oxalate polymer composition were placed, subcutaneously, in the dorsal cervical area to mediate the absorption rate. Details of the surgical procedure and methods of monitoring the release of radiolabeled by-products as well as a whole-body radiography study were reported earlier.¹¹

5.4.4.3.3 Discussion of Results and Conclusion

The cumulative amounts of generated radiolabeled by-products were detected in the expired gas, urine, and feces of the rats as depicted in Figure 5.4. The data in Figure 5.4 indicate that:

- About 80% of the initial ¹⁴C was recovered at about 16 months posttreatment.

**FIGURE 5.4**

Cumulative mean ^{14}C from rat urine (U), feces (F), and CO_2 (K).

- The majority of the radiolabeled by-products are excreted through the kidney.
- A minor and minimum fraction of the radiolabeled by-products are extracted in the feces and by expiration, respectively.
- The release profile of total radiolabeled species affected by implant location follows practically a zero order of kinetics.

Microsections resulting from a whole-body autoradiography study revealed no detectable accumulation of radiolabeled by-products in any tissue in general, and specifically the kidney and liver, during the study period, with the exception of the subcutaneous administration site.

The above results suggest strongly that no formaldehyde is formed during the absorption of this tissue adhesive, as generally claimed earlier for cyanoacrylates.¹⁰ Formaldehyde would have been incorporated and detected in body tissues other than the administration site since the only possible source of the radiolabeled by-products is the methylene group of the polymer main chain. Obviously, this disputes earlier claims that the cyanoacrylate polymers degrade by depolymerization to formaldehyde and methyl cyanoacetate. This is very unlikely to take place in the prevailing, mild biological environment. On the other hand, if formaldehyde was detected in a degrading polymethyl cyanoacrylate, it might have been an oxidation product of the methanol that forms upon hydrolysis of the highly activated methyl ester. Interestingly, if this is the case, then it is reasonable to propose that the polymethyl cyanoacrylate undergoes partial or complete hydrolysis to form a soluble species in the biologic environment. Accordingly, it is further proposed that the degradation/absorption of P-MPC takes place

through hydrolysis of the ester groups leading to a soluble, excretable polymeric chain. This is indeed consistent with the:

- Observed dependence of the P-MPC absorption or mass loss on the surface area of the polymer, which was recorded earlier in the *in vitro* studies
- Proposal that the P-MPC mass loss takes place through erosion or delamination
- The practically zero-order release kinetics for the release of the radiolabeled by-products^{7,8,11,12}

Hence, it was concluded that:

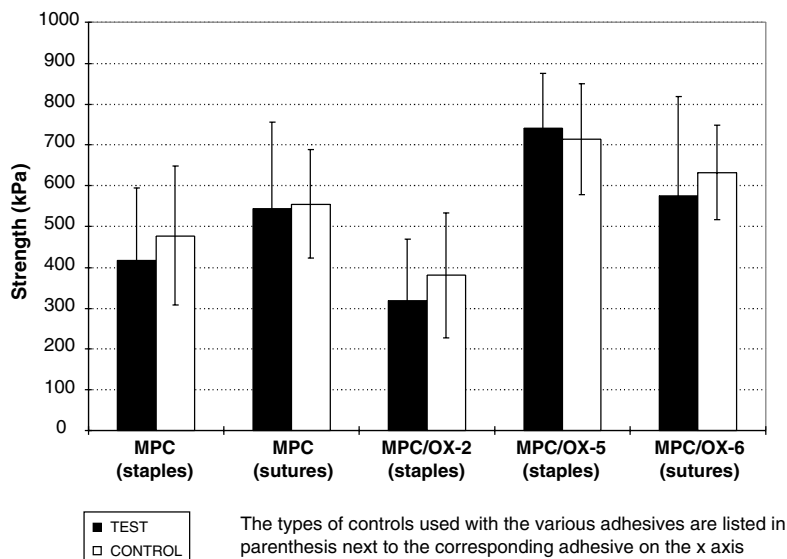
- The polymerized MPC formulation is absorbable as it releases the radiolabeled by-products in about 16 months, reflecting a similar or shorter absorption period than that determined by the direct method (Section 5.4.4.2).
- The degradation/absorption of P-MPC is not associated with formaldehyde formation.
- The P-MPC degradation is based on the hydrolysis of chain pendent ester groups and formations of water-soluble, excretable by-products.¹²

5.4.5 Evaluation of *In Vivo* Performance of Absorbable Tissue Adhesives

Using an incisional rat skin wound model, performance of absorbable tissue adhesives was compared against (1) sutures and staples; and (2) a commercial, nonabsorbable tissue adhesive.

5.4.5.1 Comparative Evaluation of V-200 Tissue Adhesive Formulations against Suture and Staple Controls

This evaluation was conducted by Flagle and co-workers.¹³ The tissue adhesive formulations were tested using an *in vivo* model in Sprague–Dawley rats (each weighing approximately 225 g). Each tissue adhesive formulation was tested on six rats. Anesthesia was induced via subcutaneous injection of 0.5 mg/kg acepromazine and 0.05 mg/kg buprenorphine; rats were maintained under anesthesia via 1.5 to 2.5% isoflurane inhalation. Once anesthetized, they were shaved and scrubbed with Nolvasan scrub. Four incisions were made on the back of each rat. Two incisions were made 2 cm lateral to the dorsal midline on each side of the rat. Each incision was approximately 3 cm long and separated by 1 cm on each side of the rat. The incisions on the left side were used as controls; these were closed with either four surgical staples or four interrupted sutures. The incisions on the right

**FIGURE 5.5**

Wound healing strength of various tissue adhesives vs. corresponding controls.

side were closed with different V-200 formulations. These were based on MPC and P-TOEO lots having variable molecular weights, and referred to as OX-2, OX-5, and OX-6. Elizabethan collars were used on the rats to prevent them from mutilating their wound sites.

At 2 weeks postoperative, rats were euthanized in a CO₂ precharged chamber. The dorsal skin from the rats was dissected from the subcutaneous tissue to remove the incisions and surrounding skin. A cut was made at the mid-point of each incision perpendicular to its length to give two test samples per incision. Healed incision strength was measured in tension using an MTS MiniBionix (Model 858) at a strain rate of 2.5 cm/min. The wound strength was calculated as the force required to separate the wound divided by the cross sectional area of the sample.

Wound healing strength data associated with V-200 and both the suture and staple controls are depicted in Figure 5.5. Due to differences among rats, the strength of the control varied from animal to animal. Therefore, each adhesive was evaluated against its corresponding control. All adhesives exhibited strengths which show no statistically significant difference as compared to the corresponding controls. Thus, the use of adhesives results in practically the same wound strength as the traditional mechanical wound closure devices, namely, sutures and staples, after a 2-week period. Hence it was concluded that:

- Methoxypropyl cyanoacrylate/poly(trioxyethylene oxalate) tissue adhesive provides an alternative to the traditional methods of wound closure.

- This tissue adhesive may be used as a stand-alone closure method or in conjunction with sutures or staples.

5.4.5.2 Comparative Evaluation of Absorbable and Nonabsorbable Tissue Adhesive

Using the ratskin incisional wound model described in Section 5.4.5.1, Corbett et al. compared the performance of the V-100 absorbable formulation against the commercial nonabsorbable tissue adhesive Nexaband®.¹⁴ The study was conducted for 9 and 15 days. The biomechanical testing results, in terms of maximum load-to-failure of healed incisions, are summarized in Table 5.6. The maximum load values at 15 days postoperative healed skin at the incision sites of the same animal appear to be practically the same (within a reasonable experimental error) for V-100 and Nexaband®. However, the preliminary results for 9-days postoperative healed incisions show a significant difference in maximum load-to-break values for wounds approximated by V-100 and Nexaband®. Incisions adjoined by V-100 showed an average maximum load value that is almost double that of Nexaband®. These results suggest that at 15-days postoperative, the two adhesives contribute similarly in supporting the regain of wound strength. However, at 9-days postoperative, the performance of V-100 far exceeds that of Nexaband® as it provides a wound strength regain comparable to those attained at 15 days. This may suggest that V-100 is associated with an exceptionally high rate of wound strength regain.

TABLE 5.6

Biomechanical Strength Testing Data of Healed Skin Wounds

Rat No.	Study Period	Average Maximum Load (N) ^a	
		Nexaband®	V-100
S1	15 days	6.57	5.90
S2	15 days	5.88	6.30
S3	15 days	6.04	5.56
S7	9 days	3.35	6.25

^a Normalized to 1-cm precise wound length.

The available biomechanical testing results allowed Corbett et al. to conclude that:

- The absorbable tissue adhesive V-100 contributes similarly to Nexaband® toward strength regain of adjoined skin wounds at 15 days.
- V-100 may offer an exceptional advantage over the nonabsorbable Nexaband® in terms of faster strength regain at the early stages of healing.
- A study of wound repair at 3 to 8 days postoperative using V-100 to verify the second conclusion is warranted.

5.5 Conclusion and Perspective on the Future

Development of absorbable cyanoacrylate tissue adhesives with comparable or superior properties to their clinically accepted, nonabsorbable counterparts, presents a milestone in sutureless wound repair. As was the case in the suture area, the absorbable tissue adhesives are expected to replace their non-absorbable counterparts in their most important topical applications. Moreover, the absorbable tissue adhesives, and not the non-absorbable ones, are expected to be used for internal wound repairs. This is provided that a practical sterilization method is developed to achieve product sterility.

References

1. Spotnitz, W. D., History of tissue adhesives, in *Surgical Adhesives and Sealants: Current Technology and Application*, Sierra, D. and Saltz, R, Eds., Technomic Publishing Co., Lancaster, PA, 1996, chap. 1.
2. Linden, C. L., Jr. and Shalaby, S. W., Absorbable Tissue Adhesive, U.S. Patent (to U.S. Army) 5,350,798, 1994.
3. Shalaby, S. W., Polyester/Cyanoacrylate Tissue Adhesive Formulations, U.S. Patent (to Poly-Med, Inc.) 6,299,631, 2001.
4. Shalaby, S. W., Stabilized Polyester/Cyanoacrylate Tissue Adhesive Formulation, a CIP to U.S. Patent 6,299,631, filed in December 2002.
5. Bruce, T. F., Corbett, J. T., Atkins, G. G., Kline, J. D., Hinds, M. and Shalaby, S. W., Study of anionic and free-radical polymerization of an absorbable cyanoacrylate tissue adhesive, *Trans. Soc. Biomater.*, 24, 451, 2001.
6. Linden, C. L., Jr. and Shalaby, S. W., Performance of modified tissue adhesives for soft and hard tissue, *J. Biomed. Mater. Res., Appl. Biomater.*, 38(4), 348, 1997.
7. Flagle, J., Kline, J. D., Allan, J. M. and Shalaby, S. W., *in vitro* Evaluation of Absorbable Tissue Adhesives, *Trans Soc. Biomater.*, 22, 376, 1999.
8. Linden, Jr., C. L., M.S. Thesis, Clemson University, Clemson, SC, 1992.
9. Domb, A. J., Amselem, S., Langer, R. and Maniar, M., Polyanhydrides as carriers of drugs in *Biomedical Polymers: Designed-to-Degrade Systems*, Shalaby, S. W., Ed., Hanser Publishers, 1994, chap. 3.
10. Anderson, J. M., *Biomater. Med. Dev. Artif. Org.*, 2, 235, 1974.
11. Linden, Jr., C. L., Ph.D. Dissertation, Clemson University, Clemson, SC, 1994.
12. Shalaby, S. W., Linden, C. L., Jr. and Shalaby, M., Absorption of radiolabelled methoxypropyl cyanoacrylate tissue adhesive composition in rats, *Trans. Soc. Biomater.*, 26, 293, 2003.
13. Flagle, J. A., Allan, J. M., Kline, J. D., Dooley, R. L., Fulton, L. K., Farris, H. M. and Shalaby, S. W., A Preliminary *In vivo* study of absorbable synthetic tissue adhesives, 22nd Annual Meeting, Adhesion Society, 101, 1999.
14. Corbett, J. T., Anneaux, B. L., Quirk, J. R., Fulton, L. K., Shalaby, M., Linden, D. E., Woods, D. W. and Shalaby, S. W., Comparative study of absorbable and non-absorbable tissue adhesives: A preliminary report, *Trans. Soc. Biomater.*, 25, 636, 2002.

6

Chitosan-Based Systems

Shalaby W. Shalaby, John A. DuBose, and Marc Shalaby

CONTENTS

6.1	Introduction	77
6.2	Advances in Chitosan-Based Systems	78
6.2.1	Advances in Chitosan-Based Materials and Clinical Relevance	78
6.2.2	Advances in Processing of Chitosan-Based Systems and Clinical Relevance	79
6.3	Advances in Chitosan-Based Systems (CBS) Applications	80
6.3.1	Chitosan-Based Systems for Pharmaceutical Applications.....	81
6.3.2	Chitosan-Based Systems for Biomedical Applications	83
6.3.3	Chitosan-Based Systems in Healthcare Applications.....	84
6.3.4	Chitosan-Based Systems for Tissue Engineering.....	84
6.4	Conclusion and Perspective on the Future	85
	References	85

6.1 Introduction

Chitosan is a copolymer of glucosamine and *N*-acetylglucosamine derived from the natural polymer, chitin. The latter is a poly(*N*-acetylglucosamine) and can be obtained in an impure form mostly from crab and shrimp shells. For the preparation of chitosan, chitin is deacetylated under basic conditions to yield a copolymeric chain with variable glucosamine to *N*-acetylglucosamine ratios. Most commonly used chitosans have 70 to 90% of their repeat units deacetylated.¹ A major challenge in the production of chitosan is its purification to achieve a sufficiently low endotoxin level, which is suitable for biomedical and pharmaceutical applications. High purity chitosan has been described to have good compatibility and low toxicity.² Chito-

san can be hydrolyzed by lysosomes, and its degradation can be controlled by changing (1) the ratio of glucosamine to *N*-acylglucosamine; (2) the length of the acyl side group; and/or (3) its molecular weight.³ It has also been reported that the degradation of products of pure chitosan are nontoxic, nonimmunogenic, and noncarcinogenic.⁴ Prior to the 1970s, chitosan was primarily used in nonbiomedical applications.¹ During the 1980s and early 1990s, interest in chitosan grew significantly for use in biomedical and pharmaceutical applications.⁵ With the availability of new biocompatibility data, chitosan has been investigated further over the past 10 years as a premium biodegradable material for those applications as well as for tissue engineering.

Some of the compelling data pertaining to chitosan safety and hemostatic potential that have intensified interest in it as a biomaterial are those reported by Rao and Sharma.⁶ Results noted in this report led to the conclusion that:

- Autoclaving appeared to be an ideal sterilizing method for chitosan.
- Purified chitosan can be converted to films, which after sterilization were shown to be pyrogen-free and nontoxic when tested *in vivo*.
- Coagulation and hemoagglutination tests showed that the hemostatic mechanism of chitosan seems to be independent of the classical coagulation cascade and appears to be an interaction of the cell membrane of erythrocytes and chitosan.

6.2 Advances in Chitosan-Based Systems

6.2.1 Advances in Chitosan-Based Materials and Clinical Relevance

Most of the early studies on chitosan addressed its *N*-acylation with fatty acids to increase its hydrophobicity. Fewer studies were conducted on partial *N*-carboxylmethylation to produce materials for a variety of industrial applications. On the other hand, the growing interest in chitosan as a biomaterial and source for a suitable carrier for bioactive agents over the past 15 years led to a substantial increase in research activities relevant to chitosan modification as outlined below.

Alkenyl succinic acid anhydrides were used to acylate chitosan in order to increase its hydrophobicity while reversing its net charge at pH 7.4 from positive to negative.⁷ Films made of chitosan and its acylated derivatives were used as carriers to study the release profile of (1) ibuprofen and tolectic acid as examples of acidic, nonsteroidal, antiinflammatory drugs, and (2) cefazolin as a basic typical antibiotic.⁷ The results show that altering the net charge, via acylation, and changing chitosan from polycation to polyanion led to significant alteration of the release profiles of the basic and acid drugs. Collectively favorable ionic interaction of the drug with an oppositely

charged matrix was associated with a decrease in release rate as compared to the similarly charged counterparts.

Low molecular weight chitosan was made via nitrous acid chain cleavage of high molecular weight commercial chitosan. Mixed acylation with succinic acid (glutaric anhydride) and acetic (or propionic acid) was then used to convert the polycationic chitosan to polyanionic material.⁸⁻¹¹ The latter was used to form ionic conjugates with a series of bioactive oligopeptides. Typical examples of these conjugates were used as controlled release systems of LHRH and somatostatin analogs for a period of 3 to 14 weeks.¹¹ Both types of oligopeptides are clinically effective agents for treating colon cancer, and their availability in controlled release systems will allow their prolonged efficacy with a minimum amount of drugs.

Other than ionic conjugates of the carboxyl-bearing chitosan derivatives noted above, Song and co-workers have previously conjugated *N*-succinylated chitosan covalently to mitomycin C (MMC).¹² The covalent binding of MMC to the carboxyl group of succinylated chitosan was achieved using a carbodiimide. The covalently conjugated MMC was shown to release about 20% of its initial loading over 72 h following pseudo-first order kinetics, using a phosphate buffered solution at 37°C and pH 7.4. This represented a potentially viable means of controlling the release of MMC in a typical clinical setting.

Because of their interest in biological or naturally derived adhesives, Ono and co-workers designed a new photocrosslinkable chitosan molecule that contains both lactose moieties and photoreactive azide groups (AZ-CH-LA).¹³ Introduction of the lactose moieties resulted in a more water-soluble chitosan at neutral pH. Application of ultraviolet light (U.V.) to photocrosslinkable AZ-CH-LA produced an insoluble hydrogel within 60 sec. The hydrogel adhered firmly to soft biological tissue. Based on this and other results, the authors suggested that the hydrogel has the potential of serving as a new tissue adhesive for medical applications.

6.2.2 Advances in Processing of Chitosan-Based Systems and Clinical Relevance

Most of the early studies on chitosan system processing dealt with the purification of chitosan itself to remove impurities such as proteins, pyrogens, toxic metals, and low molecular weight polysaccharides.¹ Chitosan purification was pursued primarily to allow its use in parenteral pharmaceutical products and/or implantable biomedical devices. Parallel to chitosan purification, a great deal of effort was directed toward chitosan processing into:

- Solution-spun fibers and conversion to different textile constructs
- Beads as microcarriers of bioactive agents and substrates for cell immobilization

- Solution-cast films and membranes
- Microporous sponges

Advances beyond these traditional processes are summarized below.

In an effort to improve the blood compatibility of chitosan in a fiber form, a methanol–acetic acid solution of chitosan and tropocollagen was wet-spun into reasonably strong fibers. Using an ammonia solution with ammonium sulfate as a coagulation bath, acylation of these fibers was shown to increase their tenacity.¹⁴

Recognizing the versatility of injectable, gel-forming liquids, or solutions in pharmaceutical and biomedical applications, Chenite and co-workers developed a novel, injectable gel-forming chitosan-based solution.^{15–17} For this, an aqueous chitosan salt solution was mixed with a polyol derivative bearing a single anionic head, such as glucose-phosphate and glycerol-2-phosphate (β -GP) salts, to produce a thermally sensitive, neutral solution that undergoes gelation at body temperature. The biocompatibility of chitosan salt/ β -GP thermosensitive gel was investigated by Molinaro et al.¹⁸ These authors concluded that a high aminoglucosamine to *N*-acetylglucosamine ratio in the chitosan component of the gel-former is desirable to achieve superior biocompatibility. These systems were used to (1) deliver, successfully, active growth factors, and (2) encapsulate living chondrocytes for tissue engineering applications.¹⁷

There has been consistent interest in polyelectrolyte complexes, such as those of polycationic chitosan with polyanionic polymers, as vehicles for the controlled delivery of bioactive agents. This directed Tan and co-workers to develop a process for preparing chitosan/alginate complex as microcapsules for the controlled delivery of ketoprofen.¹⁹ These authors used an air extrusion process, which entails air-driven extrusion (through a properly sized nozzle) of a mixed solution of ketoprofen (in ethanol) and sodium alginate (in water) as droplets into a chitosan coagulation bath. The latter contains a chitosan solution in aqueous acetic acid containing calcium chloride. The *in vitro* release profile of the ketoprofen (a nonsteroidal, antiinflammatory drug), from different chitosan/alginate microcapsules at different pHs, allowed Tan and co-workers to advocate their use as pH-controlled, oral delivery systems. Thus, in the acidic stomach pH, the release is minimal and it increases as the microcapsule encounters higher pH in the intestine.¹⁹

6.3 Advances in Chitosan-Based Systems (CBS) Applications

Most of the early biomedical and pharmaceutical application of chitosan-based systems dealt with topical applications and a few controlled drug

delivery systems with limited exploitation of chitosan's unique properties. This, in part, was due to limited availability of pure chitosan with an acceptable pyrogen level. Recently, availability of highly pure chitosan paralleled by advances in the development of potent bioactive agents and interest in tissue engineering has evoked a number of new pharmaceutical and biomedical applications, a few of which are noted below.

6.3.1 Chitosan-Based Systems for Pharmaceutical Applications

Chitosan microspheres used as an injectable intramuscular drug-delivery agent biodegrade rapidly. However, spray-dry processing compromises the crystallinity of the spheres, exposing substrate sites for lysozymic degradation. Glutaraldehyde as a crosslinking agent delays degradation, but its cytotoxic degradation products incite inflammatory response in tissues, as evidenced in bovine pericardium studies.²⁰ Mi et al. showed that the use of genipin instead of glutaraldehyde to crosslink chitosan microspheres further extended the structural life of the spheres while reducing inflammation in muscular tissues.²¹ While either system caused a higher inflammatory response than untreated spheres, the number of lymphocytes present in the tissues of genipin-treated chitosan was less than that in those tissues with glutaraldehyde-treated chitosan, suggesting that genipin-treated chitosan is more biocompatible than that treated with glutaraldehyde.

Without the use of additives to assuage the response of chitosan to pH, its use as a drug carrier is unpredictable.²² Antibiotic-releasing chitosan bone scaffolds are stabilized by the addition of calcium phosphates, prolonging their useful drug release period and leveling their concentration profiles. Zhang and Zhang showed that the addition of tricalcium phosphate and calcium phosphate glasses to chitosan scaffolds laden with gentamicin-sulfate decreased the initial burst of drug by nearly 50% in a phosphate buffered solution.²² The critical drug concentration emanated from the hybrid scaffolds for the ensuing 3 weeks, whereas pure chitosan only sustained concentrations for a few days. Culturing of MG63 osteoblast-like cells on the modified and control scaffolds indicated equivalent cell growth and no reduced biocompatibility from the addition of the calcium phosphates. The chitosan-calcium phosphate complex, then, provides an effective drug delivery carrier for osteomyelitis-inflicted bone.²³

The chemical and physical properties of a novel chitosan-xanthan (CH-X) complex hydrogel lend it promise as a drug delivery vehicle.²⁴ Its high concentration of polar functional groups and porosity leads to macrophage stimulation and invasion, encouraging steady biodegradation.²⁵ According to evidence provided by Chellat et al. the extracts of CH-X are not cytotoxic, and its particles do not inhibit growth of L-929 fibroblast cell lines at concentrations below 1 mg/mL *in vitro*.²⁵ Furthermore, the production of cytokines and generation of nitric oxide by macrophages was not significantly increased by said concentrations of CH-X. *In vivo* studies by the same team

indicated phagocytic innervations of tabular Wistar rat implants, and showed extensive biodegradation of the hydrogel.²⁶

Chitosan microparticles provide a potential system for oral vaccination. While oral vaccinations would cost less and be more comfortable than traditional injections, antigen degradation in the acidic stomach environment and unpredictable immune response at Peyer's patches render them inefficient.²⁷ However, vaccines delivered in biodegradable microspheres can weather the harsh gastrointestinal environment and be phagocytized by Peyer's patch cells.^{28,29} Van der Lubben et al. demonstrated that chitosan microspheres loaded with FITC labeled ovalbumin relayed their antigens to Peyer's patches.²⁷ Stained intestinal epithelium showed high uptake of loaded microspheres, while pure administered FITC-ovalbumin indicated no uptake.

Dermal drug administration is yet another pharmaceutical application of chitosan. Topical all-*trans*-retinoic acid (ATRA) is an effective treatment for serious malignant melanoma.³⁰ However, this topical retinoid incites skin irritation in the wide majority of patients, rendering it an ineffective treatment.^{31,32} As evidenced by the research of Cattaneo and Demierre, chitosan gels avail themselves to sustained, topical release of ATRA.³³ These studies showed that manipulation of the viscosity or chitosan concentration of the gel enabled control of percutaneous penetration of the drug in mouse skin samples. In addition, their clinical trials on healthy human subjects indicated minimal erythema occurrence from application of 0.1% ATRA in 1% and 3% chitosan gel.

Cancer treatments facilitated by chitosan extend further to tumoral injection systems. Clinical malignant melanoma and glioma neutron-capture therapy (NCT) involves boron-10 compounds.^{34,35} If gadolinium-157 (Gd-157) could be used instead, a greater therapeutic effect would result due to its high thermal neutron-capture cross-section.³⁶ The efficacy of Gd-NCT, however, is contingent upon the delivery and retention of gadolinium in the tumoral site.³⁷ Tokumitsu et al. presented evidence that novel emulsion-droplet coalesced chitosan nanoparticles loaded with gadopentetic acid (Gd-DTPA) held nearly 70% of the Gd in tumoral tissue of mice 24 h after injection, whereas tumors treated with conventional formulations of solutions of Gd-DTPA in a MRI contrasting agent retained only 0.4% of the original Gd load.³⁸

Coadministration of therapeutic polypeptides such as insulin with protease inhibitors increases their bioavailability.³⁹⁻⁴² However, introduction of protease inhibitors leads to disruption of natural intestinal processes including digestion of nutritive proteins.⁴³ According to Bernkop-Schnorch and Pasta, chitosan-EDTA (ethylene-diamine-tetra-acetic acid), a bioadhesive copolymer, can be covalently linked to the Bowman-Birk inhibitor, which inhibits the proteases trypsin, chymotrypsin, and elastase, providing a mucoadhesive drug-carrier matrix with local prevention of enzymatic degradation.^{43,44} These researchers showed that the conjugate system prevented local enzymatic activity of trypsin and chymotrypsin nearly completely and lowered

the enzymatic activity of elastase. In addition, the presence of EDTA inhibited carboxypeptidase activity and reduced the activity of aminopeptidase.

The polyelectrolytic properties of chitosan may further be used to form complexes with DNA plasmid, which are protected from enzymatic degradation.⁴⁵ MacLaughlin et al. found that plasmid-chitosan complexes with a 1:2 ionic charge ratio were stable *in vitro*.⁴⁶ Furthermore, they found that the chitosan complexes, when containing the endosomolytic peptide GM225.1, led to transgene expression in small intestine of rabbits, while naked plasmids yielded no expression.

6.3.2 Chitosan-Based Systems for Biomedical Applications

Application of U.V. irradiation to an aqueous solution of the photocrosslinkable chitosan (AZ-CH-LA), discussed in Section 6.2.1, resulted in an insoluble, flexible hydrogel-like soft rubber within 60 sec.⁴⁷ It was shown that the chitosan hydrogel can completely stop bleeding from a cut mouse tail within 30 sec of irradiation and can firmly adjoin two pieces of mouse skin. Ishihara et al. also demonstrated that the hydrogel accelerates wound healing.⁴⁷ The authors pointed out its clinical potential as an excellent dressing for wound occlusion and tissue adhesives in urgent hemostasis situations.

Phosphorylated chitosan (P-C) was prepared and used as an additive for calcium phosphate cement (CPC) to improve its mechanical properties and particularly its compressive strength.⁴⁸ The CPC/P-C system was proposed for use as a bone filler.

An earlier study by the Xiufang group in China showed that:

- Neurons cultured on a chitosan membrane can grow well.
- Chitosan conduits can greatly promote repair of the peripheral nervous system.⁴⁹

These results and interest of this group in repairing the central nervous system prompted the pursuit of a study of the ability of chitosan and certain chitosan-derived materials to facilitate the growth of nerve cells.⁵⁰ Results of this study led to the conclusion that:

- Chitosan has excellent nerve cell affinity besides its good biocompatibility.
- Chitosan-derived materials, such as chitosan coated with polylysine (CAP) and chitosan-polysine mixture (CPL), have higher affinity to nerve cells than chitosan itself.
- Precoating with extracellular matrix molecules and particularly laminin can greatly improve nerve cell affinity.

It has been recognized by a number of investigators that chitosan plays an important role in cell regulation and osteoconductive activities.⁵¹⁻⁵³ Addi-

tionally, it has been reported that chitosan and its degradation products can be involved in the synthesis of several substances, including hyaluronic acid, that are necessary for nutrition of its cartilage.⁵⁴ This led Lu and co-workers to study the biological effect of chitosan on cartilage tissue in rat knee.⁵⁵ Results of the study suggest that chitosan could act on the growth of epiphyseal cartilage and wound healing of articular cartilage.

Chitosan facilitates wound healing, particularly through the acceleration and stimulation of wound-cleaning polymorphonuclear leukocytes (PMN).^{56,57} Not only do the PMN cells phagocytize foreign bodies but they also produce cytokines, which contribute to local inflammatory response.⁵⁸ Ueno and co-workers illuminated the role of chitosan in wound healing.⁵⁹ They showed that the presence of fibrous chitosan at canine wound sites significantly stimulated osteopontin (OPN) expression in granular tissue. Previous studies had shown that OPN, a glycosylated phosphoprotein, encourages cell attachment.⁶⁰⁻⁶⁴ Furthermore, Ueno et al. found that human PMN stimulated *in vitro* with chitosan expressed OPN mRNA much more readily than nonstimulated cells.

6.3.3 Chitosan-Based Systems in Healthcare Applications

Chitosan polyelectrolyte (PEC) systems provide membranous dressings for expedient wound healing.⁶⁵⁻⁶⁸ Recently, Wang et al. evaluated chitosan-alginate PEC systems, for their pliability and control of water loss, for *in vivo* wound dressing.⁶⁹ *In vitro* studies showed that the PEC system was not cytotoxic and that it had a water vapor transmission rate very near that of skin, encouraging its use on granulating, but not highly exudative, wounds. The Wang et al. rat wound model provided evidence that a PEC membrane adhered well to granulating wounds and encouraged cellular ingrowth. Wounds treated with the membranes closed much faster than open wounds and gauze-wrapped wounds, and they closed slightly faster than wounds dressed with leading polyurethane films.

6.3.4 Chitosan-Based Systems for Tissue Engineering

Chitosan shows promise in the field of tissue engineering, as it has been linked to the synthesis of components of cartilage-nutritive fluids, including chondroitin and hyaluronic acid.⁵⁵ Chitosan possesses a molecular structure similar to that of glycosaminoglycan (GAG) chains, which are major components of articular cartilage.⁷⁰ Zhu et al. exploited the bioactivity of chitosan and the good mechanical properties of poly D-L lactide (PDL-LA).⁷⁰ They immobilized amino acid-grafted chitosan to the surface of PDL-LA. The resulting extracellular matrix-like surface encouraged attachment and proliferation of chondrocytes. SEM investigation showed that chondrocytes had a much higher affinity for the surfaces than virgin PDL-LA, indicating that they present good options for cartilage tissue engineering.

Deep wounds are traditionally treated with hydrogel or sponge wound dressings. Yannas et al. developed artificial skin composed of a silicone film layer and a collagen sponge layer for this purpose.⁷¹ Collagen sponge, however, is wrought with complications for tissue engineering, as it fails to maintain structural integrity upon introduction to bodily fluids and can become immunogenic.^{72,73} Ma et al. created a bilayer wound dressing with a chitosan film and a chitosan sponge layer, which efficaciously retained water *in vitro*, even with the extensive use of porogens.⁷⁴ Seeding the sponge with neonatal dermal fibroblasts led to proliferation in the pores, as the polycationic chitosan bound fibroblast cells. Over a 4-week trial, the sponge layer maintained its form, not contracting as the collagen sponge did. Their chitosan bilayer scaffold, therefore, provides an advantageous alternative to collagen-based options.

6.4 Conclusion and Perspective on the Future

Having the ability to produce high-purity chitosan propelled the great interest of contemporary investigators in exploring novel derivatives and applications of such an abundant natural polymer with unique properties. Effective exploitation of these properties for the development of novel biomedical devices, pharmaceutical and wound repair products, and tissue engineering has just begun. Chitosan and a certain number of its derivatives having controlled solubility and charge concentrations of one or two types are expected to be of great value in the fast-growing area of localized delivery of highly potent peptides and proteins, as well as in traditional and *in situ* tissue engineering.

References

1. Sandford, P. A. and Steinnes, A., Biomedical applications of high-purity chitosan, in *Water Soluble Polymers*, Vol. 467, Shalaby, S. W., Ed., ACS Symposium Series, Vol. 467, 1991, chap. 28.
2. Thomas, C. and Sharma, P., Chitosan as a biomaterial, *Biomater. Artif. Cells Artif. Org.*, 18, 1, 1990.
3. Tomihata, K. and Ikada, Y., In vitro and *in vivo* degradation of films of chitin and its deacetylated derivatives, *Biomaterials*, 18, 567, 1997.
4. Muzzarelli, R. A., Biochemical significance of exogenous chitins, chitosan in animals, patients, *Carbohydr. Polym.*, 20, 7, 1993.
5. Kimura, Y., Biodegradable polymers, in *Biomedical Applications of Polymeric Materials*, Tsuruta, T., Hayashi, T., Kataoka, K., Ishihara, K., and Kimura, Y., Eds., CRC Press, Boca Raton, FL, 1993, chap 3.

6. Rao, S. B. and Sharma, C. P., Use of chitosan as a biomaterial: Studies on its safety and hemostatic potential, *J. Biomed. Mater. Res.*, 34, 21, 1997.
7. Tayab, F. A., Hydrophobic chitosan in controlled release delivery systems, M.S. Thesis, Department of Bioengineering, Clemson University, Clemson, SC, 1995.
8. Shalaby, S. W. and Ignatious, F. S., Ionic Molecular Conjugates of Biodegradable Fully n-Acylated Derivatives of Poly(2-amino-2-deoxy-d-glucose) and Bioactive Polypeptides, U.S. Patent (to Biomeasure, Inc.) 5,665,702, 1997.
9. Shalaby, S. W. and Ignatious, F., Ionic Molecular Conjugates of Biodegradable Fully n-Acylated Derivatives of Poly(2-amino-2-deoxy-d-glucose) and Bioactive Polypeptides, U.S. Patent (to Biomeasure, Inc.) 5,821,221, 1998.
10. Shalaby, S. W., Jackson, S. A., Ignatious, F. S. and Moreau, J. P., Ionic Molecular Conjugates of n-acylated derivatives of poly(2-amino-2-deoxy-d-glucose) and polypeptides, U.S. Patent (to Biomeasure, Inc.) 6,479,457, 2002.
11. Shalaby, S. W., Poly-Med, Inc., internal reports, 1996 and 1998.
12. Song, Y., Onishi, H. and Nagai, T., Synthesis and drug-release characteristics of the conjugates of mitomycin C with N-succinyl-chitosan and carboxymethyl-chitin, *Chem. Pharm. Bull.*, 40(10), 2822, 1992.
13. Ono, K., Saito, Y., Yura, H., Ishikawa, K., Kurita, A., Akaike, T. and Ishihara, M., Photocrosslinkable chitosan as a biological adhesive, *J. Biomed. Mater. Res.*, 49, 289, 2000.
14. Hirano, S., Zhang, M., Nakagawa, M. And Miyata, T., Wet spun chitosan-collagen fibers, their chemical N-modifications, and blood compatibility, *Biomaterials*, 21, 997, 2000.
15. Shalaby, S.W., Hydrogel-Forming, Self-Solvating Absorbable Polyester Copolymers, and Methods for Use Thereof, U.S. Patent (to Poly-Med, Inc.) Composition 5,612,052, 1997.
16. Jeong, B., Bae, Y. J., Lee, B. S. and Kim, S. W., *Nature*, 388, 860, 1997.
17. Chenite, A., Chaput, C., Wang, D., Combes, C., Buschmann, M. C., Hoemann, C. D., Leroux, J. C., Atkinson, B. L., Binette, F. and Selmani, A., Novel injectable neutral solutions of chitosan form biodegradable gels in situ, *Biomaterials*, 21, 2155, 2000.
18. Molinaro, G., Leroux, J. C., Damas, J. and Adam, A., Biocompatibility of thermosensitive chitosan-based hydrogels: an *in vivo* experimental approach to injectable biomaterials, *Biomaterials*, 23, 2717, 2002.
19. Tan, T. W., Hu, B., Jin, X. H. and Zhang, M., Release behavior of ketoprofen in chitosan/alginate microcapsules, *J. Bioact. Biocomp. Polym.*, 2003 (in press).
20. Sung, H. W., Chang, Y., Chiu, C. T., Chen, C. N. and Liang, H. C., Crosslinking characteristics and mechanical properties of a bovine pericardium fixed with a naturally occurring crosslinking agent, *J. Biomed. Mater. Res.*, 47, 116, 1999.
21. Mi, F. L., Tan, Y. C., Liang, H. F. and Sung, H. W., *In vivo* biocompatibility and degradability of a novel injectable-chitosan-based implant, *Biomaterials*, 23, 181, 2002.
22. Zhang, Y. and Zhang, M., Calcium phosphate/chitosan composite scaffolds for controlled *in vitro* antibiotic drug release, *J. Biomed. Mater. Res.*, 62, 378, 2002.
23. Korkusuz, F., Uchida, A., Shinto, Y., Araki, N., Inoue, K. and Ono, K., Experimental implant-related osteomyelitis treated by antibiotic-calcium hydroxyapatite ceramic composites, *J. Bone Joint Surg.*, 75-B, 111, 1993.
24. Chu, C. H., Kumagai, H. and Nakamura K., Application of polyelectrolyte complex gel composed of xanthan and chitosan to the immobilization of *Corynebacterium glutamicum*, *J. Appl. Polym. Sci.*, 60, 1041, 1996.

25. Chellat, F., Tabrizian, M., Dumitriu, S., Chornet, E., Magny, P., Rivard, C. H. and Yahia, L. H., *In vitro* and *in vivo* biocompatibility of chitosan-xanthan polyionic complex, *J. Biomed. Mater. Res.*, 51, 107, 2000.
26. Chellat, F., Tabrizian, M., Dumitriu, S., Chornet, E., Rivard, C. H. and Yahia, L. H., HPLC analysis of chitosan-xanthan microspheres degradation, *Proc 18th Can. Biomater. Soc. Conf.*, 1998.
27. Van der Lubben, I. M., Verhoef, J. C., Van Aelst, A. C., Borchard, G. and Junginger, H. E., Chitosan microparticles for oral vaccination: preparation, characterization and preliminary *in vivo* uptake studies in murine Peyer's patches, *Biomaterials*, 22, 687, 2001.
28. Fasano, A., Innovative strategies for the oral delivery of drugs and peptides, *TiBtech.*, 16, 152, 1998.
29. Lydyard, P. and Grossi, C., Secondary lymphoid organs and tissues, in *Immunology*, Roitt, I., Brostoff, J., and Male, D., Eds., Mosby, London, 1998, 33.
30. Halpern, A. C., Retinoids and the chemoprevention of melanoma, in *Advances in the Biology and Treatment of Cutaneous Melanoma*, Meeting Abstracts, Boston, MA, November 6 and 7, 1998.
31. Gilchrist, B. A., Treatment of photodamage with topical tretinoin: an overview, *J. Am. Acad. Dermatol.*, 36, S27, 1997.
32. Stan-Posthuma, J. J., Vink, J., le Cessie, S., Bruijn, J. A., Bergman, W. and Pavel, S., Effect of topical tretinoin under occlusion on atypical naevi, *Melanoma Res.*, 8, 539, 1998.
33. Cattaneo, M. V. and Demeirre, M. F., Biodegradable chitosan for topical delivery of retinoic acid, *Drug Delivery Techno.*, 1, 45, 2001.
34. Barth, R. F. and Soloway, A. H., Boron neutron capture therapy of primary and metastatic brain tumors, *Mol. Chem. Neuropathol.*, 21, 139, 1994.
35. Mishima, Y., Ichihashi, M., Hatta, S., Honda, C., Yamamura, K. and Nakagawa, T., New thermal neutron capture therapy for malignant melanoma: melanogenesis-seeking ^{10}B molecule-melanoma cell interaction from *in vitro* to first clinical trial, *Pigment Cell Res.*, 2, 226 1989.
36. Greenwood, R. C., Reich, C. W., Baader, H. A., Koch, H. R., Breitig, D., Schult, O. W. B., Fogelberg, B., Backlin, A., Mampe, W., von Edigy, T. and Schreckenbach, K., Collective and two-quasiparticle states in ^{158}Gd observed through study of radiative neutron capture in ^{157}Gd , *Nucl. Phys.*, A304, 327, 1978.
37. Akine, Y., Tokita, N., Tokuyue, K., Satoh, M., Churei, H., Pechoux, C. L., Kobayashi, T. and Kanda, K., Suppression of rabbit VX-2 subcutaneous tumor growth by gadolinium neutron capture therapy, *Jpn. J. Cancer Res.*, 84, 841, 1993.
38. Tokumitsu, H., Ichikawa, H. and Fukumori, Y., Chitosan-gadopentetic acid complex nanoparticles for gadolinium neutron-capture therapy of cancer: preparation by novel emulsion-droplet coalescence technique and characterization, *Pharma. Res.*, 16, 1830, 1999.
39. Fujii, S., Yokoyama, T., Ikegaya, K., Sato, F. and Yoko, N., Promoting effect of the new chymotrypsin inhibitor FK-448 on the intestinal absorption of insulin in rats and dogs, *J. Pharm. Pharmacol.*, 37, 545, 1985.
40. Langguth, P., Merkle, H. P. and Amidon, G. L., Oral absorption of peptides: The effect of absorption site and enzyme inhibition on the systemic availability of metkephamid, *Pharm. Res.*, 11, 528, 1994.
41. Yamamoto, A., Taniguchi, T., Rikyuu, K., Tsuji, T., Fujita, T., Murakami, M. and Muranishi, S., Effects of various protease inhibitors on the intestinal absorption and degradation of insulin in rats, *Pharm. Res.*, 11, 1496, 1994.

42. Morishita, L., Morishita, M., Takayama, K., Machida, Y. and Nagai, T., Hypoglycemic effect of novel oral microspheres of insulin with protease inhibitor in normal and diabetic rats, *Int. J. Pharm.*, 78,9, 1992.
43. Bernkop-Schnorch, A. and Pasta, M., Intestinal peptide and protein delivery: Novel bioadhesive drug-carrier matrix shielding from enzymatic attack, *J. Pharm. Sci.*, 4, 430, 1998.
44. Reseland, J. E., Holm, H., Jacobsen, M. B., Jenssen, T. G. and Hanssen, L. E., Proteinase inhibitors induce selective stimulation of human trypsin and chymotrypsin secretion, *Hum. Clin. Nutr.*, 126, 634, 1996.
45. Richardson, S., Kolbe, H. V. J. and Duncan, R., Evaluation of highly purified chitosan as a potential gene delivery vector, *Proc. Int. Symp. Contr. Rel. Bioact. Mater.*, 24, 649, 1997.
46. MacLaughlin, F. C., Mumper, R. J., Wang, J., Tagliaferri, J. M., Gill, I., Hinchcliffe, M. and Rolland, A. P., Chitosan and depolymerized chitosan oligomers as condensing carriers for *in vivo* plasmid delivery, *J. Cont. Rel.*, 56, 259, 1998.
47. Ishihara, M., Nakanishi, K., Ono, K., Sato, M., Kikuchi, M., Saito, Y., Yura, H., Matsui, T., Hattori, H., Uenoyama, M. and Kurita, A. Photocrosslinkable chitosan as a dressing for wound occlusion and accelerator in healing process, *Biomaterials*, 23, 833, 2002.
48. Wang, X., Ma, J., Wang, Y. and He, B., Structural characterization of phosphorylated chitosan and their applications as effective additives to calcium phosphate cement, *Biomaterials*, 22, 2247, 2001.
49. Jianchun, L., Yinghui, Z., Haipeng, G., Yandao, G., Nanming, Z. and Xiufang, Z., A primary study of using chitosan for nerve repair conduit, in *5th IUMRS Int. Conf. Adv. Mater.*, Beijing, China, 1999.
50. Haipeng, G., Yinghui, Z., Jianchun, L., Yandao, G., Nanming, Z. and Xiufang, Z., Studies on nerve cell affinity of chitosan-derived materials, *J. Biomed. Mater. Res.*, 52, 285, 2000.
51. Hirano, S. and Noishiki, Y., The blood compatibility of chitosan and N-acyl-chitosans, *J. Biomed. Mater. Res.*, 19, 413, 1984.
52. Klokkevold, P. R., Vandemark, L., Kenney, E. B. and Bernard, G. W., Osteogenesis enhanced by chitosan (poly-N-acetyl glucosamineglycan) in vitro, *J. Periodontol.*, 67, 1170, 1996.
53. Muzzarelli, R., Baladasarre, V., Conti, F., Ferrara, P., Biagini, G., Gazzanelli, G. and Vasi, V., Biological activity of chitosan: ultrastructural study, *Biomaterials*, 9, 247, 1988.
54. Moskowitz, R. W., Schwartz, H. J., Michel, B., Ratnoff, O. D. and Astrup, T., Generation of kinin-like agents by chondroitin sulfate, heparin, chitin sulfate, and human articular cartilage: possible patho-physiologic implications, *J. Lab. Clin. Med.*, 76, 790, 1970.
55. Lu, J. X., Prudhommeaux, F., Meunier, A., Sedel, L. and Guillemain, G., Effects of chitosan on rat knee cartilages, *Biomaterials*, 20, 1937, 1999.
56. Prudden, J. G., Migel, P., Hanson, P., Friedrich, L. and Balassa, L., The discovery of a potent pure chemical wound-healing accelerator, *Am. J. Surg.*, 119, 560, 1970.
57. Scott, D. W., Miller, W. H. and Griffin, C. E., *Muller and Kirk's Small Animal Dermatology*, W. B. Saunders, PA, 1995, 262.
58. Cassatella, M. A., The production of cytokines by polymorphonuclear neutrophils, *Immunol. Today*, 16, 21, 1995.

59. Ueno, H., Murakami, M., Okumura, M., Kadosawa, T., Uede, T. and Fujinaga, T., Chitosan accelerates the production of osteopontin from polymorphonuclear leukocytes, *Biomaterials*, 22, 1667, 2001.
60. Oldberg, A., Franzen, A. and Heinegard, D., Cloning and sequence analysis of rat bone sialoprotein (osteopontin) cDNA reveals an Arg-Gly-Asp cell-binding sequence, *Proc. Natl. Acad. Sci., USA*, 83, 8819, 1986.
61. Somerman, M. J., Prince, C. W., William, T. B., Foster, R. A., Moehring, J. M. and Sauk, J. J., Cell attachment activity of the 44 kilodalton bone phosphoprotein is not restricted to bone cells, *Matrix*, 9, 49, 1989.
62. Miyauchi A., Alvarez, J., Greenfield, E. M., et al., Recognition of osteopontin and related peptides by an $\alpha_v\beta_3$ integrin stimulates immediate cell signals in osteoclasts, *J. Biol. Chem.*, 266, 20369, 1991.
63. Ross, F. P., Chappel, J., Alvarez, J. I. et al., Interactions between the bone matrix proteins osteopontin and bone sialoprotein and the osteoclast integrin $\alpha_v\beta_3$ potentiate bone resorption, *J. Biol. Chem.*, 268, 9901, 1993.
64. Senger, D. R., Perruzzi, C. A., Papadopoulos-Sergiou, A. and Van De Water, L., Adhesive properties of osteopontin: regulation by a naturally occurring thrombin-cleavage in close proximity to the GRGDS cell-binding domain, *Mol. Biol. Cell*, 5, 565, 1994.
65. Takeuchi, H., Yasuji, T., Yamamoto, H. and Kawashima, Y., Spray-dried lactose composite particles containing an ion complex of alginate-chitosan for designing a dry-coated tablet having a time-controlled releasing function, *Pharm. Res.*, 17, 94, 2000.
66. Kim, H. J., Lee, H. C., Oh, J. S., Sin, B. A., Oh, C. S., Park, R. D., Yang, K. S. and Cho, C. S., Polyelectrolyte complex composed of chitosan and sodium alginate for wound dressing application, *J. Biomater. Sci., Polym. Ed.*, 10, 543, 1999.
67. Gaserod, O., Smidsrod, O. and Skjak-Braek, G., Microcapsules of alginate-chitosan—I. A quantitative study of the interaction between alginate and chitosan, *Biomaterials*, 19, 1815, 1998.
68. Chandy, T., Mooradian, D. L. and Rao, G. H., Chitosan/polyethylene glycol-alginate microcapsules for oral delivery of hirudin, *J. Appl. Polym. Sci.*, 70, 2143, 1998.
69. Wang, L., Khor, E., Wee, A. and Lim, L. Y., Chitosan-alginate PEC membrane as a wound dressing: assessment of incisional wound healing, *J. Biomed. Mater. Res., Appl. Biomater.*, 63, 610, 2002.
70. Zhu, H., Ji, J., Lin, R., Gao, C., Feng, L. and Shen, J., Surface engineering of poly(D,L-lactic acid) by entrapment of chitosan-based derivatives for the promotion of chondrogenesis, *J. Biomed. Mater. Res.*, 62, 532, 2002.
71. Yannas, I. V., Burke, J. F., Gordon, P. L. and Huang, C., Collagen-like membranes for synthetic skin, *Ger. Offen.*, 2631, 909, 1977.
72. Yannas, I. V., Burke, J. F., Qrigill, D. P. and Skraubut, E. M., Wound tissue can utilize a polymeric template to synthesize a functional extension of skin, *Science*, 215, 174, 1982.
73. Heimbach, D., Luterman, A. and Burke, J. F. et al., Artificial dermis for major burns: a multi-center randomized clinical trial, *Ann. Surg.*, 208, 313, 1988.
74. Ma, J., Wang, H., He, B. and Chen, J., A preliminary *in vitro* study on the fabrication and tissue engineering applications of a novel chitosan bilayer material as a scaffold of human neonatal dermal fibroblasts, *Biomaterials*, 22, 331, 2001.

Hyaluronic Acid-Based Systems

Shalaby W. Shalaby and Waleed S. W. Shalaby

CONTENTS

7.1	Introduction	91
7.2	Advances in the Application of Sodium Hyaluronate (HA-Na).....	92
7.3	Modification of HA and Advances in the Application of Modified Forms.....	93
7.3.1	Ionic Interaction of HA with Divalent and Trivalent Metallic Ions.....	93
7.3.2	Complex Formation of HA with Other Functional Polymers	93
7.3.3	Covalent Modification of HA	94
7.4	Specific Key Roles of HA and its Derivatives in Therapeutic Applications.....	97
7.4.1	HA Is an Adjuvant in Drug Delivery Cryopreservation.....	97
7.4.2	Drug-HA Bioconjugates	98
7.5	Conclusion and Perspective on the Future	98
	References	98

7.1 Introduction

Hyaluronic acid (HA) is a biomacromolecule having an anionic polysaccharide chain made up of alternating *N*-acetyl glucosamine and glucuronic acid repeat units. A high degree of HA solubility in water is due to its presence as a sodium hyaluronate. Being a natural tissue lubricant, it has been obtained by extracting tissues and particularly cartilaginous ones. More recently, it has been produced in sufficient quantities by fermentation. Sodium hyaluronate (HA-Na) exhibits a helical conformation when present as a crystalline solid, but undergoes conformational changes upon dissolu-

tion in aqueous solvents.¹ Soluble HA-Na, a key component of the extracellular matrix, is responsible for attaining a high degree of lubricity at different tissues due to its high capacity to absorb and retain water. These characteristics and its presence as an exceptionally high molecular weight polyelectrolyte result in its extraordinary viscoelastic properties. Accordingly, in its anionic form, HA plays a central role in monitoring the mechanical properties of cartilage as it maintains the structure of various glycosaminoglycans' aggregates, thus conferring resilience and elastic strength to the cartilaginous matrix.² HA-Na is one of the major components of synovial fluids that are present as high molecular weight ($M_w = 10^6$ to 10^7 g/mol) macromolecules at high concentrations (2 to 4 g/mL) to yield a highly viscoelastic solution with optimum lubricating function at low shear rates and excellent shock-absorbing properties at high shear rates.³ Due to their viscoelastic properties, sodium hyaluronate solutions are used for the prevention of postsurgical adhesion (as noted later in Chapter 9) and also in many ophthalmic and orthopedic applications to minimize or eliminate undesirable friction-induced effects, as will be seen later in this chapter. In the meantime, the water-solubility of HA-Na and its high susceptibility to enzymatic degradation in the presence of hyaluronidase limit its use in many other applications requiring limited or highly reduced solubility and increased enzyme stability. These include applications as a matrix for controlled drug release and barrier membranes for the prevention of postoperative adhesion. This prompted many investigators to explore HA modification to modulate its solubility among other useful properties, as will be seen later in this chapter.

7.2 Advances in the Application of Sodium Hyaluronate (HA-Na)

Of the growing applications of HA-Na over the past two decades, those pertaining to ophthalmic and orthopedic areas are paramount. Recent ophthalmic applications include the use of HA-Na solution in situations dealing with:

- Anterior segment surgery
- Penetrating keratoplasty of corneal perforation
- Retinal detachment with proliferative vitreoretinopathy
- Closed vitrectomy
- Reduction of postoperative intraocular pressure after penetrating keratoplasty⁴⁻⁸

A combination of HA-Na and the nonsteroidal antiinflammatory drug Timolol was used for managing early postoperative intraocular pressure

after extracapsular cataract extraction with implantation of posterior chamber lens.⁹

Application of HA-Na and formulations thereof in the orthopedic areas entailed those dealing with treatment of inflammatory and noninflammatory knee effusions, and rheumatoid arthritis and osteoarthritis.^{10–12} Meanwhile, (1) the role of HA-Na in rheumatology and orthopedics in general was reviewed by Strachan; and (2) the pharmacologic and clinical aspects of intra-articular injection of HA-Na solution were discussed in some detail in a report by Iwata.^{12,13}

The use of combinations of HA-Na and nonsteroidal antiinflammatory drugs (e.g., naproxen sodium, tolmetin sodium), antimitotic agents (e.g., trapidil), and cytokines (e.g., interleukin-4) for preventing postoperative adhesion is discussed in more detail in Chapter 9.

7.3 Modification of HA and Advances in the Application of Modified Forms

Modification of HA to optimize its performance as a biomedical device or a vehicle for the controlled release of bioactive agents entails:

- Ionic interaction with multivalent ions to modulate its viscosity and solubility
- Complex formation with heterochain polymers to control its rheological properties and solubility
- Chemical crosslinking to produce practically insoluble gels or membranes

7.3.1 Ionic Interaction of HA with Divalent and Trivalent Metallic Ions

Interaction of calcium ions with HA to modulate its viscosity pre- and postadministration around the severed flexor tendon to minimize postoperative adhesion formation in leghorn chickens was reported by Shalaby and co-workers as noted in Chapter 9.^{14,15} Thornton and co-workers explored the use of ferric hyaluronate as a more viscous gel analog of HA-Na for postoperative adhesion.¹⁶

7.3.2 Complex Formation of HA with Other Functional Polymers

Complexes comprising HA-Na and carboxymethyl cellulose have been developed as gel-coats or membrane barriers for the reduction of postoperative adhesion formation^{17–19} (see also Chapter 8 for details).

In an effort to create a biomaterial that combines inherent biological properties which can specifically trigger desired cellular responses (e.g., angiogenesis) with electrical properties that encourage tissue regeneration, Collier and co-workers prepared unique composites of the polyanionic HA and polycationic polypyrrole (PP).²⁰ The latter is an oxidized form of PP, which can be obtained as electrically conductive film capable of supporting *in vitro* growth and differentiation of multiple cell types including neurons and endothelial cells.^{21,22} In the Collier study, composites of the biologically active polysaccharide HA and the electrically conducting polymer PP were synthesized and characterized.²⁰ Electrical conductivity of the composite biomaterial (PP/HA) was measured by a four-point probe technique. Scanning electron microscopy was used to characterize surface topography. X-ray photoelectron spectroscopy and reflectance infrared spectroscopy were used to evaluate surface and bulk chemistry. An assay with biotinylated hyaluronic acid binding protein was used to determine surface HA content. PP/HA materials were also evaluated for *in vitro* cell compatibility and tissue response in rats. Smooth, conductive, HA-containing PP films were produced; these films retained HA on their surfaces for several days *in vitro* and promoted vascularization *in vivo*. Results of the study led Collier and co-workers to conclude that the PP/HA bilayer biomaterial, with its conductive, noncytotoxic, and angiogenic properties, is an attractive candidate for further studies in tissue engineering strategies that can benefit from electrical stimulation.²⁰

7.3.3 Covalent Modification of HA

The presence of carboxylic, hydroxylic, and acetamido functionalities in HA has provided strong incentive to many investigators to pursue its modification to improve its performance in existing applications or confer unique properties for new applications. These modifications were, for the most part, directed toward the preparation of (1) crosslinked, insoluble gels and membranes; and (2) covalent conjugates with several small and chain molecules with diverse chemical, pharmaceutical, and biological activities.

In a review by Shalaby and Shah, activities on the modification of HA prior to 1990 were summarized.²³ This entails a discussion of key modifications of HA to produce biodegradable materials for use by the biomedical and pharmaceutical industries. Della Valle disclosed a key modification of HA in which the carboxyl groups of the polymer were esterified with monohydric alcohols or reacted with basic drugs.²⁴ Additionally, Della Valle used polyhydric alcohols to produce crosslinked hyaluronic acid for use in the preparation of biodegradable plastics for the production of surgical articles.²⁵ Hunt and co-workers have studied transport properties of thin films formed from alkyl esters of hyaluronic acid where the length of the alkyl group was varied. They reported that small, neutral, and positively charged molecules showed relatively high permeability, whereas low permeability values were

observed for negatively charged molecules and for solutes having molecular weights greater than 3000.²⁶ Malson and Debelder have described crosslinking of hyaluronic acid with polyfunctional reagents, such as diepoxides, to produce water-swellaable and biodegradable materials for use as surgical implants and adjuvants for the prevention of postsurgical adhesions.²⁷

Interest in suitable replacement materials for damaged cartilage that must display physical and morphological properties similar to those of healthy cartilage prompted Pelletier and co-workers to pursue a study on amphiphilic derivatives of sodium alginate and hyaluronate for cartilage repair.²⁸ Accordingly, various amphiphilic derivatives of sodium alginate and hyaluronate were prepared by covalent binding of long alkyl chains (dodecyl and octadecyl) in variable amounts on the polysaccharide backbones through esterification. In the semidilute regime, aqueous solutions of the resulting compounds exhibited the typical rheological properties of hydrophobically associating polymers. These entailed enhancement of zero shear rate Newtonian viscosity, steep shear-thinning behavior, and formation of physically crosslinked gel-like networks. The influence of the alkyl chain length, its content on the polysaccharide, and of the polymer concentration in the solution was determined. Available results were discussed with respect to the schedule of conditions related to materials which could be used for cartilage repair, such as in synovial fluid viscosupplementation, as well as in cartilage replacement. In particular, it was seen that HA-C₁₂-5 (hyaluronate substituted with 5% of dodecyl chains) and HA-C₁₈-1 (hyaluronate substituted with 1% of octadecyl chains) in a 0.15N NaCl solution at 8 g/L have rheological properties quite similar to those of healthy synovial fluid. On the other hand, the rheological parameters of solutions at 8 g/L in 0.15N NaCl of some derivatives, such as AA-C₁₂-8 (alginate substituted with 8% of dodecyl chains) or HA-C₁₈-2, were considered well fitted for use in cartilage repair. Collectively, the authors concluded that from the rheological point of view, some of the described products can fulfill numerous points of the schedule of conditions related to materials useful for cartilage repair, either for viscosupplementation or for cartilage replacement.²⁸

Toward preparing water insoluble derivatives of HA, several approaches for its crosslinking and/or derivatizing its carboxyl or hydroxyl groups have been explored by a number of investigators. Some of these entailed (1) the conversion of the carboxyl groups into amides of aminoesters; and (2) crosslinking using divinyl sulfone, epichlorhydrin, and phosphonyl chloride.²⁹⁻³² However, all of these approaches were associated with chemical reactions that were conducted under alkaline conditions to yield HA hydrogels with low crosslinking and up to 95% water content but very low mechanical strength and high susceptibility to enzymatic degradation. This prompted Tomihata and Ikada to investigate the preparation of crosslinked HA films of low water content and evaluate their tissue reactivity as a useful biomaterial.³³ Accordingly, HA was chemically crosslinked with poly(ethylene glycol) diglycidyl ether to yield slowly degradable films with low water content when brought into contact with water. The crosslinking reaction was

performed under acidic and neutral conditions, since the epoxy group is readily hydrolyzed in alkaline media. To allow the reaction to proceed at high HA concentrations, a solution casting method was employed for the crosslinking. The lowest water content of the crosslinked HA films obtained was 60 wt% when swollen with buffered saline at 37°C. Since IR spectra of the crosslinked films did not change significantly as a result of the crosslinking, intermolecular formation of ether bonds between the hydroxyl groups belonging to different polysaccharide molecules was assumed to take place. It was difficult to detect the ether bonds in the crosslinked HA films because the virgin HA film itself contained ether bonds in the molecule. The crosslinked HA film with a water content of 60 wt% exhibited practically no weight loss after 10 days of immersion in phosphate-buffered saline (pH 7.4). In the meantime, the film underwent *in vivo* degradation as indicated by a 30% weight loss after 7 days of subcutaneous implantation in rats. The inflammation reaction elicited around the implanted film was not significant. The results of this study led these investigators to conclude that HA molecules can be efficiently crosslinked with poly(ethylene glycol) diglycidyl ether by the solution casting method to produce a biodegradable, water-insoluble hydrogel material of low water content. The mild tissue reaction of the hydrogel was attributed to the fact that the crosslinks release bioinert alcohol upon degradation. To reduce the biodegradation rate to a greater extent without compromising the nontoxicity of HA was noted to be difficult because the main chain of HA is readily scissioned in the biological environment.³³

To control the hydrophilicity and/or solubility of HA substantially and modulate related properties, benzylation of the carboxyl groups of the glucuronic acid sequence was pursued in the preparation of linear and crosslinked HA-based molecules.^{34–36} These linear and crosslinked HA-based materials were developed into different forms of sponges by Fidia Advanced Biopolymers of Italy and denoted as HYAFF-11 and ACP sponges, respectively. More specifically, the HYAFF sponges were made of a linear derivative of hyaluronan modified by complete esterification of the carboxylic function of the glucuronic acid with benzyl groups.^{34,35} They had 10 to 400- μm pores, a porosity of 80%, and a surface area of 10.00 m^2/cm^3 . ACP is a crosslinked derivative of hyaluronan that was generated by condensation and, as such, has no residues different from hyaluronan. The stability of the polymer is achieved by directly esterifying some of the carboxylic groups of glucuronic acid along the chain with hydroxyl groups of the same or different hyaluronan molecules. The sponge form of this polymer has 10 to 300- μm pores, a porosity of 85%, and a surface area of 7.34 m^2/cm^3 . Recognition of the limited ability of articular cartilage in adults for self-repair prompted Solchaga and co-workers to investigate the use of HYAFF-11 and ACP sponges in the treatment of osteochondral defects.³⁷ Thus, hyaluronan-based polymers were tested for their ability to enhance the natural healing response. The researchers hypothesized that hyaluronan-based polymers create an embryonic-like milieu where host progenitor cells can regenerate the dam-

aged articular surface and underlying bone. Osteochondral defects were made on the femoral condyles of 4-month-old rabbits and were left empty or filled with hyaluronan-based polymers. The polymers tested were ACP and HYAFF-11 sponges. The rabbits were euthanized 4 and 12 weeks after surgery, and the condyles were processed for histology. All 12-week defects were scored on a 29-point scale, and the scores were compared with a Kruskal–Wallis analysis of variance on ranks. Untreated defects filled with bone tissue up to or beyond the tidemark, and the noncalcified surface layer varied from fibrous to hyaline-like tissue. Four weeks after surgery, defects treated with ACP exhibited bone filling to the level of the tidemark, and the surface layer was composed of hyaline-like cartilage well integrated with the adjacent cartilage. At 12 weeks, the specimens had bone beyond the tidemark that was covered with a thin layer of hyaline cartilage. Four weeks after surgery, defects treated with HYAFF-11 contained a rim of chondrogenic cells at the interface of the implant and the host tissue. In general, the 12-week defects exhibited good bone fill and the surface was mainly hyaline cartilage. Treated defects received significantly higher scores than untreated defects, and ACP-treated defects scored significantly higher than HYAFF-11 treated defects.³⁷ Results of the study led these investigators to note that:

- HA immobilized in the sponge formats has different biologic effects than its degradation products.
- These HA-based vehicles provide differential cuing as intact scaffolds.
- The sequential cuing is similar to that observed in major mesenchymal transitions during embryonic development.

The successful mimicking of embryonic extracellular matrix changes may be a guiding principle for engineering reparative processes in adult tissues as suggested by other authors.^{37–40}

7.4 Specific Key Roles of HA and its Derivatives in Therapeutic Applications

This topic was discussed in a report by Prestwich and Vercruysse, and segments pertinent to the subject of this chapter are summarized herein.⁴¹

7.4.1 HA Is an Adjuvant in Drug Delivery Cryopreservation

Unmodified HA is used as an adjuvant for ophthalmic drug delivery and for enhancing the absorption of drugs and proteins by mucosal tissues. The efficacy of several steroidal and nonsteroidal antiinflammatory drugs can be enhanced in the presence of HA. In reproductive medicine, HA improves

the retention of the mobility of cryopreserved and thawed spermatozoa. This property can be applied to the selection of viable spermatozoa and improvement of artificial *in vitro* fertilization procedures.

7.4.2 Drug-HA Bioconjugates

The derivatization of HA and the synthesis of drug-HA bioconjugates offer several advantages over simple HA-drug admixtures. First, chemical modification allows the physicochemical properties of HA to be tailored according to the desired applications, and this can have a significant impact on the natural turnover and clearance of the HA derivative. For instance, HA has a half-life of 0.5 to 3 days in tissues, but is rapidly cleared from plasma by receptor-mediated uptake by liver endothelial cells with a half-life of several minutes. The HA-drug bioconjugates may exhibit improved water solubility relative to the parent drug. HA-drug hydrogels may be used in localized controlled drug release systems. The high-affinity HA receptors overexpressed in metastatic cells may provide important targeting opportunities for cell-selective delivery of anticancer agents. The receptor on rat liver endothelial cells has been shown to be only partially selective for HA, as HA uptake can be inhibited by coadministration of chondroitin sulfate; by contrast, rat colon cancer cells bear receptors that specifically recognize HA.⁴¹

7.5 Conclusion and Perspective on the Future

The use of unmodified HA in ophthalmic and orthopedic applications, primarily as highly viscoelastic lubricants, has been successful and is expected to grow slowly but steadily. Meanwhile, the use of unmodified HA as a vehicle for drug delivery has been moderately successful and is likely to be phased out with the availability of more enzymatically stable forms of modified HA. To date, ionic and covalent conjugates of HA have encountered limited interest and use. However, this is most likely to become an area for substantial future growth in view of increasing interest in contemporary approaches to controlled delivery of bioactive agents and *in situ* tissue engineering. Applications of crosslinked HA are limited and expected to remain so until new approaches to network formations are developed.

References

1. Feder-Davis, J., Hittner, D. M. and Cowman, M. K., Comparison of solution and solid-state structure of sodium hyaluronan by ¹³C NMR spectroscopy, in *Water Soluble Polymers* Shalaby, S. W., McCormick, C. L. and Butler, G., Eds., ACS Symposium Series, American Chemical Society, Washington, DC, Vol. 467, 1991, chap. 32.

2. Abatangelo, G. and O'Reagan, J., Hyaluronan: Biological role and function in articular joints, *Eur. J. Rheumatol. Inflamm.*, 15, 6, 1995.
3. Schurtz, J., Rheology of synovial fluids and substitute polymers, *Pure Appl. Chem.*, A33, 1249, 1996.
4. Balazs, E. A. and Pape, L. G., The use of sodium hyaluronate (Healon®) in human anterior segment surgery, *Ophthalmology*, 87, 699, 1980.
5. Maguen, E., Nesburn, A. and Macy, J. I., Combined use of sodium hyaluronate and tissue adhesive in penetrating keratoplasty of corneal perforations, *Ophthalm. Surg.*, 15, 55, 1984.
6. Gerke, E., Meyer-Schwickerath, E. and Wessing, A., Healon in retinal detachment with proliferative vitreoretinopathy, *Graefe's Arch. Clin. Exp. Ophthalmol.*, 221, 241, 1984.
7. Folk, J. C., Weigeist, T. A., Packer, A. J. and Howcroft, M. J., Sodium hyaluronate (Healon) in closed vitrectomy, *Ophthalm. Surg.*, 17, 299, 1986.
8. Burke, S., Sugar, J. and Farber, M. D., Comparison of the effects of two viscoelastic agents, Healon and Viscoat, on postoperative intraocular pressure after penetrating keratoplasty, *Ophthalm. Surg.*, 21, 821, 1990.
9. Anmarkrud, N., Bergaust, B. and Bulle, T., The effect of Healon and Timolol on early postoperative intraocular pressure after extracapsular cataract extraction with implantation of posterior chamber lens, *Acta. Ophthalmol.*, 70, 96, 1992.
10. Punzi, L., Schiavon, F., Ramonda, R., Malatesta, V. and Bambari, P., Intra-articular hyaluronic acid in the treatment of inflammatory and non-inflammatory knee effusions, *Curr. Ther. Res.*, 43, 643, 1988.
11. Strachan, R. K., Smith, P. and Garner, D. L., Hyaluronate in rheumatology and orthopaedics: is there a role?, *Ann. Rheum. Dis.*, 49, 949, 1990.
12. Isdale, A. H., Hordon, L. D., Bird, H. A. and Wright, V., Intra-articular hyaluronate (Healon): a dose-ranging study in rheumatoid arthritis and osteoarthritis, *J. Drug. Dev.*, 4, 93, 1991.
13. Iwata, H., Pharmacologic and clinical aspects of intraarticular injection of hyaluronate, *Clin. Orthop.*, 289, 285, 1993.
14. Miller, J., Furgusen, R., Powers, D., Burns, J. and Shalaby, S. W., Efficacy of hyaluronic acid/nonsteroidal anti-inflammatory drug systems in preventing post-surgical tendon adhesions, *J. Biomed. Mater. Res./Appl. Biomater.*, 38(1), 25, 1997.
15. Shalaby, S.W. and Miller, J.A., Composition for Prevention of Inflammation and Adhesion Formation and Uses Thereof, U.S. Patent (to Poly-Med, Inc.) 5,866,554, 1999.
16. Thornton, J. et al. Clinical evaluation of 0.5% ferric hyaluronate adhesion prevention gel for the reduction of adhesion following peritoneal cavity surgery: Open-label pilot study, *Hum. Reprod.*, 13, 1480, 1998.
17. Becker, J. et al., Prevention of post-operative abdominal adhesion by a sodium hyaluronate-based absorbable membrane: A prospective, randomized, double-blind multicenter study, *J. Am. Coll. Surg.*, 183, 297, 1996.
18. Burns, J. et al., Reduction of post-surgical adhesion formation in rabbit uterine horn model with use of hyaluronate/carboxymethyl cellulose gel, *Fertil. Steril.*, 69, 415, 1998.
19. Greenawalt, K., Basi, L., Muir, C. and Burns, J., Physical properties of hyaluronic acid-based bioabsorbable membrane for the prevention of post-surgical adhesion, *Mater. Res. Soc. Symp. Proc.*, 292, 265, 1993.

20. Collier, J. H., Camp, J. P., Hudson, T. W. and Schmidt, C. E., Synthesis and characterization of polypyrrole hyaluronic acid composite biomaterials for tissue engineering applications, *J. Biomed. Mater. Res.*, 50, 574, 2000.
21. Schmidt, C. E., Shastri, V. R., Bacanti, J. P. and Langer, R., Stimulation of neurite outgrowth using an electrically conducting polymer, *Proc. Natl. Acad. Sci. USA*, 94, 8948, 1997.
22. Garner, B., Georgevich, B., Hodgson, A. J., Liu, L. and Wallace, G. G., Polypyrrole-heparin composites as stimulus-responsive substrates for endothelial cell, *J. Biomed. Mater. Res.*, 44, 121, 1999.
23. Shalaby, S.W. and Shah, K.R., Chemical modifications of natural polymers and their technological relevance, in *Water Soluble Polymers*, ACS Symposium Series, American Chemical Society, Washington, DC, Vol. 467, 1991, chap. 4.
24. Della Valle, F., European Patent Application (to Fidia, SpA), 0,216,453A₂, 1987.
25. Della Valle, F., European Patent Application (to Fidia, SpA), 0265,116-A₂, 1998.
26. Hunt, J. A., Joshi, H. N., Stella, V. J. and Topp, E. M., *J. Control. Rel.*, 12, 159, 1990.
27. Malson, T. and Debelder, European Patent 272,300, 1988.
28. Pelletier, S., Hubert, P., Payan, E., Marchal, P., Choplin, L. and Dellacherie, E., Amphiphilic derivatives of sodium alginate and hyaluronate for cartilage repair: Rheological properties, *J. Biomed. Mater. Res.*, 54, 102, 2001.
29. Danishefsky, I. and Siskovic, E., Conversion of carboxyl groups of mucopolysaccharides into amides of amino acid esters, *Carbohydr. Res.*, 16, 199, 1971.
30. Hamilton, R. G. and Raksha, R. A., PCT International Application WO 89/02445, 1989.
31. Francesco, D. V. and Aurelio, R., European Patent Application EP-265, 116, 1987.
32. Thomas, J., PCT International Application WO 90/09401, 1990.
33. Tomihata, K. and Ikada, Y., Preparation of cross-linked hyaluronic acid films of low water content, *Biomaterials*, 18,(3), 189, 1997.
34. Campoccia, D., Doherty, P., Radice, M., Brun, P., Abatangelo, G. and Williams, D.F., Semisynthetic resorbable materials from hyaluronan esterification, *Biomaterials*, 19, 2101, 1998.
35. Rastrelli, A., Beccro, J., Biviano, F., Calderini, G. and Pastorello, A., Hyaluronic acid esters, a new class of semisynthetic biopolymers: Chemical and physico-chemical properties, *Clin. Implant. Mater.*, 9, 199, 1990.
36. Solchaga, L. A., Dennis, J. E., Goldberg, V. M. and Caplan, A. I., Hyaluronic acid-based polymers as cell carriers for tissue-engineered repair of bone and cartilage, *J. Orthop. Res.*, 17, 205, 1999.
37. Solchaga, L.A., Yoo, J. U., Lundberg, M., Dennis, J. E., Huibregtse, G. A., Goldberg, V. M. and Caplan, A. I., Hyaluronan-based polymers in the treatment of osteochondral defects, *J. Orthop. Res.*, 18, 773, 2000.
38. Toole, B. P., Banerjee, S., Turner, R., Munaim, S. and Knudson, C., Hyaluronan-cell interactions in limb development, in *Developmental Patterning of the Vertebrate Limb*, Hinchliffe, J. R., Hurlle, J. M. and Summerbell, D., Eds., Plenum Press, New York, 1991, 215.
39. Toole, B. P., Hyaluronan in morphogenesis, *J. Intern. Med.* 242, 35, 1997.
40. Turley, E. A., Hyaluronan and cell locomotion, *Cancer Metastasis Rev.*, 11, 21, 1992.
41. Prestwich, G. D. and Vercruysse, K. P., Therapeutic applications of hyaluronic acid and hyaluronan derivatives, *PSTT*, 1(1), 42, 1998.

Section C

Developments in Preparative, Processing, and Evaluation Methods

8

New Approaches to the Synthesis of Crystalline Fiber-Forming Aliphatic Copolyesters

Shalaby W. Shalaby, Kimberly A. Carpenter and Bruce L. Anneaux

CONTENTS

8.1	Introduction	103
8.2	One-Step Synthesis of Caprolactone-Glycolide Segmented Copolymers and Monofilament Sutures Thereof	104
8.2.1	Design of the Polymerization Scheme and Rationale.....	104
8.2.2	Properties of Typical Polymers	105
8.2.3	Physicochemical and Biological Properties of Typical Monofilament Sutures	105
8.3	Copolyesters Made by End-Grafting Cyclic Monomers onto Polyalkylene Succinate and Monofilament Sutures Thereof.....	108
8.3.1	Design of Polymerization Scheme and Rationale.....	108
8.3.2	Properties of Typical Polymers	109
8.3.3	Physical and <i>In Vivo</i> Properties of Typical Monofilament Sutures.....	109
8.4	Conclusion and Perspective on the Future	110
	References	110

8.1 Introduction

Segmented copolymers geared for the production of compliant monofilament sutures described in Chapter 3 dealt with the use of end-grafting of an amorphous, or low melting, polyaxial polymeric initiator with cyclic monomers to form crystalline end-grafts. In this particular chain design, the

amorphous core, due to the polyaxial initiator, is responsible for the imparted high compliance. In a search for other approaches to the production of absorbable, segmented copolyesters for conversion to compliant monofilament sutures, two new experimental strategies were recently explored.¹⁻³ The first strategy was to:

- Use two monomers with vastly different rates of polymerization to yield segmented chains by direct copolymerization
- Use the two monomers in certain relative amounts to allow the formation of soft, noncrystalline segments that resist ester-ester interchange under prevailing polymerization and extrusion conditions
- Rely on a fast polymerizing comonomer as the source of the crystalline fraction, which retains its crystalline morphology through most of the polymerization and subsequent processes
- Conduct the copolymerization well below the T_m of the crystalline component of the segmented polymer

Accordingly, the first part of this chapter deals with the copolymerization of an ϵ -caprolactone/glycolide mixture that is rich in glycolide wherein the critical stage of the copolymerization is conducted in the solid state below 200°C, which is well below the 225°C of the T_m of polyglycolide.¹

The second strategy deals with the design of an aliphatic, segmented, high glycolide-based copolymer with soft segments that are free of the hydrolytically labile glycolyl group as is the case in earlier segmented/block, high glycolide copolyesters.³⁻⁵ More specifically, the new strategy is based on using hydroxy-terminated polyalkylene succinate as the polymeric initiator for preparing glycolyl-free amorphous, or low T_m , prepolymer for end-grafting with glycolide or glycolide-rich mixtures of monomers.^{2,3}

8.2 One-Step Synthesis of Caprolactone-Glycolide Segmented Copolymers and Monofilament Sutures Thereof

8.2.1 Design of the Polymerization Scheme and Rationale

Strategies for the synthesis of crystalline absorbable glycolide-based polymers based primarily on glycolide for the production of medical devices that exhibit in-use dimensional stability have been limited to:

- Random copolymers with at least 90% of their chains derived from glycolide

- Segmented/block copolymers which are made by two-step synthesis entailing the preparation of a prepolymer containing a minor fraction of glycolate sequence, following end-grafting with glycolide or a mixture of monomers containing more than 65% glycolide⁴⁻⁶

Composition limitation associated with the random copolymer approach and process complexity, and fair-to-inadequate reproducibility encountered in the two-step synthesis of segmented glycolide copolymer, provided the incentive to explore a simple yet reliable approach to prepare crystalline glycolide copolymers with a broad range of physicochemical properties and possibly unique functional performance.^{2,3}

Accordingly, this approach deals with the direct, one-step copolymerization of a monomer mixture containing less than 80% glycolide with the balance being caprolactone using a mono- or di-functional diol, amine, or aminoalcohol, an organometallic catalyst, and the appropriate reaction temperature/time scheme to yield crystalline copolymers. In a typical example, a monomer mixture containing less than 80% glycolide and more than 20% caprolactone is copolymerized in the presence of 1,3-propanediol at a monomer to indicator ratio of 500 to 1200 and catalytic amounts of stannous octanoate at a monomer-to-catalyst ratio of 40,000 to 70,000 to produce crystalline segmented copolymers containing less than 90% glycolide-based chain sequences that melt between 150°C and 220°C, and a crystalline fraction exhibiting a heat of fusion of 20 to 85 J/g.⁶

8.2.2 Properties of Typical Polymers

Table 8.1 depicts the properties of typical polymer products at the early stage of polymer development. The data in Table 8.1 show clearly that these polymers are indeed crystalline. However, the molecular weight was less than optimal and this led to further studies to produce higher molecular weight polymers as described in Table 8.2.

8.2.3 Physicochemical and Biological Properties of Typical Monofilament Sutures

Two of the early polymers described in Table 8.1 were melt spun into monofilament sutures, which exhibit the tensile properties shown in Table 8.3.

A new series of high molecular copolymers was prepared; typical properties of these polymers are outlined in Table 8.4.⁷ Monofilaments produced from these polymers were evaluated for their physical and *in vivo* properties as monofilament sutures. Typical results of such evaluation are summarized in Table 8.4.

TABLE 8.1
Early Glycolide/Caprolactone Segmented Copolymers: Synthesis and Properties¹

Polymer Number	Monomer Molar Ratios	Monomer Charge		Initiator Weight (g)	Reaction Conditions ^a			Polymer Properties		
		Glycolide (g)	Caprolactone (g)		Temp (°C)	Time (h)	Tm (°C)	ΔH (J/g)	Viscosity (dL/g)	
A-1	C/CL: 70/30	105.5	44.5	0.146	180	6	218	76.2	0.89	
A-2	G/CL: 60/40	90.0	60.0	0.327	180	6	157	22.1	0.62	
A-3	G/CL: 70/30	105.0	45.0	0.327	180	6	209	66.9	0.74	
A-4	G/CL: 70/30	105.5	44.5	0.198	180	6	204	43.9	0.82	
A-5	G/CL: 70/30	105.5	44.5	0.151	180	2	199	140.0	0.69	
A-6	G/CL: 75/25	226.0	74.0	0.282	180	3	204	82.8	1.12	

^a A 0.2 M solution of stannous octanoate in toluene was used to provide a mole ratio of 60,000 for monomer/catalyst; 1,3- propane diol was used as the initiator.

TABLE 8.2

Typical Fiber Properties of Early Glycolide/Caprolactone Segmented Copolymers¹

Polymer Number ^a	Diameter (mm)	Elongation (%)	Tensile Strength (Kpsi)	Modulus (Kpsi)
A-1	10.6	43	70	160
A-6	16.6	44	83	290

^a See Table 8.1 for composition.

TABLE 8.3

Typical Properties of High Molecular Weight Segmented ϵ -Caprolactone/Glycolide Copolyesters Prepared by One-Step Synthesis¹

Polymer Number	Initial Monomer Charge (CL/G ^a)	Polymer Properties		
		I.V. ^b (dL/g)	DSC Data	
			T _m (°C)	ΔH_f (J/g)
A-7	30/70	1.66	190	51
A-8	28/72	1.24	193	60
A-9	26/74	1.56	204	43

^a Molar ratio.

^b In HFIP.

TABLE 8.4

Typical Suture Properties of Monofilaments of High Molecular Weight Segmented CL/G Copolymers Prepared by One-step Synthesis¹

Polymer Number ^a	Monofilament Suture Physical Properties					Suture <i>In Vivo</i> BSR at One Week	
	Diameter (mm)	Linear Tensile Strength (Kpsi)	Young's Modulus (Kpsi)	Elongation (%)	Knot Strength (N)	1	2
A-7	0.23	84	114	68	25	—	—
A-8	0.30	85	75	49	23	—	—
A-9	0.41	90	64	67	50	63	26

^a See Table 8.3 for composition.

8.3 Copolyesters Made by End-Grafting Cyclic Monomers onto Polyalkylene Succinate and Monofilament Sutures Thereof

For this group of new polymers, a prepolymeric polyalkylene succinate was prepared, end-grafted with ϵ -caprolactone (CL) and/or trimethylene carbonate (TMC), and the product was then end-grafted with glycolide or a glycolide-rich mixture of monomers. Discussion in this chapter is focused on these copolyesters based on polytrimethylene succinate.

8.3.1 Design of Polymerization Scheme and Rationale

Interest in segmented copolymers having soft segments of less hydrolabile linkage than those described earlier as containing glycolide-based sequences provided an incentive to pursue the study noted in this section.⁴⁻⁶ To this end, polyalkylene succinate, and specifically polyethylene succinate and polypropylene succinate, were selected as main parts of the soft component of segmented copolymers because of their less hydrolabile properties as compared to those described earlier in the literature.⁴⁻⁶ The respective new study was directed toward the design of segmented/block copolymeric chains to yield absorbable materials for the production of biomedical articles with controlled absorption and strength retention profiles. The copolymers of the present family of polymers have an amorphous or low melting temperature phase that is based primarily on soft segments or blocks whose chains are essentially devoid of distinctly hydrolytically labile ester linkages and hence provide an overall minimized hydrolytic instability.

The present copolymers are defined as blocked or segmented because they are of the type having blocks or segments made from "hard" phase-forming monomers and one or more blocks or segments made from "soft" phase-forming monomers. Generally, the hard phase blocks or segments lend mechanical strength to the overall copolymer and the soft phase blocks or segments render the copolymer compliant. The term "block copolymer" typically refers to a copolymer having two or more blocks or long structures of repeat units such as the general form A-B, A-B-A, or (A-B)_n. A "segmented copolymer" is typically considered to be one with multiple relatively short structures such as -a-b-a-b ... or -a-b-c-a-b ..., where the a, b, and c are shorter than the A and B of the block copolymers. The present copolymers are referred to as "block/segmented copolymers" herein because they may contain a limited number of long blocks or several short segments per chain. These terms are intended to distinguish the present copolymers from random copolymers.

The copolymers which are the subject of this section are formed by the copolymerization of a prepolymer, which will ultimately form the soft block or segments, with one or more monomers which will form the hard blocks

TABLE 8.5

Typical Polymer Properties^a of Segmented Copolyesters of End-grafted Polytrimethylene Carbonate (PTS)^{2,3}

Polymer Number	Polymer Composition ^b PTS/TMC/G	Thermal Data	
		T _m (°C)	ΔH _f (J/g)
B-1 ^c	15/25/60	207	53
B-2	15/25/63	225	63
B-3 ^c	15/25/60	224	72

^a All polymers were insoluble in hexafluoro-2-propanol for viscosity measurement.

^b Based on contributed amounts of PTS, TMC, and glycolide to the two-stage, end-grafting polymerization charges.

^c End-grafting conditions for B-1 and B-3 were not identical charges.

or segments. A typical prepolymer of the present system is a polyalkylene dicarboxylate, such as a polytrimethylene succinate. The polytrimethylene succinate is typically end-grafted first with ϵ -caprolactone (CL) and/or trimethylene carbonate (TMC). The product of this reaction is then end-grafted with glycolide or a glycolide-rich mixture containing a small amount of TMC. Generally, the soft blocks or segments must be incapable of crystallization between 25 and 50°C and display a high degree of chain mobility at about room temperature. That is, preferably the prepolymer which will ultimately form the soft block is either amorphous or has a melting temperature of 50°C or less. However, the second end-grafting step is designed to produce crystalline terminal segments, such as those derived exclusively or primarily from glycolide.

8.3.2 Properties of Typical Polymers

A number of polyesters made by two-stage end-grafting with trimethylene carbonate and glycolide were prepared and their respective properties are shown in Table 8.5. The data in Table 8.5 show that these polymeric high-melting materials, with a sufficiently high degree of crystallinity (measured in terms of ΔH_f), are well-suited for use as fiber formers.

8.3.3 Physical and *In Vivo* Properties of Typical Monofilament Sutures

Tensile and *in vitro* and breaking strength retention data of typical monofilament sutures made of the polymers described in Section 8.3.2 are summarized in Table 8.6. The data in Table 8.6 indicate that the polymers described in Table 8.5 can be converted to monofilament sutures with competitive strength retention and breaking strength profiles as the commercially available braided sutures made of polyglycolide or 90/10 poly(glycolide-co-L-lactide).

TABLE 8.6

Typical Suture Properties of Monofilaments Made from Segmented Copolymer of End-Grafted Polytrimethylene Succinate^{2,3}

Polymer Number	Monofilament Suture Physical Properties				Suture <i>In Vivo</i> BSR ^a at One Week		
	Diameter (mm)	Linear Tensile Strength (Kpsi)	Young's Modulus (Kpsi)	Elongation (%)	2	3	4
B-1	0.30	78	251	39	—	43	22
B-2	0.14	96	568	43	80	65	34
B-3	0.26	67	452	23	73	48	44

^a *In vitro* breaking strength retention in phosphate buffer solution at pH 7.4 and 37°C.

8.4 Conclusion and Perspective on the Future

Available data relevant to the two new approaches to the design and preparation of novel, absorbable chain molecules illustrate the great flexibility that is now available in tailor-made absorbable polymeric materials as preferred substitutes for existing ones. Segmented CL/G copolyester made by one-step copolymerization and the end-grafted polyalkylene succinate copolymers may provide preferred monofilament suture alternatives to surgical gut sutures and high glycolide braided sutures, respectively. It is also anticipated that the availability of these two new classes of polymers will propel the growing use of absorbable polymers in vascular applications.

References

1. Shalaby, S. W., Direct Synthesis of Segmented Glycolide Copolymers and Crystalline Materials Therefrom, U.S. Patent (to Poly-Med, Inc.) 6,498,229, 2002.
2. Shalaby, S. W., Copolyesters with Minimized Hydrolytic Stability and Crystalline Absorbable Copolymers Thereof, U.S. Patents (to Poly-Med, Inc.) 6,255,408, 2001; 6,503,991, 2003.
3. Schiretz, F. R., Jr., Anneaux, G. L., Shalaby, W. S., Linden, D. E., Pilgrim, J. A., Quirk, J. R. and Shalaby, S. W., End-grafted polyalkylene succinate copolymers: A new family of crystalline absorbable materials, *Trans. Soc. Biomater.*, 25, 162, 2002.
4. Shalaby, S. W. and Johnson, R. A., Synthetic absorbable polyesters, in *Biomedical Polymers: Designed-to-Degrade Systems*, Shalaby, S. W., Ed., Hanser Publishers, New York, 1994, 1.
5. Shalaby, S. W. and Jamiolkowski, D. D., Surgical Articles of Copolymers of Glycolide and ϵ -caprolactone and Methods of Producing the Same, U.S. Patent (to Ethicon, Inc.) 4,700,704, 1987.

6. Bezwada, R. S., Jamiolkowski, D. D. and Shalaby, S. W., Segmented copolymers of ϵ -caprolactone and glycolide, U.S. Patent (to Ethicon, Inc.) 5,133,739, 1992.
7. Carpenter, K. A., Anneaux, G. L., Taylor, M. S. and Shalaby, S. W., Poly-Med, Inc., unpublished work, 2002.

9

Advances in Morphological Development to Tailor the Performance of Absorbable Medical Devices

Saša Andjelic, Benjamin D. Fitz, and Dennis D. Jamiolkowski

CONTENTS

9.1	Introduction	114
9.2	Methods and Techniques for Monitoring Crystallinity	116
9.2.1	Supramolecular Crystal Developments.....	116
9.2.2	Overall Crystallization Kinetics.....	119
9.3	Effect of Crystallinity on Segmental Dynamics.....	122
9.3.1	Effect on Glass Transition Temperature	122
9.3.2	Intra- and Inter-Spherulitic Amorphous Phase Dynamics.....	127
9.4	Advanced Methods to Accelerate Crystallization Kinetics of Absorbable Copolymers	130
9.4.1	Physical Route: Stress-Induced Crystallization.....	130
9.4.2	Chemical Route: a Novel Synthetic Method Using Mixed Initiators	132
9.5	Effect of Morphology on Polymer Absorption Profiles	135
9.5.1	Effect of Molecular Orientation	135
9.5.2	Effect of Crystallinity	136
9.5.3	Hydrolysis Profiler.....	137
9.5.4	Drug Delivery Vehicles	138
9.6	Novel Polyesters: POE Polymers.....	138
9.7	Conclusion and Perspective on the Future	139
	Acknowledgment.....	139
	References	140

9.1 Introduction

Since the early to mid-1970s, absorbable polymers have been finding uses in a number of medical applications. First came fibers. Multifilament sutures based on polyglycolide and a poly(lactide-co-glycolide) random copolymer were followed by monofilament sutures based on poly(*p*-dioxanone) homopolymer and then other copolymers with nonrandom sequence distributions. Injection molded products of poly(*p*-dioxanone) and polylactide presented opportunities for medical devices with relatively complex shapes. Additionally, with its ability to retain its mechanical properties for longer time periods, polylactide was recognized as having utility for medical devices in the area of orthopedics. Eventually, researchers were able to develop devices that were valued not for their mechanical properties and how they changed with time but for their diffusional properties. With this, the area of controlled drug delivery vehicles presented yet another wonderful opportunity for absorbable polymers.

In all this work, chemistry plays a major role. Ponder, for example, a glycolate ester with its alcohol-based moiety, primary in nature, vs. a lactate ester with its secondary alcohol moiety. Steric effects and electronic considerations explain the slower hydrolysis rate of the latter. Chemistry is then a dominant player in determining reaction rates that then greatly influence tissue absorption profiles and biological compatibility. But even samples of the same polymer, with the same molecular weight distributions, indistinguishable in all chemical features, can behave very differently with regard to their biological and mechanical performances if they exhibit different morphologies.

The word “morphology” is from the Greek *morph*, meaning form or shape, and *logos*, meaning study or knowledge. Polymer morphology then refers to the shape or patterns in assemblies of the macromolecular chains. When the chains can go to a lower energy state in which regular packing of the molecules occurs, the polymer is said to crystallize. The driving force for such an occurrence is generally enthalpic, and there are symmetry requirements that must be met. At its simplest, morphological characterization of a semicrystalline polymer includes the relative amount of the crystalline and amorphous phases, the amount of crystalline and amorphous orientation present, the nature of the crystal structure, and the size distribution of the crystals. These characteristics are usually influenced by the thermal and mechanical processing history the polymer was exposed to during morphological development. From an ease-of-manufacturing standpoint, the rate at which morphology is developed is very important. Thus kinetic information as a function of processing conditions is vital in creating fabrication schemes.

For a given polymer system, the crystal size distribution is influenced by the initial nucleation density, the nucleation rate, the rate of crystal growth, and the state of orientation. When the polymer is subjected to conditions in which nucleation predominates over radial growth, smaller crystals result. Larger crystals will form when there are relatively fewer nucleation sites and faster growth rates. Consider when a crystallizable amorphous polymer undergoes strain; a nonspherulitic stress-induced crystalline texture will generally develop, as well as a partially oriented amorphous phase. This morphology is influential on final mechanical and end use properties and needs to be understood.

Unlike the influence of morphology on mechanical behavior, the effect on biological behavior is a less mature area of endeavor. For absorbable polymers, the effect of crystalline structure on diffusion and reaction rates provides insight. The relative amount of crystalline phase influences the rate of diffusion of water into a hydrolytically unstable polymer. Furthermore, the rate of hydrolysis of a given ester group in the polymeric chain will depend on whether the group resides in a self-protecting crystal or whether it exists in an unprotected, easily accessed, amorphous phase.

It should be recognized that although molecular orientation can be used to develop great strength in the "machine direction," under unfortunate circumstances it can play havoc with dimensional stability in some parts. Molecular orientation is sought in fibers, for instance, to increase physical properties — the "machine direction" is the fiber direction and orientation is developed by the drawing process. The orientation is "locked in" by crystallizing the polymeric fiber during an annealing step, usually under some amount of force or other constraint. In the case of injection molding, orientation may be unwanted in amorphous parts because the orientation, or stress, is now a driving force to cause distortion in the part anytime the storage temperature exceeds the glass transition temperature. More than one fabricator without an understanding of the polymer physics involved has produced intricately shaped parts, such as screws of polylactide, only to have them distort and warp upon sterilizing by ethylene oxide (EO). The glass transition of the amorphous polymer, not very high to begin with, is reduced even lower by the absorption of EO gas. Once the new T_g drops below the temperature profile of the sterilizing process, molecular mobility is greatly enhanced, allowing the article to relieve the stress by distorting.

If we are to develop an understanding of the relationship in absorbable polymers between key physical/biological properties and morphological characteristics, it is important to investigate how morphology is developed and to understand how it is controlled by processing parameters and molecular characteristics. With ultimate design and control of morphology as a goal, this chapter will highlight the application of existing and new methodologies in characterizing and understanding the structural development of both the crystalline and amorphous phases of synthetic absorbable polymers.

9.2 Methods and Techniques for Monitoring Crystallinity

9.2.1 Supramolecular Crystal Developments

Synthetic absorbable polymers are generally semicrystalline, with crystalline lamella incorporated into a variety of supramolecular structures depending on crystallization conditions and chemical characteristics of a material. Typically, under quiescent conditions axialitic or variants of spherulitic morphologies develop. Visual characterization of developing supramolecular structures can be performed by a variety of techniques including hot-stage optical microscopy (HSOM), scanning electron microscopy (SEM), transmission electron microscopy (TEM), small-angle light scattering (SALS), or the recently developed atomic force microscopy (AFM). As an example of such measurements, Figure 9.1a to 9.1c shows a series of morphological images captured during isothermal crystallization of poly(*p*-dioxanone), PDS, at 85°C by AFM, HSOM, and SALS, respectively.

An advantage of a visual characterization method over nonvisual alternatives, such as x-ray or thermal analysis, is that nucleation rates and spherulitic growth rates can be determined separately.¹ Separately studying nucleation and growth significantly enhances our understanding of crystallization behavior — ultimately providing processing and device optimization. One experimental characterization technique providing benefits of direct visualization of the development of morphology is arising from the recently developed AFM. The tremendous resolution and range of viewable length-scales, from millimeters to nanometers, imaged rapidly and nondestructively, allows for real-time observation of microscopic transient phenomena. Recently this technique has been used to visualize nucleation and lamellar growth fronts in crystallizing polymers.^{2,3} This level of insight is possible on absorbable medical polymers. For example, we show in Figure 9.1 the “birth” of a spherulite of PDS; the new emerging spherulite is identified by an arrow.

To illustrate the value of intensive characterization of the polymer crystallization process for absorbable medical polymers, we continue with a case study of PDS. If we look sequentially through the crystallization process, the first stage is the formation of active nuclei. This occurs when segments of adjacent polymer chains register and group. The grouping may be temporary, and the group may be disrupted by the thermal kinetic jostling that occurs in the polymer melt. But when the group exceeds a critical size, the nucleus is activated and stable, and will provide the starting point for lamellar growth. This creation, destruction and critical nucleation size were impressively captured in dynamic flux by direct visualization via AFM in a recent study.² Once lamellae begin to grow from a stable nucleus, they grow radially, but due to the statistical nature of the trajectory of this growth, the lamellar structures tend to curve at the distal ends, resembling bundles of wheat.⁴ Polymer chains in the space between crystalline lamellae are amor-

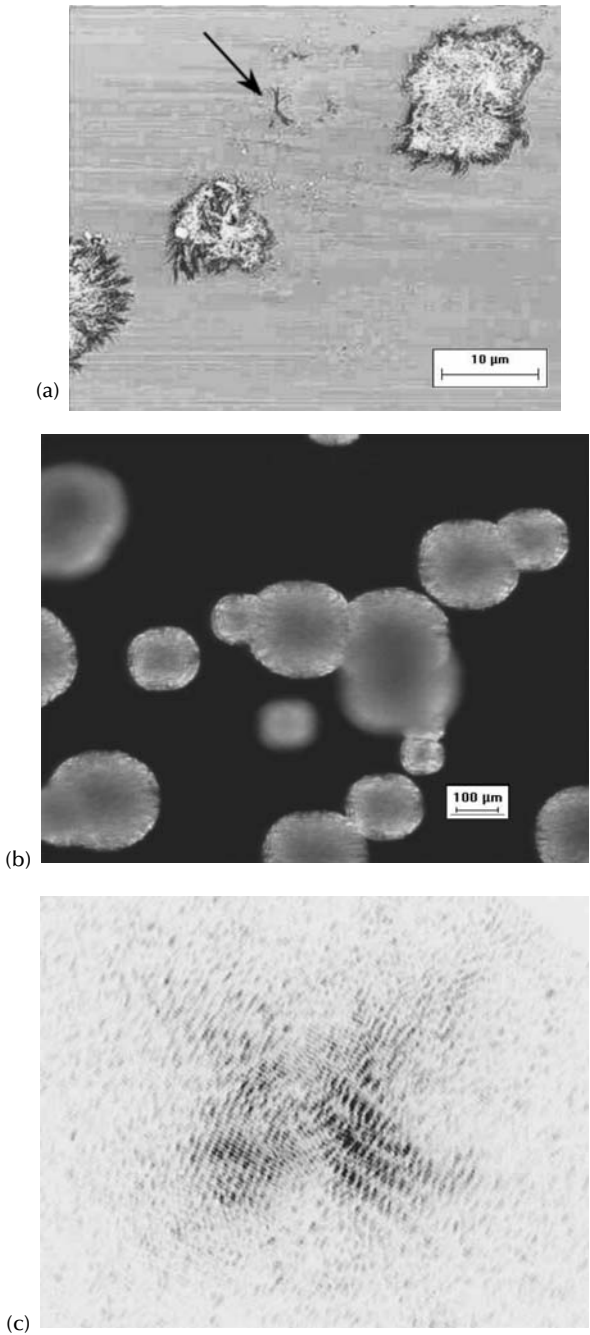


FIGURE 9.1
A series of morphological images captured during isothermal crystallization of poly(*p*-dioxanone), PDS, at 85°C by (a) AFM, (b) HSOM, and (c) SALS.

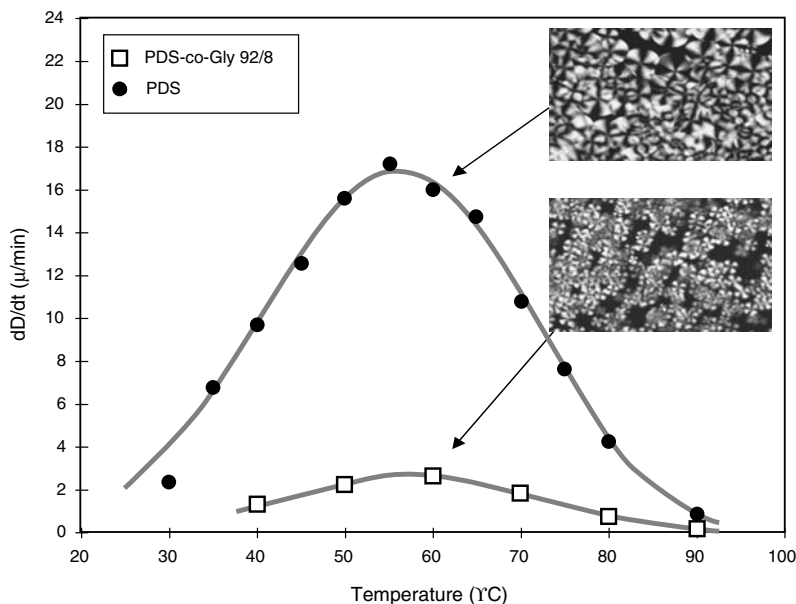


FIGURE 9.2

Isothermal spherulitic growth rates of PDS and one of its slower-to-crystallize copolymers (PDS-co-Glycolide, 92/8) as a function of crystallization temperature. HSOM images of PDS and its copolymer captured after isothermal crystallization at 60°C after 15 and 30 min, respectively, are also included.

phous. In addition to lamellar growth is the appearance of new lamellae in the amorphous intralamellar spacing, known as secondary crystallization. This process can be detected by small-angle x-ray scattering. However, in order to observe secondary crystallization in real time, a powerful x-ray source, available at a synchrotron, is required.⁵ Less powerful x-ray sources have integration times that are too long to capture the dynamic process. During further crystal growth, eventually these assemblies of lamellae continue to grow to the point of being recognizable in an optical microscope as spherulitic morphologies.

Once the supramolecular structure of a crystallizing polymer reaches a mature spherulitic shape, and the diameter is greater than $\sim 5 \mu\text{m}$, the HSOM method (Figure 9.2) becomes particularly useful to monitor spherulitic growth and nucleation rate parameters in real-time. These measurements provide insights into crystallization phenomena, such as:

- The determination of the nature of nucleation (homogeneous or heterogeneous)
- The fact that spherulites grow linearly with time at a given crystallization temperature

- Spherulite radial growth continues at a constant rate, even after other portions of the spherulite have impinged with its neighbors — indicating that lamellae within a given spherulite grow independently
- The spherulite growth rate, dD/dt , varies with crystallization temperature, T_c , by decreasing as the melting point is approached.

This last point has been described by the Lauritzen and Hoffmann (LH) nucleation theory.^{6,7}

To illustrate the above, we consider the crystallization of the absorbable polymer PDS. Isothermal spherulitic growth rates of PDS and one of its slower-to-crystallize copolymers (PDS-*co*-Glycolide, 92/8, mole basis) are plotted in Figure 9.2 over a broad range of crystallization temperatures. The maximum growth rate for these polymers is about 60°C. The spherulitic growth rate of PDS homopolymer is significantly higher (~8×) than that of the copolymer. This is due to the disruptive role of the comonomer in the chain packing of lamellae. HSOM images of PDS and its copolymer captured after isothermal crystallization at 60°C after 15 and 30 min, respectively, are also included in Figure 9.2. A slower growth rate of the copolymer is clearly evident, but nucleation density does not appear to be reduced by the presence of the glycolide moiety in the structure.

In contrast to polarized optical microscopy, SALS can measure crystal structures of a smaller size (Figure 9.1c) in the range of 0.05 μm to several microns.⁸ Additionally, SALS transmission measurements can be used to obtain real-time crystallization kinetics since density fluctuations in the material increase with time.⁹ This technique may also be used for the detection of an induction period in crystallization.

Supramolecular spherulitic structures shown in Figure 9.1a to c are composed of alternating stacks of crystalline and amorphous layers. The size, direction, and orientation of these lamellar subunits may also play a role in the physical and biological characteristics of implanted absorbable medical devices. In order to gain important information on the real-time development of the length-scale of the crystalline lamella during crystallization, small-angle x-ray (SAXS) synchrotron radiation must be used.⁵ For example, recent SAXS studies on PDS and its glycolide-containing copolymer revealed that the crystal thickness of both materials increases linearly with temperature, indicating the gradual formation of thicker lamellae at higher crystallization temperatures. On the other hand, the thickness of the amorphous layer does not change with crystallization temperature for either polymer.

9.2.2 Overall Crystallization Kinetics

The overall crystallization rates depend on two factors: the concentration of growing spherulites with time (nucleation density) and the rate of spherulitic growth. Contributions of both processes to the overall crystallization kinetics can be studied in real time by a variety of techniques such as differential

scanning calorimetry (DSC), dielectric relaxation spectroscopy (DRS), small-angle x-ray scattering (SAXS), wide-angle x-ray diffraction (WAXD) using synchrotron radiation, and small-angle light scattering (SALS).^{5,9-12}

An inherent characteristic of many absorbable polyesters is their relatively slow crystallization rate. This difficulty for polymer processing, however, presents an advantage in that these materials can be easily quenched into the completely amorphous state and studied isothermally over an unusually wide temperature range. These slow processes present experimental challenges in terms of measuring their crystallization rates in a time-resolved fashion. Here are some examples of standard characterization tools that are inadequate for these studies. For example, calorimetrically, the enthalpy change during a slow process can be near or below instrument sensitivity. Even small- and wide-angle x-ray techniques have limited utility if a material has a low (<15%) degree of crystallinity, resulting in a large error resolving the amorphous and crystalline diffraction peaks. Furthermore, in the case of polymers that exhibit a nonspherulitic crystalline morphology with an unusually high nucleation density, crystal growth analysis via hot-stage optical microscopy will not be of use since the feature size will be smaller than the instrument's capability to resolve. These latter material considerations will then also rule out small-angle light scattering to study crystal growth.

One advanced experimental tool with sufficient sensitivity to monitor crystallization of both slow and fast crystallizable materials is dielectric relaxation spectroscopy, DRS.^{6,11} Dielectric measurements can provide real-time monitoring of crystallization for a wide variety of semicrystalline polymers. Real-time data on developing crystalline morphology are of great utility since such information may be directly incorporated into the design for optimal biological performance. The underlying mechanism enabling DRS to follow crystallization kinetics is via monitoring **the decrease of** relaxed (low-frequency) permittivity, ϵ_0' , with crystallization time. This decrease can be associated with the progressive reduction of the amorphous phase as segments of the polymer chains (and therefore dipoles on the chains) become immobilized in crystals. As an illustration, in Figure 9.3 relaxed permittivity of PDS is plotted against time for a series of selected isothermal crystallization temperatures at a frequency of 25 kHz. Before crystallization, all of the samples are in a fully amorphous state. Initial values of ϵ_0' (at $t = 0$) are lower with increasing temperature due to decreasing dipole relaxation strength with temperature.

A quantitative measure of isothermal crystallization is the crystallization half-time, $t_{1/2}$. Crystallization times expressed as the reciprocal of $t_{1/2}$ (crystallization rate) are shown in Figure 9.4 as a function of crystallization temperature. These results indicate that the fastest crystallization for the PDS homopolymer can be obtained at approximately 47°C. For the sake of comparison, Figure 9.4 also includes spherulitic growth rates from HSOM.

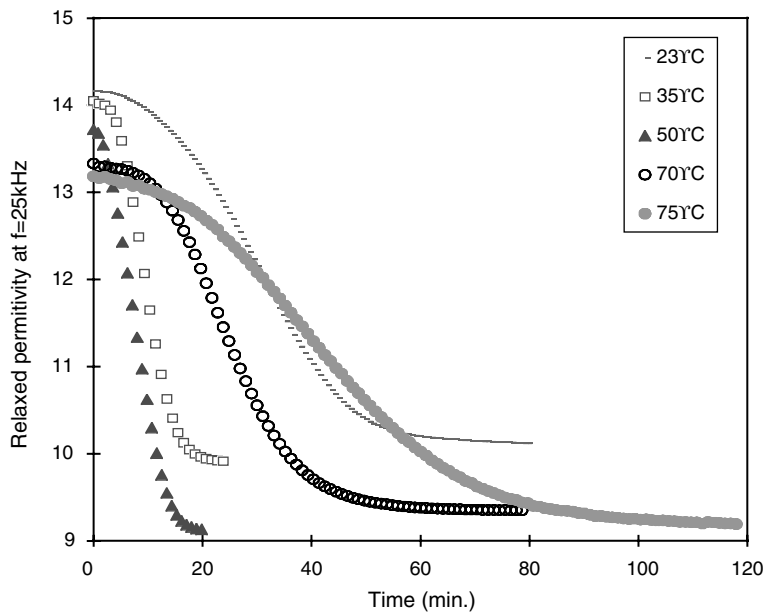


FIGURE 9.3
Relaxed permittivity of PDS against time for a series of selected isothermal crystallization temperatures at a frequency of 25 kHz.

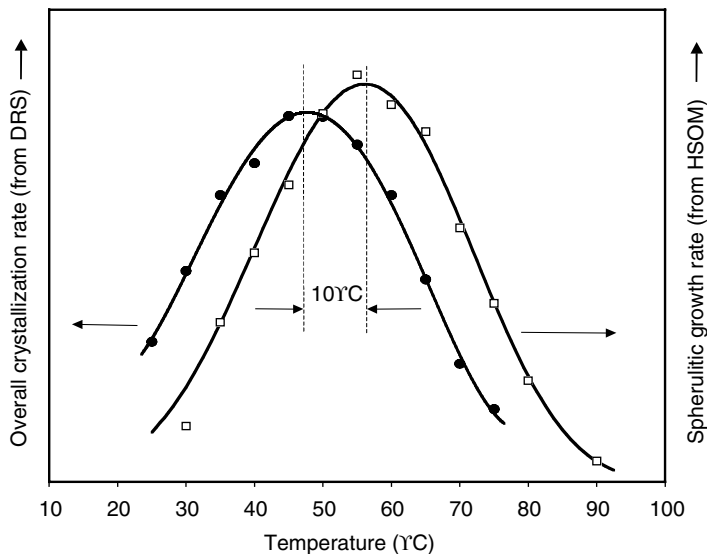


FIGURE 9.4
Overall crystallization rate (from DRS) and spherulitic growth rate (from HSOM) for PDS homopolymer as a function of temperature.

9.3 Effect of Crystallinity on Segmental Dynamics

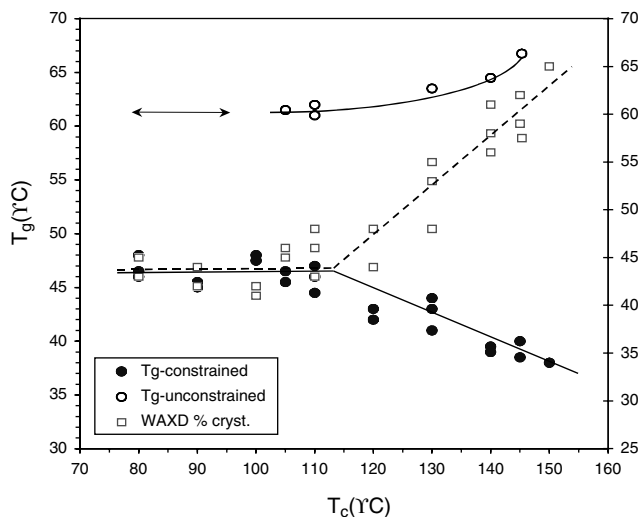
In this section we present an in-depth examination of the different types of amorphous phases in crystallizing polymer melts and of how the polymer chain segmental dynamics vary between these different regions. For absorbable polymers used in medicine, such a detailed understanding of the polymer may seem excessive. However, dismissing these details would not be prudent since there is an ever increasing trend towards the fabrication of smart devices and active devices, for which understanding and characterizing the microscopic morphology and diffusion characteristics are crucial. An example of this is in controlled release applications, or for micro electromechanical systems (MEMS).

9.3.1 Effect on Glass Transition Temperature

It is widely recognized that the degradation rate of absorbable polymers *in vivo* or in appropriate environmental conditions depends on polymer morphology and glass transition temperature, T_g . In general, the T_g of a polymer is unchanged or increases slightly with the degree of crystallinity. The argument made for the T_g increase with crystallinity is that the segmental mobility in the amorphous phase is reduced near crystal lamellae. To acquire sufficient energy to mobilize these hindered chains in a vitrified amorphous phase, a higher temperature is required, and thus a higher T_g is commonly found.

Contrary to this well-known and widely observed T_g trend with polymer crystallinity, there have been some recent reports that are at odds with the conventional observations.^{13–15} The last two studies described an unusual decreasing trend in the glass transition temperature of poly(L-lactide), PLLA, observed during isothermal crystallization under special, constrained crystallization conditions. Constrained conditions are those in which the volumetric contraction during crystallization is restricted. This is due to the crystallizing polymer being nominally prevented from shrinking during crystallization by the polymer affinity to the walls of the vessel containing it. Unconstrained conditions have no constraints on one or more surface of the crystallizing polymer (e.g., an open-topped vessel, where during crystallization the polymer is free to contract from the top surface).

It was found that the T_g of PLLA crystallized under partially constrained conditions is dramatically lowered compared to that obtainable under standard conditions. Interestingly, it was observed that the T_g also decreases systematically with an increase in the crystallization temperature. On the other hand, the T_g of PLLA samples crystallized under unconstrained conditions had the expected trend of increasing with increasing T_c . A summary of the observed T_g depression is shown in Figure 9.5. In this composite figure, the T_g of the constrained samples, and unconstrained samples and their corresponding crystallinity levels, are plotted against the crystallization tem-

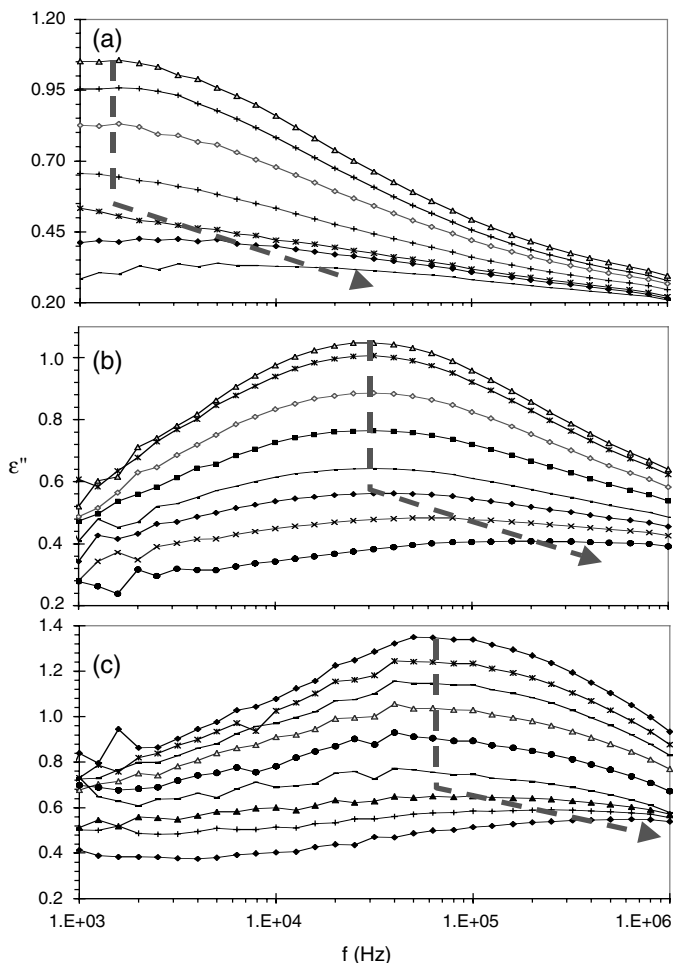
**FIGURE 9.5**

The glass transition temperature, constrained PLLA, and an unconstrained PLLA sample and their corresponding crystallinity levels (from WAXD) as a function of crystallization temperature.

perature. This figure shows how crystallinity increases with T_c for both sample types. Despite the fact that T_g differs considerably depending on the crystallization method used, all other physical parameters that were measured, including the melting point and degree of crystallinity, were not affected.

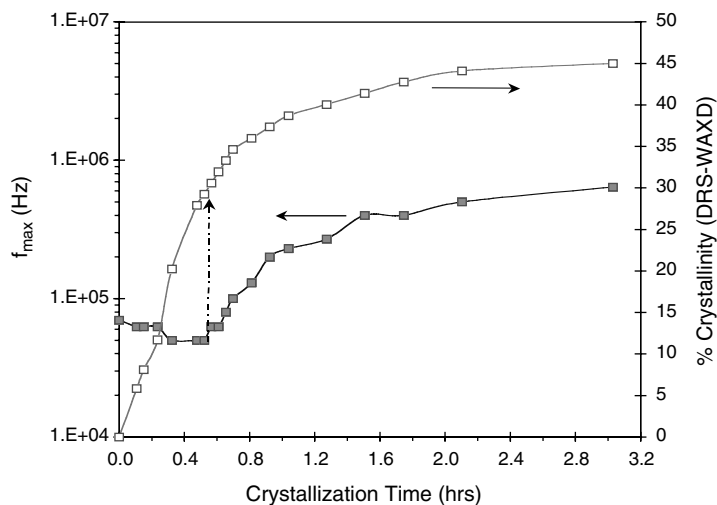
The phenomenon may be understood in the following way. For the constrained samples, provided that voids do not form in the polymer, the free volume in the amorphous phase of the polymer will increase with crystallization. The increasing crystal volume fraction has a higher density than the amorphous fraction, depleting mass from the amorphous phase, which is not able to contract to maintain its normal density. On cooling from the crystallization temperature, the polymer vitrifies in its high-free-volume state, fixing the sample's overall volume, which is preserved when the sample is removed from the constraining environment. The crystallites which span the bulk of the polymer may also act to fix the overall sample volume. Because of this, prepared samples exhibit a depressed T_g on the first DSC heating step above the melting point.

The initial findings of the T_g depression in PLLA were *ex situ* characterization by thermal analysis. In the remainder of this section the use of advanced characterization methods is illustrated to provide additional insight into the novel behavior. The methods used to address the polymer were those appropriate to provide *in situ*, real-time information on morphology via SALS, and on segmental dynamics via DRS.¹⁵ The rationale for the use of these tools is that the dipolar loss peak in the frequency domain (from DRS) is closely related to the glass transition of a given polymer system — hence, under isothermal conditions, a change in the loss peak frequency is

**FIGURE 9.6**

Dipole loss data of constrained PLLA in the frequency domain as a function of crystallization time at (a) 75, (b) 85, and (c) 90°C.

an indicator of a T_g shift. Figure 9.6 is a representative example of such a case. In this figure, the dipolar loss data of constrained PLLA are shown in the frequency domain as a function of crystallization time at selected isothermal conditions. Due to the fact that PLLA can be easily supercooled upon applying moderate cooling steps, the first spectra shown in Figure 9.6 belong to the fully amorphous polymer melt. The onset of crystallization is marked by the first drop in the intensity of the dipole peak. The reduction in the dipolar peak intensity is related to the portion of polymer chains that become dielectrically inactive due to their incorporation in the crystal lattice. As crystallization progresses, the intensity of the dipole peak decreases. This figure also shows that in the later stage of crystallization the dipolar relax-

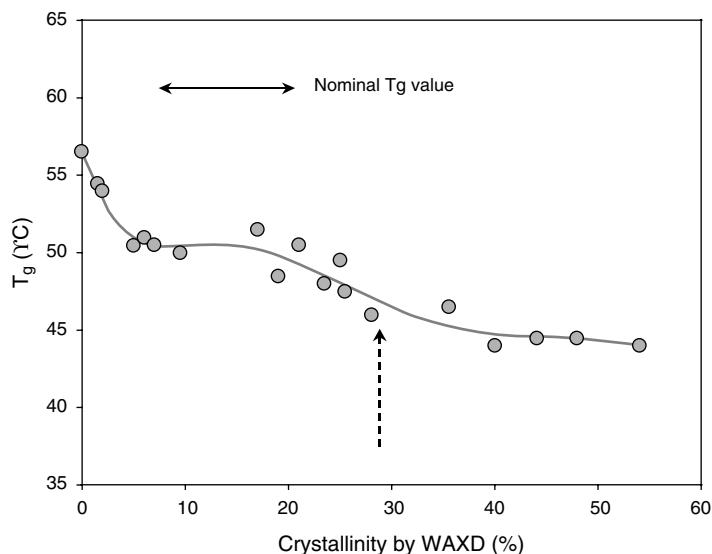
**FIGURE 9.7**

The frequency at the maximum loss peak and overall crystallinity vs. crystallization time for constrained PLLA crystallized isothermally at 90°C.

ation peak shifts to higher frequency (the bold dashed arrow connects the loss maxima of each curve in the figure). The shift of the dipole peak to higher frequency clearly reveals the T_g -depression that occurs during isothermal crystallization and is not generated on cooling from the crystallization temperature. The unique *in situ* measurement via DRS of a T_g change provides valuable information towards understanding the T_g -depression in PLLA found by calorimetric measurements.

Another approach to interpreting the DRS findings is shown in Figure 9.7, where the frequency at the maximum loss peak is plotted vs. crystallization time for PLLA crystallized isothermally at 90°C. In the same figure, the degree of crystallinity obtained by DRS and WAXD methods that corresponds to the observed τ frequency shifts is included. Up to about 30% crystallinity there is practically no change in the dipole peak position. At a later crystallization time, a gradual shift of the peak to a higher frequency region is clearly evident. The effect of crystallinity on the glass transition behavior of PLLA was further explored. T_g and the corresponding degree of crystallinity for a series of samples that had been partially crystallized in the DOS cell at 90°C were determined using the kinetics profile displayed in Figure 9.7. The relationship between T_g and crystallinity is shown in Figure 9.8.

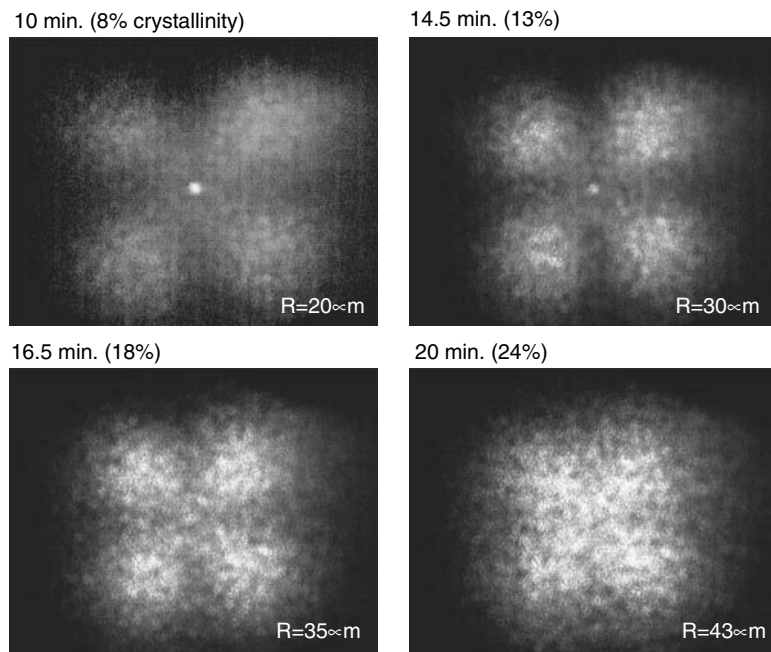
To discover whether a morphological change is occurring in PLLA that is affecting T_g , a novel combination of experimental methods is required. This combination of techniques operates simultaneously on the polymer sample so that both types of information are given on exactly the same sample at the same time thus alleviating any difficulties on quenching samples and ensuring that any thermal history between samples is matched. Simulta-

**FIGURE 9.8**

The glass transition temperature and the corresponding degree of crystallinity for a series of constrained PLLA samples partially crystallized in the DOS cell at 90°C.

neous DRS measurements and SALS scattering patterns on PLLA are collected. As an illustration of the SALS measurements, Figure 9.9 shows digital images of SALS scattering patterns taken at different times during the isothermal crystallization of PLLA at 90°C. Very early in the process, a wide-spread, four-lobed pattern of low intensity is evident, indicating an early development of spherulitic structure. These patterns are seen preceding the first detection of crystallinity by DRS, suggesting that SALS is a more sensitive technique to follow induction periods in crystallization.

Determination of structural parameters from the SALS images involves evaluating the scattering pattern along the 45° azimuthal line.⁹ Analyzing the SALS data, the spherulitic size can be computed.¹⁶ For the patterns shown in Figure 9.9, the average spherulite diameters range from an average of 20 μm at 10 min to 43 μm at 20 min. At the same time, the overall crystallinity increases from 8 to 24%. The SALS images captured at slightly longer crystallization times ($t > 20$ min, percent crystallinity $> 24\%$) exhibit distorted four-lobed patterns. The qualitative change in the patterns over this time period in crystallization indicate that spherulitic impingement has occurred at approximately 25 to 30% overall crystallinity. This time period is coincident with the shift of the dipole peak to higher frequencies, pointing to the intralamellar material as responsible for the change in segmental dynamics.

**FIGURE 9.9**

Digital images of SALS scattering patterns at selected times during the isothermal crystallization of PLLA at 90°C.

9.3.2 Intra- and Inter-Spherulitic Amorphous Phase Dynamics

In this section we delve further into the molecular dynamics of the amorphous phase. For a different case study than PLLA, we focus on PDS in this section. Since PDS has a T_g below body temperature, segmental dynamics will surely play a role in diffusion of biologically active compounds from the implanted polymer. In order to observe whether crystallization influences the segmental dynamics in PDS, as was found for PLLA in the previous section, a series of investigations were conducted. Informative aspects of those studies are summarized and highlighted in the section that follows.

It is important to first identify the segmental dynamics of an amorphous polymer melt, and if possible, observe any changes in the amorphous phase mobility during crystallization. As an example of such measurements, changes in the dielectric loss and dielectric constant in the frequency domain as a function of crystallization time at 22°C are presented in Figure 9.10. Short-time frequency sweeps were taken from 100 Hz to 1 MHz (the duration of a frequency sweep is ~1min and much shorter than the time-scale of the crystallinity changes occurring). The curve at $t = 0$ corresponds to the fully amorphous polymer that was quenched prior to crystallization. As crystal-

lization proceeded, several important features were observed. As shown in Figure 9.10, the frequency of the maximum loss, f_{\max} , (inversely proportional to the most probable relaxation time, τ) for a fully amorphous α -relaxation was initially located in the high-megahertz region.

Soon after the first crystals developed, the maximum of this peak shifted to about 1 MHz. With further crystal growth, a gradual reduction of the intensity of the α -relaxation was observed denoting the loss of the amorphous portion in the polymer. However, the location of this peak remained unchanged until the very late stages of the process. The insensitivity of the relaxation time, τ , throughout most of the process suggests that the domain size of this segmental motion is sufficiently small so that the growing crystal units do not perturb dipole relaxation. However, after 60 min at 22°C, where crystallization was apparently near completion, a shift of the frequency of the maximum loss, f_{\max} , towards lower frequency was detected as shown in Figure 9.10. The f_{\max} downward shift occurs after the crystalline phase achieves a significant volume fraction. This indicates a slowing down of the chain mobility as rigid crystalline lamellae encroach. This slowing of amorphous molecular dynamics is the typical behavior and has been observed for a wide range of semicrystalline polymers, but it is contradictory to the behavior described in the previous section regarding the T_g depression in PLLA.

In addition to the primary segmental relaxation, a new dipolar relaxation process located at a lower frequency range emerges and systematically increases with time, highlighted by the upward arrow in Figure 9.10. Two isosbestic points on both sides of the peak accompany this relaxation. The existence of isosbestic frequencies at which ϵ'' is independent of crystallization time is an important feature and may suggest that the two relaxations in Figure 9.10 are complementary. It is likely that the origin of the new relaxation comes from a highly restricted amorphous portion located between crystalline lamella within the spherulites of the polymer — the intraspherulitic amorphous phase. The other type of amorphous phase fills the interspherulitic space between spherulites; the polymer chain segments here are unrestricted. The segmental relaxation in this space remains unaffected by the presence of crystalline lamellae. With further crystal growth, this dominant part of the relaxation, *interspherulitic* in nature, is gradually transformed into an *intraspherulitic* form at crystallization times greater than 60 min when the frequency shift of the main α -relaxation is observed.

To gain further insight into the crystallization mechanism of PDS, the shape and breadth of the relaxation spectrum were examined before and after crystallization. The comparison is made in Figure 9.11, where a normalized plot of dielectric loss as a function of frequency was constructed. Before the onset of crystallization (temperatures below 8°C), dipole loss curves superimpose quite well suggesting thermodielectric simplicity in the applied frequency interval between 100 Hz and 1 MHz.¹⁷ As crystalli-

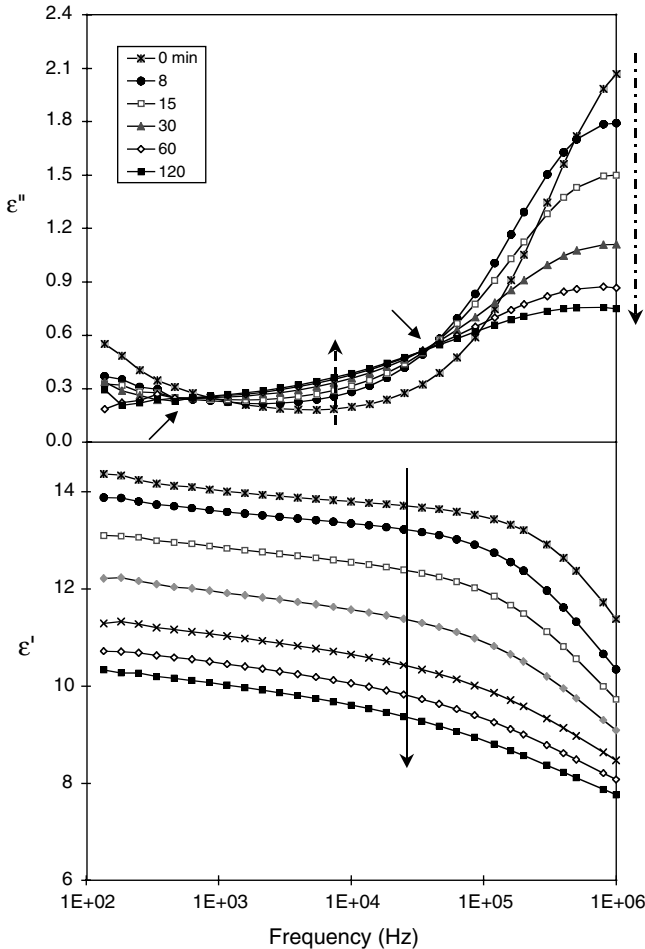
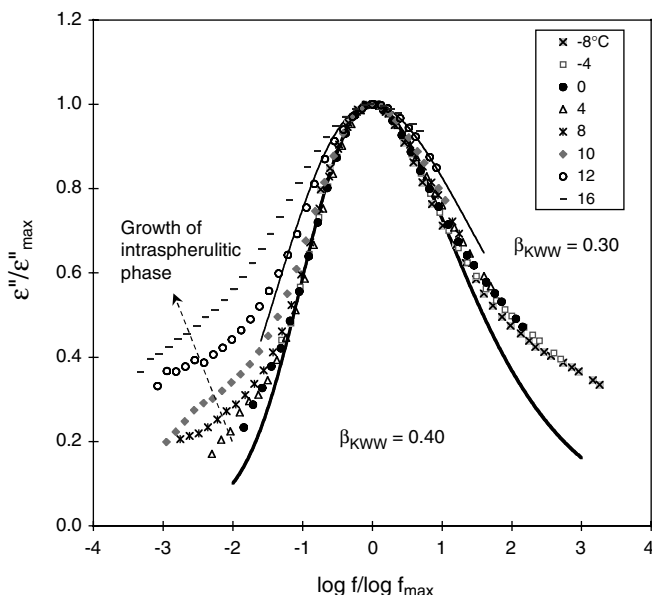


FIGURE 9.10

The dielectric loss and dielectric constant of PDS in the frequency domain as a function of crystallization time.

zation proceeds at higher temperatures, a significant but rather gradual broadening of the relaxation spectrum was observed. The value of the parameter β in the Kohlrausch–Williams–Watts (KWW) function (solid lines) remained constant at 0.40 prior to PDS crystallization. The value of β systematically decreased as crystallization proceeded, and with a possible exception of the low and high-frequency tails, maintained a relatively good fit through the rest of the data. The main reason for broadening of the relaxation spectrum during PDS crystallization is the increase of chain confinement of the amorphous phase manifested by the new process located at lower frequency.

**FIGURE 9.11**

Normalized plot of dielectric loss as a function of frequency for PDS as a function of crystallization temperature.

9.4 Advanced Methods to Accelerate Crystallization Kinetics of Absorbable Copolymers

9.4.1 Physical Route: Stress-Induced Crystallization

This section discusses the use of shear to accelerate the development of crystallinity. By this route, crystallization kinetics may be manipulated without introducing a foreign substance (nucleating agent) into the polymer. The influence of shear can be understood through molecular-level physics. Polymer crystallization can be viewed as a molecular ordering process consisting of two components, nucleation and growth. Polymer crystal nucleation in bulk molten material is considered to be a result of chains forming a stable layer on an *activated* heterogeneity (e.g., a particulate impurity, such as dust, edge on a vessel wall, etc.). This nucleated layer generates a new surface on which epitaxial growth will occur. The requirement of the heterogeneity to be *activated* gives rise to the time and temperature dependence of nucleation density; nucleation rates are generally constant with time for quiescent isothermal crystallization processes, although exceptions have been found.^{1,18} The growth process involves polymer chains reorienting and registering onto the primary or secondary nuclei surface.¹⁹ In this way crystal growth will depend on chain mobility, and hence the temperature dependence of crystal growth rates can be understood from the temperature dependence of poly-

mer chain dynamics. To modify crystallization rates, one or both of the processes of nucleation or growth must be manipulated.

The modification of these processes by shear is now explained. When a polymer melt is sheared, the polymer chains are perturbed from their random coils to elongate essentially parallel to the shear direction. This results in two consequences: (1) the system entropy is reduced, effectively increasing the degree of undercooling and the polymer's melting temperature, and (2) the induced chain extension provides a higher probability for favorable chain conformation for registry with heterogeneous nuclei, secondary nuclei and other extended chains. The latter allows a significant degree of homogeneous nucleation to occur. Additionally, small crystal aggregates may form from deformed or broken spherulites, which may act as additional self-heterogeneous nuclei.¹⁹

The influence of mechanical stress (shear) on a crystallizing polymer can also induce other morphological changes: spherulite to fibril transformation, polymorphic crystal forms/habits can be altered (e.g., poly(vinylidene fluoride), and polypropylene α and β polymorphs), reorientation of already formed crystalline lamellae, formation of oriented crystallites, orientation of amorphous polymer chains, and combinations of these (e.g., core-shell morphologies). In addition to morphological changes, shear can result in temperature fluctuations and shear-induced degradation in the crystallizing polymer melt.

These morphological changes occur under conditions of high strain or high shear rate. At lower strains or shear rates ("mild" shear), only nucleation density is affected.⁹ Figure 9.12 shows an enhancement in nucleation density due to a "mild" shear. The polymer is PDS, crystallized under the two conditions given in the figure: quiescent and with a 1-sec step-shear at 60 (1/sec). The obvious enhancement in nucleation density results in greatly accelerated crystallinity development, as shown in Figure 9.13. The effect of shear is temperature dependent, being more effective at higher temperature where the quiescent homogeneous nucleation rate is normally low.⁹

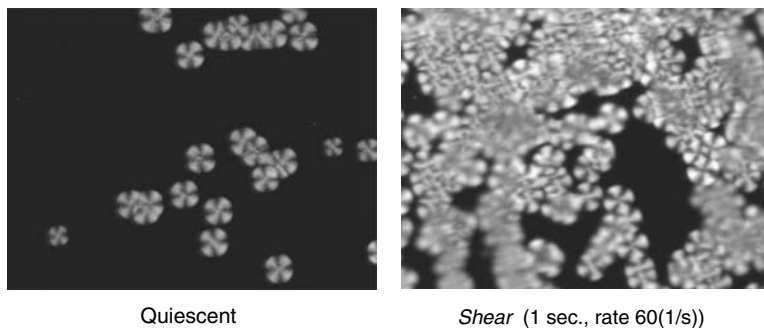
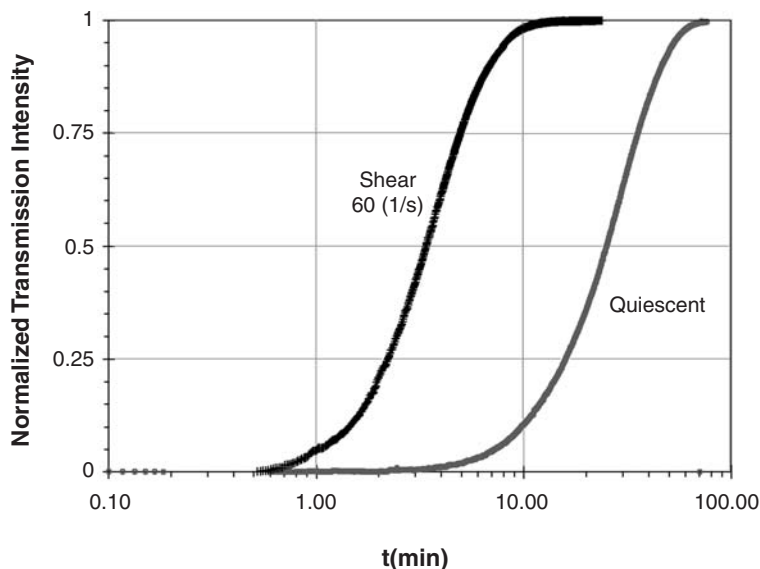


FIGURE 9.12

Optical polarized micrographs of PDS isothermally crystallized at 75°C for 12 min under the given shear conditions.

**FIGURE 9.13**

Normalized SALS transmission during isothermal crystallization of PDS at 75°C under quiescent and shear conditions of a 1-sec step-shear at a shear rate of 60 (1/sec).

9.4.2 Chemical Route: a Novel Synthetic Method Using Mixed Initiators

This section describes a means to enhance the crystallization kinetics of absorbable polymers via polymer chemistry. It will show how this can be achieved by using an appropriate combination of mono- and difunctional alcohol initiators for ring-opening polymerization (ROP). Diols have been used commercially in ring-opening “prepolymerizations” to produce α,β -dihydroxy macroinitiators that are then used in a subsequent copolymerization to produce materials with special sequence distributions. This sequential addition ROP, in which a monomer feed portion is added in a subsequent step, is one method to make block copolyesters. An example is a glycolide/ ϵ -caprolactone copolymer that has enjoyed considerable commercial success.²⁰

In the course of the ROP of lactones, mono- and difunctional initiators will both normally produce linear materials because one chain, without branch points, is produced from each molecule of the initiator. Recently, the effect of the functionality of the initiator in the sequential addition ROP of lactones was explored by using a combination of mono- and difunctional alcohols in different molar ratios.²¹ It was anticipated that the properties of polymers made using a mixture of initiators should lie between the extremes exhibited by materials based on only mono- or only difunctional initiators. However, it was discovered that employing a mixture of these initiator types could produce polymers with significantly different properties. They include much

TABLE 9.1

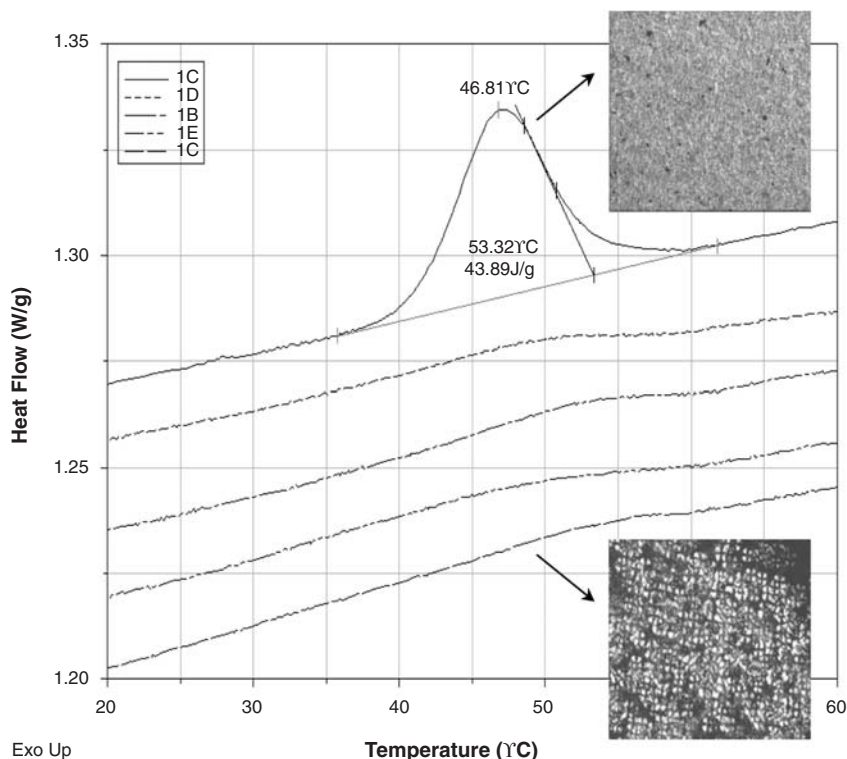
92/8 PDS/Glycolide Copolymers Used in This Study

Polymer	DD/DEG Molar Ratio (%)	Monomer-to-Initiators Ratio	IV (dL/g)	M _w (g/mol)
1A	100/0	~1,200:1	1.73	80,000
1B	75/25	~1,000:1	1.77	73,000
1C	50/50	~1,000:1	1.61	68,000
1D	25/75	~1,000:1	1.55	55,000
1E	0/100	~800:1	1.41	49,000

more rapid crystallization kinetics, resulting in enhanced processability and mechanical performance; mixing initiators is expected to alter biological properties as well.

The lactone-based polymers found to be susceptible to enhancement by mixing initiators were made in the following manner. A series of undyed PDS/Glycolide segmented block copolymers were prepared by ring-opening polymerization using stannous octanoate at a monomer-to-catalyst mole ratio of 30,000:1, utilizing various ratios of the mono-functional initiator, dodecanol (DD), to a difunctional initiator, diethylene glycol (DEG), as shown in Table 9.1. The polymer composition was determined by NMR, yielding 92 mol% polymerized *p*-dioxanone and 8 mol% polymerized glycolide. Although there is a difference in molecular weight in the polymer series as shown in Table 9.1, it has been shown separately that the molecular weight differences do not play a role in the crystallization properties of the polymers.

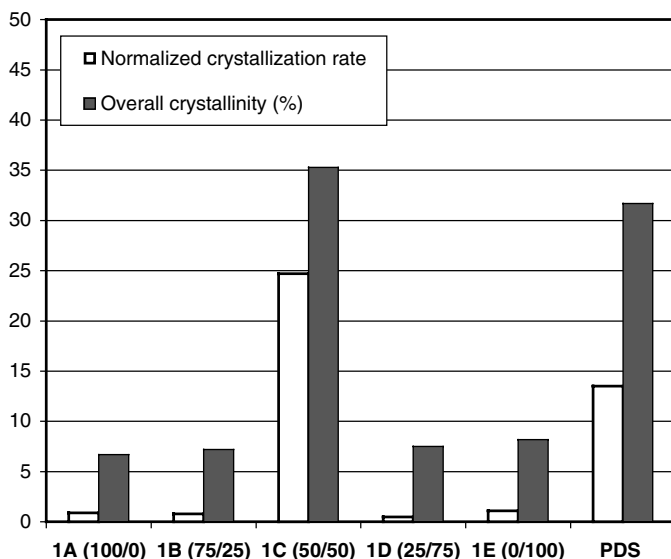
Throughout this chapter, the separation of overall crystallization into crystal growth and nucleation has been discussed. Separating these features will be shown to be crucial in the present section in order to understand how the molecular-level polymer structure can influence these aspects of crystallization. The first indication of a difference in crystallizability in the set of polymers in Table 9.1 was from calorimetric measurements (providing overall crystallinity information). This is best illustrated in Figure 9.14, where a set of thermograms taken during a cooling rate of 0.5°C/min is presented for the series of copolymers. Under the given thermal history, during cooling from the melt, copolymer 1C produced a large exotherm, suggesting that a significant crystallization took place. On the other hand, the other copolymers in the series do not show a significant change in the heat flow signal (i.e., no crystallization). To understand why 1C crystallized on cooling at this rate and the others in the series did not, polarized microscopy images of the copolymers 1C and 1A (obtained using the same crystallization conditions) are also included in Figure 9.14. These images show extensive nucleation in copolymer 1C, much higher than in the others. It was also found that copolymer 1C exhibits a higher degree of crystallinity on cooling from the melt at 0.5°C/min than even the pure PDS homopolymer. A comparison of the crystalliz-

**FIGURE 9.14**

Thermograms taken during a cooling rate of $0.5^{\circ}\text{C}/\text{min}$ for the series of PDS/Gly copolymers. HSOM images of copolymers 1C and 1A captured during isothermal crystallization at 40°C are also included.

ability of all copolymers and the PDS homopolymer on cooling from the melt at $0.5^{\circ}\text{C}/\text{min}$ are displayed in Figure 9.15. It can be seen that copolymer 1C crystallizes 25 times faster than the other copolymers; the total extent of crystallinity was four to five times higher as well. When compared to the PDS homopolymer, the copolymer 1C exhibits twice the overall crystallization rate and a 4% higher degree of crystallinity. Similar trends were observed for other thermal histories.²¹

The spherulite growth rates obtained with HSOM ($G = dD/dt$) for a series of PDS/Gly copolymers, when plotted against temperature, showed a characteristic “bell-shaped” curve with the maximum rate observed at intermediate temperature $\sim 60^{\circ}\text{C}$. Although all copolymers in this series have very similar spherulitic growth rates at a given temperature, their growth rates were about eight times slower than the PDS homopolymer. To restate the results: the combination of initiators does not influence the *growth rate* in the copolymer; however, the copolymer *growth rate* is slower than that of the PDS homopolymer. Thus it can be concluded that the controlling feature for this system of enhancing crystallizability is nucleation.²²

**FIGURE 9.15**

A comparison of the crystallizability of all PDS/Gly copolymers and the PDS homopolymer on cooling from the melt at 0.5°C/min. Numbers in parentheses on the x-axis are the ratios of mono- to difunctional initiators.

The feature of the polymer that will be shown to have contributed to the difference in nucleation density was the distribution of monomer sequences in the polymer chain. To determine the sequence distribution, carbon-13 NMR can be employed. Analysis of C^{13} data for the copolymer determined that the copolymer 1C was the most blocky in glycoyl (gly) runs. The distribution of sequences in the polymer chain containing gly were found to have a higher propensity of sequences of five or more consecutive gly units. The other copolymers had lower levels of these blocky gly-containing sequences. This structural difference may result in high-melting blocks of a glycoyl-rich phase in copolymer 1C that are not disrupted on melting and that, upon subsequent cooling, act as nucleating seeds. The enhanced crystallization has been observed in other copolymers containing glycolide.^{21,22} However, depending on the copolymer composition, the mixture of initiators needed to give the effect was unique to each copolymer system.

9.5 Effect of Morphology on Polymer Absorption Profiles

9.5.1 Effect of Molecular Orientation

A good example of the effect of molecular orientation on the rate of absorbable polymer breakdown can be found in the recent patent literature.²³ In an effort to define a process for making synthetic absorbable, autoclaveable,

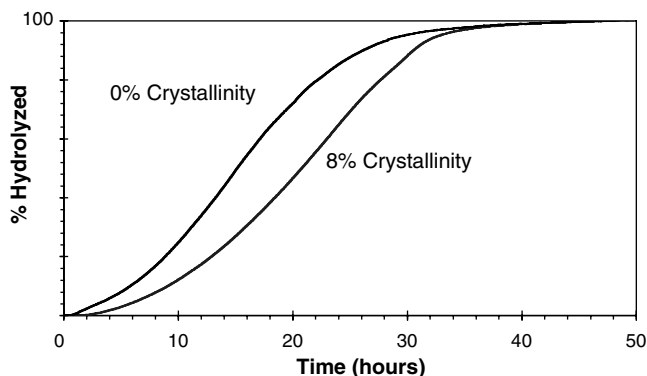
monofilament fibers for use as brachytherapy seed spacers, data was developed that showed the effect of draw ratio. At draw ratios of 1.5 and 3.4, molecular orientation was still very low, and the resulting fibers disintegrated during autoclaving. At higher draw ratios (4.8 and 5.5), there was more molecular alignment, resulting in a profound effect on the fibers' ability to resist premature hydrolysis.

9.5.2 Effect of Crystallinity

Crystallinity can play a major role in reducing the rate of hydrolysis. Likewise, even a small amount of hydrolysis can increase the extent of crystallinity that a sample can attain. This phenomenon was demonstrated by Zong et al., who showed in 1999 that crystallization of some absorbable polymers can be cleavage-induced.²⁴ The effect is as follows. As polymer chains crystallize, some get incorporated into separate crystals. As growth continues, the chain segments anchored between two crystals (the so-called "tie molecules") are physically constrained and prevented from crystallizing. When tie molecules are cleaved, this constraint is removed, allowing these chain segments to participate in secondary crystallization. With the added degree of molecular freedom, these chain segments can either add to an existing crystal of which they are already a part, or these segments now can crystallize on their own. Fu et al., also found that certain absorbable materials exhibit cleavage-induced crystallization during *in vitro* degradation testing.²⁵

It is interesting to find in this work that polydispersity (M_w/M_n) decreased during *in vitro* degradation. In further work, both the weight-average and the number-average molecular weight of all the polyglycolide and poly(glycolide-co-lactide) fiber samples tested were observed to decrease almost linearly with *in vitro* exposure time.²⁵ Polydispersity of all the samples decreased during *in vitro* degradation; weight-average molecular weight decreased faster than number-average molecular weight, even on a percent basis. This is firm evidence of a greater likelihood of larger molecules undergoing chain cleavage — the greater the length of the chain, the greater the probability of cleavage. Morphology may also play a role here. If one considers individual chains of increasing length, it will be the longer chains that will be "tie molecules," stretched between two crystals. It will be these molecules, with segments in the susceptible amorphous phase, that will have a greater probability of cleavage. As the longer chains are cleaved, although both M_w and M_n decrease, M_w decreases faster, thus decreasing the ratio of M_w/M_n .

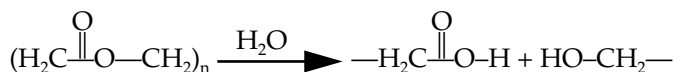
To be clear, the phenomenon of cleavage-induced crystallization should not be confused with solvent-induced crystallization, in which mobility is increased by the lowering of the glass transition temperature. We are also not referring to the well-known effect of molecular weight on mobility and hence crystallizability. Instead, it is based on removing a physical restraint of the molecular chain.

**FIGURE 9.16**

Extent of polymer hydrolysis at pH 7.27 and 75°C by titration of carboxylic acid groups generated. Samples are polyesters having 0 or 8% crystallinity (by WAXD).

9.5.3 Hydrolysis Profiler

Many absorbable biomedical polymers rely on the hydrolytic instability of polyester linkages for their *in vivo* degradation. A direct means of assessing this mode of polymer breakdown is via the titration of carboxylic acid groups generated. An example of the hydrolytic degradation reaction scheme is the following:



Monitoring hydrolysis in this way may be used to demonstrate the role of morphology (crystallinity) on chain degradation. As an example, in Figure 9.16 we show degradation time courses for two film samples prepared from the same polymer resin but processed under different thermal histories to result in 0 and 8% crystallinity. It is clear that the hydrolytic degradation is greatly slowed by crystallinity. The role of morphology has been examined previously, where it was found that hydrolytic degradation occurs preferentially in the amorphous regions of a semicrystalline polymer.^{26–28} There are several reasons for this:

- The amorphous regions are less dense so that water may diffuse in and degradation products diffuse out more rapidly.
- The arrangement of functional groups in crystalline lamellae may present hydrophobic surfaces to the ingress of water.
- The self-protecting crystal phenomena referred to earlier in this chapter.

One consequence of this, as mentioned above, is an increase in crystallinity during degradation. Another role for morphology is with respect to enzymatic activity, where during *in vivo* degradation it has been suggested that amorphous components are preferentially degraded by enzymes.²⁹

The range of polymer properties influencing *in vivo* absorption of implanted devices is quite large, but for completeness we should list some of them here: intrinsic ester cleavage energy (polymer composition), rates of diffusion of water into the device, rate of diffusion of degradation products from the device, copolymer sequence distribution, catalyst level, initiator type, chain architecture (branched, linear, star-shaped, dendritic), residual monomer, residual moisture, degradation-modifying ability of degradation product (e.g., acid catalysis), hydrophilicity, miscibility of degradation products with physiological fluids, degree of crystallinity, polymer orientation (both amorphous and crystalline lamellae), tertiary structure (spherulites, microfibrils, phase separation, and miscibility), feature size (spherulite, fibril, domain size), macroscopic geometry — filamentitious vs. monolithic (fiber, film, rod, etc.), surface-to-volume ratio, porosity, and molecular weight distribution.³⁰

9.5.4 Drug Delivery Vehicles

Absorbable polymers have been getting a lot of attention as controlled drug delivery vehicles, as well they should. There are trade-offs when considering morphology; amorphous materials cannot generally be exposed above their glass transition temperatures without consequence. Although semicrystalline materials may have dimensional stability, there are other problems related to absorption profiles and to release rates. Very often formulations are chosen that are fully amorphous, such as the racemic lactide copolymers. This may be in part because of the complexities a more sophisticated morphology would impose. Imagine release from an amorphous phase and another release process from a crystalline phase. Although this degree of freedom may present a wonderful design tool, the manufacturer would need to provide a very highly developed morphology control system to ensure reproducibility. It is thus not surprising that amorphous materials get so much attention in the drug delivery world. Besides offering faster release rates, they are not complicated by crystallization phenomena.

9.6 Novel Polyesters: POE Polymers

A new class of synthetic absorbable polyesters, the polyoxaesters (POEs), was disclosed in the mid- to late 1990s by Bezwada and Jamiolkowski.^{31,32} POEs are made by poly-condensation, and if made to insure hydroxy termination, they can be used as α,ω -dihydroxy macroinitiators for further

(co)polymerization with lactone monomers. The resulting segmented block copolyesters can be made to be semicrystalline if the blocks are crystallizable. A report was published describing a semicrystalline POE homopolymer that was made without having to resort to copolymerization.³²

Utilizing the Gibbs equation relating free energy to the changes in enthalpy and entropy, $\Delta G = \Delta H - T\Delta S$, one can gain insight into the melting point, or T_m , of the polymer:

$$T_m = \Delta H_f / \Delta S_f$$

A diol was selected that would result in a stiffer chain, decreasing ΔS_f , the entropy of fusion, and thus increasing T_m . The material was prepared with the diacid, 3,6-dioxaoctanedioic acid, and the diol *trans*-1,4-cyclohexanedimethanol (*t*-CHDM). At a weight-average molecular weight of 84,000, the T_g and T_m were -10 and 115°C , respectively; crystallinity was 64% as determined by x-ray diffraction. This is an example of researchers utilizing thermodynamics to control morphology. By employing the relatively rigid diol, *t*-CHDM, the chain was stiffened, the entropy of fusion lowered, and the melting point raised above room temperature.

9.7 Conclusion and Perspective on the Future

A manufacturer who does not understand the complexities of polymer morphology in absorbable polymeric medical devices may be in serious trouble. This ominous statement is a reminder that we need to have a sound technology base when we choose to improve lives by providing medical devices. What will the future bring? Wonderful things we hope, if the past is any indicator: shorter product development cycle times and better performance characteristics. We have learned so much in the last 25 years — about how to synthesize the right material, how to control molecular weight, and how to control processing conditions to get the right performance characteristics. With proper characterization the seemingly impossible may be made possible; with improper characterization the seemingly possible may be made impossible.

Acknowledgment

The authors thank Prof. Inaki Mondragon and Cristina Marieta from The Universidad Del Pais Vasco, San Sebastian, Spain, for providing the AFM images and for helpful discussions.

References

1. Andjelic, S., Jamiolkowski, D. D., McDivitt, J., Fischer, J. and Zhou, J., Spherulitic growth rates and morphology of absorbable poly(p-dioxanone) homopolymer and its copolymer by hot stage optical microscopy, *J. Polym. Sci. Polym. Phys. Ed.*, 39, 3073, 2001.
2. Li, L., Chan, C., Li, J., Ng, K., Yeung, K. and Weng, L., A direct observation of the formation of nuclei and the development of lamellae in polymer spherulites, *Macromolecules*, 32, 8240, 1999.
3. Hobbs, J., McMaster, J., Miles, M. and Barham, P., Direct observations of the growth of spherulites of poly(hydroxybutyrate-co-valerate) using atomic force microscopy, *Polymer*, 39, 2437, 1998.
4. Woodward A., *Atlas of Polymer Morphology*, Hanser Publishers, New York, 1989.
5. Andjelic, S., Jamiolkowski, D. D., McDivitt, J., Fischer, J., Zhou, J., Wang, Z. G. and Hsiao, B. S., Time-resolved crystallization study of absorbable polymers by synchrotron small angle x-ray scattering, *J. Polym. Sci. Polym. Phys. Ed.*, 39, 153, 2001.
6. Andjelic, S., Fitz, B. D. and Jamiolkowski, D. D., Crystallization in synthetic absorbable polymers, in *Recent Research Developments in Biomaterials*, Ikada, Y., Ed., Research Signpost, Kerala, India, 2002, chap. 8.
7. Hoffman, J. D., Davis, G. T. and Lauritzen, J. I. *Treatise on Solid State Chemistry*, Hannay, N., Ed., Plenum Press, New York, 1976, chap. 7.
8. Andjelic, S. and Richard, R. E., Crystallization behavior of ultrahigh molecular weight polyethylene as a function of *in vacuo* gamma irradiation, *Macromolecules*, 34, 896, 2001.
9. Abuzaina, F., Fitz, B. D., Andjelic, S. and Jamiolkowski, D. D., Time resolved study of shear-induced crystallization of poly(p-dioxanone) polymers under low-shear, nucleation-enhancing shear conditions by small angle light scattering and optical microscopy, *Polymer*, 43, 4699, 2002.
10. Andjelic, S., Jamiolkowski, D. D., McDivitt, J., Fischer, J., Zhou, J. and Vetrecin, R., Crystallization study on absorbable poly(p-dioxanone) polymers by differential scanning calorimetry, *J. Appl. Polym. Sci.*, 79, 742, 2001.
11. Andjelic, S. and Fitz, B. D., Study of reorientational dynamics during real-time crystallization of absorbable poly(p-dioxanone) by dielectric relaxation spectroscopy, *J. Polym. Sci. Polym. Phys. Ed.*, 38, 2436, 2000.
12. Wang, Z. G., Wang, X., Hsiao, B. S., Andjelic, S., Jamiolkowski, D. D., McDivitt, J., Fischer, J., Zhou, J. and Han, C. C., Morphological development in absorbable poly(glycolide), poly(glycolide-co-lactide) and poly (glycolide-co-caprolactone) copolymers during isothermal crystallization, *Polymer*, 42, 8965, 2001.
13. Andjelic, S. and Jamiolkowski, D. D., Tensile property examinations of isothermally grown semicrystalline films made from absorbable poly(p-dioxanone), *J. Appl. Med. Polym.*, 5, 1, 2001.
14. Fitz B., Andjelic S. and Jamiolkowski, D. D., T_g depression in poly(L-lactide) crystallized under partially constrained conditions, *Macromolecules*, 35, 5869, 2002.
15. Fitz, B. and Andjelic, S., *Polymer*, Real-time monitoring of segmental dynamics during crystallization of poly(L(-)-lactide) by simultaneous DRS/SALS technique, *Polymer*, 44, 3031, 2002.

16. Stein, R. and Rhodes M., Photographic light scattering by polyethylene films, *J. Appl. Phys.*, 31, 1873, 1960.
17. Fitz, B., Andjelic, S. and Mijovic, J., Reorientational dynamics and intermolecular cooperativity in reactive systems: (1) model epoxy-amine systems, *Macromolecules*, 30, 5227, 1997.
18. Wolkowicz, M., Nucleation and crystal growth in sheared poly(1-butene) melts, *J. Polym. Sci.: Polym. Symp.*, 63, 365, 1978.
19. Magill, J., Rates of crystallization of polymers, in *Polymer Handbook* 4th ed., Brandrup, J., Immergut, E. and Grulke, E., Eds., John Wiley & Sons, New York, 1999, chap. VI.
20. Bezwada, R. S., Jamiolkowski, D. D., Lee, I. Y., Agarwa, V., Persivale, J., Trenka-Benthin, S., Erneta, M., Suryadevara, J., Yang, A. and Liu, S., Monocryl® suture, a new ultra-pliable absorbable monofilament suture, *Biomaterials*, 16, 1141, 1995.
21. Andjelic, S., Jamiolkowski D., Kelly B. and Newman H., *Polymer*, submitted.
22. Patents pending.
23. Karl, J. J., Popadiuk, N., Jamiolkowski, D. D., Keilman, K. M., Andjelic, S., U.S. Patent (assigned to Ethicon, Inc. Somerville, NJ), 6,419,866.
24. Zong, X. H., Wang, Z. G., Hsiao, B. S., Chu, B., Zhou, J. J., Jamiolkowski, D. D., Muse, E. and Dormier, E., Structure and morphology changes in absorbable poly(glycolide) and poly(glycolide-co-lactide) during *in vitro* degradation, *Macromolecules*, 32, 8107, 1999.
25. Fu, B., Hsiao, B., Chen, G., Zhou J., Koyfman, I., Jamiolkowski D. D. and Dormier E., Structure and property studies of bioabsorbable poly(glycolide-co-lactide) fiber during processing and *in vitro* degradation, *Polymer*, 43, 5527, 2002.
26. Fischer, E. W., Sterzel, H. J. and Wegner, G., Investigation of the structure of solution grown crystals of lactide copolymers by means of chemical reactions, *Kolloid-Z. Z. Polym.*, 251,980. 1973.
27. Fredericks, R., Melveger, A. and Dolegiewitz, L., Morphological and structural changes in a copolymer of glycolide and lactide occurring as a result of hydrolysis, *J. Polym. Sci.: Polym. Phys. Ed.*, 22, 57, 1984.
28. King, E. and Cameron, R., Effect of hydrolytic degradation on the microstructure of poly(glycolic acid): an x-ray scattering and ultraviolet spectrophotometry study of wet samples, *J. Appl. Polym. Sci.*, 66, 1681, 1997.
29. Pitt, C., Non-microbial degradation of polyesters: mechanisms and modifications, in *Proceedings of the Second International Scientific Workshop on Biodegradable Polymers and Plastics*, Vert M., Feijen J., Albertsson A., Scott G. and Chiellini E., Eds., Royal Society of Chemistry, Cambridge, UK, 1992, page 7.
30. Fitz, B. and Jamiolkowski, D. D., in preparation.
31. Bezwada, R. S. and Jamiolkowski, D. D., U.S. Patents (assigned to Ethicon, Inc.): 5,464,929; 5,595,751; 5,597,579; 5,607,687; 5,618,552; 5,620,698; 5,645,850; and 5,648,088. Jamiolkowski, D. D. and Bezwada, R. S. U.S. Patents (assigned to Ethicon, Inc.): 5,698,213; 5,700,583; 5,844,017; 5,859,150; 5,962,023; 6,074,660; 6,100,346; 6,147,168; 6,224,894; and 6,251,435.
32. Bezwada, R. S., Jamiolkowski, D. D., Andjelic, S. and Vhora, I., Crystalline and amorphous absorbable polyoxaester homopolymers, *Transactions of the 28th Annual Meeting of the Society for Biomaterials*, Tampa, FL, XXV, 255, 2002.

10

Polymer Biocompatibility and Toxicity

Karen J.L. Burg, Shalaby W. Shalaby, and Griet G. Atkins

CONTENTS

10.1 Historical	143
10.2 Evolution and Status.....	144
10.2.1 Forms of Polymer Toxicity	144
10.2.2 Polymer Processing and Its Effect on Toxicity	145
10.2.3 Methods of Toxicity Testing	146
10.2.3.1 Specifics of Testing.....	148
10.2.3.2 <i>In Vitro</i> Cell Culture Toxicity Assays.....	148
10.2.3.3 <i>In Vivo</i> Toxicity Testing.....	150
10.3 Toxicity and Biocompatibility for Specific Absorbable/Biodegradable Systems	151
10.3.1 Absorbable/Biodegradable Devices	151
10.3.1.1 Cyanoacrylate	152
10.3.1.2 Polylactide and Polyglycolide	152
10.3.1.3 Alginates, Chitosans, and Collagens	152
10.3.2 Absorbable/Biodegradable Drug Carriers	153
10.4 Critical Test Methods for Implants and Drug Carriers.....	154
10.4.1 Implants	154
10.5 Conclusion and Perspective on the Future	154
References	155

10.1 Historical

Biomaterials, particularly absorbables/biodegradables, undergo rigorous processing and characterization as well as comprehensive safety testing prior to final conversion to a biomedical device or drug carrier. The International Organization for Standardization (ISO), the U.S. Food and Drug Adminis-

tration, and the American Society for Testing and Materials continue to oversee the development of guidelines for systematically testing the cytotoxicity and biocompatibility of these materials and devices. Absorbables are generally evaluated in a similar fashion as drugs since their residence time *in vivo* is limited and since these specialized, designed-to-degrade materials release components systemically. One of the immediate chief safety concerns is the evaluation of the biocompatibility and toxic potential of materials in the body's harsh environment. Toxicity describes a change in form or function of a cell or cells due to chemical injury, whereas biocompatibility describes the interaction of a material with the host tissue. A toxic material may stimulate a slight and reversible change in cellular behavior, or it may cause cell death. Generally, toxic responses are caused by the disturbance of multiple cell processes; increases in chemical dose generally result in a greater disruption.¹ Biocompatibility is determined in a relative manner; a biocompatible material is one which demonstrates appropriate interaction with the host in a specific application and implant site.

10.2 Evolution and Status

Biocompatibility reflects an interaction that may be influenced by a number of material factors, including surface topography, charge, and chemistry. It is also influenced by properties of the host tissue, including local pH, blood transport rate, presence of lipids, and tissue type. Absorbable materials may be fashioned into very diverse device forms; thus, the ensuing discussion of toxicity and biocompatibility will be focused on the chemical as well as physical influence of the bulk material or device and its degradants on the host tissue. Usually, toxicity is first tested *in vitro* early in material development stages. At this point, it is determined whether or not the toxicological profile of the material is suitably low to warrant further investigation of the material. Biocompatibility testing is performed *in vivo* at a later developmental stage, after extensive *in vitro* characterization. This is critical to minimizing the time and expense associated with a given material. A polymer's toxicology profile will be measured again, once the final device has been produced, in order to ensure that the handling and processing steps (including sterilization and storage) have not altered the toxicological features of the material.

10.2.1 Forms of Polymer Toxicity

Generally, toxicity may occur due to bulk material or due to leachables from the material. Bulk toxicity may be an immediate effect or it may occur with the gradual degradation of the polymer with time. It has been found that

cells from different tissues tend to react similarly in identically controlled toxicity tests, which minimizes the number of cell lines that must be maintained in cell culture for toxicity testing. Acute studies are generally less than 30 d in length. Chronic toxicity studies are required for materials contacting tissue for more than 30 d. Acute toxicity is largely due to leachables, which may be impurities, oligomers, or monomers resulting from less than optimal preparation or processing schemes, or they may be additives of purposeful design, i.e., dyes, plasticizers, radiopacifiers, or ultraviolet absorbents. The processing conditions may be examined and improved to minimize this occurrence and/or the impurity may be extracted to purify the end product. This can be accomplished through solvent extraction and/or evaporation under reduced pressure. The material properties should be tested following any such treatment in order to confirm that no detrimental effects (e.g., decrease in molecular weight) have occurred. It may be necessary to acquire higher grade reactants to achieve an acceptable product.

Leaching is the process of solubilizing low-molecular weight entities from the surface of a material. If these entities are not present at the surface they will migrate to the surface over time and may be a cause for concern only after days or weeks *in vivo*. Thus, the rate of diffusion depends on the bulk polymer and its physicochemical properties as well as the properties of surrounding fluid (media, blood, etc.). Absorbable systems are purposefully designed to gradually solubilize *in vivo*, so chronic studies also are a necessity.

The interaction of the host tissue with the polymer depends on the implantation site. For example, a pH sensitive suture that exhibits no degradation at a subcutaneous location may exhibit rapid degradation at an acidic location such as the stomach. A material may therefore demonstrate a toxic response at one implantation location but not at another. Similarly, the issue of patient diversity (age, gender, health status, physical condition, size, etc.) lends itself to distinctive device interactions specific to patient characteristics.

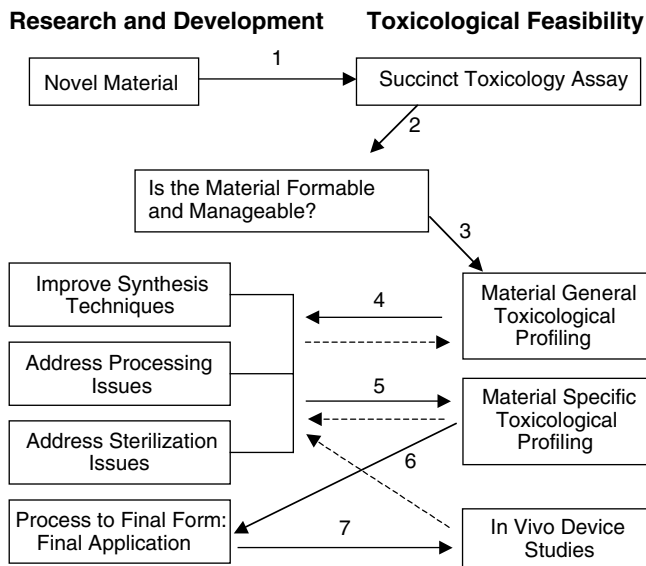
10.2.2 Polymer Processing and Its Effect on Toxicity

Processing (exposure to heat and chemicals) and sterilization can cause degradants to form; therefore, it is imperative to test toxicity initially as well as post-processing, even if the initial material is known to be nontoxic. Excessive heat during synthesis and melt processing generates monomer, linear and cyclic dimers, and oligomers. Additionally, oxidation may readily occur during processing in the presence of trace amounts of oxygen. Although autoclave is used in the sterilization of many biomedical devices, the most common form of sterilization for absorbable/biodegradable polymers is by exposure to ethylene oxide. Many of the absorbable/biodegradable polymers cannot withstand the high temperatures or exposure to moisture and may degrade immediately or after a given number of cycles, so it is necessary to be aware of the lifetime of the product. Absorbable/biodegradable polymers are sensitive to high-energy radiation; hence radi-

ation sterilization is only used in a few cases. In the event that radiation is used, there is likely to be chain cleavage and a subsequent decrease in molecular weight as well as an increase in radiation degradation products. This, therefore, may result in the formation of leachables within the product. Gamma irradiation may also crosslink polymers, thus changing key physical characteristics of the bulk material.² When ethylene oxide is used as a gas sterilant, products are placed under vacuum post-ethylene oxide sterilization in order to remove residual gas. If the residual is not completely removed, it will leach and cause local tissue necrosis. The more porous and "thick" the device, the more cause for concern; this has particular relevance to tissue engineering scaffolds which tend to be polymeric masses with tortuous channels. The least common sterilants are gaseous formaldehyde and glutaraldehyde aqueous solution, which are both difficult to completely and consistently remove from a variety of device masses. These aldehydes, if left in an implanted material, will leach and cause tissue necrosis. Recent advances have suggested that a combination of formaldehyde gas (minimal amount) with a high-energy, low-dose gamma irradiation may be a satisfactory method of sterilization for sensitive polymers.³ This new technology may allow greater advancements and use of absorbable materials that are not readily processed to a sterile, mechanically able form using standard sterilization processes.

10.2.3 Methods of Toxicity Testing

Toxicity testing occurs in stages while the many other questions concerning the design of a biomedical device are simultaneously being posed and addressed (Figure 10.1). The type and extent of testing that a given polymer requires depend on the extent of past use of the material in the desired applications as well as other applications. A newly developed absorbable polymer is subjected to succinct preliminary testing in which both the bulk material and leachables are scrutinized. Extracts are taken from the material, using aqueous and nonaqueous liquids, in order to mimic responses in tissue environment extremes ranging from aqueous to lipid. The *Ames salmonella* bacteria reverse mutation assay, for example, is used to determine mutagenic potential of absorbable leachables. The leachables are placed in proximity to genetically altered bacteria. The bacterial nutrient requirements will shift toward normal in the presence of a mutagenic material. This test is used to determine if, in the given chemical state, the polymer warrants further development before making a large-scale investment of time and money. All devices that will contact the body for over 30 d require mutagenic screening. If the material passes these tests and appears formable, manageable, and a potential biomaterial, it undergoes general toxicology profiling. This is a battery of very general toxicological tests which are not specific to the end use of the polymer. The battery can guide the end use in that it may elucidate appropriate and inappropriate end uses (final form and/or application). As

**FIGURE 10.1**

Order of toxicity testing in absorbable biomaterial design. Solid, numbered lines indicate direct pathway of a material to a device. Dashed lines indicate potential revisions and the resulting iterative process.

the design phase progresses, an endpoint use is targeted, and processing and design related testing is initiated; cytotoxic potential is continuously scrutinized. At this point a material-specific toxicological profile will be run. This will pinpoint tests that are specific to the device's use (for example, *in vitro* mechanical degradation testing and examination of products in media, and degradation of the specimen) and allow the collection of a large amount of safety data. The form of the material tested depends on the device and application of interest. Also, forms of the material must be tested that take into account sterilization or other post-processing steps that may potentially alter tissue response. The last series of tests is an *in vivo* animal study in which the device is tested in as close an approximation to the final endpoint application as possible. These are time-course studies designed to observe the polymer's initial characteristics as well as their changes with implantation time.

A general material class may be considered "toxic," but specific devices fashioned from the material may be acceptable in particular applications. Thus, the toxicity test results should be carefully evaluated, realizing the sensitivity and/or relevance of each and weighing each accordingly in the final diagnosis. For example, studies in the literature have shown that select subcutaneous implants in rats, mice, and hamsters can cause fibrosarcomas during long-term studies.⁴ These results do not extrapolate to human studies, and therefore the *in vivo* test should be lightly weighted. Similarly, many natural absorbable materials, which absorb largely by enzymatic degrada-

TABLE 10.1Standard Methods for *In Vitro* Toxicity Assessment⁷⁻¹³

Description	Material Form	ASTM
Agar diffusion	Bulk or extract	F-895
Direct contact	Bulk or extract	F-813
Extract, method for	Extract	F-619
Hemolysis	Bulk or extract	F-756
Evaluation	Bulk, thermoplastic PU	F-624

tion, behave very differently in a rodent model than in a larger animal model. Two factors are largely responsible — the differences in respective mass ratios of polymer to host and the presence of a large foreign body mass that may alter the rat enzymatic processes. Because of these inconsistencies, the battery of tests should be selected and the results considered on a case by case basis. Histologic methods may be used to evaluate toxicity; however, “qualitative” histologic assessments should be made carefully to distinguish a normal foreign body response from ensuing degradation or absorption from a cytotoxic response.

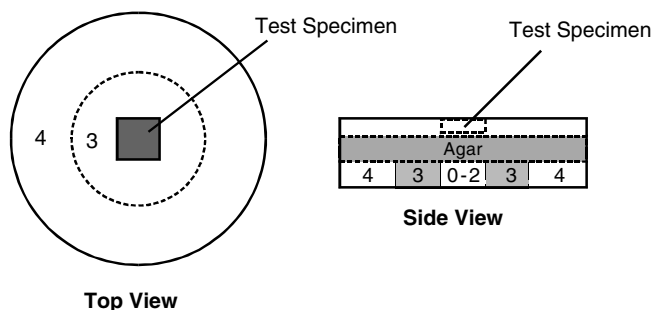
10.2.3.1 Specifics of Testing

Methods of cytotoxicity testing are described in the literature, the ASTM Standards, the U.S. Pharmacopeia, and in ISO 10993-5 (Tests for Cytotoxicity: *In Vitro* Methods).^{5,6} Selected tests are briefly outlined here and listed in Table 10.1.⁷⁻¹³

10.2.3.2 In Vitro Cell Culture Toxicity Assays

The actions of chemicals that cause disease or death occur at the cellular level; therefore, it is necessary to conduct an array of *in vitro* cell culture tests to determine cytotoxicity.⁸ The bulk absorbable material is tested; also, hydrolyzed products as well as extracts are assessed. The most obvious marker of toxicity is cell death. Necrosis, as compared with normal cellular apoptosis, is characterized by cellular and organelle swelling followed by rupture. Apoptosis, in contrast, is programmed cell death, which is characterized by a reduction in cell volume and basophilic staining of the chromatin. There are three common *in vitro* screens for toxicity — agar, direct contact, and elution assays.

Agar diffusion involves cultivating a monolayer of cells, then overlaying it with agar, and placing the test specimen on top. Specimens used for *in vitro* cell toxicity tests are usually 1 cm². The agar layer prevents the specimens from mechanically damaging the cells but allows diffusion of leachables from the specimen to the monolayer. This method is inappropriate for materials that are heavy enough to compress the agar and/or materials with leachables unable to diffuse through agar. The cell death after 24 to 72 h is

**FIGURE 10.2**

Agar diffusion assay. Reactivity grades of 0 to 4 determined by extent of degenerated cells in monolayer. Side view shows layers (bottom to top) of cells, agar, and test specimen.

observed microscopically and “zones” of affected cells are measured (Figure 10.2). The further from the material abnormal cells are observed, the wider the zone of influence, indicating a more dramatic cytotoxic effect. This is measured and correlated to a reactivity grade.

The classic direct contact assays involve cultivating a monolayer of cells and placing the test specimen directly on top. A zone grading system is used in assessment, and cell death is similarly measured after 24 h. This method allows the potential mechanical damage of the monolayer by the test specimen and does not allow the assessment of biochemical behavior of cells in the respective zones. In order to more closely define biochemical behavior of direct cell–biomaterial interaction, cells may be directly cultured onto discs of the material of interest. By examining sufficient replicates, biochemical activity of the cells may be assessed. In the past, this test has been problematic because the discs tend to float in culture, or due to the complicating factors added by glues used in securing the films to their culture vessel. Now, with the introduction of a new multiwell cell culture insert that integrates with a standard multiwell plate, these types of cultures and assays are possible and provide a great deal of additional toxicity data.¹⁴

Extract assays are conducted by cultivating a monolayer of cells for 24 h in a standard media. An extract of a biomaterial is taken, placed in fresh medium, and used to replace the standard medium after 24 h. The cells are incubated for 24 to 72 h, after which time the changes in monolayer density due to cell necrosis are noted. The reactivity grade is assigned based on the percentage of affected cells.

Other *in vitro* methods include evaluation of hemolytic properties of material extracts for blood-contacting polymers and evaluation of specific materials in their final form. An example of this is given in Table 10.1 for the standard evaluation of thermoplastic polyurethanes (PU). These standard evaluations have been developed for many commercially used biomaterials and include toxicity testing as well as methods of final form assessment for other physical properties.

TABLE 10.2Standard Methods for *In Vivo* Toxicity Assessment^{17–19}

Description	Material Form
Intracutaneous injection	Extract
Transcutaneous	Bulk
Subcutaneous	Bulk
Ocular	Extract/bulk
Teratology	Bulk
Radiolabeling	Bulk
Systemic injection	Extract
Skin irritation	Extract
Allergenicity	Bulk
Intramuscular	Bulk

10.2.3.3 *In Vivo* Toxicity Testing

The final toxicity tests are performed *in vivo*; examples are listed in Table 10.2.^{17–19} Skin irritation tests are used in animal studies to test toxicity of topically used devices. These are performed by placing the device “as is” on a patch of skin for 4 to 24 h and evaluating it according to an irritation index. Mucosal irritation tests have been developed for dental, ocular, vaginal, rectal, bladder, and urethral implants, for which skin patch tests are not adequate.^{18–20} Intracutaneous injections of polymer extracts are used to pinpoint toxicities caused by leachables. Acute systemic toxicity may be evaluated through intravenous or intraperitoneal mouse injections of saline and/or oil-based polymer extracts. The mice are monitored for 24 to 72 h for adverse reactions and compared with control animals. Devices that are not exposed to mucosal tissue or blood and that are not implanted may be evaluated by oral dose or by dermal test, where a defined amount of material is placed in contact with the skin. There are also methods to assess genotoxicity (to evaluate DNA and chromosomal changes) and subchronic toxicity (to evaluate repeated contact instead of sustained contact). Chronic toxicity studies are conducted for periods of time equivalent to the human absorption rate of the material under investigation in order to observe possible systemic effects of leachables.

Absorbable devices may be radiolabeled and the excreted amounts of material quantified by scintillation counts. Any radiolabeled material remaining *in vivo* may be visualized by radiography. Absorption rates are estimated by subcutaneous implantation and visual evaluation of shape, mass, and dye retention. Diffusion chambers are also used to prevent the host cells from encapsulating the absorbable material while allowing contact with tissue fluids. Chambers are placed subcutaneously or intraperitoneally; the absorbable material may be chemically evaluated on retrieval.

10.3.1 Absorbable/Biodegradable Devices

During this discussion, absorbable implants are defined as those materials whose purpose is to interact directly with the host; that is, the material is the biomedical device performing or assisting in a tissue repair function. Table 10.3 details biocompatibility and toxicity tests pertinent to absorbable devices.²¹ Of particular importance to biocompatibility testing is histological evaluation. Histological evaluation involves retrieval of tissue and implanted material at predetermined timepoints and processing the explants to obtain a thin section of the material-implant for microscopic evaluation. Cells surrounding or invading the implant are typed and counted and the surrounding collagen capsule measured. This information is weighted accordingly to

Biocompatibility and Toxicity Material and Extract Screens for Absorbable Devices

Cytotoxicity
Sensitization
Irritation
Acute Systemic Toxicity
Subchronic Toxicity
Genotoxicity
Implantation
Chronic Toxicity
Carcinogenicity
Hemocompatibility
Reproductive/ Developmental
Biodegradation

Soft Tissue contact < 24 h

Soft Tissue contact between 24 h and 30 d

Soft Tissue contact >30 d

Hard Tissue contact < 24 h

Hard Tissue contact between 24 h and 30 d

Hard Tissue contact >30 d

Blood contact < 24 h

Blood contact between 24 h and 30 d

	Blood contact >30 d
1	1
2	1
3	1
4	1
5	1
6	1
7	1
8	1
9	1
10	1
11	1
12	1
13	1
14	1
15	1
16	1
17	1
18	1
19	1
20	1
21	1
22	1
23	1
24	1
25	1
26	1
27	1
28	1
29	1
30	1
31	1
32	1
33	1
34	1
35	1
36	1
37	1
38	1
39	1
40	1
41	1
42	1
43	1
44	1
45	1
46	1
47	1
48	1
49	1
50	1
51	1
52	1
53	1
54	1
55	1
56	1
57	1
58	1
59	1
60	1
61	1
62	1
63	1
64	1
65	1
66	1
67	1
68	1
69	1
70	1
71	1
72	1
73	1
74	1
75	1
76	1
77	1
78	1
79	1
80	1
81	1
82	1
83	1
84	1
85	1
86	1
87	1
88	1
89	1
90	1
91	1
92	1
93	1
94	1
95	1
96	1
97	1
98	1
99	1
100	1

provide a semi-quantitative measurement of tissue response to the biomaterial.¹⁶ Histological methods can similarly provide additional information about systemic response to leachables and can provide a picture of the material behavior *in vivo*.

10.3.1.1 Cyanoacrylate

Cyanoacrylates are regarded as devices and are used in tissue adhesives to minimize the need for sutures and staples. Varying cyanoacrylates have varying toxicity profiles according to their compositions and use. In the application of adhesives and other devices, where free monomer is present, the monomer is toxic.^{22,23} The degradation products of some of these materials have also been found to be toxic.

10.3.1.2 Polylactide and Polyglycolide

Absorbable biomaterials, specifically lactide and lactide-glycolide copolymers, have been used to fabricate devices and applications including sutures and fracture fixation pins, as well as drug release systems. The majority of information provided on the toxicity of these materials, regardless of application, shows that they are nontoxic locally and systemically. There have been reports of inflammation, foreign body response, and cell lysis although normally within acceptable limits.²⁴ Such problems have occurred when the devices have been used in areas of low fluid transport, where the material by-products are not readily removed from the local area. This response is local and does not relate to systemic toxicity; therefore, these materials are well tolerated by the body. Although there are certainly advantages and disadvantages for each specific system, the use of absorbable materials has increased dramatically for many applications; the most prominent of these are within the tissue engineering and the suture industries.

10.3.1.3 Alginates, Chitosans, and Collagens

Natural degradable materials such as alginates, chitosans, and collagens tend to elicit a strong inflammatory response when implanted in the body. These materials are used in wound dressing and wound closure devices as well as drug delivery systems. Alginates and chitosans are derived from seaweed and crab shells, respectively, while collagens are derived from a variety of tissue sources. Degradation of chitosans and collagens depends on the macrophage proteolytic enzymes present at the implant site. The human body does not contain alginases; thus, the degradation of alginate raises interesting compatibility issues. Alginate is gelled in the presence of a divalent cation such as calcium; thus, in the body the cations may exit the gel, resulting in loss of structural integrity and separation of the molecular chains from each other. The chains will not degrade, however, and if the molecular weight of the alginate is sufficiently high, the chains will not exit the body via normal

lating vehicle for cellular xenotransplantation, e.g., diabetes therapies, and as such is a drug delivery system. The alginate acts as a semipermeable barrier, allowing diffusion of growth factors and other cell signals to the host but protecting the transplanted cells from immunologic destruction. Again, the challenge is to track the systemic effects of alginate in the long term.

10.4 Critical Test Methods for Implants and Drug Carriers

10.4.1 Implants

The ability of an implanted polymeric biomaterial to induce carcinogenicity, either locally or systemically, is certainly a question of concern with the popularity of uses of these materials as sutures, bearing surfaces, grafts, etc. Although short-term assays of these materials have not led to conclusions of malignancy, longer term studies are necessary to eliminate all concern regarding toxic effects. This is particularly important as the patient population becomes younger and materials are expected to have longer lifetimes. Fortunately, cancers associated with polymers are rare to nonexistent.²⁶

10.5 Conclusion and Perspective on the Future

Unfortunately, there is no one test that can decisively determine cytotoxicity of a new material. Nothing less than a complete battery of tests over extended durations can determine the safety of a material that is to be implanted. It is likely that the rapid expansion of absorbable polymer technology and new fields such as tissue engineering and nanotechnology will drive the development of new and customized toxicity tests. For example, with vastly improved gene identification methods, it is anticipated that detection of gene expression by microarray and other molecular biology techniques will become integrated with biocompatibility and cytotoxicity testing. With problems of cross-contamination over microplate cultures, false positives, and difficulties with cell lines, only careful planning and quality experiments can ensure successful development of new materials for use in today's medical industry.

References

1. Seibert, H., Gülden, M. and Voss, J.-U., Comparative cell toxicology: the basis for *in vitro* toxicity testing, *ALTA*, 22, 168–174, 1994.
2. Burg, K. J. L. and Shalaby, S. W., Radiation sterilization of medical and pharmaceutical devices, in *Radiation Effects on Polymers: Chemical and Technological Aspects*, American Chemical Society, Washington, DC, 1996, 240.
3. Correa, D. E., Kline, J. D., Barefoot, S. F., Corbett, J. T. and Shalaby, S. W., Radiochemical sterilization: the fate of trace formaldehyde gas in suture packages, *Trans. Sixth World Biomater. Congr.*, II, 461, 2000.
4. Woodward, S. C., Evaluation by light microscopy, in *Handbook of Biomaterials Evaluation*, von Recum, A. F., Ed., Taylor & Francis, Philadelphia, PA, 1999, 599.
5. Biological reactivity tests, *in vitro*, *U.S. Pharmacopeia*, 23, 1697, 1995.
6. Tests for cytotoxicity: *in vitro* methods, *Biological Evaluation of Medical Devices, Part 5*, ANSI/AAMI, 1993, 10993.
7. Shalaby, S. W., Fibrous Materials for Biomedical Applications, in *High Technology Fibers*, Part A, Lewin, M. and Preston, J., Eds., Marcel Dekker, New York, 1985, 87.
8. Darby, T. D., Safety evaluation of polymer materials, *Annu. Rev. Pharmacol. Toxicol.*, 27, 157, 1987.
9. ASTM F-895 Agar Diffusion Cell Culture Screening for Cytotoxicity.
10. ASTM F-813 Direct Contact Cell Culture Evaluation of Materials for Medical Devices.
11. ASTM F-619 Extraction of Medical Plastics.
12. ASTM F-756 Assessment of Hemolytic Properties of Materials.
13. ASTM F-624 Evaluation of Thermoplastic Polyurethane Solids and Solutions for Biomedical Applications.
14. Gevaert, M., Burg, K. J. L., Weinbrenner, D. and LaBerge, M., Novel direct contact cell culture apparatus for evaluation of cell-material interaction, *Trans. 29th Annu. Meeting Soc. Biomater.*, 2003.
15. ASTM F-749 Evaluating Material Extracts by Intracutaneous Injection in the Rabbit.
16. ASTM F-750 Evaluating Material Extracts by Systemic Injection in the Mouse.
17. ASTM F-719 Testing Biomaterials in Rabbits for Primary Skin Irritation.
18. Eckstein, P., Jackson, M. C., Millman, N. and Sobrero, A. J., Comparison of vaginal tolerance tests of spermicidal preparations in rabbits and monkeys, *J. Reprod. Fertil.*, 20, 85, 1969.
19. Chvapil, M., Chvapil, T. A., Owen, J. A., Kantor, M., Ulreich, J. B. and Eskelson, C., Reaction of vaginal tissue of rabbits to inserted sponges of various materials, *J. Biomed. Mater. Res.*, 13, 1, 1979.
20. Burg, K. J. L. and Shalaby, S. W., Absorbable materials and pertinent devices, in *Handbook of Biomaterials Evaluation*, von Recum, A. F., Ed., Taylor & Francis, Philadelphia, PA, 1999, 99.
21. Upman, P., Testing, in *Handbook of Biomaterials Evaluation*, von Recum, A. F., Ed., Taylor & Francis, Philadelphia, PA, 1999, 275.
22. Rubin, J. P. et al., Complications and toxicities of implantable biomaterials used in facial reconstructive and aesthetic surgery: a comprehensive review of the literature, *Plast. Reconstr. Surg.*, 100, 1336, 1997.

23. Thumwanit, V. et al., Cytotoxicity of polymerized commercial cyanoacrylate adhesive on cultured human oral fibroblasts, *Austr. Dent. J.*, 44, 248, 1999.
24. Kyriacos, A. A. et al., Sterilization, toxicity, biocompatibility and clinical applications of polylactic acid/polyglycolic acid copolymers, *Biomaterials*, 17, 93, 1996.
25. ASTM F-748-98 Selecting generic biological test methods for materials and devices.
26. Busch, H., Silicone toxicology, *Semin. Arthr. Rheum.*, 24, 11, 1994.

Section D

Growing and Newly Sought Applications

11

Tissue Engineering Systems

Chuck B. Thomas and Karen J.L. Burg

CONTENTS

11.1	Historical	159
11.1.1	Synthetic Polymers.....	160
11.1.2	Natural Polymers	161
11.2	Evolution and Status.....	162
11.2.1	Nonabsorbable and Absorbable Polymers.....	162
11.2.2	Synthetic and Natural Polymers	162
11.2.3	Scaffold Design	164
11.2.3.1	Application of Processing Methods.....	164
11.2.3.2	Improving Biocompatibility	167
11.2.3.3	Promoting Vascularization	168
11.3	Clinical Relevance.....	169
11.3.1	Injectable Polymers	169
11.3.2	Synthetic Polymer Degradation.....	170
11.4	Conclusion and Perspective on the Future	171
	References	171

11.1 Historical

Tissue engineering is generally defined as the development of biologically based replacement tissues and organs. This is a broad definition and may incorporate cellular or acellular devices. In the case of acellular tissue engineering devices, the implant will promote growth of the existing tissue (Figure 11.1). The cellular device will supply new cells to the implant site that will either augment the existing cell population or reintroduce a missing population (Figure 11.1). Additionally, the cellular device may or may not incorporate a materials element. In many cases, however, an absorbable

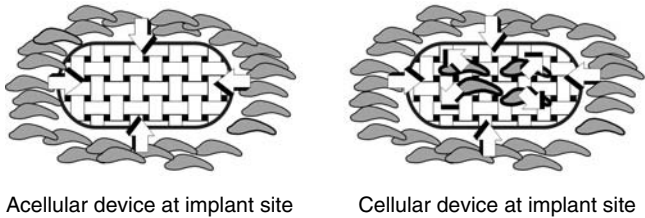


FIGURE 11.1
Acellular mesh induces tissue ingrowth (left) while cellular mesh integrates with surrounding tissue (right).

Synthetic Absorbable	Natural Absorbable
Synthetic Nonabsorbable	Natural Nonabsorbable

FIGURE 11.2
Four classifications of polymeric biomaterials.

polymeric substrate (otherwise termed as a "matrix" or "scaffold") is a key component and is sculpted to provide the appropriate form for the cellular component. The substrate may be used as a temporary delivery vehicle on which cells are housed; following implantation, the substrate absorbs at a defined rate as the tissue acquires the initial shape.

Although the term "tissue engineering" was coined years earlier in a clinical explant study of a polymethylmethacrylate (PMMA) keratoprosthesis,¹ Langer and Vacanti brought the terminology into the public eye with their review of the field in 1993.² Langer and Vacanti detailed how the field of tissue engineering could be used to provide clinical solutions for the replacement of ectodermal, endodermal, and mesodermal-derived tissue. At least 26 times they noted the importance of polymers in tissue engineering research, ranging from the treatment of Parkinson's disease and the regeneration of peripheral nerves to the design of vascular grafts and the regeneration of cartilage. Two properties are typically used to classify the tissue engineering polymers. First, the material is categorized by its affinity to break down *in vivo*; that is, it is termed either absorbable or nonabsorbable. Second, the source of the material is used to classify the material as natural or synthetic. All four combinations of these characteristics (Figure 11.2) have found use in tissue engineering.

11.1.1 Synthetic Polymers

Poly lactides have been researched for over 30 years in applications such as rods and films for bone fixation and sutures.³ Polyesters such as polygly-

colide (PGA) and poly-L-lactide-co-glycolide (PLGA) have been used since the 1970s as biodegradable sutures.⁴⁻⁸ Polydioxanone, a polyetherester, has been utilized as a biodegradable suture since the early 1980s.^{9,10} Polyorthoesters have been evaluated for drug delivery applications due to their surface erosion characteristics; they have complex degradation products, and they require additives to promote erosion.^{11,12} Polyanhydrides have also been researched for drug delivery. Langer conducted studies on polycarboxy-bisphenoxypropane (PCPP) and found that by incorporating sebacic acid (SA) with PCPP, the degradation rate could be improved.¹²

Since the 1960s, hydrogels have been employed in biomedical applications such as wound dressings and thus were incorporated immediately into tissue engineering research.¹³ One of the earliest hydrogels studied, Hydron™ (Hydro Med Sciences, Cranbury, NJ), consisted of a composite system of polyhydroxyethylmethacrylate (PHEMA) and polyethylene glycol (PEG).¹⁴ It was studied for various applications including wound dressings; however, results from different studies of this material were conflicting.¹⁵ While it was lauded for alleviating patient pain and being easily applied, reports were also published that indicated Hydron had difficulty in adhering to the wound, cracking in many instances, and requiring removal from the wound.¹⁶⁻¹⁸ Vigilon® (C. R. Bard, Inc., Covington, GA), a wound dressing hydrogel, was developed in the 1980s.¹⁹ Vigilon consisted of 96% water and polyethylene oxide (PEO) placed between two polyethylene films, and it was found to be impermeable to bacteria and permeable to oxygen. Vigilon also was able to absorb exudate from the tissue without adhering to it, and the hydrogel was practically translucent.^{20, 21}

11.1.2 Natural Polymers

The first polymers used as tissue engineering scaffold materials were natural polymers. In the late 1970s and early 1980s, Bell and co-workers researched collagen-based polymers in what are now considered tissue engineering applications.^{22,23} These studies included the development of full thickness skin-equivalent grafts that consisted of a rat collagen lattice initially cast with rat fibroblasts. After an *in vitro* growth phase, the subsequent dermal layer was seeded with epidermal cells from the same host animal, and the entire construct was implanted into an open skin wound on the back of the host. The grafts became vascularized, inhibited wound contraction, filled the original wound space, and, other than the absence of hair follicles and sebaceous glands, resembled normal skin. Yannas and co-workers performed studies in the 1970s and 1980s with porous crosslinked copolymers of collagen and glycosaminoglycans for the purpose of designing artificial skin.^{24,25} Yannas also developed copolymers of collagen and proteoglycans for skin and peripheral nerve repair.²⁶

Alginate, a natural polysaccharide, is obtained from seaweed and finds widespread use in tissue engineering research. Alginate is comprised of chains of guluronic acid and mannuronic acid, with the amount and length

of the guluronic blocks having a direct impact on its physical and mechanical properties. When alginate is combined with a source of divalent cations such as Ca^{++} or Mg^{++} , it forms a gel. Early research with alginate gels in the 1980s focused on their potential use as microencapsulation vehicles for cells.²⁷ Although alginate has good biocompatibility, it cannot be broken down enzymatically in the human body. Another drawback of alginate is that, depending on the seaweed source, the relative amounts and ratio of guluronic acid and mannuronic acid vary considerably.

11.2 Evolution and Status

11.2.1 Nonabsorbable and Absorbable Polymers

Focus has changed with time from nonabsorbable to absorbable polymers. Absorbable polymers typically take the form of fibrous meshes, porous scaffolds, or hydrogels. If the polymer can degrade at a controlled rate, the body's own cells can infiltrate the matrix and replace the polymer space with natural tissue. The use of an absorbable polymer can have many advantages, such as the following:

- Absorbable polymers provide less risk of permanent infection than nonabsorbable polymers.²⁸
- Absorbable polymers can be optimized for specific applications. For example, they can be manufactured to provide a local acidic or basic environment for the cells. Their porosity and pore size can be tailored to alter mechanical properties and to provide optimal growth parameters for specific cell types. In addition, their degradation can be altered so that the polymer erodes from the inside (bulk erosion) or by surface erosion. Side chains can also be included in the polymer design so that drugs, growth factors, hormones, and nutrients can be released during degradation.²⁹
- Absorbable implants do not necessitate a removal operation, which is advantageous to both the patients and the economy.³⁰

11.2.2 Synthetic and Natural Polymers

Selection of a tissue engineering substrate includes a choice between absorbable and nonabsorbable material, as well as a choice between synthetic and naturally derived materials. The most common synthetic polymers used for fibrous meshes and porous scaffolds include polyesters such as polylactide and polyglycolide and their copolymers, polycaprolactone, and polyethylene glycol. Synthetic polymers have advantages over natural polymers in select instances, such as the following:³¹

- Synthetic polymers can be fabricated by molding, extrusion, and solvent processing into reproducible shapes and sizes with little batch-to-batch variation.
- Synthetic polymers can be designed to degrade at a controllable rate rather than the variable rate found with the typically enzymatic degradation of natural polymers.
- Synthetic polymers can be fabricated with customized molecular weight and hydrophobicity.
- Synthetic polymers generally elicit a lower immune response and lower antigenicity.
- Synthetic polymers are generally more versatile in that their properties can be adjusted to meet the needs of the application.

In contrast, natural polymers have certain advantages over synthetic polymers. For example, naturally derived materials provide a natural surface for better cell attachment and a greater capability of promoting cell differentiation.

A notable disadvantage of synthetic polymers is their lack of cell-recognition signals, and a distinct disadvantage of the naturally derived polymers is their propensity to rapidly remodel in the body.³² Regardless of the type of material selected (i.e., synthetic or natural), scaffolds must have the following characteristics:³¹

- Surface properties that promote cell adhesion, proliferation, and differentiation
- Controllable degradation rate
- Biocompatibility
- Degradation products that are excreted by normal physiologic metabolic pathways
- Large surface-area-to-volume ratio
- Easy processability into three-dimensional shapes of complex geometry
- Mechanical properties capable of withstanding stresses in specific applications

One important disadvantage of absorbable poly-L-lactide (PLLA), PGA, and PLGA is that a sharp drop in the pH of the local environment often results from degradation. The release of the lactic acid and glycolic acid degradation products contributes to the rise in acidity and can promote an inflammatory reaction in areas of low fluid transport. Thus, a constant release of degradation products (instead of a bolus release) is desired so that the body has sufficient time to rid waste products from the implant area.³¹ The degradation of absorbable polymers depends on many factors, including

crystallinity, chain mobility, degradative medium, molecular orientation, surface/volume ratio, chemical composition, shape, molecular weight, molecular weight distribution, hydrophilicity/hydrophobicity, impurities, porosity, surface texture, and mass.³³

11.2.3 Scaffold Design

11.2.3.1 Application of Processing Methods

Since many of our tissues are three-dimensional in shape, a strong effort has been made in the last 15 years to design three-dimensional polymer matrices for implantation. Such polymer scaffolds can be prepared by fiber bonding, solvent-casting and particulate-leaching, membrane lamination, melt molding, emulsion/freeze-drying, high pressure (gas foaming), or phase inversion.^{31,34} Cima and co-workers were among the first to design a three-dimensional polymer matrix by fiber bonding for tissue engineering applications.³⁵ They manufactured a PGA fiber-based felt by entangling 15 μm -diameter fibers into a matrix of 2 mm thickness. They investigated the use of the matrix as a support for transplanting cartilage and liver cells, and they concluded that the method, in general, is feasible for cell transplantation and tissue regeneration (Figure 11.3). They also noted that many obstacles must be overcome before such technology can be made clinically available. These obstacles include modification of the surface chemistry, three-dimensional microstructure, porosity, and shape of the absorbable polymer.

In a similar study, osteoblasts, osteocytes, and chondrocytes were grown on fibers obtained from a nonwoven mesh of polyglycolide. Vacanti and co-workers demonstrated that polyglycolide can be used as a matrix for bone and cartilage cell transplantation.³⁶ A drawback to the use of these fibrous meshes was their insufficient compressive properties. In a study by Mooney

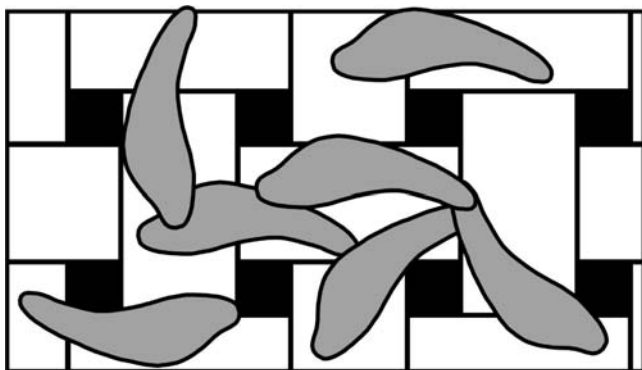
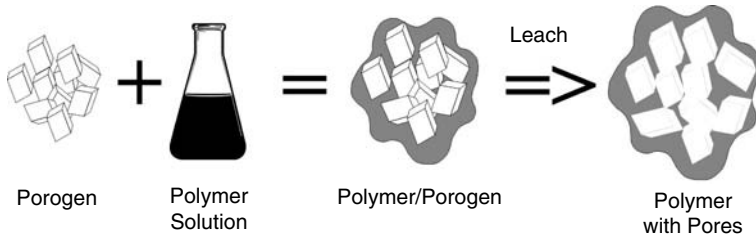


FIGURE 11.3

Cellular attachment to a polymeric matrix is affected by many factors, including matrix topography.

**FIGURE 11.4**

Solvent-casting, particulate-leaching is a common method of creating porous foams.

and co-workers, PGA meshes were coated with atomized solutions of PLLA or PLGA, which physically bonded to the PGA fibers.³⁷ Compression properties increased with the extent of bonding; the PLLA coating provided more strength than the PLGA coating. PGA meshes coated with PLGA degraded more rapidly than those with the PLLA coating.

Another method to improve the compressive properties of a porous scaffold was proposed by Thomson and co-workers.³⁸ Using a modified solvent-casting, particulate-leaching technique with compression molding, three-dimensional porous scaffolds of PLGA and short hydroxyapatite fibers were fabricated. Results from these studies, however, were mixed. The compressive strength increased in low porosity foams that had large amounts of hydroxyapatite fibers; however, these foams were not suitable for cell seeding due to their low porosity. Conversely, the compressive strength of the highly porous scaffolds did not increase with the amount of hydroxyapatite fibers incorporated; yet, the highly porous scaffolds were most suitable for cell seeding.

In another study, Ishaug and co-workers grew enzymatically isolated rat calvarial osteoblasts on different compositions of poly(α -hydroxy ester) films *in vitro* to evaluate feasibility of cell growth on these polymers and to determine if copolymer composition had any effect on osteoblast adhesion, growth, and phenotype.³⁹ The compositions tested were 100% PLLA, 75/25 PLGA, 50/50 PLGA, and 100% PGA. Ishaug and co-workers concluded that the osteoblasts attached, proliferated, and maintained their phenotype on all four compositions.

Mikos and co-workers developed a solvent-casting, particulate-leaching technique aimed at producing highly porous, three-dimensional foams of PLLA (Figure 11.4).⁴⁰ This technique was similar to those used previously in the filter industry to manufacture nonabsorbable porous filters. The resultant highly porous structure provided a greater surface area-to-volume ratio than a film construct, and it created extra space for cellular growth and extracellular matrix deposition. Large surface areas are critical for growth of anchorage-dependent cells, as is an interconnected pore network that allows cells to be freely distributed throughout the scaffold. Mikos and co-workers reported that foams of targeted crystallinity, porosity, and surface area-to-volume ratio were fabricated. They also concluded that the foam properties

were not affected by solvent selection or particulate type; the properties only depended on particle size and initial particulate weight fraction.

Extending the scope of Mikos' work, Ishaug and co-workers grew rat stromal osteoblasts *in vitro* on PLGA foams with pore sizes ranging from 150 to 710 μm , and found that pore size did not affect cell proliferation and function.^{40,41} They then grew rat neonatal calvarial osteoblasts *in vitro* on PLGA foams with pore sizes ranging from 150 to 710 μm and confirmed that calvarial osteoblasts could similarly form bonelike tissue *in vitro*.⁴²

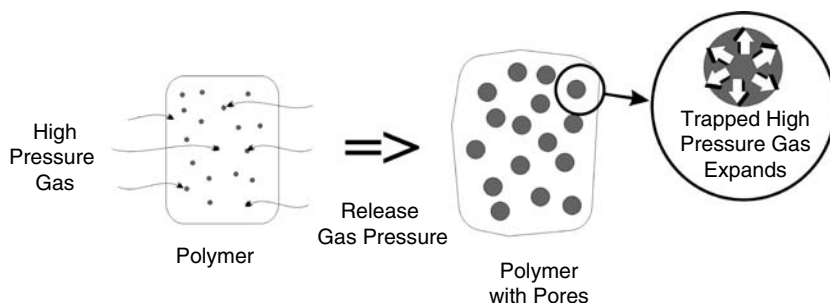
In a related study, Goldstein and co-workers tested the effect of cell culture conditions on PLGA porous scaffolds seeded with rat marrow stromal cells.⁴³ They discovered that high porosity foams had the greatest shrinkage in cell culture and might not be suitable for load-bearing applications such as treatment of orthopedic defects. The researchers recommended using foams with a maximum porosity of 80%.

In an effort to engineer soft tissues, Wake and co-workers used a solvent-casting, particulate-leaching method to fabricate pliable, porous scaffolds made of blends of PLGA and PEG.⁴⁴ They investigated the effects of PLGA copolymer ratio, PLGA/PEG blend ratio, initial salt weight fraction, and salt particle size on pliability and pore morphology. The study indicated that initial particulate weight fraction and PLGA/PEG blend ratio had the most significant effects on the physicomaterial properties of the scaffolds. Pliability was shown in that the PLGA/PEG scaffolds were able to be rolled into tubes without macroscopic damage.

Polyesters have also been processed into tubular form for orthopedic and cardiovascular tissue engineering applications. Meinig and co-workers evaluated bone regeneration using tubular PLLA membranes in mid-diaphyseal defects in rabbit radii.⁴⁵ The membrane prevented soft tissue formation in the defect area, and it allowed woven bone to fill the defect. Local inflammation or systemic intolerance was not observed, and the membranes remained intact for the entire 64-week study.

In a similar study, Pineda and co-workers investigated the role of pore size in tubular PLLA membranes.⁴⁶ They found that a thin connective tissue layer formed between the membrane and the newly formed bone, indicating a lack of osseointegration of the membrane. They also concluded that bone formation was not as intensive as the pore size of the membranes increased. Finally, they concluded that the primary function of such a membrane in this application was to support the growth of cells in the "medullary cavity" formed by the membrane.

Niklason and Langer studied the feasibility of using PLGA and PGA for tissue-engineered, small diameter blood vessels.⁴⁷ They reported that PLGA films supported confluent monolayers of aortic smooth muscle and endothelial cells, and PGA mesh scaffolds developed a tissue-like appearance when seeded with aortic smooth muscle cells. They also claimed that PGA scaffolds formed into a tube did not maintain sufficient strength required for blood vessels, even with smooth muscle tissue formed on the polymer. In an effort to improve the results, they applied pulsatile stretch forces to the cell-polymer

**FIGURE 11.5**

Gas foaming is a method of forming porous scaffolds without the use of solvents.

constructs during the culture period. To mimic *in vivo* conditions, they used pulsatile intraluminal pressure and flow. Strength properties improved, but the constructs could not withstand arterial pressure.

One of the criticisms often heard about porous scaffold fabrication of polylactides and polyglycolides is that toxic organic solvents are used that cannot be completely removed through processing. To address this issue, Holy and co-workers used a multistep extraction method for producing porous foams of PLGA.³⁴ They began by dissolving PLGA in dimethylsulfoxide (DMSO) and placing the solution in aluminum molds. The DMSO was then removed by extraction in distilled water and the foams were freeze-dried.

Another study that was performed to fabricate porous scaffolds without organic solvents or high temperatures was reported by Harris and co-workers.⁴⁸ They proposed the use of a gas-foaming/particulate-leaching technique to form PLGA foams (Figure 11.5). Gas foaming methods typically result in a scaffold having a closed pore structure, which is undesirable for most cell transplantations. Harris and co-workers compression-molded mixtures of PLGA and sodium chloride (NaCl) particles at room temperature. The pressed disks were then subjected to carbon dioxide at 800 psi for 48 h. After releasing the pressure, the disks were washed in distilled water for 48 h to remove the salt particles. Control scaffolds were also prepared using a standard solvent-casting, particulate-leaching technique. Harris and co-workers found that foams produced by the new technique had significantly greater compressive and tensile moduli than the control scaffolds. Smooth muscle cells readily adhered and proliferated on the new scaffolds as well.

11.2.3.2 Improving Biocompatibility

In addition to the release of acidic degradation products, another deficiency of polyesters used in tissue engineering is their lack of functional groups. To improve biocompatibility of PLLA and PGA, some researchers have processed these polyesters with amino acids such as glycine and lysine.^{49,50}

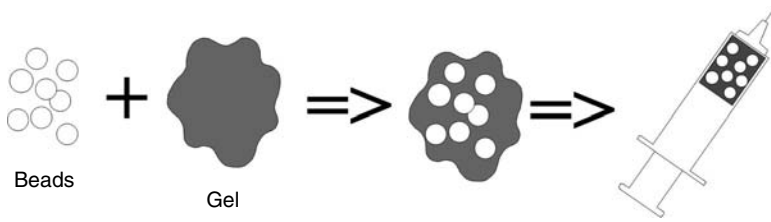
Polymers that can guide development of tissue through the addition of arginine-glycine-aspartic acid (RGD) or other polypeptide sequences have also been fabricated. The RGD sequence of amino acids is found in proteins of the extracellular matrix such as fibronectin, and one of the sequence's roles is to promote cell adhesion. The purpose of synthesizing such polymers is to manipulate the body into treating the synthetic material, which mimics the extracellular matrix, like natural tissue. If successful, cells should then readily attach and proliferate on the scaffold. Shakesheff and co-workers provide a review of the three major techniques used to create polymer-peptide hybrid materials.⁵¹

While the future of poly(amino acids) in tissue engineering looks promising, their use is restricted due to issues involving immunogenicity and contamination during large-scale production.³² Despite these problems, positive results have been obtained. Laurencin and others designed a three-dimensional scaffold made out of a degradable amino acid-containing polymer, poly[(methylphenoxy)(ethyl glycinato) phosphazene].⁵² Osteoblasts from cell line MC3T3 were seeded onto the matrix, and the cells attached and grew during the study. Poly(amino acids) have been produced using *in situ* techniques such as irradiation by ultraviolet light.⁵³

11.2.3.3 Promoting Vascularization

One of the constraints in designing a porous scaffold for tissue engineering applications is the thickness of the scaffold and how it relates to cell proliferation. Most cells (with the notable exception of chondrocytes) require support from the vascular system to receive nutrients and oxygen. Unfortunately, vascularization of thick porous scaffolds often does not occur quickly enough to allow survivability of cells located in the interior. Holder and co-workers addressed this concern by adding vascular endothelial cells to PGA meshes in an attempt to increase *in vivo* vascularization of the implant.⁵⁴ After a 4-week implantation time in rats, the researchers found that seeding the scaffolds with endothelial cells increased the number of capillaries and lymphatic-like structures. The scaffolds also supported vascular structures that contained blood and were factor-VIII positive. Holder and co-workers concluded that adding vascular endothelial cells to tissue engineering scaffolds might allow development of thicker constructs.

Eiselt and co-workers developed another method for promoting vascularization of large engineered tissues, such as soft tissue for breast reconstruction.⁵⁵ Vascular endothelial growth factor (VEGF) and heparin were incorporated into a solution of PLGA, and microspheres were fabricated using a double-emulsion technique. The microspheres were sized, and drug incorporation and release were measured. The researchers were able to design the spheres to release a burst of VEGF initially to trigger angiogenesis, followed by a slower, stable release to maintain a positive response.

**FIGURE 11.6**

Development of tissue engineered composite, injectable materials.

11.3 Clinical Relevance

11.3.1 Injectable Polymers

Tissue-engineered constructs have an advantage over many implants in that they offer the possibility of implantation by minimally invasive surgery such as laparoscopy. Hydrogels have a significant advantage over fibrous meshes and porous scaffolds in that they can be implanted by injection, making them even less invasive than implants of fibrous meshes or porous scaffolds (Figure 11.6).

The ideal injectable polymer should have the following characteristics:⁵⁶

- Fill spaces of various sizes and shapes
- Polymerize *in situ* without harming surrounding tissue
- Degrade according to a planned degradation profile
- Produce degradation products that can be eliminated by normal metabolic pathways
- Maintain desirable properties as it degrades
- Exhibit required physical, chemical, and mechanical properties for the application
- Be routinely sterilized without harming properties
- Have a long shelf-life
- Be available to surgeon on short notice

Polypropylene fumarate (PPF) has been in development since the mid-1990s as an injectable, absorbable bone cement with tissue engineering potential. In a 5-week *in vivo* study in rats, a PPF-based composite crosslinked with *N*-vinylpyrrolidinone showed good biocompatibility with bone ingrowth and no inflammatory response.⁵⁷ Peter and co-workers provide an extensive review of the early development of PPF composite materials, including information about its synthesis, crosslinking, degradation, and

biocompatibility.⁵⁶ Briefly, PPF is formed by combining fumaryl chloride and propylene glycol to form a diester intermediate, which undergoes a transesterification to obtain the polymer. PPF can be crosslinked with a vinyl monomer such as *N*-vinyl pyrrolidinone. Injectable PPF composites can be fabricated by adding components (such as sodium chloride to create porosity or β -tricalcium phosphate to improve mechanical properties) to the PPF-monomer mixture. The maximum crosslinking temperature for the various formulations ranges between 38 and 48°C.

Recent approaches in fabrication of injectable tissue engineering materials involve crosslinking of polymers *in situ*. Advantages of crosslinkable systems include good mechanical properties, processing ease, and implant flexibility. Important factors include the crosslinking temperature and reagent toxicity.⁵⁸ Burg and co-workers introduced the concept of a composite, injectable material, in which cellular microbeads or fragments of injectable size are delivered to a tissue defect site via syringe injection.⁵⁹ The microbeads provide a sufficiently high modulus for anchorage-dependent cells, and the delivery gel facilitates the injection and prevents the beads from compressing post implantation. This system is ideal for irregular defects formed by traumatic injury or surgical tissue removal in cancer treatment.

11.3.2 Synthetic Polymer Degradation

PGA and PLLA go through a process of hydrolytic degradation that causes a decline in the molecular weight of the implant; however, the mass remains nearly constant. At low molecular weights, the implant can disintegrate and produce small fragments that elicit an immune response from macrophages.⁶⁰ PLLA and PGA degrade in a time period of 6 months to several years, depending on initial molecular weight and crystallinity; copolymers of the two pure forms typically degrade in a few months.⁶¹ Copolymers of these polyesters have been formed with polyethylene glycol to reduce the inflammatory reaction upon degradation, and the PEG also aids in improving biocompatibility for some applications.⁶² Polylactides, polyglycolides, and their copolymers degrade *in vivo* by hydrolysis of the polyester bond.³¹ Numerous polyester bonds are broken throughout the polymer until lactic acid and/or glycolic acid remains. These products can then be processed through normal metabolic pathways, and they finally break down to carbon dioxide and are eliminated by the respiratory system.

PGA is highly crystalline and hydrophilic, and its degradation rate depends on its crystallinity. PLLA is less crystalline and more hydrophobic (due to the presence of a methyl group, which sterically hinders hydrolysis of the ester bond) than PGA; thus, it degrades at a slower rate. PLLA has good strength properties among biodegradable polymers. PLGA copolymers have the advantage of being able to manipulate their degradation rate through varying the content of glycolic acid between 25 and 70%. PLGA

copolymers are amorphous, and they do not have strength properties that match PLLA.³¹

11.4 Conclusion and Perspective on the Future

There is an urgent need for characterizing polymers implanted in the body by histological techniques. Many polymers used in tissue engineering require special care and consideration when histologically examined. For example, the poly (α -hydroxy acids) are especially prone to the organic solvents and high temperatures used in traditional histological sample preparation. Histological techniques need to be developed in order for these tissue constructs to be properly evaluated after explantation. Since histological examination of tissues is routine in a clinical setting, this development is imperative for improved communication and collaboration between tissue engineers and clinical researchers.

The functions of tissue-engineered systems also need to be properly evaluated. For example, thorough biomechanical testing of polymer constructs developed for tissue engineering will be required in addition to the biological and physicochemical properties so often studied. It is not sufficient to show that a construct excels in promoting cellular attachment, proliferation, and differentiation of the desired phenotypes and has a desirable degradation profile if it cannot meet the mechanical requirements of the intended application.

References

1. Wolter, J. R. and Meyer, R. F., Sessile macrophages forming clear endothelium-like membrane on inside of successful keratoprosthesis, *Trans. Am. Ophthalmol. Soc.*, 82, 187, 1984.
2. Langer, R. and Vacanti, J. P., Tissue engineering, *Science*, 260, 920, 1993.
3. Kulkarni, R. K. et al., Biodegradable poly(lactic acid) polymers, *J. Biomed. Mater. Res.*, 5, 169, 1971.
4. Herrmann, J. B., Kelly, R. J., and Higgins, G. A., Polyglycolic acid sutures. Laboratory and clinical evaluation of a new absorbable suture material, *Arch. Surg.*, 100, 486, 1970.
5. McCarthy, W. H., A new synthetic absorbable suture material: a clinical trial of polyglycolic acid suture in general surgery, *Aust. NZ J. Surg.*, 39, 422, 1970.
6. Postlethwait, R. W., Polyglycolic acid surgical suture, *Arch. Surg.*, 101, 489, 1970.
7. Conn, J., Jr., et al., Vicryl (polyglactin910) synthetic absorbable sutures, *Am. J. Surg.*, 128, 19, 1974.
8. Horton, C. E. et al., Vicryl synthetic absorbable sutures, *Am. Surg.*, 40, 729, 1974.

9. Bartholomew, R. S., PDS (polydioxanone suture): a new synthetic absorbable suture in cataract surgery. A preliminary study, *Ophthalmologica*, 183, 81, 1981.
10. Ray, J. A. et al. Polydioxanone (PDS), a novel monofilament synthetic absorbable suture, *Surg. Gynecol. Obstet.*, 153, 497, 1981.
11. Heller, J., Controlled release of biologically active compounds from bioerodible polymers, *Biomaterials*, 1, 51, 1980.
12. Langer, R., 1994 Whitaker Lecture: polymers for drug delivery and tissue engineering, *Ann. Biomed. Eng.*, 23, 101, 1995.
13. Wichterle, O. and Lim, D., Hydrophilic gels for biological use, *Nature*, 185, 117, 1960.
14. Levowitz, B. S. et al., Biologic compatibility and applications of hydon, *Trans. Am. Soc. Artif. Intern. Organs*, 14, 82, 1968.
15. Nathan, P. et al., A new biomaterial for the control of infection in the burn wound, *Trans. Am. Soc. Artif. Intern. Organs*, 22, 30, 1976.
16. Brown, A. S., Hydon for burns, *Plast. Reconstr. Surg.*, 67, 810, 1981.
17. Curreri, P. W. et al., Safety and efficacy of a new synthetic burn dressing: a multicenter study, *Arch. Surg.*, 115, 925, 1980.
18. Warren, R. J. and Snelling, C. F., Clinical evaluation of the Hydon burn dressing, *Plast. Reconstr. Surg.*, 66, 361, 1980.
19. Geronemus, R. G. and Robins, P., The effect of two new dressings on epidermal wound healing, *J. Dermatol. Surg. Oncol.*, 8, 850, 1982.
20. Eaglstein, W. H., Experiences with biosynthetic dressings, *J. Am. Acad. Dermatol.*, 12, 434, 1985.
21. Yates, D. W. and Hadfield, J. M., Clinical experience with a new hydrogel wound dressing, *Injury*, 16, 23, 1984.
22. Bell, E. Ivarsson, B. and Merrill, C., Production of a tissue-like structure by contraction of collagen lattices by human fibroblasts of different proliferative potential in vitro, *Proc. Natl. Acad. Sci. USA*, 76, 1274, 1979.
23. Bell, E. et al., Living tissue formed *in vitro* and accepted as skin-equivalent tissue of full thickness, *Science*, 211, 1052, 1981.
24. Yannas, I. V. and Burke, J. F., Design of an artificial skin. I. Basic design principles, *J. Biomed. Mater. Res.*, 14, 65, 1980.
25. Yannas, I. V. et al., Design of an artificial skin. II. Control of chemical composition, *J. Biomed. Mater. Res.*, 14, 107, 1980.
26. Yannas, I. V., Biologically active analogs of the extracellular matrix: artificial skin and nerves, *Angew. Chem. Int. Ed. Engl.*, 29, 20, 1990.
27. Lim, F. and Moss, R. D., Microencapsulation of living cells and tissues, *J. Pharm. Sci.*, 70, 351, 1981.
28. Gristina, A. G., Biomaterial-centered infection: microbial adhesion versus tissue integration, *Science*, 237, 1588, 1987.
29. Vacanti, C. A. and Vacanti, J. P., Bone and cartilage reconstruction with tissue engineering approaches, *Otolaryngol. Clin. North. Am.*, 27, 263, 1994.
30. Rokkanen, P. et al., Absorbable devices in the fixation of fractures, *J. Trauma*, 40, S123, 1996.
31. Thomson, R. C. et al., Biodegradable polymer scaffolds to regenerate organs, *Adv. Polym. Sci.*, 122, 245, 1995.
32. Kim, B. S. and Mooney, D. J., Development of biocompatible synthetic extracellular matrices for tissue engineering, *Trends Biotechnol.*, 16, 224, 1998.
33. Burg, K. J. and Shalaby, S. W., Physicochemical changes in degrading polylactide films, *J. Biomater. Sci. Polym. Ed.*, 9, 15, 1997.

34. Holy, C. E., Davies, J. E., and Shoichet, M. S., Bone tissue engineering on biodegradable polymers: preparation of a novel poly(lactide-co-glycolide) foam, in *Biomaterials, Carriers for Drug Delivery and Scaffolds for Tissue Engineering*, Peppas, N. A. et al., Eds., AIChE Press, New York, 1997, 272.
35. Cima, L. G. et al., Tissue engineering by cell transplantation using degradable polymer substrates, *J. Biomech. Eng.*, 113, 143, 1991.
36. Vacanti, C. A. et al., Tissue-engineered growth of bone and cartilage, *Transplant. Proc.*, 25, 1019, 1993.
37. Mooney, D. J. et al., Stabilized polyglycolic acid fibre-based tubes for tissue engineering, *Biomaterials*, 17, 115, 1996.
38. Thomson, R. C. et al., Hydroxyapatite fiber reinforced poly(α -hydroxy ester) foams for bone regeneration, *Biomaterials*, 19, 1935, 1998.
39. Ishaug, S. L. et al., Osteoblast function on synthetic biodegradable polymers, *J. Biomed. Mater. Res.*, 28, 1445, 1994.
40. Mikos, A. G. et al., Preparation and characterization of poly(L-lactic acid) foams, *Polymer*, 35, 1068, 1994.
41. Ishaug, S. L. et al., Bone formation by three-dimensional stromal osteoblast culture in biodegradable polymer scaffolds, *J. Biomed. Mater. Res.*, 36, 17, 1997.
42. Ishaug-Riley, S. L. et al., Three-dimensional culture of rat calvarial osteoblasts in porous biodegradable polymers, *Biomaterials*, 19, 1405, 1998.
43. Goldstein, A. S. et al., Effect of osteoblastic culture conditions on the structure of poly(DL-lactic-co-glycolic acid) foam scaffolds, *Tissue Eng.*, 5, 421, 1999.
44. Wake, M. C., Gupta, P. K. and Mikos, A. G., Fabrication of pliable biodegradable polymer foams to engineer soft tissues, *Cell. Transplant.*, 5, 465, 1996.
45. Meinig, R. P. et al., Bone regeneration with resorbable polymeric membranes: treatment of diaphyseal bone defects in the rabbit radius with poly(L-lactide) membrane. A pilot study, *J. Orthop. Trauma*, 10, 178, 1996.
46. Pineda, L. M. et al., Bone regeneration with resorbable polymeric membranes. III. Effect of poly(L-lactide) membrane pore size on the bone healing process in large defects, *J. Biomed. Mater. Res.*, 31, 385, 1996.
47. Niklason, L. E. and Langer, R. S., Advances in tissue engineering of blood vessels and other tissues, *Transplant. Immunol.*, 5, 303, 1997.
48. Harris, L. D., Kim, B. S., and Mooney, D. J., Open pore biodegradable matrices formed with gas foaming, *J. Biomed. Mater. Res.*, 42, 396, 1998.
49. In 'T Veld, P. J. et al., Glycine/glycolic acid based copolymers, *J. Polym. Sci. Polym. Chem.*, 32, 1063, 1994.
50. Barrera, D. A. et al., Copolymerization and degradation of poly(lactic acid-co-lysine), *Macromolecules*, 28, 425, 1995.
51. Shakesheff, K., Cannizzaro, S. and Langer, R., Creating biomimetic micro-environments with synthetic polymer-peptide hybrid molecules, *J. Biomater. Sci. Polym. Ed.*, 9, 507, 1998.
52. Laurencin, C. T. et al., A highly porous 3-dimensional polyphosphazene polymer matrix for skeletal tissue regeneration, *J. Biomed. Mater. Res.*, 30, 133, 1996.
53. Elisseff, J. et al., Synthesis and characterization of photo-cross-linked polymers based on poly(L-lactic acid-co-L-aspartic acid), *Macromolecules*, 30, 2182, 1997.
54. Holder, W. D. et al., Increased vascularization and heterogeneity of vascular structures occurring in polyglycolide matrices containing aortic endothelial cells implanted in the rat, *Tissue Eng.*, 3, 149, 1997.
55. Eiselt, P. et al., Development of technologies aiding large-tissue engineering, *Biotechnol. Prog.*, 14, 134, 1998.

56. Peter, S. J. et al., Polymer concepts in tissue engineering, *J. Biomed. Mater. Res.*, 43, 422, 1998.
57. Yaszemski, M. J. et al., The ingrowth of new bone tissue and initial mechanical properties of a degrading polymeric composite scaffold, *Tissue Eng.*, 1, 41, 1995.
58. Behraves, E. et al., Synthetic biodegradable polymers for orthopaedic applications, *Clin. Orthop.*, S118, 1999.
59. Burg, K. J. L. et al., A novel approach to tissue engineering: injectable composites, *Trans. 2000 World Biomater. Congr.*, Kona, HI, May 2000.
60. Huffman, K. R. and Casey, D. J., Effect of carboxyl end groups on hydrolysis of polyglycolic acid, *J. Polym. Sci. Polym. Chem.*, 23, 1939, 1985.
61. Miller, R. A. et al., Degradation rates of oral resorbable implants (polylactates and polyglycolates): rate modification with changes in PLA/PGA copolymer ratios, *J. Biomed. Mater. Res.*, 11, 711, 1977.
62. Hubbell, J. A., Biomaterials in tissue engineering, *Biotechnology (NY)*, 13, 565, 1995.

12

Synthetic Vascular Constructs

Shalaby W. Shalaby and Waleed S.W. Shalaby

CONTENTS

12.1 Introduction	175
12.2 Early Development of Synthetic Vascular Grafts.....	176
12.3 Evolution in the Use of Synthetic Absorbable Polymers for Vascular Grafts and Patches	176
12.4 New Approaches to the Development of Vascular Grafts and Allied Devices	178
12.4.1 General	178
12.4.2 Absorbable Grafts	178
12.4.3 Partially Absorbable Vascular Grafts and Wraps	179
12.4.4 Vascular Wraps or Patches	183
12.5 Contemporary Vascular Applications of Absorbable Polymers	184
12.5.1 Absorbable Femoral Sealing Devices.....	184
12.5.2 Absorbable Stent Mantle.....	185
12.5.3 Absorbable Sealant/Drug Carrier for Polytetrafluoroethylene (ePTFE) Grafts	186
12.5.4 Partially Absorbable Bicomponent Fibers for Vascular Grafts.....	186
12.6 Conclusion and Perspective on the Future	186
References	187

12.1 Introduction

Vascular diseases are among the leading causes of death in Western countries. Surgical treatments developed over the past half century were associated with significant early clinical successes. However, further advances in this field have been hampered because of the limited availability of effective reconstructive biomaterials. This is particularly the case for biomaterials that

meet certain hemocompatibility and biomechanical requirements used in repairing or reconstructing vascular walls, which have been pathologically or mechanically compromised. Most common among known synthetic vascular constructs, which contain absorbable polymers, are vascular grafts. Other forms of vascular constructs, which are receiving increased attention, include vascular patches and wraps and arterial seals.

12.2 Early Development of Synthetic Vascular Grafts

Since Voorhees and co-workers first used Vinyon “N” cloth as a vascular graft and their conclusion that synthetic materials could serve as conduits, development in this area did not keep pace with impressive advances in materials and medical device technologies.¹ Meanwhile, the considerable health concerns associated with vascular diseases and inadequate supply of native vessels for bypass procedures have led to the development of synthetic vascular grafts made from expanded polytetrafluoroethylene (ePTFE), polyethylene terephthalate (PET), or polyurethanes (PU). For all practical purposes, these grafts satisfy the need for large size vascular grafts with patency approaching those of autologous grafts. However, the synthetic, small-diameter grafts are yet to match the autologous grafts in terms of long-term patency regardless of the enormous commercial efforts that were driven by a market that can exceed \$2 billion per annum. For the past 20 years, no major developments have been accomplished in this area in spite of the recent rush to exploit the new findings associated with tissue engineering. This may be attributed to the fundamental disconnect between highly focused areas of academic vascular research and industrial efforts where interests broadly extend from abstract cell biology and tissue engineering to short-term, applied vascular research. It is well acknowledged that functional failures of synthetic vascular grafts are associated with:

- Loss of patency due to platelet aggregation and subsequent thrombosis
 - Delayed or inadequate surface endothelialization
 - Blood leakage and/or mechanical failure due to improper graft construction and/or biomechanical properties
 - Infection, which may be traced to compromised graft sterility
-

12.3 Evolution in the Use of Synthetic Absorbable Polymers for Vascular Grafts and Patches

Many attempts have been made at engineering vascular grafts by providing a tubular, porous, polymer support structure. The structure must be mechan-

ically sound so as not to collapse or interfere with blood transport through the conduit. Absorbable polymers made from glycolide (G) and/or *l*-lactide (LL) have shown favorable responses to such mechanical stresses. Absorbable LL/G copolymers can be made to have different compositions in order to provide a range of degradation times from several weeks to a few years.²

The poor biocompatibility of traditional synthetic materials and the persistent dilemma of clinically unacceptable graft diameters (<6 mm) provided the incentive to improve clinical performance through substrate modification. One such attempt is the surface modification of synthetic tubular materials or type I collagen with endothelial cells and smooth muscle cells to provide a more biologically "friendly" implant.³⁻⁵ Other investigators have tried coating 90/10 poly(glycolide-co-*l*-lactide)-based grafts with absorbable materials such as a mixture of poly-DL-lactide/poly-(2,3-butylene maleate) or poly-(2,3-butylene fumarate)/poly-DL-lactide.⁶⁻⁸ Fumarate leads to a more uniform and predictable absorption rate without evidence of complications due to aneurysm or rupture. Alternatively, the porosity of a tubular implant may be adjusted to provide a diminishing array of pore sizes from the exterior to the interior of the implant, thus potentially allowing increased capillarization and improved biocompatibility.⁹

Traditionally, the ideal vascular graft material was assumed to be biologically inert. Today, however, research has shifted toward creating an active material that will interact and integrate favorably with the surrounding biological environment. Thus, the use of absorbable materials appears to meet this dynamic requirement and in some systems has been shown to stimulate growth factor release through macrophage induction. Both polyglycolide (PGA) 90/10 glycolide/*l*-lactide copolymer and polydioxanone (PDS) woven grafts have successfully demonstrated in animal studies inner capsule development as well as capillary invasions, thus resulting in an integrated, mechanically stable prosthesis.¹⁰⁻¹² The inner capsule was shown to contain layers of myofibroblasts covered by endothelial-like cells, which were assumed to originate from a capillary endothelial source. In similar studies, Dacron-reinforced PGA showed no such capsule development and low amounts of transinterstitial macrophage migration, presumably due to the inhibitive nature of Dacron.¹³ Similarly, partially absorbable vascular patches based on woven composite yarn comprising polyglycolide (24 to 82%) and polyethylene terephthalate (18 to 76%) yarns were evaluated in dogs.¹⁴ Results indicate that the patch biocompatibility and effect on blood components increased with the increase in the polyglycolide content. This highlights the importance of tissue ingrowth to the construction of successful synthetic vascular grafts.

The compliance and longevity of a potential vascular graft material can influence the retention of mechanical integrity.^{15,16} Studies in the polyurethane/poly-*l*-lactide (PU/PLLA) system have shown that a decrease in the percentage of polyurethane causes a decrease in compliance and an increase in aneurismal degeneration.¹⁷ These studies further showed that high mechanical compliance of the graft at implantation stimulates elastin forma-

tion and an absorbable graft material allows maintenance of the mechanical stability of the newly formed tissue. The PU/PLLA system was initially compliant; however, long-term incidences of aneurismal dilation were significantly greater in this system than in the polyester ones. It was postulated that the long-term presence of PU leads to fibrodysplasias which decrease compliance and elastin deposition. Another important criterion in scaffold development, as with other applications, is establishing sufficient mechanical strength prior to absorption. If this is not feasible, the absorbable scaffold may be reinforced by an inert component or developed into a composite material whereby the tissue ingrowth occurs through a series of polymers. These types of multicomponent, absorbable vascular prostheses appeared to be efficacious.¹⁸ Studies have shown that, in contrast to the absorbable component, the biomechanical properties of the nonabsorbable component modulate the histologic attributes and longevity of the final tissue structure.

Other attempts at tissue engineering blood vessels have been made by constructing the vessels *ex vivo* directly from the cellular components. This may be accomplished by culturing a sheet of human vascular smooth muscle cells in collagen and placing it within a luminal support to produce the media.¹⁹ A fibroblast sheet is then similarly cultured and placed about the media to form the adventitia. Endothelial cells are later seeded into the lumen of the vessel, thus forming a mechanically sound, three-dimensional vessel.

12.4 New Approaches to the Development of Vascular Grafts and Allied Devices

12.4.1 General

Of the new approaches to the development of vascular grafts using absorbable polymers, it is believed by the authors that those dealing with tissue engineering, and more specifically, *in situ* tissue engineering, are most promising. For *in situ* tissue engineering, use of absorbable polymers, as with nonabsorbable polymers, to form partially absorbable grafts is a logical approach to the application of absorbable polymers in vascular grafts as well as patches. This view is shared by other investigators.²⁰⁻²²

12.4.2 Absorbable Grafts

Greisler and co-workers have examined the use of commercial absorbable fibers for the production of absorbable vascular grafts.²³ Using multifilament yarn of 90/10 poly(glycolide-co-l-lactide) and monofilaments of poly-*p*-dioxanone to produce totally absorbable grafts was shown to be impractical. This is because of the insufficient strength retention profile of these grafts postoperatively.

12.4.3 Partially Absorbable Vascular Grafts and Wraps

As early as the 1950s and 1960s, use of compound, partially absorbable, vascular grafts was evaluated by Wesolowski et al. and Fox et al.^{24,25} They evaluated 24 different combinations of graft materials in dogs and pigs. In general, it was found that coated grafts performed less favorably than compound grafts wherein the absorbable component was an integral part of the fabrication. Deleterious changes such as calcification did occur in the compound grafts; however, this occurred in a delayed fashion and was felt to be due to the absorbable component. The most satisfactory results were achieved with grafts composed of a compound yarn of absorbable catgut that had been wrapped with multifilament polyester yarn.²⁴

More recent work on compound vascular grafts has focused largely on the incorporation of lactide polymers. An early report came from Ruderman's group at Walter Reed. They evaluated woven grafts composed of 24% PLLA and 76% Dacron implanted into the abdominal aorta of dogs.²⁶ After 100 days, they found all grafts to be patent with extensive tissue ingrowth.²⁶

Bowald's group investigated compound grafts and compared double layer Vicryl grafts with Vicryl grafts anchored inside ePTFE or Dacron mesh tube grafts.²⁷ The grafts were implanted into the descending aorta of pigs. Nearly half of the pigs receiving Vicryl grafts experienced graft rupture. The pigs receiving grafts with external support did not experience graft rupture. Histologically, the supported Vicryl grafts were found to have the microscopic picture of arterial regeneration, although areas of degenerative change and calcification were noted. Increased collagen formation was noted in the Vicryl/Dacron group.²⁷

Greisler's group also investigated Vicryl in combination with Dacron, ePTFE, and polypropylene.^{12,28-31} Vicryl grafts surrounded by Dacron or ePTFE showed no incidence of aneurysmal dilatation as compared to a 20% dilatation rate for unwrapped Vicryl grafts. Arterial regeneration occurred in the wrapped grafts, but in an incomplete manner. In grafts made of Vicryl and Dacron yarn blends, the rate of aneurysmal dilatation increased proportionally with the percentage of Dacron in the blended yarn. A maximum dilation rate of 83% was seen with the 56% Dacron grafts. No dilatation was seen when 20% Dacron was used. Cellularity of the regenerated tissue generally decreased in the presence of Dacron, suggesting an inhibitory effect of this nonabsorbable biomaterial.¹³ Subsequent work demonstrated decreased prostaglandin content of the inner capsules of Dacron/Vicryl composite grafts as compared to those of Vicryl grafts.²⁸ In order to avoid the deleterious effects of Dacron, compound grafts were constructed using polypropylene, which possesses greater biocompatibility and incites a relatively low-grade inflammatory response.²⁶ And grafts comprising 69% Vicryl and 31% polypropylene were implanted into rabbit infrarenal aortas. Over 2 weeks to 12 months, all grafts remained patent without aneurysm formation. Production of 6-keto-PGF_{1 α} was in the normal range.²⁹ Vicryl/polypropylene prostheses were also implanted into the aorto-iliac positions

of dogs, and all grafts were without aneurysm formation over 1 year. Patency was enhanced as compared to Dacron and ePTFE control grafts; arterial regeneration was demonstrated.³⁰ Greisler's group also evaluated grafts made of polyglycolide (PGA) fabric reinforced by a Dacron outer wrap for up to 9 months after implantation. The incidence of aneurysmal dilatation in these grafts was zero at 9 months after implantation, and Dacron appeared to have an inhibitory effect on the cellularity of the luminal surface and inner capsule.¹³

Chu and co-workers at Cornell investigated the combination of PGA and Dacron.³² They produced knitted fabric grafts composed of PGA and Dacron fibers blended at various compositional ratios. They studied the properties of these bicomponent fabrics *in vitro*. Their major finding was the achievement of increasing water porosity over time without significant losses in the structural integrity and strength of the specimens.

Having demonstrated the effectiveness of partially resorbable arterial prostheses in rabbits, Greisler sought to evaluate longer grafts in a higher order species. Conduits (4 mm × 5 cm) were woven from composite yarns containing 70/30 PDS/polypropylene and implanted into the aorto-iliac positions of dogs for periods of up to 1 year.³³ No aneurysms or perigraft hematomas developed. The patency of the PDS/polypropylene grafts was significantly greater than that of Dacron or ePTFE control grafts. Inner capsules were completely endothelialized by 1 month. IC cellularity and thickness were greater than those within Dacron or ePTFE.³³

Van der Lei and co-workers investigated compound grafts of ePTFE fitted around PU/PLLA.³⁴ Compared to grafts composed entirely of bioresorbable PU/PLLA or biostable but compliant PU, the ePTFE-wrapped PU/PLLA grafts had diminished regeneration of all layers of the arterial wall. This was attributed to the decreased compliance associated with the ePTFE wrap. In their study of absorbable composite, small diameter vascular grafts, Prechtel and co-workers noted that current autologous and synthetic small diameter vascular grafts fail to satisfy the mechanical and biocompatible criteria required to sustain blood flow.²² Consequently, it was postulated that:

- The ideal coronary artery vascular graft must restore blood flow to the heart as well as endure high fatigue cycling and retain patency over time.
- These requirements can be satisfied through the use of a tissue-engineered construct that gradually replaces synthetic materials with natural tissue, assembling a new vessel native to the individual.³⁵⁻³⁷

Prechtel and co-workers also focused on the construction of tissue engineered, small-caliber vascular grafts that mimicked the structure of the host coronary artery.²² The design employed biodegradable polymeric fibers in a braided construct utilizing an inner and outer layer with fiber orientations similar to those of the native coronary artery to enable matched mechanical

performance and cell orientation. The fiber preform was impregnated with a crosslinked, degradable collagen matrix to enhance mechanical performance and aid tissue integration. The methodology intended to apply the principles of tissue engineering in the use of a temporary scaffold to provide the body with a structural blueprint that encourages natural tissue to integrate and eventually assume physiological responsibility for natural function. Results of the study allowed these investigators to conclude that surface erosion in the collagen matrix created stress concentrations around preexisting pores and allowed crack propagation, thus reducing the stiffness of the material and increasing the compliance of the structure. The construct retained sufficient integrity of structure to provide a conduit for fluid flow over the first 48 h of degradation *in vitro*.

In a study by Cohn et. al., a selectively biodegradable filament-wound vascular graft was prepared and its performance was compared to an expanded Gore-Tex graft.²⁰ In rationalizing the need for a selectively or partially absorbable graft, the authors noted that developing a new vascular graft is a multifaceted challenge where hemocompatibility, porosity, and compliance requirements must be organically integrated into the prosthesis design. The selectively biodegradable arterial graft was manufactured by the filament winding technique. A basic feature of filament winding is its ability to tailor the mechanical properties of the prosthesis so that a closer match with the anisotropic behavior of the native artery is achieved. These elastomeric vascular grafts are produced in a two-stage process whereby a filamentous scaffold is first wound on a rotating mandrel and subsequently impregnated with a block copolymer of polyethylene oxide and polylactic acid (PELA), a biodegradable elastomer. Due to the gradual degradation and dissolution of the PELA elastomer, the initially impervious grafts display gradually increasing mural porosity. *In vitro* degradation studies showed that PELA degrades substantially over a 2- to 4-week period, with concomitant increased porosity. As a result, the elastic modulus of the graft decreases steadily by approximately one decade over a short period of time. Axial and hoop compliance were measured under static and pulsatile internal pressure loading. The results show that the filament-wound structures exhibit an anisotropic behavior, which can be tailored to mimic that of natural arteries. Under dynamic loading at a frequency of 60 strokes/min frequency, no measurable phase difference between the applied stress and strain response was found. The hysteresis curve was seen to be a straight line. Aiming at closely matching the prosthesis and host arteries compliance, the grafts were engineered using a 50° winding angle and a wall thickness of 440 μm . The initial compliance of these prostheses was $2.5\% \text{ Hg}^{-1} 10^{-2}$, which is equivalent to an initial tensile modulus of 7.1 MPa. The as-manufactured graft exhibited extremely low water permeation (1 to 2 ml water/min cm^{-2} mm Hg). However, leakage gradually developed as a function of increased porosity from the degradation of PELA. The wound graft exhibited excellent handling and suturability characteristics as well as enhanced burst strength. In a short-term study, these small-diameter (I.D. = 6 mm)

arterial prostheses were implanted in the canine carotid and their biological performance was compared to that of expanded Gore-Tex. During their implantation, the filament-wound grafts were impervious to blood. Due to their biodegradable component, the grafts combine minimal intraoperative blood loss and high healing porosity. The luminal surface of the filament-wound prostheses was coated with a thin layer of pseudointima, which was strongly adhered to the grafts' surface. Contrasting with the stiff Gore-Tex grafts, the filament-wound prostheses retained high compliance pulsatility upon explanation. Due to its enhanced hydrophilicity, the PELA-rich mural composition attained high water uptake levels, resulting in a prosthesis which combines hydrogel soft consistency with high compliance and enhanced strength provided by the elastomeric scaffold. The selectively biodegradable graft resulted in excellent healing and incorporation processes, which was corroborated by histological studies. It is surmised that PELA plays an important role as the gradually degrading sealant of the graft and enhancing surface thromboresistance.

The two above approaches were in concert with Burg and Shalaby's earlier call for using newly developed technologies by Shalaby and co-workers.³⁸ Of these, two recently developed technologies are expected to be of value in tissue engineering applications. First, Shalaby developed a series of injectable, absorbable liquid copolymers which undergo gel formation upon contacting moist biological tissues.³⁹ These copolymers are based on polyethylene glycol segments and copolymeric segments derived from glycolide, lactide, trimethylene carbonate, ϵ -caprolactone, and/or *p*-dioxanone. These monomers are used in the production of commercial absorbable sutures. The injectable liquid polymers were described as a suitable vehicle for housing living cells for injection into desired biological sites to continue propagation into three-dimensional constructs with the gradual absorption of the gel carrier. Surface phosphonylation or sulfonation of preformed devices, including microporous open-cell foams, is described by Shalaby and co-workers.^{40,41} This technology represents a second area of promise for tissue engineering. It entails the formation of covalently bonded surface phosphonate or sulfonate groups which can (1) introduce hydrophilicity to hydrophobic substrates; and (2) bind specific proteins or peptides to direct cell attachment. Among the substrates suitable for surface phosphonylation or sulfonation are certain hydrophobic absorbable polyesters.

In outlining the future use of absorbable polymers in tissue engineering, Burg and Shalaby cited a number of key factors that need to be addressed.³⁸ One of the drawbacks to the synthetic materials as potential vascular graft materials is that, as homopolymers, they do not have the cell surface receptors required for cellular recognition. The polymers must be optimized to best modulate features such as crystallinity, surface texturing, and surface wettability in order to selectively attract specific biological components while preventing spreading of blood platelets. Surface modification, such as that described by Shalaby and co-workers, may be of value in overcoming some of these issues.⁴⁰ The need for a vascular graft implies that the sur-

rounding target tissue may be “abnormal” (atherosclerotic, for example). It has been shown in animal studies that the quality of such tissues (e.g., in the presence of excessive amounts of lipoprotein) may have a profound effect on the development of new tissue.³³ It would therefore be useful to study the absorbable material in such suboptimal conditions or in compromised tissue environments.

In their study of partially absorbable vascular grafts made of bicomponent fibers having a polypropylene core and polyglycolide sheath, King and co-workers showed that the absorbable sheath mediates considerably the tissue response to the graft.²¹

12.4.4 Vascular Wraps or Patches

Of the few studies conducted in this area, those of Moritz et al. and Hinrichs et al. are most pertinent.^{42,43}

Moritz and co-workers reported that a satisfactory biologic graft can be created if dilated, but otherwise unusable, veins are wrapped with a constrictive mesh tube.⁴² The purpose of this study was to determine whether or not an absorbable constrictive tube creates an appropriately sized vascular graft by induction of neoarterial wall growth. In eight sheep, a 5-cm segment of the carotid artery was resected and the external jugular vein inserted as a tubular graft. The vein was either wrapped with a polydioxanone (PDS) reinforced Vicryl mesh ($n = 4$), a Vicryl mesh ($n = 4$), or a Dacron mesh tube ($n = 3$) to achieve a diameter reduction to 7 mm; or the vein was used without reinforcement ($n = 3$). At angiography after 6 months, the unreinforced veins had an average diameter of 19 mm. The Vicryl-reinforced veins on the average measured 9.4 mm, but three or four developed aneurysmatic dilatations at sites of valve sinuses with a mean diameter of 19 mm. PDS-reinforced veins on the average measured 7.4 mm. Two of four had minor aneurysms of 13 and 16 mm. The two remaining PDS-reinforced grafts were indistinguishable from the native artery. Dacron tubes reduced the vein size reliably on the average to 7.6 mm, but showed narrowing at the proximal anastomosis (PDS 7.2 ± 0.4 , Dacron 6.1 ± 0.4 , $p = 0.016$). PDS wrapping reduced maximal graft diameter to 10.9 ± 4 mm as compared to that of the native vein, 18.7 ± 3.5 ($p < 0.05$). Absorbable meshes can reduce the diameter of a venous graft by strengthening the vessel wall, but PDS reinforcement needs further technical refinement to prevent local dilatation at the sites of venous valves. Dacron seems to be a safe alternative in this respect but tends to create anastomotic narrowing.⁴²

In their study on improving the arterialization of autologous vein grafts, Hinrichs and co-workers noted that arterial reconstructions with vein grafts fail more frequently than with arterial grafts.⁴³ One of the causes of graft failure is damage due to overstretching of the graft wall. Overstretching took place because the vein graft, which has a poorly developed medium, cannot withstand the arterial blood pressures. The aim of the study was to evaluate

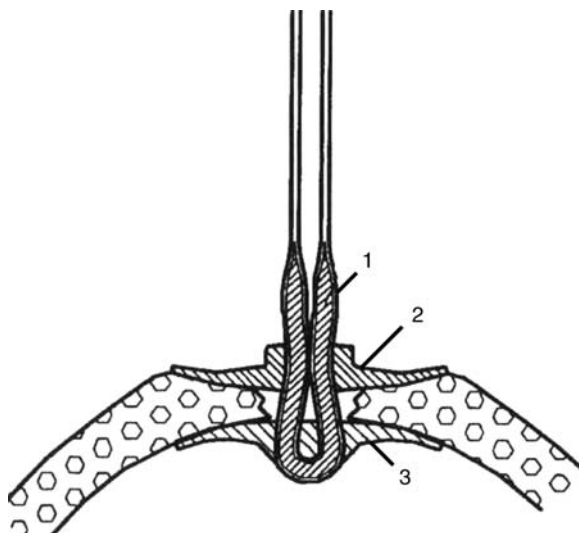
whether damage due to overstretching can be prevented and a gradual adaptation of the vein graft to the arterial blood pressures can be induced by applying a microporous, elastomeric, degradable prosthesis around the vein graft. Accordingly, autologous vein grafts (length 1.0 cm) with and without supporting prostheses were interposed into both carotid arteries of rabbits. Microporous, elastomeric, polyurethane-based prostheses and microporous, elastomeric, biodegradable prostheses made of poly- ϵ -caprolactone or a copolymer of ϵ -caprolactone (CL) and 3,6-dimethyl-1,4-morpholine-2,5-dione (DMD), based on 95.5/4.5 CL/DMD, were prepared. The grafts were evaluated up to 6 weeks after implantation. The control vein grafts showed severe destructive changes such as de-endothelialization, disruption of the media with edema, degradation of the elastic laminae, and infiltration of polymorphonuclear leucocytes into the vein graft wall, leading eventually to a fibrotic wall. In contrast, the composite vein grafts showed a preservation of the smooth muscle cell layers and the elastic laminae with only few polymorphonuclear leucocytes infiltrated into the vein graft wall. It was also noted that the wall of the vein graft gradually increased in thickness by the formation of regular circularly oriented cellular layers beneath the original longitudinally oriented smooth muscle cell layers, indicating a gradual adaptation of the vein graft to the arterial conditions. It appeared that the arterialization rate depended on the degradation rate of the supporting prostheses. Microporous prostheses made of the copolymer of CL and DMD were recommended as a support for the vein grafts.⁴³

12.5 Contemporary Vascular Applications of Absorbable Polymers

12.5.1 Absorbable Femoral Sealing Devices

An advanced, absorbable, femoral sealing device has been developed for use in repairing femoral artery holes following angioplasty.^{44,45} The sealing component of the device is made of polyaxial, highly compliant, absorbable copolymer, similar to those described in Chapter 3 and proposed for use as transient sealants and vehicles for the controlled release of bioactive agents.

The femoral sealing device comprises three separate parts as shown in Figure 12.1: a first sealing member 1, an elongated member 2, and a second sealing member 3. The first sealing member 1 is attached to a distal end of the elongated member 2. The first sealing member comprises two openings through which a multifilament, coreless suture is threaded so as to make it house the elongated member 2. A second sealing member 3 is provided with an opening (Figure 12.1), which is adapted to the elongated member 2, i.e., the opening is greater than the thickness of the proximal portion of the elongated member 2. With a structure like this, the second sealing member

**FIGURE 12.1**

A typical design of a femoral absorbable sealing device.

3 is threadable onto and along the elongated element 2. The most distal portion of the elongated member 2 has a constant thickness that is slightly greater than the opening of the second sealing member 3, and constitutes the distal lock portion. This will allow for frictional engagement between the inside of the opening of the second sealing member 3 and the distal lock portion of the elongated member 2, which makes the sealing device infinitely variably lockable along the distal lock portion.

The multifilament, coreless suture is preferably made of an absorbable material, such as a segmented lactide copolymer (such as those described in Chapter 2 of this book). The first sealing member 1, second sealing member 3, and the elongated member 2 are made of the flexible absorbable polyaxial copolymer, such as those described in Chapter 3.

12.5.2 Absorbable Stent Mantle

As noted in Section 12.5.1, a family of polyaxial copolyesters described in Chapter 2 can be used to prepare two or more of the critical components of a femoral sealing device. Other compliant members of this family of polymers, which can be converted to compliant, stretchable membranes and strong, stretchable monofilament fibers, can be used to construct a mantle or cover for metallic endovascular stents. Thus, a composite of thin film, reinforced with a monofilament in cross-coiled configuration, can be assembled into a highly compliant, expandable, tubular mantle or sleeve. This can be placed tightly as a cover outside an expandable metallic or polymeric stent so that under concentric irreversible expansion at the desired site of

a treated biological conduit, such as blood vessels or urethra, both components will simultaneously expand, and the mantle will provide a barrier between the inner wall of the conduit and the outer wall of the stent. The polymers are used as a stretchable matrix of a fiber-reinforced cover, sleeve, or mantle for a stent, where the fiber reinforcement is in the form of a spirally, coiled yarn.^{44,45}

12.5.3 Absorbable Sealant/Drug Carrier for Polytetrafluoroethylene (ePTFE) Grafts

This is a member of the absorbable gel-forming family of liquid copolyesters, comprising polyethylene glycol end-grafted with cyclic monomers as described in Chapter 4. Trudel and co-workers have investigated the use of a typical member of the gel-forming family of polymers as a sealant and carrier of bioactive agents to enhance tissue ingrowth in ePTFE grafts.⁴⁶

12.5.4 Partially Absorbable Bicomponent Fibers for Vascular Grafts

Concentric bicomponent fibers comprising a polypropylene core and polyglycolide sheath have been developed by a team of industrial and academic investigators for use as partially absorbable vascular grafts. Preliminary *in vivo* study on small-diameter grafts made of the corresponding multifilament yarn showed great promise for this system as a novel scaffold for *in situ* vascular tissue engineering.^{21,47}

12.6 Conclusion and Perspective on the Future

In spite of the great success of synthetic, absorbable surgical sutures and the growing applications of absorbable polymers in orthopedics and tissue engineering, the use of these polymers in vascular constructs is limited. This, in part, is due to the limited awareness of vascular investigators of the attributes of absorbable polymers and the fact that, in addressing these failure modes, individual investigators have (1) addressed one particular mode and practically ignored others, which can affect the collective performance during in-use applications; (2) rushed to use extreme animal models in early stages of graft evaluation, which can obliterate simple findings leading to hasty interpretation of results and failure when tested in humans; and/or (3) rushed to rely heavily on tissue engineering as the solution for existing problems without acknowledging the lengthy process required to provide a prototype graft. Needless to say, it is timely to evoke a radical but modest approach to address the issue of vascular graft failures. Such an approach is expected

to (1) address the different modes of graft failure in a collective manner and to provide an integrated solution to the root causes of these failures; (2) use existing knowledge of tissue engineering in tandem with established principles of bioengineering and device design, while taking advantage of advances made in the development of transient bioabsorbable implants; and (3) select a simple animal model to allow early identification of design defects and progress gradually to a more complex model in an effort to yield meaningful pre-clinical results.

References

1. Voorhees, A. P. et al., *Ann. Surg.*, 135, 322, 1952.
2. Shalaby, S. W. and Johnson, R. A., Synthetic absorbable polyesters, in *Biomedical Polymers: Designed-to-Degrade Systems*, Shalaby, S. W., Ed., Hanser Publishers, New York, 1994, chap. 1.
3. Herring, M. B., Gardner, A. K. and Glover, J. L., Seeding human arterial prostheses with mechanically derived endothelium. The detrimental effect of smoking, *J. Vasc. Surg.*, 1, 279, 1984.
4. Kempczinski, R. F., Rosenman, J. E., Pearce, W. H. et al., Endothelial cell seeding of a new PTFE vascular prosthesis, *J. Vasc. Surg.*, 2(3), 424, 1985.
5. Yue, X., van der Lei, B., Schakenraad, J. M. et al., Smooth muscle cell seeding in biodegradable grafts in rats: A new method to enhance the process of arterial wall regeneration, *Surgery*, 103, 206, 1988.
6. Galletti, P. M., Ip, T. K., Chiu, T.-H. et al., Extending the functional life of bioresorbable yarns for vascular grafts, *Trans. ASAIO*, 31, 399, 1984.
7. Galletti, P. M., Trudell, L. A., Chiu, T.-H. et al., Coated bioresorbable mesh as vascular graft material, *Trans. ASAIO*, 31, 257, 1985.
8. Galletti, P. M., Aebischer, P., Sasken, H. F. et al., Experience with fully bioresorbable aortic grafts in the dog, *Surgery*, 103, 231, 1988.
9. van der Lei, B., Blaauw, E. H., Dijk, F. et al., Microporous compliant biodegradable graft materials: A new concept for microvascular surgery, in *Recent Advances in Vascular Grafting*, Skotnicki, S. H., Buskens, F. G. M., Reinaerts, H. H. M., Eds., Nijmegen, The Netherlands, 1984, 19.
10. Greisler, H. P., Arterial regeneration over absorbable prostheses, *Arch. Surg.*, 177, 1425, 1982.
11. Greisler, H. P., Kim, D. U., Price, J. B. et al., Arterial regenerative activity for prosthetic implantation, *Arch. Surg.*, 120, 315, 1985.
12. Greisler, H. P., Ellinger, J., Schwarcz, T. H. et al., Arterial regeneration over polydioxanone prostheses in the rabbit, *Arch. Surg.*, 122, 715, 1987.
13. Greisler, H. P., Schwarcz, T. H., Ellinger, J. et al., Dacron inhibition of arterial regenerative activity, *J. Vasc. Surg.*, 3, 747, 1986.
14. Yu, T. J., Ho, D. M. and Chu, C. C., Bicomponent vascular grafts consisting of synthetic absorbable fibers: Part II: in vivo healing response, *J. Invest. Surg.*, 7(3), 195, 1994.

15. Greisler, H. P., Pham, S. M., Endean, E. D. et al., Relationship between changes in biomechanical properties and cellular ingrowth in absorbable vascular prosthesis, *ASAIO Abstracts*, 16, 25, 1987.
16. Greisler, H. P., Joyce, K. A., Kim, D. U. et al., Spatial and temporal changes in compliance following implantation of bioresorbable vascular grafts, *J. Biomed. Mater. Res.*, 26(11), 1449, 1992.
17. Lei, V., Bartels, H. L., Nieuwenhuis, P. et al., Microporous, compliant, biodegradable vascular grafts for the regeneration of the arterial wall in rat abdominal aorta, *Surgery*, 98, 955, 1985.
18. Endean, E. K., Kim, D. U., Ellinger, J. et al., Effects of polypropylene's mechanical properties on histological and functional reactions to polyglactin 910/polypropylene vascular prostheses, *Surg. Forum*, 38, 323, 1987.
19. Germain, L., L'Heureux, N., Labbe, R. et al., Human blood vessel produced *in vitro* by tissue engineering, *Workshop on Biomaterials and Tissue Engineering Abstracts*, 23, 1997.
20. Cohn, D., Marom, G. et al., A selectively biodegradable filament wound vascular graft, *Trans. Soc. Biomater.*, 28, 403, 2002.
21. King, M. W., Ornberg, R. L., Marios, Y., Marinov, G. R., Cadi, R., Roy, R., Cossette, F., Southern, J. H., Joardar, S. J., Weinberg, S. L., Shalaby, S. W. and Guidon, R., *Trans. Soc. Biomater.*, 22, 60, 1999.
22. Prechtel, E., Young, K., Goldman, S. et al., Design, synthesis, and mechanical characterization of a resorbable composite small diameter vascular graft as a tissue engineered construct, *Trans. Soc. Biomater.*, 28, 200, 2002.
23. Greisler, H. P., *New Biologic & Synthetic Vascular Prosthesis*, R.G. Landes, Austin, TX, 1991.
24. Wesolowski, S. A. et al., The compound prosthetic vascular graft. A pathologic surgery, *Surgery*, 53, 19, 1963.
25. Fox, D. et al., in *Tissue Engineering of Prosthetic Vascular Grafts*, Zilla, P. and Greisler, H. P., Eds., R.G. Landes, Austin, TX, 1999, chap. 45.
26. Ruderman, R. J. H., Andrew, F., Hattler, B. G. et al., Partially biodegradable vascular prosthesis, *Trans Am. Soc. Artif. Intern. Organs*, 18, 30, 1972.
27. Bowald, S., Busch, C. and Eriksson, I., Absorbable material in vascular prosthesis: A new device, *Acta. Chir. Scand.*, 146, 391, 1980.
28. Schwarcz, T. H., Nussbaum, M. L. et al. and Greisler, H. P., Prostaglandin content of tissue lining vascular prostheses, *Curr. Surg.*, 44, 18, 1987.
29. Greisler, H. P., Kim, D. U., Dennis, J. W. et al., Compound polyglactin 910/polypropylene small vessel prostheses, *J. Vasc. Surg.*, 5, 572, 1987.
30. Greisler, H. P., Tattersall, C. W., Klosak, J. J. et al., Partially bioresorbable vascular grafts in dogs, *Surgery*, 110, 645, 1991.
31. Zenni, G. C., Gray, J. L., Appelgren et al., Modulation of myofibroblast proliferation by vascular prosthesis biomechanics, *ASAIO J.*, 39, M496, 1993.
32. Chu, C. C. L. et al., Design and in vitro testing of newly made bicomponent knitted fabrics for vascular surgery, *Polym. Sci. Technol.*, 35, 185, 1987.
33. Greisler, H. P., Klosak, J. J., Endean, E. D. et al., Effects of hypercholesterolemia on healing of vascular grafts, *J. Invest. Surg.*, 4(3), 299, 1991.
34. Van der Lei, B., Wildevuur, C. R. and Nieuwenhuis, P., Compliance and biodegradation of vascular grafts stimulate the regeneration of elastic laminae in neoarterial tissue: An experimental study in rats, *Surgery*, 99, 45, 1986.
35. Ratcliffe, A., *Matrix Biology*, 8, 1, 2000.
36. Auger, F. A., *FASEB J.*, 12, 1, 1998.

37. Nerem, R. M., *Tissue Eng.*, 1, 1, 1995.
38. Burg, K. J. L. and Shalaby, S. W., in *Tissue Engineering of Prosthetic Vascular Grafts*, Zilla, P. and Greisler, H. P., Eds., R.G. Landes, Austin, TX, 1999, chap. 46.
39. Shalaby, S. W., Hydrogel-Forming, Self-Solvating Absorbable Polyester Copolymers, and Methods for Use Thereof, U.S. Patent (to Poly-Med, Inc.) 5,612,052, 1997.
40. Shalaby, S. W. and McCaig, S. M., Process for Phosphonylating the Surface of an Organic Polymeric Preform, U.S. Patent 5,491,198, 1996.
41. Shalaby, S. W. and Roweton, S. L., Continuous Open-Cell Polymeric Foams Containing Living Cells, U.S. Patent 5,677,355, 1997.
42. Moritz, A., Grabenwoger, F., Windsich, A. et al., A method for constricting large veins for use in arterial vascular reconstruction, *Artif. Organs*, 14(5), 394, 1990.
43. Hinrichs, W. L. J., Zweep, H.-P., Satoh, S. et al., Supporting, microporous, elastomeric, degradable prostheses to improve the arterialization of autologous vein grafts, *Biomaterials*, 15(2), 83, 1994.
44. Shalaby, S. W., Amorphous Polymeric Polyaxial Initiators and Compliant Crystalline Copolymers Therefrom, U.S. Patent (to Poly-Med, Inc.) 6,462,169, 2002.
45. Shalaby, S. W., Akerfeldt, D., Freinz, F. and Egnelöv, P., Amorphous Polymeric Polyaxial Initiators and Compliant Crystalline Copolymers Therefrom, International Patent Application (to Poly-Med, Inc.) WO 01/40348 A2, 2001.
46. Trudel, J., Shalaby, S. W., Massia, S. and LaBerge, M., Cytocompatibility of an absorbable gel-forming sealant candidate for vascular applications, *Trans. Soc. Biomater.*, 22, 162, 1999.
47. King, M. W., Ornberg, R. L., Marios, Y., Marinov, G. R., Cadi, R., Roy, R., Cossette, F., Southern, J. H., Joardar, S. J., Weinberg, S. L., Shalaby, S. W. and Guidon, R., *Proc. Sixth World Biomater. Congr., Trans. Soc. Biomater.*, II, 533, 2000.

13

Postoperative Adhesion Prevention

Waleed S.W. Shalaby and Shalaby W. Shalaby

CONTENTS

13.1 Introduction	192
13.2 Approaches to Postoperative Adhesion (POA) Prevention	192
13.2.1 Surgery	192
13.2.2 Adjuvants	193
13.2.3 Barrier Systems	194
13.3 Advances in the Use of Absorbable/Biodegradable Polymers for POA Prevention	194
13.3.1 Multivalent Ion-Modified Hyaluronic Acid Formulations	195
13.3.2 Covalently Crosslinked HA Films	196
13.3.3 Effect of Pharmacological Adjuvants on Hyaluronic Acid Performance	196
13.3.4 Absorbable Gel-Forming Liquid Copolyesters as Transient Barriers and Multifaceted Compositions for POA Prevention	198
13.3.4.1 Preparation of a Mixed Gel-Forming Vehicle Comprising PEG-400 End-Grafted with a Mixture of Trimethylene Carbonate (TMC) and Glycolide	198
13.3.4.2 <i>In Vitro</i> Evaluation of Gel-Forming Absorbable Copolyester Placebos	199
13.3.4.3 Preparation of Nonaqueous Gel-Forming Formulations and Control Systems	200
13.3.4.4 Comparative Study of the Copolyester Gel-Former and Other Controls	200
13.3.4.5 Effect of Pharmacological Agent on the Performance of the Copolyester Gel-Former	201
13.4 Conclusion and Perspective on the Future	202
References	202

13.1 Introduction

Tissue injury in response to surgery, chronic inflammatory processes, or accidental trauma evokes a series of wound healing processes involving inflammation, cell proliferation/matrix deposition, and matrix remodeling.¹ The process is initiated by an active coagulation phase that produces a fibrin clot to act as a scaffolding moiety. Within the first 3 h, the release of various cytokines and prostaglandins increases vascular permeability to coordinate the recruitment of macrophages, granulocytes, fibroblasts, and mesenchymal cells. Mediators of this process include histamine and prostaglandins. The next 24 to 48 h of repair is characterized by cell migration and organization. Fibrinolysis usually begins by day 3 as fibroblast proliferation leads to matrix deposition. Angiogenesis plays a critical role in the matrix remodeling since wound healing is a multifocal process of fibrinolysis and matrix deposition which lasts for up to a year. Under normal circumstances, the majority of these fibrin clots are lysed as part of the normal healing process. However, in some cases, matrix deposition and vascularization occur in persistent fibrin clots that organize into permanent thick, fibrous adhesions. The formation of such fibrous adhesions has been the subject of significant clinical problems across many different fields of medicine. These include:

- Postsurgical peritoneal adhesions, which can cause abdominal pain and bowel obstruction
- Pelvic adhesions that can impair fertility
- Postsurgical tendon and joint adhesions that cause chronic pain and decreased mobility²⁻⁷

13.2 Approaches to Postoperative Adhesion Prevention

It is generally agreed that the propensity to form adhesions following surgery or tissue trauma results from a deviation or imbalance in one or more phases of normal wound repair. It has yet to be determined which are the critical factors involved; however, efforts to prevent adhesion have focused on various surgical techniques, the use of anticoagulants, barriers to permanently or transiently separate tissue surfaces, and adjuvants to impair the inflammatory phase or some component of matrix deposition/remodeling.

13.2.1 Surgery

Surgical efforts to minimize postoperative adhesions have been limited. It was originally felt that separate closure of the peritoneal defect after laparo-

tomy would decrease adhesion formation, and hence, adhesion-related complications such as intestinal obstructions. However, multiple animal and human studies have shown that nonclosure of the peritoneum is not detrimental in terms of adhesion formation or postoperative complications.⁸ The argument against closure is that the peritoneum heals rapidly without separate reapproximation, and there is less tissue handling and suture placement with nonclosure, as well as decreased operative time.⁹ Furthermore, the presence of excess suture can cause tissue strangulation/ischemia which promotes adhesion formation. For this reason, re-peritonealization of raw surfaces after dissection is no longer the standard of surgical practice. Studies comparing laparoscopy vs. laparotomy (pfannenstiel or vertical incision) have shown dramatic decreases in the formation of anterior abdominal wall adhesions.¹⁰ However, morbidity outcomes have not been studied to date. Second-look procedures to evaluate the efficacy of adhesiolysis have observed reformation rates as high as 97% irrespective of surgical technique (microsurgical vs. laser).¹¹⁻¹³ Although adhesion reformation rates are high, improved fertility has been observed.

13.2.2 Adjuvants

The marginal improvements seen with improved surgical technique prompted a wide range of adjuvant strategies. Early studies focused on the intraperitoneal administration of crystalloid or colloid solutions to minimize tissue-tissue contact by creating a thin film. It was expected that the presence of a thin film would minimize contact between raw surfaces and thus inhibit adhesion formation. To date, however, numerous studies have shown no proven efficacy. Examples include phosphate buffered saline, lactated ringer's, normal or hyperosmotic saline, and dextran 70.¹⁴ Furthermore, the addition of heparin had no influence on adhesion formation. In practice, these solutions are rapidly absorbed from the peritoneum, and thus any potential efficacy from a thin filmy layer is lost. It is estimated that the peritoneal cavity absorbs up to 500 cc of physiologic saline in less than 24 h.¹⁵ Thus, it is not surprising that crystalloid/colloid solutions are ineffective given that peritoneal wound healing/adhesion formation requires up to 5 to 8 d. Given the apparent importance of inflammation, it was felt that inhibiting their response would decrease adhesion formation. Modulating the inflammatory response was first studied using corticosteroids without success.¹⁶ However, nonsteroidal antiinflammatory agents (NSAIDs) and other immunomodulators have recently shown decreased adhesion formation in animal models. These include low-dose aspirin, ketorolac and IL-10, monocyte chemotactic protein 1, antibodies to vascular permeability factor, and antioxidants.¹⁷⁻²¹ Agents designed to promote fibrinolysis have also demonstrated efficacy in animal models. These strategies range from the use of t-PA, to inhibitors of collagen synthesis, and thrombin formation.²²⁻²⁴

13.2.3 Barrier Systems

The concept of using mechanical barriers to prevent the apposition of raw intraabdominal surfaces has received considerable interest. While tissue barriers such as omental grafts have not proven useful, much of our current interest has focused on various synthetic barriers. It can be appreciated that the ideal barrier would be expected to eliminate adhesion formation, exhibit ease of handling, application, and retention at the sites of interest, be applicable to both open surgical and laparoscopic procedures and biodegradable to facilitate removal. To date, the ideal barrier has yet to be developed. Currently available products have shown only a modest reduction in adhesion prevention. Sites of interest have included the anterior abdominal wall after vertical incisions, the uterus after myomectomy, and other adnexal structures after adhesiolysis.^{25–27} Prospective studies are currently under way to examine morbidity; however, some improvements have been noted in terms of fertility. The list of available synthetic barriers are Seprafilm® (carboxymethylcellulose/hyaluronic acid), Interceed® (oxidized regenerated cellulose), and Gore-Tex Surgical Membrane® (expanded polytetrafluoro-ethylene). While only a marginal decrease in adhesions is noted, these materials suffer from additional shortcomings including ease of handling (Seprafilm), retention at tissue surface (Interceed), compromised efficacy in the presence of blood (Interceed), and need for secondary surgery for removal (Gore-Tex Surgical Membrane). A number of materials have shown promise in clinical and animal studies. These include Sepracoat® (hyaluronic acid gel), ferric hyaluronate, crosslinked hyaluronic acid (Incert®), and photopolymerized hydrogels.^{28–31}

13.3 Advances in the Use of Absorbable/Biodegradable Polymers for Postoperative Adhesion (POA) Prevention

Most pertinent to the subject of this chapter are modifications of the earlier strategies that have shown some promise for use in preventing or minimizing POA. This approach combines the use of a biodegradable synthetic material to function as a transient barrier system while providing local drug delivery to prevent POA. Advances made in this area during the last 10 years have dealt primarily with:

- Hyaluronic acid modified with multivalent ions
- Covalently crosslinked hyaluronic acid
- Nonaqueous, gel-forming liquid copolyesters

In conducting pertinent *in vivo* studies, the type of animal model used can influence the results and produce great variability. In this review, the majority

of studies highlight the rat sidewall model, which is more reliable and reproducible than others.³² In tendon adhesion studies, however, a well-accepted model is the white leghorn chicken model and used by contemporary investigators.^{6,33,34}

13.3.1 Multivalent Ion-Modified Hyaluronic Acid Formulations

Miller and co-workers investigated the effect of intraoperative treatments of high viscosity absorbable gels, made of various combinations of hyaluronic acid and nonsteroidal, antiinflammatory drugs, on adhesion formation in a flexor tendon model.^{6,34} Part of the study was designed to determine the effect of calcium ion on the viscosity of the HA before and after administration at the surgical site. For this, mature white leghorn chickens were used to verify the chosen surgical model and to test five different gel treatments. The gels were formed from a base of 2% sodium hyaluronate in phosphate buffered saline, plus:

- No additional substance
- 1 mg/mL tolmetin sodium
- 1 mg/mL naproxen sodium (NP)
- 0.216 g/mL calcium acetate
- 0.216 g/mL calcium acetate plus 1 mg/mL naproxen sodium

The gels were applied by injecting 0.2 mL of the specified composition into the intra-sheath space near the conclusion of the surgical procedure. Gross histological evaluations were conducted to analyze the efficacy of each treatment in terms of adhesion prevention.⁶ All treatments significantly reduced the extent and severity of postsurgical tendon adhesions in this animal model as compared to the control ($p < 0.05$). While the addition of calcium acetate alone to HA significantly improved adhesion scores ($p < 0.01$), more significant efficacy was noted using the NSAIDs. Each composition that included an NSAID and/or calcium acetate was significantly more effective ($p < 0.05$) than the plain sodium hyaluronate gel in preventing adhesion formation. However, the combination of naproxen sodium and calcium acetate in a high viscosity sodium hyaluronate carrier produced the most effective composition. The mean score of the HA+CA+NP gel was significantly lower than both the HA+NP scores ($p < 0.05$). The results suggest that maintaining the natural separation between the tendons and their sheath while controlling the local tissue inflammation were critical to effective adhesion prevention. Thus, the apparent synergism noted in this multimodal approach may be a promising strategy for future postsurgical adhesion prevention strategies. It was also noted that the addition of NSAIDs and calcium acetate, as a crosslinking agent, has a profound effect on the *in vivo* performance of the gels in the leghorn chicken model. It was hypothesized that this effect would

be due to the combined effect of the antiinflammatory drug and the expected increase in viscosity from crosslinking the gels. However, the inherent viscosities of the gels with the calcium acetate were substantially lower than expected. In fact, the inherent viscosities of simple HA and HA-NSAID gels were higher than those containing calcium acetate. The unexpected decrease in inherent viscosity was explained as follows: When calcium acetate is added to these gels in a closed system such as a preparation vial or an Ostwald viscometer, it does not appear to affect the molecular weight of the hyaluronic acid. The addition merely changes the ionic concentration of the gel, resulting in a lower inherent viscosity. However, when these gels are placed in an open system, such as the *in vivo* environment, ion exchange occurs, and the by-product of the reaction rapidly diffuses out of the hyaluronic acid matrix. In this case, the reaction byproduct is sodium acetate. This *in situ* crosslinking leaves a higher viscosity gel at the surgical site and accounts for the effectiveness of the HA+CA and HA+CA+NP systems. The increased viscosity yields a longer *in vivo* residence time for these compositions and supports the above findings.⁶

A second form of HA modified with multivalent metal ions was clinically evaluated by Thornton and co-workers.²⁹ This entailed the addition of a small amount of ferric salt to high molecular weight HA to form ferric hyaluronate with sufficient ionic crosslinking, which, in turn, increased the modified HA viscosity.

13.3.2 Covalently Crosslinked HA Films

A combination of hyaluronic acid and carboxymethyl cellulose was chemically crosslinked to form a barrier membrane that is used clinically as Seprafilm® for preventing POA.²⁸ Another form of crosslinked hyaluronic acid is used clinically for reducing POA under the trade name Incert®.³⁰

13.3.3 Effect of Pharmacological Adjuvants on Hyaluronic Acid Performance

In a study on the effect of different pharmacological adjuvants on the performance of hyaluronic acid for POA prevention, a rat sidewall model, was used by Shalaby and co-workers to determine adhesion scores associated with HA formulations containing:

- The nonsteroidal antiinflammatory drug naproxen (NP)
- Trapidil (TP) as an NSAID and antimetogenic compound
- The cytokine interleukin-4 (IL-4)^{35,36}

Results of all segments of the study were compared with a suitable HA control as shown in Tables 13.1, 13.2, and 13.3. The cumulative adhesion scores depicted in Table 13.1 indicate that NP in HA formulations had little effect in preventing adhesion using the rat sidewall model. The data in Table

TABLE 13.1

Cumulative Postsurgical Adhesion Pilot Data with HA/Naproxen Sodium Formulations and Placebos

Active Formulation or Placebos Composition ^a	Suture Used in Model	Adhesion Score ^b
20 mg/ml HA in H ₂ O	4-0 Silk	3.7 (N = 3)
21 mg/ml NP + 20 mg/ml HA + 4 mg/ml CaAc	4-0 Silk	4 (N = 1)
4 mg/ml NP	4-0 Silk	3 (N = 1)
4 mg/ml NP + 20 mg/ml HA	4-0 Silk	5 (N = 1)
1 mg/ml NP + 20 mg/ml HA + 4 mg/ml CaAc	4-0 Silk	5 (N = 1)
1 ml/ml NP + 20 mg/ml HA	4-0 Silk	3 (N = 2)
0.5 mg/ml NP in H ₂ O	4-0 Silk	3 (N = 1)
20 mg/ml HA in H ₂ O	6-0 Silk	4 (N = 3)
20 mg/ml HA + 1 mg/ml NP + 1.5 mg GA	6-0 Silk	4 (N = 1)
20 mg/ml HA + 4 mg GA	4-0 Silk	5 (N = 1)
20 mg/ml HA + 1 mg NP + 4 mg GA	4-0 Silk	5 (N = 1)
Saline	6-0 Silk	4* (N = 1)
1 mg/ml NP in H ₂ O	6-0 Silk	5* (N = 1)
1 mg/ml NP + 20 mg/ml HA	6-0 Silk	4* (N = 1)
20 mg/ml HA	6-0 Silk	3.5 (N = 2)
20 mg/ml HA + 1.5 mg/ml GA + 1 mg NP	6-0 Silk	0 (N = 1)

Note: NP = Naproxen sodium; HA = Sodium hyaluronate; GA = Glycolic acid.

^a Volume used = 1 ml.

^b Using a *provisional* scoring system with a scale of 0 to 5 reflecting no and maximum adhesion at one week or as otherwise indicated, respectively; where N = number of rats used.

* POA at 6 d.

TABLE 13.2

Postsurgical Adhesion Data at One Week with HA/Interleuken-4 (IL-4) Formulations and Placebos Using Sidewall Model with Silk Sutures

Active Formulation or Placebos ^a Composition	Suture Used in Model	Average Adhesion Score ^b
20 mg/ml HA	6-0	7.6 ± 0.5 (N = 5)
20 mg/ml HA in H ₂ O + 1.5 µg IL-4	6-0	5.0 ± 1.4 (N = 5)
20 mg/ml HA + 0.5 mg GA + 1.33 µg IL-4	6-0	5.7 ± 2.8 (N = 3)
20 ml/ml HA + 0.5 mg GA + 2 µg IL-4	6-0	6.7 ± 0.7 (N = 3)

Note: HA = Sodium hyaluronate; GA = Glycolic acid.

^a Volume used = 1 ml.

^b Using an averaged cumulative scoring system with a scale of 0 to 10 reflecting no and maximum adhesion at 1 week; where N = number of rats used.

13.2 dealing with IL-4 indicate that incorporation of IL-4 in the HA formulation generally improves HA performance in preventing POA. The data also show that:

- 1.5 µg of IL-4/site (1 cm² in area) is the optimum dose within a range of 1.33 to 2µg.
- IL-4 has a positive effect on HA performance.

TABLE 13.3

Postsurgical Adhesion Data at 1 Week with Trepidil Formulations and Placebos Using Sidewall Model with Silk Suture

Active Formulation or Placebos ^a Composition	Suture Used in Model	Average Adhesion Score ^b
20 mg/ml HA + 1 mg Trepidil	6-0	8 (N = 1)
20 mg/ml HA + 0.5 mg GA + 0.5 mg Trepidil	6-0	8.3 ± 0.3 (N = 2)
20 ml/ml HA + 0.5 mg GA + 2 mg Trepidil	6-0	5.5 (N = 2)
20 mg/ml HA + 0.5 mg/ml GA + 1 mg Trepidil	6-0	6.8 PM 0.4 (N = 5)

Note: HA = Sodium hyaluronate; GA = Glycolic acid.

^a Volume used = 1 ml.

^b Using an averaged cumulative scoring system with a scale of 0 to 10 reflecting no and maximum adhesion at 1 week; where N = number of rats used.

- The use of glycolic acid (GA) does not appear to have significant effect on the performance of the IL-4 formulation.

Meanwhile, the data in Table 13.3 show clearly that:

- Trepidil has a discernable effect on HA performance in reducing the level of POA.
- The presence of GA may increase the HA viscosity and increase its effectiveness in providing a prolonged bioavailability of trepidil.
- Concentration of 2 mg/site represents the most functional concentration in the range of 0.5 to 2 mg/site.³⁵

13.3.4 Absorbable Gel-Forming Liquid Copolyesters as Transient Barriers and Multifaceted Compositions for POA Prevention

Special liquid gel-formers were prepared for evaluation as transient barriers and controls for multifaceted formulations using antiinflammatory, antian-giogenic, and immunomodulating agents. A few of these agents were used in the HA formulations and discussed in Section 13.3.3.

13.3.4.1 Preparation of a Mixed Gel-Forming Vehicle Comprising PEG-400 End-Grafted with a Mixture of Trimethylene Carbonate (TMC) and Glycolide

Trimethylene carbonate (TMC) and glycolide (G) were purchased from Boehringer Ingelheim Chemicals, Inc. (Virginia). Polyethylene glycol-400 (PEG-400) was purchased from Sigma-Aldrich (Missouri). Modified/stabilized methoxypropyl cyanoacrylate tissue adhesive (MS-MPC) was prepared at Poly-Med, Inc. (South Carolina).

The first step entailed the preparation of relatively hydrophobic copoly-ester, P1 (11.2/88.8 PEG/copolyester, by mole). Thus, PEG-400 (45 g) was

mixed under a dry nitrogen environment in a predried glass reactor (equipped for mechanical stirring) with TMC (93.2 g, 0.913 mol) and glycolide (11.8 g, 0.102 mol) and stannous octanoate (0.203 mmol as a 0.2 M solution in dry toluene) as a catalyst. The end-grafting of PEG with the cyclic monomers was conducted at 150°C for 5 h while mixing after the melting of the reaction charge at about 110°C. Using gel permeation chromatography (GPC), the conversion of the monomer was shown to be practically complete. Trace amounts of residual monomers were removed by distillation at 110°C under reduced pressure. The purified polymer was characterized for molecular weight (by GPC), identity (by IR), and composition (by NMR), and exhibited the expected properties based on the polymerization charge.

The second step entailed the preparation of a more hydrophilic copolymer, P2 (80/20 PEG/copolyester, by mole) following the same reaction scheme as that described above for P1. However, the polymerization charge consisted of PEG (120g), TMC (26.6 g, 0.888 mol), glycolide (3.34 g, 0.029 mol), and stannous octanoate (0.203 mmol as a 0.2 M solution in dry toluene).

The third step entailed the selection of P1/P2 mixture. Several compositions comprising different ratios of P1/P2 were made and characterized for:

- Bulk viscosity (using capillary rheometry)
- Adhesion to moist substrate (using the fabric peel test cited in Chapter 5)
- Ability to form a thin hydrogel membrane upon contacting water
- Retention of mechanical integrity over 4 to 48 h (using an incubator shaker at pH 7.4 and 37°C)
- Capacity to dissolve the different bioactive agents³⁷

Similar experimental conditions to those described in Section 13.3.4.1 were used to prepare and characterize P3 and P4 and pursue the preparation of analogous gel-forming mixtures. The compositions of P3 and P4 are given below:

P3: 30/70 (PEG-900)/(90/10 TMC/G, by mole) by weight

P4: 80/20 (PEG-900)/(90/10 TMC/G, by mole) by weight

13.3.4.2 In Vitro Evaluation of Gel-Forming Absorbable Copolyester Placebos

This segment of the study was intended to identify a gel-forming placebo that can be easily extruded at the administration site and display a desirable degree of gel-formation as a transient barrier. Additional properties which were sought in a useful transient barrier include:

- Having very mild adhesive properties to allow coating the traumatized site for 8 to 48 h

- Dispersing into colloidal droplets after an initial site coating period
- Generating a minimum amount of acidic acid by-product as it absorbs at the site or in the peritoneum

Accordingly, mixtures of the primary gel-formers P1 to P4 were made to identify the two most suitable systems for evaluation with a series of drugs having a broad scope of pharmacological activities. Mixtures of P2 and P1 or P3 were also used in this study; however, P4 was too viscous to mix effectively.

13.3.4.3 Preparation of Nonaqueous Gel-Forming Formulations and Control Systems

A selected mixed gel-forming composition, such as that made of 70/30 P1/P2 (by weight), was heat sterilized at 120°C for 1 h. The sterile liquid vehicle was allowed to reach room temperature in a laminar flow hood. The specific amount of the bioactive agent was mixed in a closed, sterile container until complete dissolution of the bioactive agent was achieved. Control systems consisted of:

- Size 6-0 braided silk
- Sodium hyaluronate (HA) as described in Section 13.3.1
- Methoxypropyl cyanoacrylate tissue adhesive (C-TA) as a positive control

13.3.4.4 Comparative Study of the Copolyester Gel-Former and Other Controls

This study is designed to compare the effect of the gel-former selected in Section 13.3.4.2 on POA with a size 6-0 silk suture/saline, HA, and C-TA as basic barrier and positive controls, respectively.³⁸ The adhesion formation was studied using a rat sidewall model. The abdominal cavity was entered into in female Sprague–Dawley rats through a small midline incision. A 1-cm² area of peritoneal sidewall was excised with a scalpel blade. The 6-0 silk was then sutured around the perimeter of the excised area with a square knot at each corner. Aliquots of either the gel-former (100 μ L) or the controls (1 mL) were injected on the excised site. One week postoperative, the adhesion prevention score was recorded for the different formulations on a scale of 0 to 10. A score of 10 represents maximum adhesion whereas 0 reflects the absence of any adhesions. Adhesion rating criteria were based on the work by Burns et al.³²

Table 13.4 illustrates the adhesion scores for the various synthetic barriers and silk control. The P1/P2 gel former alone was the only vehicle that showed statistically significant decrease in adhesion formation based on the rat sidewall model.

TABLE 13.4

Adhesion Scores of Barriers and Silk Control

Vehicle	n	Adhesion		
		Score (\pm SE)	<i>p</i> -value ^a	<i>p</i> -value ^b
Silk Control	6	7.2 \pm 0.5	—	NS
HA	5	7.6 \pm 0.5	NS	—
C-TA	5	9.6 \pm 0.2	0.001	0.004
P1/P2 Gel-former	7	5.1 \pm 0.6	0.004	0.01

^a Against silk control.

^b Against HA control.

13.3.4.5 Effect of Pharmacological Agent on the Performance of the Copolyester Gel-Former

A number of pharmacological agents, with known effects, may be pertinent to the biological events that control POA. A brief description of these agents is shown in Table 13.5.

Table 13.6 illustrates the adhesion scores when the modulating agents were incorporated in the P1/P2 gel-former. These agents showed no statistically significant reductions in adhesion scores when incorporated in the HA vehicle.

TABLE 13.5

Investigated Active Agents

Modulating Target	Type	Agent
Antiinflammatory	NSAID	Naproxen Sodium
Antiangiogenic	Triptoreline	Peptide-03
	Lanreotide	Peptide-14
	Pyrimidine analog	Trapidil
Antiplatelet/Antiproliferative	Antimicrotubule	Paclitaxel

TABLE 13.6

Adhesion Scores of Active Gel-Former

P1/P2 Gel-Former with	n	Adhesion		
		Score (\pm SE)	<i>p</i> -value ^a	<i>p</i> -value ^b
Naproxen	10	2.9 \pm 0.98	0.01	0.05
Triptoreline	5	2.8 \pm 1.25	0.005	0.005
Lanreotide	5	0.8 \pm 0.8	0.001	0.004
Trapidil	5	4.0 \pm 1.16	0.02	NS
Paclitaxel	10	4.9 \pm 0.89	0.05	NS

^a Against silk control.

^b Against HA control.

13.4 Conclusion and Perspective on the Future

Available results discussed in this chapter on POA prevention were used to develop the following conclusions and prospective advances:

- An optimized rat sidewall model can be used reproducibly to evaluate antiadhesion formulations in conjunction with an adopted composite score and multiple photographic documentation of the surgical site.
- The copolyester gel-forming transient barriers are more effective than HA.
- HA-based formulations with IL-4 are promising candidates for further development.
- The cyclic octapeptide somatostatin analog, lanreotide acetate in P1/P2 gel-former, is the most effective in reducing POA, and to a lesser extent, the LHRH analog, triptoreline acetate, the NSAID naproxen and, possibly trapidil, are effective in the same vehicle.

Optimization of the gel-former system in terms of the composition of the polymer as well as the concentration of NP and/or lanreotide is expected to lead to the most effective approach to POA prevention.

References

1. Stangel, J. J., Nisbet, D. and Settles, T., Formation and prevention of post-operative abdominal adhesions, *J. Reprod. Med.*, 29, 143, 1984.
2. Ellis, H., The cause and prevention of post-operative intraperitoneal adhesions, *Surg. Gynecol. Obstet.*, 133, 497, 1971.
3. Holtz, G., Prevention and management of peritoneal adhesions, *Fertil. Steril.*, 41, 497, 1984.
4. Holtz, G., Gynecologic surgery and adhesion prevention: Overview of classical adjuvant approaches, *Prog. Clin. Biol. Res.*, 381, 81, 1993.
5. Gelberman, R. H. and Manske, P. R., Factors influencing flexor tendon adhesions, *Hand Clin.*, 1, 35 (1985).
6. Miller, J. A., Efficacy of Hyaluronic Acid/Non-steroidal Anti-inflammatory Drug Systems on Post-surgical Tendon Adhesions, M.S. Thesis, Clemson University, Clemson, SC, 1994.
7. Shalaby, S. W. and Miller, J. A., Composition for Prevention of Inflammation and Adhesion Formation and Uses Thereof, U.S. Patent (to Poly-Med, Inc.) 5,866,554, 1999.
8. Tulandi, T., Hum, H. S. and Gelfand, M. M., Closure of laparotomy incisions with or without peritoneal suturing and second-look laparoscopy, *Am. J. Obstet. Gynecol.*, 158, 536, 1988.

9. Duffy, D. and diZerega, G. S., Is peritoneal closure necessary?, *Obstet. Gynecol. Surg.*, 49, 817, 1994.
10. Levrant, S. G., Bieber, E. J. and Barnes, R. B., Anterior abdominal wall adhesions after laparotomy or laparoscopy, *J. Am. Assoc. Gynecol. Laparosc.*, 4, 353, 1997.
11. Operative Laparoscopy Study Group, Postoperative adhesion development after operative laparoscopy: evaluation at early second-look procedures, *Fertil. Steril.*, 55, 700–704, 1991.
12. Diamond, M., Daniell, J., Martin, D., Feste, J., Vaughn, W. K. and McLaughlin, D. S., Tubal patency and pelvic adhesions at early second-look laparoscopy following intraabdominal use of the carbon dioxide laser: initial report of the intraabdominal laser study group, *Fert. Steril.*, 42, 717, 1984.
13. Hershlag, A., Diamond, M. P. and DeCherney, A. H., Adhesiolysis, *Clin. Obstet. Gynecol.*, 34, 395, 1991b.
14. DeCherney, A. H., diZerega, G. S. et al., Clinical problem of intraperitoneal postsurgical adhesion formation following general surgery and the use of adhesion prevention barriers, *Surg. Clin. N. Am.*, 77, 671, 1997.
15. Shear, L., Ching, S. and Gabuzda, G. J., Compartmentalization of ascites and edema in patients with hepatic cirrhosis, *N. Engl. J. Med.*, 282(25), 1391, 1970.
16. Fayez, J. A. and Schneider, P. J., Prevention of pelvic adhesion formation by different modalities of treatment, *Am. J. Obstet. Gynecol.*, 157, 1184, 1987.
17. Muzii, L., Marana, R., Brunetti, L., Margutti, F., Vacca, M. and Mancuso, S., Postoperative adhesion prevention with low-dose aspirin: effect through the selective inhibition of thromboxane production, *Hum. Reprod.*, 13, 1486, 1998.
18. Holschneider, C. H., Nejad, F. and Montz, F. J., Immunomodulation with interleukin-10 and interleukin-4 compared with ketorolac tromethamine for prevention of postoperative adhesions in a murine model, *Fertil. Steril.*, 71, 67, 1999.
19. Zeyneloglu, H. B., Senturk, L. M., Selin, E., Oral, N., Oliven, D. L. and Arici, A., The role of monocyte chemoattractant protein-1 in intraperitoneal adhesion formation, *Hum. Reprod.*, 13(5), 1194, 1998.
20. Saltzman, A. K., Olson, T. A., Mohanraj, D., Carson, L. F. and Ramakrishnan, S., Prevention of postoperative adhesions by an antibody to vascular permeability factor/vascular endothelial growth factor in a murine model, *Am. J. Obstet. Gynecol.*, 174(5), 1502, 1996.
21. Rodgers, K. E., Girgis, W., St Amand, K., Campeau, J. and diZerega, G. S., Reduction of adhesion formation in rabbits by intraperitoneal administration of lazaroid formulations, *Hum. Reprod.*, 13, 2443, 1998.
22. Menzies, D. and Ellis, H., Intra-abdominal adhesions and their prevention by topical tissue plasminogen activator, *J. R. Soc. Med.*, 82, 534, 1989.
23. Nagler, A., Rivkind, A. I., Raphael, J., Levi-Schaffer, F., Genina, O., Lavelin, I. and Pines, M., Halofuginone — an inhibitor of collagen type I synthesis — prevents postoperative formation of abdominal adhesions, *Ann. Surg.*, 227, 575, 1998.
24. Rodgers, K. E., Girgis, W., Campeau, J. D. and diZerega, G. S., Reduction of adhesion formation by intraperitoneal administration of a recombinant Hirudin analog, *J. Invest. Surg.*, 9, 385, 1996.
25. Becker, J. M., Dayton, M. T., Fazio, V. W., Beck, D. E., Stryker, S. J., Wexner, S. D., Wolff, B. G., Roberts, P. L., Smith, L. E., Sweeney, S. A. and Moore, M., Prevention of postoperative abdominal adhesions by a sodium hyaluronate-based bioresorbable membrane: a prospective, randomized, double-blind multicenter study, *J. Am. Coll. Surg.*, 183, 297, 1996.

26. Diamond, M., Reduction of adhesions after uterine myomectomy by Seprafilm membrane (HAL-F): a blinded, prospective, randomized, multicenter clinical study, Seprafilm Adhesion Study Group, *Fertil. Steril.*, 66, 904, 1996.
27. Nordic Adhesion Prevention Study Group, The efficacy of Interceed(TC7)* for prevention of reformation of postoperative adhesions on ovaries, fallopian tubes, and fimbriae in microsurgical operations for fertility: a multicenter study, *Fertil. Steril.*, 63, 709, 1995.
28. Diamond, M., Reduction of de novo postsurgical adhesions by intraoperative precoating with Sepracoat (HAL-C) solution: a prospective, randomized, blinded, placebo-controlled multicenter study, *Fertil. Steril.*, 69, 1067, 1998.
29. Thornton, M. H., Johns, D. B., Campeau, J. D., Hoehler, F. and diZerega, G. S., Clinical evaluation of 0.5% ferric hyaluronate adhesion prevention gel for the reduction of adhesions following peritoneal cavity surgery: open-label pilot study, *Hum. Reprod.*, 13, 1480, 1998.
30. Haney, A. et al., A barrier composed of chemically cross-linked hyaluronic acid (Incert) reduces postoperative adhesion formation, *Fertil. Steril.*, 70, 145, 1998.
31. Chowdhury, S. M. and Hubbell, J. A., Adhesion prevention with anicrod released via a tissue-adherent hydrogel, *J. Surg. Res.*, 61, 58, 1996.
32. Burns, J. et al., A hyaluronate-based gel for the prevention of post-surgical adhesions: evaluation in two animal species, *Fertil. Steril.*, 66, 814, 1996.
33. Daley, R. A., Cannistra, L. M., Walsh, W. R., Sasken, H. F. and Akelman, E., A chicken model for flexor tendon adhesion studies, *Proc. Orthop. Res. Soc.*, 38, 103, 1992.
34. Miller, J., Furgusen, R., Powers, D., Burns, J. and Shalaby, S. W., Efficacy of hyaluronic acid/nonsteroidal anti-inflammatory drug systems in preventing post-surgical tendon adhesions, *J. Biomed. Mater. Res., Appl. Biomater.*, 38(1), 25, 1997.
35. Shalaby, S. W., NIH SBIR Grant No. 1 R43 GM63291-01, Gel-forming Systems for Adhesion Prevention, Final Report, 2002.
36. Corbett, J. T., Shalaby, W. S., Fulton, L. K., Carpenter, K. A. and Shalaby, S. W., Effect of inflammatory modulators in a polymeric matrix on post-operative adhesion: A preliminary study, *Trans. Soc. Biomater.*, 25, 141, 2002.
37. Flagle, J., Kline, J. D., Allan, J. M. and Shalaby, S. W., *In vitro* evaluation of absorbable tissue adhesives, *Trans. Soc. Biomater.*, 22, 376, 1999.
38. Corbett, J. T., Shalaby, W. S. W., Fulton, L. K., Carpenter, K. A. and Shalaby, S. W., Gel-forming systems for post-operative adhesion prevention, *Trans. Soc. Biomater.*, 26, 99, 2003.

14

Implantable Insulin Controlled Release Systems for Treating Diabetes Mellitus

Marc Shalaby and Shalaby W. Shalaby

CONTENTS

14.1 Introduction	206
14.2 The Genesis and General Types of Controlled Drug Delivery Systems	207
14.3 Early Nonabsorbable Polymeric Insulin Delivery Systems.....	209
14.3.1 Crosslinked Polyacrylamide Systems.....	209
14.3.2 Ethylene-Vinyl Acetate Copolymer Pellets	209
14.4 Absorbable Polymeric Delivery Systems.....	211
14.4.1 Polylactic Acid Pellets	212
14.4.2 Polylactic Acid Microcapsules	213
14.4.3 Polylactic-co-Glycolic Acid Microcapsules.....	215
14.4.4 Block Copolymers/Hydrogels	216
14.5 Biomolecules as Drug Delivery Systems	217
14.5.1 Liposomes.....	218
14.5.2 Lipid Microparticles.....	218
14.5.3 Serum Albumin Beads.....	218
14.5.4 Chitosan Microcapsules	219
14.6 Ceramic Delivery Systems	220
14.6.1 Hydroxyapatite Ceramic Microspheres.....	220
14.6.2 Alumino-Calcium-Phosphorous Oxide Ceramic Systems	220
14.6.3 Zinc-Calcium-Phosphate Oxide Ceramic Systems.....	221
14.7 Conclusion and Perspective on the Future	221
References	224

14.1 Introduction

Diabetes mellitus is a systemic disorder of metabolism that stems from a deficiency of insulin, the hormone needed to stimulate the influx of fatty acids, amino acids, and glucose into cells. In recent years, the incidence of diabetes has reached epidemic proportions and is associated with long-term damage, dysfunction, and failure of a number of organ systems. In addition to being a leading cause of heart attacks, strokes, end-stage renal disease, and blindness, diabetes also has detrimental effects on the peripheral vasculature and the peripheral nervous system.¹

Type I diabetes is characterized by a complete lack of insulin because of an autoimmune destruction of the Islets of Langerhans, the subgroup of pancreatic cells responsible for insulin synthesis and secretion. Patients are generally diagnosed during childhood or adolescence and become dependent on lifelong, subcutaneously injected exogenous insulin. Type II diabetes, which usually occurs later in life, is the result of an insensitivity of peripheral tissues to the effects of insulin. This insensitivity is often referred to as "insulin resistance." Insulin resistance is caused by both a genetic predisposition to such factors and environmental factors such as obesity and sedentary lifestyle. Early in the course of the disease, the pancreas is able to compensate for insulin resistance by producing more insulin. When the pancreas begins to fail and is unable to secrete the additional insulin needed, there exists a state of *relative* insulin deficiency, even though total body levels of insulin are often high. This relative deficiency manifests as the hyperglycemia and other metabolic derangements associated with diabetes mellitus.

It is well established that tight glucose control can delay or prevent the long-term sequelae of both type I and type II diabetes. At present, there are several modalities to achieve glucose control. For type I diabetes, the mainstay of therapy is a combination of long- and short-acting insulin preparations given subcutaneously several times per day. For type II diabetes, there is a host of oral agents considered to be first-line therapy. These include insulin secretagogues designed to enhance pancreatic secretion of insulin, and insulin sensitizing agents designed to decrease gluconeogenesis in the liver and decrease insulin resistance in the peripheral tissues. Often, however, type II diabetes is a progressive disorder, and many type II diabetics ultimately require insulin therapy. Insulin may be given in lieu of, or in conjunction with, oral agents.

Most insulin regimes for insulin-requiring diabetics consist of long-acting (or basal) insulin preparations in conjunction with short-acting insulin preparations. The basal insulin is titrated to control basal insulin requirements and fasting glucose, and the short-acting insulin is designed to control postprandial rises in blood glucose. It is widely accepted that multiple subcutaneous injections are required to achieve tight glucose control, but such tight control may also be achieved through the use of an insulin pump in which

a continuous infusion of short-acting insulin is delivered via a subcutaneous catheter. This modality often achieves excellent glucose control, but the pumps must be worn continuously all day and have a significant rate of malfunctioning, often because of reservoir leakage or kinking and clogging of the catheter tubing.

As a result of the shortcomings of current insulin therapy, much work has been directed toward developing polymeric controlled release systems that can be implanted or injected into the body to achieve glucose control in patients with diabetes. This chapter will review the history of such systems and will discuss current technology and future trends for the sustained delivery of insulin for the treatment of diabetes mellitus. Several media serving as carriers include synthetic absorbable polymers, biomolecules, and ceramics.

14.2 The Genesis and General Types of Controlled Drug Delivery Systems

The concept of an implantable drug delivery system originated in England in the 1930s. In 1937, R. Deansley and A. S. Parkes presented their findings to the Royal Society of Medicine in London. In one experiment, they found that implanted pellets of compressed crystalline estrone caused female feathers to grow on male birds for as long as three months. In 1938, P. M. F. Bishop of Guy's Hospital in London presented research in humans in which subcutaneous implantation of pellets made of compressed estrogen limited the number of hot flashes suffered by women with premature menopause.²

In general, controlled-release systems are designed to release a drug in a fixed, predetermined pattern for a given period of time. Such systems are generally independent of local environmental conditions as the device is designed to provide the rate-limiting barrier to drug delivery. These systems have several advantages:

- Plasma drug levels may be maintained in a therapeutic range for long periods of time.
- Medications that normally require multiple administrations because of short half-lives may be given far less often.
- Sustained release may lead to lower total drug dosages, which is important when dealing with medications that have significant side-effects or toxicities.
- Patient compliance may be improved.
- Drugs with high first-pass metabolism by the liver or deactivation by the gastrointestinal tract can be delivered effectively.^{3,4}

These advantages must be weighed against the potential disadvantages including:

- Lack of biocompatibility of the implant or of residual organic solvents used in synthesis
- Production of potentially harmful by-products if a biodegradable (or absorbable) polymer system is employed
- Surgical implant and/or removal of the system
- Inadvertent drug overdose because of device
- Inability to adjust the rate of drug release if the drug's effects become undesirable after implantation
- Variability of absorption from the subcutaneous tissues because of differences in local blood supply and amount of subcutaneous fat^{2,3}

In general, controlled drug release occurs either by diffusion, chemical activation, or solvent activation. Two general types of diffusion-controlled systems are the reservoir system and the matrix system. In the reservoir model, the active drug is surrounded by a semipermeable membrane that is designed to allow osmosis to occur at a given rate. One advantage to this system is that it is relatively easy to develop with a constant and reproducible release profile. This advantage is outweighed by the dangers of overdose with a tear in the membrane, and the fact that the systems are not biodegradable and require a surgical procedure for implant and removal. In addition, it is very difficult to manufacture a membrane that permits the release of large macromolecules (MW >1000 Da).³

In nonabsorbable matrix systems, the active drug is uniformly distributed throughout a polymer matrix. Controlled release occurs through a series of interconnecting channels that allow the release of large macromolecules, such as insulin, for extended periods of time. The main advantage to such systems is the ease and low cost of manufacturing the systems and the relative safety in the event of a break in the implanted pellet. One major disadvantage is the lack of biodegradability and inconsistent release profiles that vary with time.³

Chemically controlled systems come in two versions — biodegradable systems and pendant chain systems. In the former, biodegradation of the polymer allows for the diffusion of drug into the surrounding tissues. These systems offer the advantage of being eventually absorbed by the body, thus obviating the need for surgical removal of the system. One must weigh this advantage with the potential that the breakdown products of the polymer may be toxic or cause an immunologic response. In the pendant chain system, the active drug is covalently bound to a polymer backbone. Release rates are adjusted by varying the hydrophilicity of the backbone.³ A number of researchers have taken this one step further and developed systems in which an enzymatic reaction mediates drug release from the polymer backbone.^{5,6}

With solvent-activated systems, the active drug is uniformly dispersed within a polymer matrix. The drug is effectively trapped within the polymer chains. Upon exposure to the biological environment fluids, the matrix swells, causing an increased distance between the polymer chains. This facilitates the release of the drug from the matrix to the surrounding biological environment. The rate of release is dependent upon the relaxation rate of the polymer chains as they are exposed to the fluid media.^{3,7,8}

14.3 Early Nonabsorbable Polymeric Insulin Delivery Systems

14.3.1 Crosslinked Polyacrylamide Systems

In the early 1970s, B. K. Davis developed a system in which polyacrylamide (PAA) chains crosslinked with 2% *N,N'* methylenebisacrylamide served as a mediator of insulin release. During the polymerization of PAA, bovine insulin (1 mg or 10 mg) is added to form a slurry of PAA and insulin. This slurry is then subcutaneously injected into diabetic rats. Rats who received the 40% PAA/10 mg insulin implants had essentially a normal rate of growth compared to nondiabetic controls over the 21-d study. Upon surgical removal of the implants, overt signs of diabetes (glucosuria, weight loss) immediately developed. This PAA system was one of the first to be developed for insulin delivery. What made this system attractive early on was the fact that implantation could be accomplished by injection, which obviated the need for a surgical implantation procedure. An incision is still needed to remove the polymer as the system is not bioabsorbable.⁹ In addition, the PAA implants were found to cause a significant local inflammatory reaction, leading to the search for more biocompatible polymer systems.¹⁰

14.3.2 Ethylene-Vinyl Acetate Copolymer Pellets

In 1976, Langer and Folkman published a landmark paper in which several polymer systems were studied with respect to biocompatibility and sustained release of macromolecules.¹⁰ Ultimately, they determined that two of the polymer systems were most biocompatible. Pellets made from casting of ethylene-vinyl acetate copolymer (EVAC) showed no significant inflammation after implantation as did the pellets cast of Hydron, a polymer of hydroxyethylmethacrylate. In terms of *in vitro* release kinetics, while both polymer systems exhibit a significant initial release (i.e., "burst kinetics"), the ethylene-vinyl acetate system had a slower overall release profile that persisted significantly longer, making it more ideally suited for the *in vivo* release of macromolecules. As a way to further retard the rapid release of the proteins,

the researchers coated a subset of the polymer/protein pellets with pure polymer. This was the first attempt to slow the release of the macromolecules from the polymer matrices and was found to be moderately successful.

As it appeared that the EVAC system had promise for *in vivo* applications, much work was done to study the kinetics of the system in order to improve upon the release profile. Early on, the biggest obstacle to studying the release profiles of the system was the poor reproducibility of the early studies. This was believed to be the result of inhomogeneous distribution of polymer and matrix within the pellets. Significant drug settling occurred during the casting and drying of the pellets. At room temperature, insoluble drug would migrate vertically, and lateral shifting could be visually observed to occur as if by currents (possibly thermal in nature). This led to significant variation in the distribution of the drug from pellet to pellet. As a means to compensate for this, low temperature casting procedures were developed by Rhine et al. to decrease the role of thermal currents.¹¹ Magnified photographs of the pellets prepared at low temperatures revealed a visually more homogenous appearance, implying a more uniform drug distribution. This uniformity was demonstrated by more reproducible release kinetics.¹¹

With more uniformity in the fabrication of the EVAC pellets, Bawa et al. set out to further delineate the kinetics of the system.¹² They set out to answer the question "How can a polymer that is impermeable to molecules larger than 600 Da allow for the sustained release of macromolecules as large as 2×10^6 Da?" Using an optical microscope, it was discerned that EVAC films cast without any drug were essentially homogeneous nonporous. However, when macromolecules are incorporated, and the drug/polymer matrix is formed, there appears to be a tortuous network of interconnecting pores. It is believed that this network serves as a mechanical barrier to mediate insulin release.¹² Overall, researchers determined that there are two phases of drug release. Initially there is a burst phase in which rapid release occurs, followed by a period of essentially linear drug release. It is believed that the burst effect is the result of drug dissolution from the surface of the matrix, and that the second phase is due to diffusion of the macromolecules through this interconnecting pore network.^{11,12}

With extensive *in vitro* studies completed on the EVAC-based insulin delivery system, the stage was set for *in vivo* studies to determine if the implants could improve glucose control in diabetic rats. The most commonly used model to study the *in vivo* effects of the various implants is designed to simulate type I diabetes (although one can assume some degree of applicability to type II diabetes). Insulin deficiency (and hence, diabetes) is induced in rats by the infusion of the drug streptozotocin. This agent targets the Islets of Langerhans and destroys these cells. This ultimately leads to an irreversible and complete loss of insulin secretion. Newly diabetic rats then suffer the consequences of hypoinsulinemia such as hyperglycemia, glucosuria, and weight loss. All of the *in vivo* studies done used some combination of these indicators as endpoints when comparing study groups to controls.

In a study by Creque et al., insulin-loaded EVAC polymer pellets were subcutaneously implanted into diabetic rats.¹³ Within the first 24 h after implantation, glucose levels fell from 374–412 mg/dl to 87–127 mg/dl. Glucose levels then remained stable for 26 d, after which glucose levels rose abruptly. In addition, there was steady growth and no glucosuria in the study group compared to diabetic controls during the same time period. Evaluation of the eluted insulin revealed that almost 100% of the insulin released was biologically active. One important caveat to the study was that in pellets that were no longer releasing insulin, only about 35% of the incorporated insulin was eluted. And while this study clearly showed that insulin could be effectively loaded into a polymer matrix and released without denaturation of the protein, there were clear problems with the efficiency of the system.

In an effort to further improve the efficiency and duration of insulin elution from the EVAC pellets, Brown et al. made additional modifications to their original system.¹⁴ They found that insulin release from the system can be improved by essentially two mechanisms:

1. Using a more soluble sodium insulin preparation (as opposed to zinc preparations)
2. Increasing loading of insulin into the EVAC matrix

Both of these modifications serve to increase the driving force responsible for pushing insulin from the matrix into the surrounding environment. In addition, researchers found that by altering the method of matrix fabrication and using larger insulin particles, a more porous matrix with larger pores is obtained, allowing for more efficient insulin release. These modifications allow for more complete release of insulin, but such a system would be expected to release insulin stores much too quickly. In order to counterbalance these effects, Brown et al. coated the insulin-loaded EVAC pellets with a pure polymer coating of ethylene vinyl acetate.¹⁵ On one side of the coated pellet, a small aperture is placed through which the insulin elutes. The end-product is an implant that allows for slow yet more complete insulin release. *In vivo* studies of the modified EVAC pellets led to normoglycemia for 45 d in diabetic rats. Furthermore, insulin release continued to occur for as long as 105 d, as evidenced by lower glucose values compared to untreated diabetic controls.¹⁵

14.4 Absorbable Polymeric Delivery Systems

Because of the early work done by Langer and others, researchers saw that successful sustained release of biologically active insulin from polymer sys-

tems was possible.^{3,10} In addition, studies of the kinetics of the early systems allowed for more modern systems to be developed. And while the nonabsorbable polymeric delivery systems worked, their use in humans was hampered by the fact that they needed to be surgically implanted and removed upon insulin exhaustion. This led researchers to look for insulin release systems that were biodegradable and biocompatible, thus obviating the need for surgical removal. Furthermore, efforts were made to develop systems that were not only absorbable but could be placed in the subcutaneous tissue with a simple injection, thus avoiding a surgical procedure altogether.

14.4.1 Polylactic Acid Pellets

Controlled insulin release systems in the form of an implantable polylactic acid (PLA) pellet were studied in the mid 1980s.¹⁶ The pellets were prepared via solvent casting techniques previously used in the preparation of the EVAC systems. Sephadex G-25 is added to the casting system as a means to modify insulin release from the pellets. Studies of the *in vitro* release kinetics showed that while an initial burst phase existed, it was not as profound an effect as was observed with other release systems. *In vivo* studies of the implants in diabetic rats showed that glucose control could be achieved for as long as two weeks after implantation. Retrieval of the pellets several weeks after implantation revealed no significant inflammation at the implantation site, suggesting biocompatibility. Of note, however, is that the pellets were found to be intact 3 weeks after implantation, suggesting that minimum degradation occurs despite insulin exhaustion. This implies that insulin release occurs independent of polymer degradation. This degradation is believed to be the result of the slow hydrolysis of the high molecular weight PLA pellets.¹⁷

Even though the PLA pellets ultimately degrade, having a hibernating implant imbedded in the subcutaneous tissue is considered undesirable. Having a system in which the degradation profile of the polymer more closely parallels its insulin release profile is clearly advantageous. Up until this point, most of the PLA used in these insulin-loaded implants had a molecular weight of >20,000 Da. Yamakawa et al. studied implants that utilized PLA with lower molecular weights (<10,000 Da). While the lower molecular weight PLA/insulin pellets degrade much more quickly, they exhibit a significant initial burst effect and a short duration of action *in vivo* (3 d). As a means to combat this unfavorable release profile, one side of the pellet was coated with a thin layer of pure low molecular weight PLA as a retardant to insulin release. These double layer implants were then compared to the single layer implants. *In vivo* experiments demonstrated a blunted burst effect and 19 d of glucose control. Interestingly, a biphasic release profile was observed *in vivo*. In the first phase (days 1 to 9), insulin release is thought to occur as a result of diffusion from the uncoated side of the pellet. In the second phase (days 9 to 19), insulin release appears to be

accelerated by erosion of the coating layer and/or the disintegration of the PLA matrix. This second phase seems to be perfectly timed as the release from the first phase seems to near exhaustion around the time the second phase begins. Studies of the biodegradation of the implant revealed that the pellet had fully been absorbed by 7 to 8 weeks. And while no evidence of inflammation existed at the site of implantation, a fibrous capsule was noted around the site of the implant, suggesting a mild foreign body reaction. It is unclear whether this capsule is a reaction to the implant itself or merely the result of the implantation process. In addition, it is believed that the capsule plays a role, favorable or otherwise, in the *in vivo* release kinetics.¹⁷

Yamakawa et al. took the concept of a coated PLA tablet one step further.¹⁸ They devised an implantable pellet that consisted of an insulin/PLA (MW 5000 Da) matrix core surrounded by a coating layer comprising Polyoxymethylene (POM) and PLA (MW 11,000). In order to allow for insulin release, the coated pellets underwent oxygen plasma irradiation. Using scanning electron micrograph images, the researchers were able to demonstrate that plasma irradiation served to form pores in the outer layer of the pellet, presumably as a result of depolymerization of the POM from the coating surface. *In vivo* studies demonstrated that normal plasma glucose levels were maintained for 10 d in diabetic rats, which was a shorter duration of action compared to previous PLA implant studies.^{16–18} The reason for the shorter release profile is not well understood, but may be the result of the higher degree of PLA hydrolysis seen with the lower molecular PLA as well as the increased porosity of the plasma-irradiated outer layer.¹⁸

While the PLA pellets seemed to have potential as biodegradable sustained insulin delivery systems, the need for surgical implantation hindered their progress and attractiveness for use in humans. This directed researchers to develop biodegradable systems that could be placed via injection with a simple syringe, thus obviating the need for any surgical procedure either for implantation or removal.

14.4.2 Polylactic Acid Microcapsules

In an early study by Lin et al., insulin-loaded polylactic acid (PLA) microcapsules were synthesized by an emulsification-solvent evaporation process originally reported by Beck et al.^{4,19} Several parameters in the synthesis process were modified with the intention of optimizing the insulin release profile. Such modifications included variations in types, concentrations, and viscosities of protective colloids used in the emulsification process. Polyvinyl alcohol (PVA), when used as the protective colloid in the fabrication process, was found to produce the PLA microparticles in reproducible quality. Further studies revealed that the concentration PVA directly affects the PLA particle size and the surface characteristics of the microcapsules. With higher concentrations of PVA, microparticles tended to be smaller and to have a smoother surface. When the release profiles of the microcapsules were stud-

ied, a burst effect was followed by a period of sustained release. When a 3% PVA solution was used as the protective colloid, no initial burst was observed, just a continuous sustained release of drug. The compact size and smooth surface of the PLA microparticles were believed to be responsible for the observed release profile.⁴

Kwong et al. further studied the synthesis and release kinetics of similarly prepared PLA microbeads.¹⁶ In addition to variations in insulin loading, temperature, and evaporation pressures, investigation into the optimum solvent evaporation time was pursued. At the time, it was believed that the undesirable initial burst kinetics were secondary to dissolution of insulin crystals from the surface of the microbeads. It was also known that PVA can assist in the nucleation and growth of surface insulin crystals. The investigators postulated that removal of PVA from the microbead preparation before all of the organic solvent had been evaporated would lessen the degree of insulin crystal formation on the surface of the microparticle, thus leading to less of an initial burst release. When PVA was removed after 4 h of the 9-h evaporation process, the resultant microparticles were found to have higher insulin content and less burst kinetics.

In vivo studies were done in which the microparticles were injected into diabetic rats while serum insulin and glucose levels were simultaneously monitored. There were a small number of early deaths believed to be secondary to insulin shock and hypoglycemia because of the burst effect. However, in the surviving rats, glucose levels were controlled for approximately 2 weeks after microbead injection. Interestingly, microscopic examination of microbeads recovered as long as 6 weeks after implantation showed no signs of degradation of the polymer matrix. Because of this, the investigators concluded that degradation of the polymer was believed to play no role in the release profiles. In addition, no signs of inflammation were noted at the injection site, indicating that at minimum, the intact polymer was biocompatible. Insulin release was believed to occur via a similar mechanism as in the EVAC pellets already described — a system of interconnected pores within the microbead matrix that allows for the controlled diffusion of insulin after an initial dissolution of surface insulin.¹⁶

In an effort to further prolong the duration of insulin release, further modifications were made in the synthesis of the PLA microcapsules. It had been previously shown that additives incorporated into the fabrication process could modify release profiles.¹⁶ Furthermore, decreasing the number of pores on the surface of an implant or a microcapsule tends to act as a barrier to insulin release.¹⁴ Lin et al. used these concepts to further modify insulin release kinetics of PLA microcapsules.²⁰ They found that by adding 1% EVAC as a release-modifying agent, *in vivo* insulin release and glucose control extended from 3 to 5 d for PLA microcapsules alone to 7 to 10 d for PLA plus 1% EVAC. In addition, when the insulin-loaded microcapsules were coated with paraffin wax, 2 weeks of glucose control was observed *in vivo*. It is postulated that the wax serves as a sealant for the surface of the micro-

particles, thereby limiting the entry of aqueous environment into the PLA/insulin matrix and thus retarding insulin release.

While the PLA microparticles showed significant potential as a means of sustained insulin delivery, there were concerns regarding the use of potentially toxic organic solvents in their synthesis. Microbead analysis revealed that approximately 3% of the methylene chloride used in the fabrication process remained entrapped in the microbeads despite several days of vacuum evaporation.¹⁶ Whether or not this small amount of methylene chloride is a clinically relevant contaminant is not clear.

14.4.3 Polylactic-co-Glycolic Acid Microcapsules

Building upon previous research done on PLA microcapsules, polylactic-co-glycolic acid (PLGA) microcapsules were prepared to serve as a sustained release system for insulin. Initially, this system had the same drawbacks as previous systems — namely, an initial burst resulting in high levels of insulin early in the release profile and subsequent premature exhaustion. This is the case when a simple solid-in-oil dispersion of crystalline insulin in dichloromethane is used in the fabrication of the PLGA microcapsules. Researchers found that with this dispersion, most of the loaded insulin is deposited on the surface of the microcapsules, and very little is incorporated into the bulk of the polymer matrix. In order to combat this, Yamaguchi et al. developed a novel solvent evaporation multiple emulsion process in which water or glycerol is added to the initial insulin/dichloromethane dispersion.²¹ Using SEM analysis, the researchers observed that upon the addition of water or glycerol, mini-emulsion droplets form with a mean diameter of 300 to 500 nm. This alteration in the fabrication process allowed for a more homogenous distribution of insulin within the polymer matrix. This favorable distribution is believed to be the result of the amphiphilic properties that both insulin and PLGA possess. This amphiphilicity allowed both molecules to converge at the interface between the hydrophilic additive (water or glycerol) and the dichloromethane. With most of the loaded insulin present on the inside of the microcapsules, not on the surface, initial burst kinetics were minimized. As a result, insulin release was dependent upon diffusion through the matrix and upon degradation of the matrix itself.²¹

The initial burst was further decreased by the fact that upon the addition of the hydrophilic additive, the glass transition temperature of the PLGA decreases from 42.5°C to 36.7°C. This allows annealing of the PLGA molecules to take place upon subcutaneous administration (where the ambient temperature is 37°C). This annealing process causes the initial porous structures of the microcapsules to disappear and allows “melted” microcapsules to fuse with each other. A decreased number of surface pores and a decreased surface area to volume ratio serves to limit the release of insulin from the annealed microparticles.²¹

In vivo studies were undertaken to compare insulin release profiles between microparticles prepared from the simple solid-in-oil dispersion and those prepared from the novel multiple emulsion technique. With the former, a significant initial insulin rise was observed. This rise peaked at 6 h and insulin release was essentially exhausted by 24 h. With the latter, the initial burst was strongly suppressed, and glucose control was achieved for 2 weeks. Insulin release continued for as long as 20 d, although the levels of insulin were not adequate to achieve normal glucose levels for this entire study period.²¹

Takenaga et al. further studied the release kinetics of several different PLGA/insulin systems.²² The molecular weight of the PLGA used in the microparticle preparations was shown to be a factor in determining the initial release of kinetics. Formulations prepared with higher molecular weight PLGA (9,000 to 10,000 Da) have higher initial insulin release than those prepared with lower molecular weight PLGA (6,000 to 8,000 Da). This phenomenon is believed to be the result of weaker interactions between the insulin and the higher molecular weight polymers. This is true for most of the polymer systems until the molecular weight of PLGA approaches 4000 Da. With this molecular weight, instead of the slow insulin release that one might expect, there is a rapid insulin release into the aqueous medium. This was believed to be the result of the greater solubility of the lower molecular weight PLGA polymer.²² Further studies were suggested in order to determine the optimum ratio of LA to GA as well as the optimum molecular weight of PLGA that can be used to prepare microspheres capable of sustained insulin delivery with minimal burst kinetics.

Because of the use of a hydrophilic solvent in the fabrication of the PLGA microparticles, pure insulin would exist in an amorphous or liquid state. This is not considered desirable since amorphous insulin has a much shorter duration of action than does crystalline insulin. In order to prevent this "deactivation" of insulin, zinc has been studied as a way to stabilize the insulin molecule in the presence of hydrophilic solvent.^{23,24} Accordingly, an insulin preparation using zinc oxide is utilized in the preparation of the PLGA microcapsules.^{21,22}

14.4.4 Block Copolymers/Hydrogels

Thermosensitive, biodegradable hydrogel polymers have been of great interest with regard to the sustained release of high molecular weight bioactive molecules such as insulin. These block copolymer systems consist of two different biocompatible polymers. Most commonly used are copolymers of PLGA and polyethylene glycol (PEG) or copolymers of PLA and polyethylene oxide (PEO).^{7,25,26}

Aqueous solutions of high-PEG block copolymers possess a unique temperature-dependent reversible gel-sol transition. This allows hydrogels to be loaded with bioactive molecules, such as insulin, in an aqueous phase above the gel-sol transition temperature, usually around 45°C. As a sol, the insulin-loaded copolymer system is injectable. Upon exposure to the subcutaneous

tissues, the copolymer cools to body temperature (37°C), which is below the gel–sol transition temperature. This causes the copolymer to form a hydrophobically bonded gel state in which all interactions are physical. Once this water-insoluble gel matrix is established, bioactive molecules can then be released into the subcutaneous tissue in a sustained fashion. Initial release is mediated by diffusion of drug. Subsequent release is governed by a combination of diffusion and matrix degradation. These systems possess several advantages over previous release systems:

- Organic solvents are not necessary in the synthesis of these copolymers, so there is less potential for toxic effects compared to other systems.
- These copolymers require no surgical procedure for implantation.
- These copolymers can solubilize and stabilize poorly soluble or sensitive drugs, such as proteins.
- Because no covalent bonds are needed to form the matrix, these copolymers can repeatedly go between being a sol or gel.^{7,25}

In a study by Kim et al., a block copolymer of PLGA and PEG was shown to be capable of releasing insulin for as long as 15 d after subcutaneous injection.²⁶ Once again, zinc was shown to be an essential part of the drug delivery system. Systems prepared without zinc exhibited a cumulative release of approximately 60% at 15 d, whereas almost 90% cumulative release was obtained when zinc (0.2 wt%) was added to the system. It is thought that the zinc ion helps insulin acquire a stable hexameric state, which not only protects the insulin from degradation but allows it to freely diffuse through the polymer matrix. Without the addition of zinc ion, insulin forms an aggregate state in the slightly acidic environment of the gel matrix. This aggregate does not freely diffuse through the matrix and ultimately becomes trapped within it. This translates into a lower cumulative release.

14.5 Biomolecules as Drug Delivery Systems

Questions as to the safety and biocompatibility of synthetic insulin delivery systems led researchers to explore the possibility of using naturally occurring biomolecules as drug delivery vehicles. The thinking is that these agents would not be recognized as foreign by the body, and thus they would produce a minimal immunological response upon implantation/injection. Efforts were made to develop insulin delivery systems derived from liposomes, lipid microparticles, and microbeads of crosslinked albumin. There were varying degrees of success with each of these systems, but each had its own set of drawbacks.

14.5.1 Liposomes

Liposomes are microscopic lipid vesicles that spontaneously form when phospholipids are suspended in an aqueous medium. The vesicles formed generally possess a lipid bilayer that surrounds an aqueous compartment. The hydrophilic components of the phospholipid serve to line the inside of the vesicle as well as the outside surface. The hydrophobic chains are contained within the interior of the bilayer. This unique structure allows pharmacological agents, including bioactive molecules such as insulin, to be loaded into the interior of these liposomes, thus forming a depot of drug in a protective coating. For molecules such as insulin that are quickly degraded, the protection offered by the lipid bilayer made liposomes an attractive vehicle for study. During the 1980s, researchers studied the effects of insulin-loaded liposomes in diabetic dogs. After subcutaneous injection of these liposomes, insulin release and glucose control were documented for up to 9 h, compared to 2 h with pure insulin injection.^{27,28} Unfortunately, at the time the studies were done, there were already insulin preparations that achieved this duration of action. As a result, the use of liposomes as means to deliver basal insulin for extended periods of time was short-lived.

14.5.2 Lipid Microparticles

Even though liposomal preparations did not seem to be a suitable vehicle for basal insulin release, the concept of using lipid molecules was still attractive to some researchers. In one study, Reithmeier et al. investigated the potential of using triglycerides as a matrix material for microparticles that could serve as a subcutaneous depot for sustained insulin release.²⁹ Microparticles of glyceryl tripalmitate were prepared using either a modified solvent evaporation technique or a melt dispersion method. Both means of microparticle preparation provided good yields and produced microparticles in the size range of 200 to 1500 nm. The lipid microparticles had greater than 80% loading of insulin. These lipid microparticles were found to be at least as biocompatible as the PLGA microparticles previously described. Unfortunately, the release of insulin from the lipid microparticles was slow and incomplete, thus ending its use as an effective insulin delivery system. The undesirable release kinetics were believed to be the result of adsorption of insulin to the matrix material. And while this system may not be suitable for insulin delivery, the possibility that these lipid microparticles may be used for other agents still exists.²⁹

14.5.3 Serum Albumin Beads

Continuing efforts to formulate a device from naturally occurring biomaterials led researchers to investigate the use of albumin microbeads prepared by chemically crosslinking the protein with 1% glutaraldehyde (G). Albumin

was chosen as the protein of choice since it is biocompatible, readily available, and relatively inexpensive. In addition, since native albumin binds many drugs strongly, it would seem logical that this type of binding would also occur in an albumin matrix, thus retarding drug release until the biodegradation of the albumin matrix occurs. Initially, studies using albumin beads were done using progesterone in rabbits.³⁰ However, this work quickly translated into systems for insulin release.^{31,32}

In a study done by Goosen et al., insulin-loaded, glutaraldehyde crosslinked albumin microbeads were prepared and implanted into diabetic rats.³¹ Two implantation techniques were employed and compared. In the first method, varying doses of microbeads were implanted in a clump by means of a small subcutaneous incision. The second technique consisted of mixing the microbeads in a glycerol/saline solution and then injecting the mixture subcutaneously to achieve an equal dispersion of microbeads. With both techniques, serum insulin levels peaked at around 2 weeks postimplantation and remained elevated for at least 2 months. Also with both techniques, a fibrous capsule was found to have formed around the insulin microbeads. This capsule is believed to play an integral role in retarding insulin release from the microbeads.³¹

In comparing the two techniques, higher sustained levels of insulin were achieved when the microbeads were implanted in the form of a clump. The difference in the release kinetics was believed to be differences in fibrous capsule formation. When the evenly dispersed microbead technique was employed, fibrous capsules surrounded each individual microbead. When implanted in the form of a clump, one large fibrous capsule formed to surround the entire clump, but no fibrous material was found within the clump. As a result, the interfacial area between the tissue and implant was much greater with the dispersion method. Subsequently, when equal doses of insulin are used, a higher insulin concentration gradient is present at the interfacial surface of the microbead clump compared to the individually encapsulated microbeads. This higher insulin gradient then translates into more robust insulin release and the higher levels of insulin observed.³¹ In further studies of the insulin-loaded microbeads, it was found that variations in the size of the microbeads and the extent to which the albumin is crosslinked can greatly affect insulin release. Smaller microbeads and those with less crosslinking have been found to release insulin more quickly than larger preparations and those with a higher degree of crosslinking.^{31,32}

14.5.4 Chitosan Microcapsules

Chitin is a naturally occurring polysaccharide that is secreted by the epidermis and forms the bulk of the protective layer of many insects and crustacea. When this compound is deacetylated, the end-product is chitosan, a biocompatible, biodegradable polysaccharide. Through the use of its amino groups, chitosan possesses the ability to be covalently crosslinked to form a stable

matrix capable of the controlled delivery of bioactive molecules. In a study by Aiedeh et al., insulin-loaded chitosan microcapsules were prepared by interfacial crosslinking of chitosan ascorbyl palmitate in a water/oil dispersion.³³ The covalently linked dehydroascorbyl palmitate (obtained by the oxidation of ascorbyl palmitate) on the surface of the microparticles serves to stabilize the chitosan in an aqueous environment, allowing it to function as a vehicle for sustained insulin release. *In vitro* studies showed nearly zero-order release kinetics for as long as 80 h.

14.6 Ceramic Delivery Systems

14.6.1 Hydroxyapatite Ceramic Microspheres

Bioactive hydroxyapatite (HA) ceramic preparations are known to be biocompatible, absorbable, and porous. They have been used extensively in orthopedic surgery as a substitute for bone autografts to fill defects within traumatized bone. It is known to be noninflammatory and causes no immunological or foreign body reaction. In a study by Paul et al., insulin was loaded into porous HA microparticles and coated with a polyethylene vinyl acetate copolymer.³⁴ When these microparticles were surgically implanted into the subcutaneous tissue of diabetic rats, glucose control was achieved for approximately 2 d. The short duration of action of the insulin-loaded microspheres was believed to be a function of inefficient drug-loading and significant burst kinetics. Because of these limitations, HA as a delivery system for insulin was short-lived.

14.6.2 Alumino–Calcium–Phosphorous Oxide Ceramic Systems

Alumino–calcium–phosphorous oxide (ALCAP) ceramic technology has been explored as a means of insulin delivery. In a study by Muzina et al., several delivery systems were investigated that employed ALCAP ceramics.³⁵ Two of the systems deserve particular attention. The first was an implant consisting of a solid composite of ALCAP powder, cysteine, and insulin (ACI delivery system). With this system prolonged insulin effect was observed, believed to be the result of the integration of insulin into the hardened composite. This integration forces the insulin to first dissociate from the composite before it can be released into the surrounding environment. In addition, the composite matrix serves to protect the insulin from degradation by providing a physical barrier between the insulin and the aqueous environment. Upon subcutaneous implantation into diabetic rats, glucose control was achieved for 2 weeks with the ACI delivery system.³⁵

The second ALCAP system worthy of discussion involved the use of a refillable glass reservoir attached to the ceramic implant (GRCS delivery

system). With this system, a 1-ml reservoir filled with a suspension of vegetable oil and insulin serves as a depot of insulin for the controlled release system. The nonporous nature of the glass reservoir serves to protect insulin from degradation, while the hydrophobic nature of the oil protects the insulin once it has entered the ceramic portion of the implant. Upon implantation into diabetic rats, a steady maintenance of normoglycemia was obtained for 21 d. What makes this system even more attractive is the fact that the glass reservoir is easily refillable by injection. This offers the potential for indefinite glucose control with few injections.³⁵ It seems that increasing the reservoir size or using longer-acting insulin preparations could further increase the duration of effectiveness of the implant and reduce the number of refill injections.

14.6.3 Zinc–Calcium–Phosphate Oxide Ceramic Systems

Because of concerns about aluminum toxicity with the ALCAP systems, research into delivery systems that utilized zinc–calcium–phosphate oxide (ZCAP) ceramics were undertaken. In a study done by Arar and Bajpai, ZCAP ceramic capsules were manufactured and impregnated with PLA.³⁶ Varying doses of insulin (20, 30 and 40 mg) were incorporated into the capsules and subcutaneously implanted into diabetic rats. While all of the preparations achieved some degree of glucose control, the lowest dose of insulin, 20 mg, achieved the best glucose control for the longest duration. With this dose, glucose levels comparable to nondiabetic controls were achieved for 21 d. One might expect the higher dose preparations to possess a longer duration of action, but this was not the case. This paradoxical behavior is believed to be the result of insulin aggregation in the presence of the zinc inherent to the ceramic preparation. The tendency of insulin to aggregate is amplified by the increased insulin concentration within the system. Researchers suggest that a 1:2 glycerol:insulin solution may be effective in stabilizing the insulin molecule and may be preferable for use in ZCAP capsules over insulin alone.

14.7 Conclusion and Perspective on the Future

There have been significant advances with regards to implantable delivery systems for the controlled release of insulin. Many of the systems previously studied have characteristics considered favorable, but no one system possesses all of the necessary attributes to make such systems a reality in humans. It is clear that biocompatibility and biodegradability are vital components to the ideal delivery system. Such systems do not require surgical removal upon exhaustion of drug and are seamlessly integrated into the

host. Injectability is also advantageous as it obviates the need for surgical implantation. And while injectable, biodegradable systems currently exist, efforts to prolong the duration of insulin release or to modify the insulin release profile after implantation would make these promising systems more attractive. A review of previous attempts at optimizing insulin release from nonabsorbable matrices may serve to guide future explorations into injectable, degradable systems.

Efforts to prolong glucose control with smaller doses of insulin led researchers to study the effects of coadministration of somatostatin and insulin. It is well established that glucose levels in the blood are mediated by a balance that exists between insulin and counter-regulatory hormones. Somatostatin is a naturally occurring hormone known to inhibit the secretion of many of these endogenous counter-regulatory hormones including growth hormone, glucagon, corticosteroids, and catecholamines. It would follow that somatostatin administration, by inhibiting the hormones that tend to raise serum glucose levels, would effectively decrease the amount of insulin required to maintain glucose control. In a study by Edelman et al., EVAC pellets loaded with a combination of insulin and somatostatin were compared to EVAC pellets loaded with insulin alone.³⁷ Researchers demonstrated that glucose levels in the "insulin alone" group remained depressed for 5 d until the insulin released from the EVAC matrices fell below 11.6 units/kg/d. When somatostatin was delivered concomitantly with insulin, glucose control persisted for 12 d until insulin release had decreased below 3.6 units/kg/d. And while the insulin release profile was essentially the same between the two systems, the latter system was able to achieve glucose control for a much longer duration as somatostatin effectively decreased insulin demand. Perhaps coadministration of somatostatin can be further studied in more modern insulin delivery systems to achieve a similar effect.

Another way to potentially prolong the duration of glucose control would be to load longer-acting insulin preparations into the polymeric delivery systems. Such longer-acting preparations include NPH insulin, lente insulin, ultralente insulin, and insulin glargine. In addition, a novel long-acting insulin preparation was recently reported in which NPH insulin is cocrystallized with a lipophilically modified, more hydrophobic insulin derivative. The cocrystal preparation dissolves substantially slower than pure NPH preparations, and there is a more homogenous release profile with a longer duration of action (24 h vs. 18 h).³⁸

In their studies of bioactive derivatives, Shalaby and co-workers were able to acylate insulin with monobasic and dibasic organic acids to produce insulin derivatives with variable degrees of solubility at pH 7.4 and modulated charge type and density.³⁹⁻⁴² The latter effect on charge was used to control the iontophoretic mobility of derivatized insulin.^{40,41} Acylation of insulin with fatty acids to produce derivatives having various levels of hydrophilicity was explored. These investigators were able to achieve variable levels of bioavailability and efficacy in diabetic rats.³⁹

It seems logical that release of longer-acting preparations would still be dependent upon the factors that determine the release kinetics of short-acting insulin preparations (i.e., diffusion, matrix degradation). However, once released from the matrix, their longer half-lives would serve to control glucose for longer periods of time. Almost all of the previous release systems reviewed employed short-acting insulin preparations. Perhaps research into longer-acting agents would serve to significantly prolong and improve glucose control.

In some interesting work by Gershonov et al., two 9-fluorenylmethoxycarbonyl moieties were covalently bound to insulin to develop an inactive insulin preparation that has minimal biological potency or receptor-binding capacity.⁴³ At a pH of 7.4 and a temperature of 37°C, the modified insulin undergoes a time-dependent spontaneous conversion to fully active insulin. One subcutaneous dose of the modified insulin controlled glucose levels in diabetic rats for up to 3 d. In order to demonstrate that this effect was due to the gradual conversion of inactive insulin to active insulin in the circulation and not a factor of the subcutaneous environment, an intraperitoneal injection was done and was shown to affect glucose levels for up to 40 d. This modified insulin appears to function as a mobile depot of insulin that gradually produces active insulin. Such a preparation may have a synergistic effect on duration of insulin action if it is incorporated into a sustained delivery device.

One drawback to all of the systems reviewed is their inability to respond to increases in insulin demand such as postprandial rises in serum glucose. The ideal insulin delivery system would provide for basal insulin requirements, but would be able to modify insulin release to respond to rises in serum glucose. Early attempts to accomplish this desirable goal were made using an oscillating magnetic field to control insulin release rates. In a study done by Brown et al., tiny magnets were incorporated into an insulin/EVAC matrix.⁴⁴ When the pellets were exposed to an oscillating magnetic field, release rates increased up to 30-fold. *In vivo*, 20 min of magnetic field exposure caused serum glucose levels in diabetic rats to go from 300–450 mg/dl to 150–275 mg/dl. And while this method offers some promise, ferromagnetic materials incorporated into delivery systems would need to be surgically removed since they would not be bioabsorbable.

A more promising and elegant means of responding to increasing insulin demand utilizes a glucose-mediated, enzymatically controlled drug delivery system. The system is based upon the insulin/EVAC system previously described. Feedback control is mediated by the enzyme glucose oxidase, which is immobilized to Sepharose beads. These beads are incorporated into the EVAC matrix along with insulin. When glucose levels within the delivery system rise, gluconic acid is produced causing a drop in the pH of the matrix microenvironment. This leads to an increase in insulin solubility and, ultimately, insulin release. Such an effect is observed both *in vitro* and *in vivo*. Additionally, this pulse effect is temporary, and repeated pulses of insulin release are observed upon reexposure to increasing glucose concentrations.^{5,6}

Significant advances in sustained insulin delivery systems have been made in the past two decades. However, much work is still needed to further develop these devices. Factors such as injectability, biocompatibility, duration of action, and the ability to modify insulin release need to be further explored before such devices will be suitable for the treatment of diabetes mellitus in humans.

References

1. Report of the Expert Committee on the Diagnosis and Classification of Diabetes Mellitus, *Diabetes Care*, 20, 1183, 1997.
2. Blackshear, P. J., Implantable drug delivery systems, *Sci. Am.*, 241, 66, 1979.
3. Langer, R., Implantable controlled release systems, *Pharmacol. Ther.*, 21, 35, 1983.
4. Lin, S. Y., Ho, L. T. and Chiou, H. L., Microencapsulation and controlled release of insulin from polylactic acid microcapsules, *Biomater. Med. Devices Artif. Org.*, 13(3 & 4), 187, 1985–1986.
5. Fischel-Ghodsian, F., Brown, L., Mathiowitz, E., Brandenburg, D. and Langer, R., Enzymatically controlled drug delivery, *Proc. Nat. Acad. Sci. U.S.A.*, 85, 2403, 1988.
6. Brown, L., Edelman, E., Fischel-Ghodsian, F. and Langer, R., Characterization of glucose-mediated insulin release from implantable polymers, *J. Pharm. Sci.*, 85(12), 1341, 1996.
7. Zentner, G. M., Rathi, R., Shih, C., McRea, J. C., Seo, M. H., Oh, H., Rhee, B. G., Mestecky, J., Moldoveanu, Z., Morgan, M. and Weitman, S., Biodegradable block copolymers for delivery of proteins and water-insoluble drugs, *J. Controlled Rel.*, 72, 203, 2001.
8. Morishita, M., Lowman, A. M., Takayama, K., Nagai, T. and Peppas, N. A., Elucidation of the mechanism of incorporation of insulin in controlled release systems based on complexation polymers, *J. Controlled Rel.*, 81(1–2), 25, 2002.
9. Davis, B. K., Control of diabetes with polyacrylamide implants containing insulin, *Experientia*, 28, 348, 1972.
10. Langer, R. and Folkman, J., Polymers for the sustained release of proteins and other macromolecules, *Nature*, 263, 797, 1976.
11. Rhine, W. D., Hsieh, D. S. T. and Langer, R., Polymers for sustained macromolecule release: procedures to fabricate reproducible delivery systems and control release kinetics, *J. Pharm. Sci.*, 69(3), 265, 1980.
12. Bawa, R., Siegel, R. A., Marasca, B., Karel, M. and Langer, R., An explanation for the controlled release of macromolecules from polymers, *J. Controlled Rel.*, 1, 259, 1985.
13. Creque, H. M., Langer, R. and Folkman, J., One month of sustained release of insulin from a polymer implant, *Diabetes*, 29, 37, 1980.
14. Brown, L., Siemer, L., Munoz, C. and Langer, R., Controlled release of insulin from polymer matrices: *in vitro* kinetics, *Diabetes*, 35, 684, 1986.
15. Brown, L., Munoz, C., Siemer, L., Edelman, E. and Langer, R., Controlled release of insulin from polymer matrices: control of diabetes in rats, *Diabetes*, 35, 692, 1986.

16. Kwong, A. K., Chou, S., Sun, A. M., Sefton, M. V. and Goosen, M. F. A., *In vitro* and *in vivo* release of insulin from poly(lactic acid) microbeads and pellets, *J. Controlled Rel.*, 4, 47, 1986.
17. Yamakawa, I., Kawahara, M., Watanabe, S. and Miyake Y., Sustained release of insulin by double-layered implant using poly(D,L-lactic acid), *J. Pharm. Sci.*, 79(6), 505, 1990.
18. Yamakawa, I., Watanabe, S., Matsuno, Y. and Kuzuya, M., Controlled release of insulin from plasma-irradiated sandwich device using poly-DL-lactic acid, *Biol. Pharm. Bull.*, 16(2), 182, 1993.
19. Beck, L. R., Cowsar, D. R., Danny, H. L., Gibson, J. W. and Flowers, C. E., New long-acting injectable microcapsule contraceptive system, *Am. J. Obstet. Gynecol.*, 135, 419, 1979.
20. Lin, S. Y., Ho, L. T. and Chiou, H. L., Insulin controlled-release microcapsules to prolong the hypoglycemic effect in diabetic rats, *Biomater. Med. Devices Artif. Org.*, 16(4), 815, 1988.
21. Yamaguchi, Y., Takenaga, M., Kitagawa, A., Ogawa, Y., Mizushima, Y. and Igarashi, R., Insulin-loaded biodegradable PLGA microcapsules: initial burst release controlled by hydrophilic additives, *J. Controlled Rel.*, 81, 235, 2002.
22. Takenaga, M., Yamaguchi, Y., Kitagawa, A., Ogawa, Y., Mizushima, Y. and Igarashi, R., A novel sustained-release formulation of insulin with dramatic reduction in initial rapid release, *J. Controlled Rel.*, 79, 81, 2002.
23. Brange, J., *Galenics of Insulin: the Physico-chemical and Pharmaceutical Aspects of Insulin and Insulin Preparations*, Springer, New York, 1986, 36.
24. Scott, D. A., Crystalline Insulin, *J. Biochem.*, 28, 1592, 1934.
25. Jeong, B., Bae, Y. H., Lee, D. S. and Kim, S. W., Biodegradable block copolymers as injectable drug-delivery systems, *Nature*, 388, 860, 1997.
26. Kim, Y. J., Choi, S., Koh, J. J., Lee, M., Ko, K. S. and Kim, S. W., Controlled release of insulin from injectable biodegradable triblock copolymer, *Pharm. Res.*, 18(4), 548, 2001.
27. Stevenson, R. W., Patel, H. M., Parson, J. A. and Ryman, B. E., Prolonged hypoglycemic effect in diabetic dogs due to subcutaneous administration of insulin in liposomes, *Diabetes*, 31, 506, 1982.
28. Patel, H. M., Liposomes as a controlled-release system, *Trans. Biochem. Soc.*, 13(2), 513, 1985.
29. Reithmeier, H., Herrmann, J. and Gopferich, A., Lipid microparticles as a parenteral controlled release device for peptides, *J. Controlled Rel.*, 73, 339, 2001.
30. Lee, T. K., Sokoloski, T. D. and Royer, G. P., Serum albumin beads: an injectable, biodegradable, system for the sustained release of drugs, *Science*, 231, 233, 1981.
31. Goosen, M. F. A., Leung, Y. F., Chou, S. and Sun, A. M., Insulin-albumin microbeads: an implantable, biodegradable system, *Biomater. Med. Devices Artif. Org.*, 10(3), 205, 1982.
32. Goosen, M. F. A., Leung, Y. F., O'Shea, G. M., Chou, S. and Sun, A. M., Long-acting insulin: slow release of insulin from a biodegradable matrix implanted in diabetic rats, *Diabetes*, 32, 478, 1983.
33. Aiedeh, K., Gianasi, E., Orienti, I. and Zecchi, V., Chitosan microcapsules as controlled release systems for insulin, *J. Microencapsul.*, 14(5), 567, 1997.
34. Paul, W., Nesamony, J. and Sharma, C. P., Delivery of insulin from hydroxyapatite ceramic microspheres: preliminary *in vivo* studies, *J. Biomater. Res.*, 61(4), 660, 2002

35. Muzina, D. J., Snow, K. R. and Bajpai, P. K., Regulation of blood glucose by sustained delivery of insulin via ALCAP ceramics in rats, *Biomed. Sci. Instrum.*, 25, 191, 1989.
36. Arar, H. H. and Bajpai, P. K., Insulin delivery by zinc calcium phosphate ceramics, *Biomed. Sci. Instrum.*, 28, 173, 1992.
37. Edelman, E., Brown, L. and Langer R., Quantification of insulin release from implantable polymer-based delivery systems and augmentation of therapeutic effect with simultaneous release of somatostatin, *J. Pharm. Sci.*, 85(12), 1271, 1996.
38. Brader, M. K., Sukumar, M., Pekar, A. H., McClellan, D. S., Chance, R. E., Flora, D. B., Cox, A. L., Irwin, L. and Myers, S. R., Hybrid insulin cocrystals for controlled release delivery, *Nat. Biotechnol.*, 20(8), 800, 2002.
39. Njieha, F. K. and Shalaby, S. W., Dynamic and physico-chemical properties of modified insulin, *Polym. Prepr.*, 33(3), 536, 1992.
40. Corbett, J. T., Dooley, R. L., Michniak, B. B., Zimmerman, J. K. and Shalaby, S. W., Iontophoretic controlled delivery of modified insulin, *Proc. Fifth World Biomater. Cong.*, Toronto, Canada, 1, 28, 1996.
41. Corbett, J. T., Dooley, R. L., Michniak, B. B., Zimmerman, J. K. and Shalaby, S. W., Succinylation of insulin for accelerated iontophoretic delivery, *Proc. Fifth World Biomater. Cong.*, Toronto, Canada, 2, 157, 1996.
42. Shalaby, S. W., Allan, J. M. and Corbett, J. T., Peracylated Insulin Compositions and Process for Making the Same, U.S. Patent (to Poly-Med, Inc.) 6,162,895, 2000.
43. Gershonov, E., Shechter, Y. and Fridkin, M., New concept for long-acting insulin- spontaneous conversion of an inactive modified insulin to the active hormone in circulation: 9-fluorenylmethoxycarbonyl derivative of insulin, *Diabetes*, 48, 1437, 1999.
44. Brown, L., Munoz, C., Siemer, L., Edelman, E., Kost, J. and Langer, R., Sustained insulin release from implantable polymers, *Diabetes*, 32, 35A, 1983.

15

Absorbable Delivery Systems for Cancer Therapy

Waleed S.W. Shalaby

CONTENTS

15.1 Introduction	227
15.2 Models of Tumor Growth	228
15.3 Emerging Challenges for Cancer Chemotherapy	232
15.3.1 Dose-Densification Using Paclitaxel	234
15.3.2 Dose-Densification Using Prolonged Infusion of Paclitaxel	236
15.3.3 Clinical Model for Dose Determination and Schedule.....	237
15.3.4 Defining a Therapeutic Index for Chemotherapy Agents	240
15.3.5 Rationale for Sustained Drug Delivery	240
15.3.6 Biodegradable or Absorbable Polymers for Drug Delivery.....	242
15.3.7 Absorbable Delivery Systems to Manipulate Drug Exposure Duration (DED) "Pegylated" Systems.....	244
15.3.8 Site-Specific (Intracranial)	245
15.3.9 Site-Specific (Intratumoral).....	246
15.4 Conclusion and Perspective on the Future	249
References	250

15.1 Introduction

Despite decades of basic and clinical research and trials of promising new therapies, cancer remains a major cause of morbidity and mortality. In 1990, cancer mortality rates peaked in the U.S. and have declined steadily. By 2000, Anderson et al. reported an estimated 500,000 deaths which was 64,000 fewer

deaths compared with 1990.¹ This was 12.7% lower than expected and was attributed to 51,900 fewer cancer deaths among men and 12,200 fewer deaths among women. Most of the decline was attributed to relatively small mortality rate reductions in the four leading causes of cancer mortality (lung, colon, prostate, and breast cancers). The decline in deaths among men resulted from fewer deaths from lung, colon, and prostate cancers, whereas the decline among women resulted from fewer deaths from breast and colon cancer. However, death among women was higher than expected in those over the age of 75 and with lung cancer. A more telling statistic is the comparison of 5-year relative survival rates between 1950–1954 and 1992–1998 for the 25 most common cancers in the U.S.² With respect to solid tumors, these modest gains in survival largely reflect earlier detection through screening programs rather than dramatic improvements in chemotherapy.³

The basis of current cancer treatment, while still grounded in traditional cytotoxic agents, is rapidly evolving to incorporate targeted agents developed from advances in molecular pharmacology. These new agents are designed to target regulatory genes or proteins, growth factors, and cellular or nuclear receptors. The obvious goal is to disrupt tumor-specific pathways involving angiogenesis, signal transduction, cell-cycle kinetics, invasion/metastasis, and drug resistance without significant compromise to normal tissue. The future emphasis of cancer therapy will undoubtedly rely on identifying new classes of molecules to optimize therapy. However, recent clinical trials using dose-densification suggest that more effective strategies of drug delivery using existing cytotoxic agents may provide a tangible opportunity to improve tumor response through a more rigorous understanding of therapeutic index and drug exposure duration. The following review will attempt to address the clinical and theoretical rationale for this approach and the implementation of absorbable delivery systems to meet this objective.

15.2 Models of Tumor Growth

The mathematical modeling of tumor growth, while derived from population kinetics, should facilitate rational strategies to optimize chemotherapy administration. To date, however, an absence of unifying concepts combined with the assumption of continuous drug delivery has largely impaired the practical use of these models. The overriding explanation for these shortcomings is that *in vivo* cancer growth is influenced by a number of interrelated processes involving cell-cell, tumor-microenvironment, and tumor-host interactions which are difficult to model in the lab. Compounding this clinical disparity is that many chemotherapy agents are eliminated within 24 to 48 h, requiring a continuous infusion to meet the theoretical assumption of most tumor growth models. Thus, *in vivo* growth inhibition

models may be more predictable if the latter parameter of extended drug exposure could be attained in the clinical setting.

Assumptions on tumor growth can be empirically or functionally grounded. Empirical models base observed growth on the macroscopic behavior of the tumor in terms of volume, mass, and cellularity.⁴ Under certain assumptions, sigmoidal growth curves can be constructed to fit the interplay between tumor growth (mass gain) and cell death (mass degradation). The size $y(t)$ of the system can be expressed as two autonomous differential equations

$$y' = G(y) - D(y), y(0) = y_0 > 0$$

where $G(y)$ and $D(y)$ represent the rate of tumor growth and degradation, respectively.⁴ Both $G(y)$ and $D(y)$ represent parallel first-order processes that reach a defined steady state. These rates can be expressed as power functions originally described by von Bertalanffy as a general growth equation⁵

$$G(y) = ay^\alpha, D(y) = by^\beta$$

where a and b are effective rate constants, and α and β refer to the “fractal order” of the effective rates as described by Kopelman.⁶ A distinctive feature of this model is the ability to interpret two rate processes within the same theoretical framework. However, this synergistic model fails to adequately describe actual tumor growth.⁷ The Gompertz growth equation

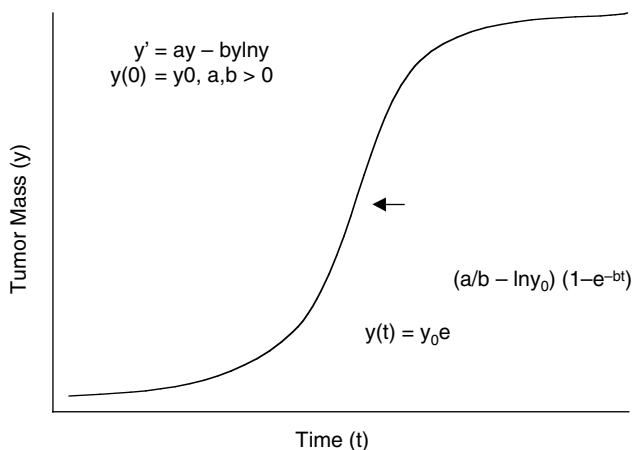
$$G(y) = ay, D(y) = by \ln y$$

and its generalized form

$$G(y) = ay^\alpha, D(y) = by^\alpha \ln y$$

are considered to provide a more accurate description of observed *in vivo* data.^{4,7,8} Gompertzian kinetics predict an initial period of increasing growth rate followed by a period of decreasing growth (Figure 15.1). The point of inflection on the curve represents the maximum rate of tumor growth. Because of its wide applicability, the Gompertz model is felt to represent empiric properties inherent to the biology of tumor growth. However, a clear understanding of these biological properties has yet to be achieved.

Functional models were later generated to predict tumor growth in terms of cell kinetics and/or cell–cell interactions. More importantly, these models allow for the incorporation of growth inhibition and stimulation by autocrine (tumor-derived), paracrine (microenvironment), or humoral/exogenous mediators. While the mathematical derivation of these relationships is beyond the scope of this chapter, it clearly represents an effort to model receptor-mediated processes, auto-stimulation, negative and positive feedback loops, and dynamic processes between competing subpopulations of

**FIGURE 15.1**

Theoretical tumor growth curve as predicted by Gompertzian kinetics. The model predicts an initial period of increasing growth rate followed by a period of decreasing growth. The inflection point (arrow) on the curve represents the maximum rate of tumor growth.

the same tumor.⁴ Recently, Sherratt et al. developed a functional model oriented to describe avascular tumor growth.⁹ In this context, tumor growth is represented as a layered structure consisting of an outer proliferating rim, quiescent band, and necrotic core (Figure 15.2). The model treats proliferating, quiescent, and necrotic cells as a continuum under the influence of environmental factors such as nutrient/growth factors from underlying tissues and cell movement in terms of migration and contact inhibition. Pertinent to this discussion is the work by Byrne et al. where tumor growth was modeled in the presence and absence of inhibitors such as chemotherapy.¹⁰ The model divides the central core of cell loss/death in terms of necrosis and apoptosis. Necrosis was treated as cell death induced by changes in the microenvironment such as decreases in local nutrient concentrations that are insufficient to sustain the tumor cell. Cell apoptosis was defined as classical programmed cell death, an intrinsic property of the cell. This model necessitates two free boundaries to track the growth of the outer tumor radius and the necrotic core radius. The latter is purported to depend on the tumor size and evolves on different timescales. The inherent advantage of this approach is that tumor growth can be evaluated as a function of two different inhibitory mechanisms. Thus, the inhibitor (chemotherapeutic agent) can act either directly on the cells to reduce proliferation or indirectly by reducing nutrient levels. The underlying assumption is that the level of inhibitor (chemotherapy) and nutrients are independent of time. Under inhibitor-free conditions, tumor configurations will depend on the relative rates of cell proliferation (σ_a), cell loss due to necrosis (σ_{nec}), and cell loss due to apoptosis (σ_{apo}) as functions of local nutrient concentrations. Therefore, under extreme conditions of strong apoptotic decay, tumor regression to zero would be favored. Conversely, weak apoptotic decay would promote a necrotic tumor

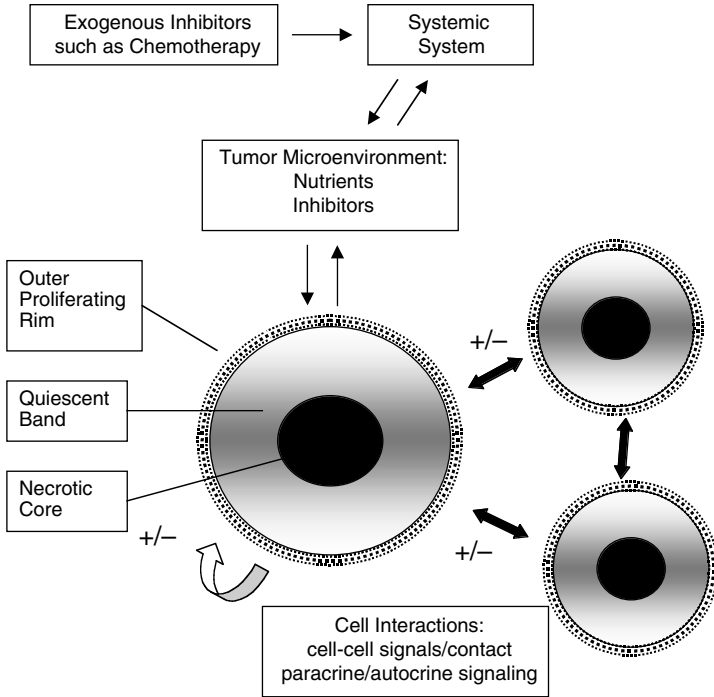


FIGURE 15.2

Conceptual description of an avascular tumor growth model. Tumor growth is represented as a layered structure consisting of an outer proliferating rim, quiescent band, and necrotic core. The model treats the proliferating, quiescent, and necrotic cells as a continuum under the influence of environmental factors such as nutrient/growth factors from underlying tissues, and cell movement in terms of migration and contact inhibition.

configuration as local nutrient concentrations wane. Under more realistic intermediate values, however, apoptotic decay would depend on the initial size of the proliferating tumor and its growth characteristics. In the presence of chemotherapy (β), tumor configurations will be coupled to the agent's influence on the cell proliferation rates (β_α), cell loss due to necrosis (β_{nec}), and cell loss due to apoptosis (β_{apo}). In their analysis, Byrne et al. examined tumor growth with a thin proliferating rim, a scenario analogous to the initial period following debulking procedures for solid tumors.¹⁰ The following mathematical relationship describes the outer tumor radius (R) over time:

$$R \sim R_o + \epsilon s_{nec} [(1 - \sigma_{apo}/\sigma_{nec})(1 - \beta_\alpha/\beta_{apo})(R_1 - \rho_1) - \lambda R_o(0)/\sigma_{nec}]t$$

where ϵ , s , and λ are constants, and ρ represents the inner core radius. It is included in this discussion to visualize trends in tumor growth as a function of σ_{nec} , σ_{apo} , β_α , and β_{apo} , respectively. When $\sigma_{nec} > \sigma_{apo}$ and $\beta_\alpha > \beta_{apo}$ exists or $(\sigma_{nec} - \sigma_{apo})(\beta_\alpha - \beta_{apo}) > 0$, tumor regression by chemotherapy is predicted. This is particularly relevant to agents that are cycle-specific in the setting of

small tumor volume where nutrient supply can be tenuous. Thus, periods of rapid tumor growth (i.e., immediately following surgical debulking) represent a critical window in which to institute adjuvant therapy. However, stable tumor configurations can evolve when $\sigma_{\text{nec}} > \sigma_{\text{apo}}$, but $\beta_{\text{apo}} > \beta_{\alpha}$ or $(\sigma_{\text{nec}} - \sigma_{\text{apo}})(\beta_{\alpha} - \beta_{\text{apo}}) < 0$. Therefore, agents that are not cycle-specific and favor apoptosis pathways will give rise to a smaller tumor when nutrient supply is marginal and cell necrosis predominates. This scenario may not only arise immediately following surgical debulking in the adjuvant setting, but more importantly at the conclusion of chemotherapy where consolidation therapy to maintain stable tumor volume may be the goal of treatment. Interestingly, the model predicts support of a stable tumor configuration when $\sigma_{\text{apo}} > \sigma_{\text{nec}}$ and $\beta_{\alpha} > \beta_{\text{apo}}$. To date, this model has not been tested *in vivo*, but could have important implications depending on the mechanism of action of the agents. This is particularly applicable in the setting of combination therapy directed at both cell proliferation and by altering local nutrient concentrations. However, this model makes a critical assumption of constant drug levels. While this can be a controlled variable in cell culture, it is not clinically viable at this time given conventional modes of drug delivery.

15.3 Emerging Challenges for Cancer Chemotherapy

Under certain conditions, the Gompertzian tumor model provides an accurate barometer for tumor growth *in vivo*. However, deviations occur over time due to selection and expansion sub-clones that are chemo-resistant. Skipper's Cell Kill Hypothesis is based on the notion that chemotherapy will lead first-order cell kill kinetics.¹¹ Therefore, each administration of chemotherapy will produce the same fraction of tumor cell death. In theory, it is believed that a log-cell drop of 9 to 11 orders of magnitude is required for tumor eradication. Clinically this scenario is complicated by the chemosensitivity of normal tissue and tumor, pharmacokinetic heterogeneity of patients, and tumor heterogeneity.

Pharmacokinetic heterogeneity can be related to drug disposition as a function of mode of drug delivery, tumor perfusion, and elimination kinetics. For example, parenteral administration of agents with relatively short half-lives (6 to 12 h) will have a brief window in which to distribute to solid tumors. Disposition will be a perfusion-dependent process whereby solid, necrotic, or ischemic tumors will receive only a fraction of the intended dose. Therefore, well-perfused tumor, but more importantly, normal tissue will see the majority of the administered dose. Elimination kinetics will also vary from patient to patient depending on the mode of elimination. As mentioned above, the dosing of many agents is based on body surface area and not elimination rates. Thus, individual differences in renal excretion and hepatic metabolism due to comorbidities or pharmacogenetics will unknowingly

influence drug clearance. Outside of toxicity to normal tissues, such variations may lead to significant underdosing as described by Gurney.¹²

Tumor heterogeneity represents a continuum of variation in terms of cell-cycle kinetics and chemosensitivity. Cells within the same tumor can vary in terms of the cell-cycle time or phase. The practical implication is that the efficacy of certain phase-specific agents will depend on the duration of drug exposure and the number of actively proliferating tumor cells. Based on Gompertzian growth kinetics, however, as a solid tumor increases in size, the rate of cell proliferation decreases. Furthermore, this growth kinetics does not take into consideration the expansion of tumor subclones that develop from sporadic mutations or by selective pressure from chemotherapy. Thus, chemo-resistance can manifest in terms of the fraction of resting cells (G_0 phase) and the ability of subclones to inactivate the drug, decrease or alter cell targets, amplify repair mechanism, or decrease drug accumulation.

In the adjuvant setting, Gompertzian kinetics would predict that the probability of achieving log kill is greatest for small volume tumors since they are likely to display the most rapid rate of proliferation. Thus, late intervention and delays in treatment due to toxicity or scheduling may actually work against the efficacy of the agent.^{13,14} The concept of dose-densification described by Norton provides an alternative mode, which is to compress the conventional schedule by decreasing treatment intervals using lower doses. In simulations, this simple manipulation achieves a considerably greater efficacy by minimizing regrowth of cells between cycles of treatment (Figure 15.3).^{13,14} Clinically, a recent randomized trial was performed using dose-dense vs. conventionally scheduled chemotherapy as postoperative adjuvant treatment in node-positive breast cancer.^{15,16} The investigators found that the

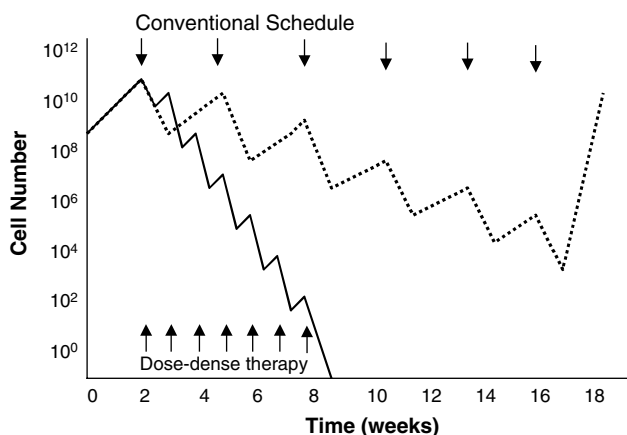


FIGURE 15.3

Simulated effect of dose-dense therapy vs. conventional scheduling on log-cell kill in Gompertzian growth. The initial time zero may represent the time of initial diagnosis at the time of surgery with subsequent treatment. (Adapted from Norton, L., Theoretical Concepts and the emerging role of taxanes in adjuvant therapy, *The Oncologist*, 6(3), 30, 2001. With permission.)

dose-dense treatment significantly improved disease-free (RR = 0.74; $P = 0.01$) and overall survival (RR = 0.69; $P = 0.013$). Four-year disease-free survival (DFS) was 82% for the dose-dense regimens and 75% for the conventional schedule. As expected, severe neutropenia was less frequent in patients who received the dose-dense regimens.

From the preceding discussion, much of our understanding of conventional chemotherapy is based on standard parenteral routes of administration. Based on Table 15.1, it is observed that the majority of these agents possess half-lives of 12 h or less. More importantly, significant variability exists for certain drugs as a function of dose, patient age, and renal or liver function. Because of this, large serum peaks and relatively rapid troughs can arise which significantly marginalize drug distribution to solid tumors. The magnitude of these fluctuations may be perfusion-dependent, dose-dependent, and/or patient-dependent. Furthermore, complicating this scenario are the inequities of dose calculations based on body-surface area (BSA), tumor heterogeneity as described below, and delayed scheduling by convention or by toxicity.

15.3.1 Dose-Densification Using Paclitaxel

In the treatment of solid tumors, drug efficacy is often marginalized by impaired delivery to centrally ischemic tissue as well as acquired drug resistance through genetic and epigenetic mechanisms. These problems are further compounded by standard scheduling regimens that administer a large dose of over brief periods of time (30 min to 3 h) at 3- to 4-week intervals. Not only does this lead to significant toxicity but also compromises efficacy since most of the agent is eliminated after 24 to 48 h. This will highlight the recent trials using dose-densified paclitaxel regimens.

In recent years, paclitaxel has been successfully incorporated in the treatment of head and neck, breast, non-small cell lung, and ovarian cancers as neoadjuvant, adjuvant, and salvage therapy. Standard parenteral regimens range from 135 mg/m² to 175 mg/m² every 3 weeks. Weekly administration of Taxol was initiated to decrease the well-known toxicities associated with higher dose regimens. Surprisingly, the lower dose weekly regimens led to significant responses in heavily pretreated patients and those thought to be paclitaxel-resistant. Klaassen et al. performed a phase I study with a weekly 1-h infusion in three patients with ovarian and seventeen with breast cancer.¹⁷ These patients were selected based on anthracycline- or platinum-refractory disease. They observed no dose limiting toxicities at a range between 70 mg/m² and 90 mg/m². Furthermore, objective responses were noted at all dose levels. At a higher dose of 100 mg/m², grade 4 neutropenia and grade 2 alopecia were observed.^{17,18} With multiple cycles, a cushing-like syndrome had also occurred due to premedication with steroids.¹⁸ Alvarez et al. were one of the first groups to show the clinical utility of weekly taxol in patients who either recurred or were refractory on the standard paclitaxel regimens.¹⁸

TABLE 15.1

Summary of Changes in 5-year Relative Survival Rates Based on the Surveillance, Epidemiology, and End Results (SEER) Program Incidence Rates and National Center for Health Statistics (NCHS) Death Rates for 1973–1997

Primary Site	5-Year Relative Survival Rates 1950–1954	5-Year Relative Survival Rates 1992–1998	Primary Site	5-Year Relative Survival Rates 1950–1954	5-Year Relative Survival Rates 1992–1998
Bladder	53	82.3	Lung (female)	9	17.0
Brain	21	31.5	Melanoma of skin	49	89.3
Breast	60	87.6	Multiple myeloma	6	29.5
Cervix	72	86.0	Oral and Pharynx	46	58.8
Colon	41	62.7	Ovary	30	52.5
Esophagus	4	14.7	Pancreas	1	4.3
Hodgkin's lymphoma	30	84.7	Prostate	43	97.8
Non-Hodgkin's	33	56.1	Rectum	40	62.5
Kidney	34	62.4	Stomach	12	20.9
Larynx	52	65.9	Testes	57	95.7
Leukemia	10	47.3	Thyroid	80	96.0
Leukemia (child)	20	78.6	Uterus	72	86.0
Liver	1	6.5	All sites	35	63.8
Lung (male)	5	13.3			

They observed a 25% complete and 42% partial response in this cohort of patients. Interestingly, weekly paclitaxel induced a nearly 63% response in those with recurrent disease. These promising results have prompted a number of phase I-II trials using weekly paclitaxel for metastatic breast, gynecologic, non-small lung, head and neck, and prostate cancers. Perez et al. evaluated the safety and efficacy of weekly paclitaxel (80 mg/m²) in women with metastatic breast cancer.¹⁹ Patients enrolled were allowed to have had up to two prior chemotherapy regimens for metastatic disease. This also included therapy with anthracyclines and taxanes. The overall response rate (complete and partial response) was 21.5%, and disease stabilization was 41.8%. Median time to progression was 4.7 months, and overall survival was 12.8 months. The authors concluded that weekly paclitaxel therapy demonstrated reasonable activity in this heavily pretreated population with advanced disease. Kaern et al. studied weekly paclitaxel in recurrent, platinum-resistant ovarian cancer.²⁰ Using a dose of 80 mg/m², the overall response rate was 55% (2 complete and 15 partial), 16% stable disease, and 29% progression. Complete responses were not seen in the 20 patients who were resistant to multiple agents (i.e., paclitaxel and platinum); however, 9(45%) had partial responses and 4 (20%) had stable disease. Response was found to be independent of prior treatment history with 50 to 60% of the

patients responding after primary, secondary, or tertiary therapy. This latter observation supports the hypothesis of paclitaxel-mediated inhibition of endothelialization over antitumor cytotoxicity. Paclitaxel is one of the most commonly used agents in the treatment of locally advanced and metastatic non-small cell lung cancer (NSCLC). Willner et al. examined the maximum tolerated dose of weekly paclitaxel in combination with radiation therapy.²¹ A total of 38 patients with inoperable NSCLC received two cycles of induction chemotherapy with paclitaxel and carboplatin followed by combined radiochemotherapy (60 Gy/6 weeks and weekly taxol). Tumor response (complete and partial) as determined by CT-scan was 88% (30/34). The 1- and 2-year survival rate was 73% and 34%, respectively. Belani has recently performed an interim analysis of a phase II study treating advanced and metastatic NSCLC with weekly paclitaxel/carboplatin followed by weekly maintenance paclitaxel.²² Patients in arm 1 received paclitaxel 100 mg/m²/wk for 3 weeks along with carboplatin on day 1 every 4 weeks. The total duration of this initial therapy was 16 weeks and was well tolerated. It was observed that the median survival had already exceeded that seen in previous phase III trials with traditional schedules of paclitaxel and carboplatin. Weekly paclitaxel and carboplatin has recently been studied in a phase II trial to improve regional control and survival in patients with advanced head and neck cancer.²³ Patients allocated to the inoperable group, received eight cycles of weekly paclitaxel and carboplatin with conventional radiotherapy. Chemoradiotherapy was followed by neck dissection for those patients who presented with clinically palpable lymph nodes. Complete and partial responses were observed in 60% and 30% of the patients, respectively. Survival data was still ongoing, but encouraging.

15.3.2 Dose-Densification Using Prolonged Infusion of Paclitaxel

Prolonging infusion schedules can alter the pharmacology of chemotherapeutic agents in terms of toxicity profiles and antitumor efficacy. Preclinical data have suggested that prolonged exposure to paclitaxel enhances its cytotoxicity, but various clinical trials utilizing long-term infusions of paclitaxel have been limited by unacceptable hematologic toxicity. Rosenthal et al. postulated that the dose-response relationship for paclitaxel may depend more on exposure duration than on peak concentration.²⁴ They conducted a phase I trial combining continuous-infusion paclitaxel (incremental dose escalation from 0.5 mg/m²/d to 17.5 mg/m²/d; 24 h a day; 7 d a week; for 7 weeks) with concurrent radiation therapy (70 Gy/7 weeks) in stage IVA/B squamous cell carcinoma of the head and neck. In terms of toxicity, grade 3 skin and mucosal reactions occurred at 10.5 mg/m²/d, but did not interrupt treatment in 5 of 6 patients. At 17 mg/m²/d, skin toxicity required a 2-week treatment break for all three patients. All grade 3 mucositis and skin toxicity resolved within 8 weeks of treatment discontinuation. There were no significant allergic reactions to the continuous infusion despite

only a single pretreatment administration of dexamethasone. Furthermore, only 2 of the 25 patients developed reversible grade 1 peripheral neuropathies. Paclitaxel serum concentrations were measured in 9 of the 25 patients and were undetectable at infusion doses ≤ 4.0 mg/m²/d. Interpatient variability with respect to steady-state paclitaxel concentrations was significant at each infusion rate. Interestingly, the plasma concentration dose level ≥ 6.5 mg/m²/d was maintained in the *in vitro* range shown to produce radiosensitization. In terms of efficacy, complete tumor clearance was observed in 14 of 19 assessable patients receiving full dose radiation therapy. Three additional partial response rates were noted for an overall response rate of 71%. Surprisingly, the response rate in patients receiving 4.0 mg/m²/d or less was similar to the higher doses despite being undetectable in the blood. This latter observation was related to the detection limits of the HPLC assay used for paclitaxel quantitation. Durable locoregional control was achieved in 9 (47%) of 19 patients treated to 70 Gy. The maximum tolerated dose for these studies was determined to be 10 mg/m²/d. In previous studies, tumor biopsies from treated patients supported the presence of paclitaxel-induced mitotic arrest. Furthermore, a slowly progressive normocytic anemia developed in conjunction with a hyporerythropoietin state in the absence of renal dysfunction. Thus, prolonged biologic activity of paclitaxel was supported by the presence of anemia and the suggestion of altered cell-cycle distributions.

Zimmerman et al. examined the efficacy of 120-h continuous infusion of paclitaxel in patients with stage IIIB and IV breast cancer who recurred after high-dose chemotherapy.²⁵ Thirty-one women underwent harvest and cryopreservation of bone marrow and/or peripheral blood progenitor cells. Patients then received high dose cyclophosphamide (2.5 g/m²) and thiotepa (225 mg/m²) followed by paclitaxel. The authors observed an overall response rate of 24% despite the high incidence of bone metastases. Skubitz performed a phase I trial where paclitaxel (17.1 mg/m²/d) was administered to 31 patients for 7 d by continuous infusion.²⁶ The study was conducted on an ambulatory basis every 28 d and was generally well tolerated. In a cohort of 15 patients with soft tissue sarcomas refractory to doxorubicin, dacarbazine, ifosfamide, and etoposide, one partial response and five with stable disease were observed. While further clinical data are needed, the aforementioned clinical trials highlight the efficacy and tolerability of dose-dense therapy, particularly in the setting of prolonged paclitaxel infusion. It also emphasizes the clinical utility of extending the drug exposure duration, presumably above a critical level, using either lower dosing over shorter intervals or by achieving steady-state concentrations in the blood.

15.3.3 Clinical Model for Dose Determination and Schedule

Phase I clinical trials are typically small, uncontrolled, and non-hypothesis-driven studies designed to determine a maximum tolerated dose (MTD) for

an experimental drug. Under this paradigm, the dose is related to toxicity in which exceeding the MTD would put the patient at unacceptable risk.²⁷ The subsequent dose determined for phase II studies is conventionally based on a tolerable level of toxicity for all patients. Thus, the end point of dose determination and scheduling is based on acceptable toxicity rather than identifying a dose and schedule for optimal antitumor effect. This problem is compounded by the inherent inaccuracy of using body surface area (BSA) for dose calculations.^{12,28,29} As Gurney points out, BSA cannot account for marked inter-patient variations in drug elimination that is known to exist.¹² A number of specific reasons for BSA-independent drug clearance include genetic variability in the activity of metabolizing enzymes and transporters, pharmacokinetic interactions due to concomitant medications, and impaired organ function due to disease, comorbidities, or prior therapy. This can lead to a nearly 4- to 10-fold variation in cytotoxic drug clearance.²⁸ For example, Gaemelin et al. defined the optimum fluorouracil (5FU) plasma concentration with a regimen of 1300 mg/m² infused over 8 h every week.³⁰ In a group of 81 patients treated with a dose calculated from BSA, 80% were found to have an ineffective 5FU plasma concentration after the first dose. The obvious consequence of this methodology is underdosing which may reduce efficacy. Gurney estimates a 20% relative reduction in survival due to BSA-related underdosing in the adjuvant treatment of node-positive breast cancer.¹²

Despite the clinical and theoretical arguments favoring dose-densification, there still exists an inability to normalize dosing regimens to account for interpatient variability. A model pharmacologic solution has been developed for carboplatin where dosing is individualized using several formulas that predict carboplatin clearance.³¹ This approach is supported by the clinical relationship between toxicity and efficacy as a function of the area under the concentration-time curve (AUC).³² Calvert and colleagues showed that it was possible to predict clearance by measuring the glomerular filtration rate (GFR) using the [51Cr]-ethylenediamine tetraacetic acid (EDTA) method according to the equation below³³

$$Cl \text{ (ml/min)} = GFR \text{ (ml/min)} + 25$$

where the carboplatin dose

$$\text{Carboplatin Dose (mg)} = AUC (CrCl + 25)$$

is calculated based on a target AUC and by substituting the creatinine clearance (CrCl) for GFR.³⁴ However, the CrCl obtained by the Cockcroft formula has led to an underestimation of the GFR and then of carboplatin clearance in patients with good renal function.³⁵ As a result, Chatelut et al. developed a more accurate equation based on four patient characteristics (i.e., body weight, age, sex, and serum creatinine level) to predict carboplatin clearance (CbCl) and dose as follows:³¹

$$\text{CbCl (Male)} = (0.134 \times \text{weight}) + (218 \times \text{weight} \times (1 - 0.00457 \times \text{age}) / \text{CrS})$$

$$\text{CbCl (Female)} = (0.134 \times \text{weight}) + 0.686 \times (218 \times \text{weight} \times (1 - 0.00457 \times \text{age}) / \text{CrS})$$

$$\text{Carboplatin dosage (mg)} = \text{AUC (mg/ml} \times \text{min)} \times \text{CbCl (ml/min)}$$

where weight is in kilograms and Crs represents the serum creatinine. In the case of obese patients, if the total body weight (TBW)/ideal body weight (IBW) is ≥ 1.2 , weight is corrected by the mean between TBW and IBW. Van Warmerdam et al. found that this equation more accurately estimates the CbCl.³⁵ The experience with carboplatin represents a reproducible model for individualizing drug dose by accounting for BSA-independent variations with respect to genetic variations in the activity of metabolizing enzymes and transporters, drug interactions due to concomitant medication, and impaired organ function due to disease, comorbidities, or prior therapy. Many propose that this pharmacologic approach should be the “gold standard” for all cancer chemotherapy. Therefore, a typical sequence would involve identifying a target AUC with subsequent adaptive dose adjustments based on measured serum concentrations and population pharmacokinetics.³⁶

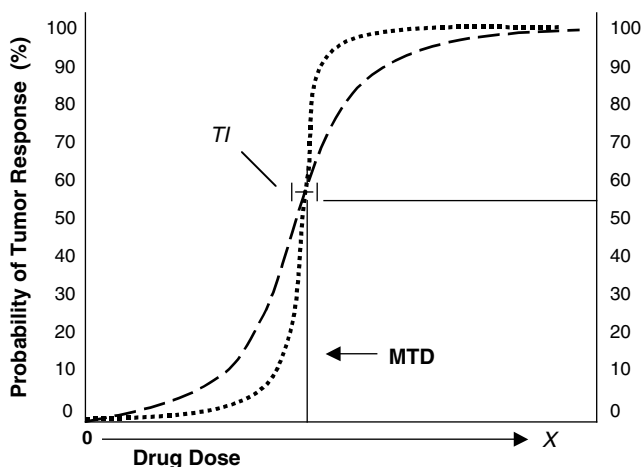


FIGURE 15.4

Theoretical probability of tumor and toxic responses as a function of drug dose. The long-dashed line represents the probability of tumor response and the short-dashed line represents the probability of a toxic response as a function of drug dose. For conventional chemotherapy, it is assumed that the therapeutic index (TI) is narrow and lies in proximity to the maximum tolerated dose (MTD) as defined by a tolerable level of toxicity.

15.3.4 Defining a Therapeutic Index for Chemotherapy Agents

The phase I trial is designed to determine a maximum tolerated dose and schedule for an agent based on acceptable toxicity profiles. Subsequent phase II and III trials use this regimen, with slight adjustments, to provide proof of clinical benefit. To date, the clinical experience with dose-densification, modest survival outcomes, and model for clinical trials argues that maximum tolerated dose and optimal tumor response are not direct correlates. While toxicity-response relationships are becoming better understood, it is the dose-toxicity relationship that defines both dose-response and scheduling. As a result, subsequent phase II and III clinical trials use the recommended dose and schedule to assess efficacy. Furthermore, the development of effective treatments is made more complicated by an incomplete knowledge of pharmacodynamic effects due to intertumor variability and prior chemotherapy treatments. Thus, the therapeutic index (TI) of a chemotherapy agent is indirectly estimated by the dose-toxicity relationship as opposed to defining a true dose-response profile. The underlying assumption is that the TI is narrow and lies in close proximity to the MTD (Figure 15.4). In retrospect, one may attribute some of the modest gains in cancer chemotherapy to a combination of antiquated methods of dose calculation and a clinical methodology that bases the optimal regimen on a maximum tolerated dose. Can a true therapeutic index be defined which is less dependent on toxicity and more predictive of response?

As discussed above, an alternative approach could use therapeutic drug monitoring to develop a dose-response relationship as defined by a target AUC and/or a cumulative AUC (cAUC; summation of individual AUCs based on repetitive dosing). This model would not only favor the clinical trends toward dose-densification but also provide a rational approach to dose individualization as described above. This would identify a true therapeutic index with acceptable toxicity profiles. In Figure 15.5, the TI is defined by the minimum effective regimen (MER) and maximum tolerated regimen (MTR) as determined by the cAUC. The MER is arbitrarily set at 20% based on the work by Gehan in the design of phase I clinical trials.³⁷ In this work a sample size of 14 was required to obtain a 95% probability of having one or more successes if a drug is at least 20% effective. Thus, the probability of tumor response may be evaluated as a function of drug exposure duration which could be normalized to account for interpatient variability in terms of drug clearance. Unfortunately, this paradigm may not be practical in the initial clinical phases of new chemotherapeutics but may be addressed once the agent has been shown to have efficacy after maturation of phase II or III studies.

15.3.5 Rationale for Sustained Drug Delivery

The assumption of dose-densification is that shorter treatment intervals or sustained drug exposure decreases tumor regrowth. However, this may be

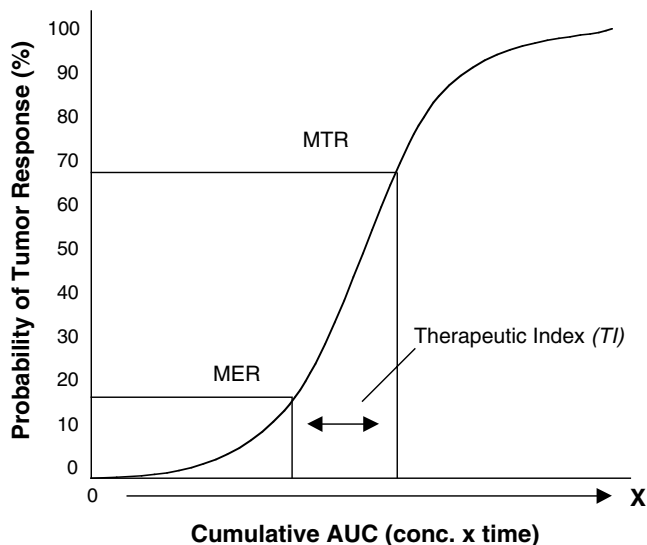


FIGURE 15.5

Theoretical probability of tumor response vs. the cumulative area under the concentration-vs.-time curve (*cAUC*). The therapeutic index (*TI*) is defined by the minimum effective regimen (*MER*) and maximum tolerated regimen (*MTR*) as determined by the *cAUC*. The *MER* is defined by the *cAUC* where a 95% probability exists of having one or more successes if the drug is at least 20% effective.

simplified by prolonging the drug exposure duration (*DED*) above a critical *MET* as compared to that achieved by conventional schedules. In this context, the theoretical treatment of tumor growth and the observed clinical data are synchronized by a common denominator, the *DED*. Examining the *DED* through dose-densified regimens can be accomplished by either shorter treatment intervals and lower doses vs. prolonged infusion. However, it could be envisioned that shorter and shorter dosing intervals and variable doses could lead to a plethora of permutations with either considerable impairment of a patient's quality of life or increased toxicity without significant benefit. The latter approach, as observed with paclitaxel, establishes a steady-state drug concentration over prolonged periods such that

$$\text{AUC} = k_0 T / \text{Cl}_s$$

where *Cl_s* represents the serum drug clearance (ml/min), *k₀* is the infusion rate constant, and *T* is the drug exposure duration.³⁸ In this context, prolonging the *DED* at a particular *C_{ss}* may identify a minimum effective *C_{ss}* such that tumor response and toxicity may be linked to *DED* (Figure 15.6). Thus, a true *TI* could be determined with acceptable toxicity profiles. For standard infusions, serum drug concentrations are within 10% of steady state after four biological half-lives of the drug.³⁸ The *C_{ss}* is proportional to the infusion rate and inversely to systemic clearance.

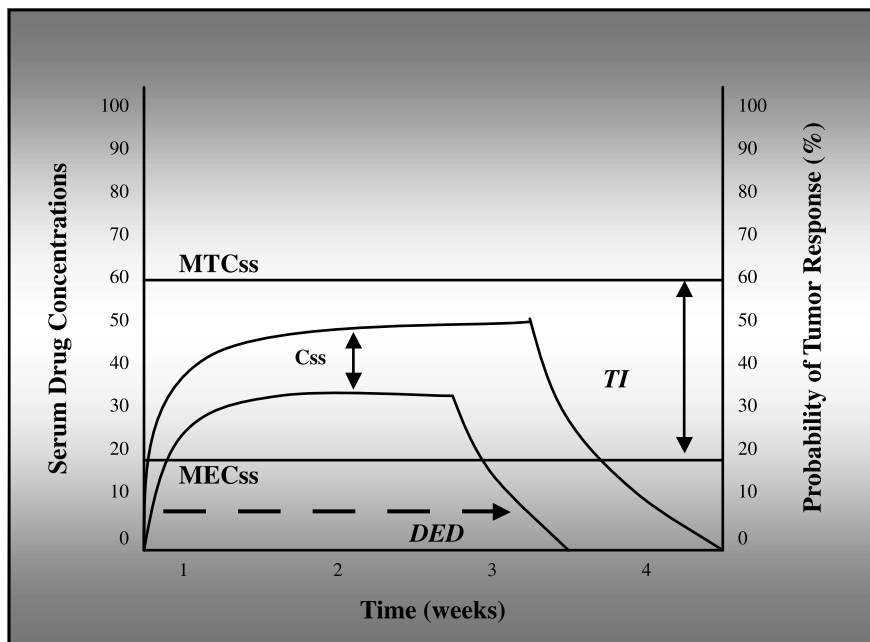


FIGURE 15.6

Ideal probability of tumor response as a function of steady state drug concentrations (C_{ss}) over time. The therapeutic index is defined by the minimum effective steady state concentration (MEC_{ss}) and the maximum tolerated steady state drug concentration (MTC_{ss}). The theoretical therapeutic index (TI) lies between the MEC_{ss} and the MTC_{ss} . The probability of tumor response can be evaluated as a function of C_{ss} and drug exposure duration (DED), which can be defined by the area under the concentration time curve (AUC).

$$C_{ss} = k_0 / Cl_s$$

Based on Table 15.2 and the kinetics of continuous infusions, the time to reach steady state is short ranging from 2 to 48 h for most agents. However, if one pursues dose-densification by reducing the dose interval, achieving steady-state using an agent with a short half-life would require unrealistically short dosing intervals. A similar impracticality may arise using continuous intravenous infusions even though proof of principle is supported using paclitaxel.²⁴ To bridge this clinical scenario, new technologies in absorbable sustained release systems may be well suited to explore these issues. In this respect, correlating tumor response with DED and C_{ss} would be simplified and may considerably improve efficacy.

15.3.6 Biodegradable or Absorbable Polymers for Drug Delivery

The term “biomaterials” has been broadly used to describe materials derived from either synthetic or biological sources that are used for clinical applica-

TABLE 15.2

Standard Chemotherapy Agents and Associated Plasma Half-Lives

Agent	Trade Name	Plasma Half-Life (h)	Agent	Trade Name	Plasma Half-Life (h)
altretamine	Hexalen	4.7–10.2	fluorouracil, 5-FU	Adrucil	0.1–0.33
bleomycin	Blenoxane	2–5	gemcitabine	Gemzar	0.7–1.6
capecitabine	Xeloda	0.7–10.6	ifosfamide	IFEX	15.0
carboplatin	Paraplatin	2.6–5.9	irinotecan	Camptosar	11.7
cisplatin	Platinol	0.4–0.8	methotrexate	Methotrexate	8–5
cyclophosphamide	Cytosan	3–12	mitomycin C	Mitozytrex	0.28
dacarbazine	DTIC-Dome	5	paclitaxel	Taxol	3.0–52.7
docetaxel	Taxotere	11.4–18.5	topotecan	Hycamtin	2–3
doxorubicin	Adriamycin	20–48	vinblastine	Velban	24.0
epirubicin	Ellence	11–25	vincristine	Oncovin	1.0
etoposide, VP-16	Vepesid	3–11	vinorelbine	Navelbine	27.7–43.6

tions. Synthetic polymers based on nylon were first studied as sutures beginning in the 1940s. Since that time, a number of materials have found important clinical applications as prosthetic devices, artificial lenses, vascular grafts, stents, and catheters. However, the development of absorbable or biodegradable sutures in the late 1950s offered additional advantages over their nondegradable counterparts. While its use in surgery has become commonplace, the application of this technology for delivery of novel therapeutics offers an array of alternatives to conventional drug administration. Absorbable delivery systems are particularly attractive since their degradation properties can be manipulated to control the rate of drug release or maintain a desired mechanical integrity, depending on the therapeutic goal.^{39–41} They can be designed to release therapeutics over extended periods of time or to act as platforms for which cell interactions may take place. One of their biggest advantages is that they may be formulated in various shapes and sizes ranging from monolithic implants to injectable nanoparticles.

Biodegradation is defined as the conversion of materials into less complex intermediates or end products by solubilization, simple hydrolysis, or enzyme-catalyzed hydrolysis. The biodegradation of polymers occurs in three stages, beginning with hydration, loss of strength and mass integrity, followed by mass loss.^{42,43} A number of polymers undergo extensive chain scission to form small soluble oligomers or monomers which are subsequently eliminated from the body. An overwhelming number of biodegradable polymers are based on polyesters. They include poly(glycolic acid) (PG), poly(lactic acid) (PLA), poly(ϵ -caprolactone)(PCL), poly(*b*-hydroxybutyric acid), poly(*b*-hydroxyvaleric acid), polydioxanone, and poly-orthoesters.⁴² PG was one of the first synthetic polymers to be used for the preparation of bioabsorbable sutures. Hydrolysis occurs by a bulk degradation process. As water penetrates the matrix, polymer chain relaxation leads to hydrolysis of accessible ester groups. Thus, the kinetics of hydrolysis will directly depend on the hydrophilicity of the polymer and the surface area for water penet-

tration. Semicrystalline polymers such as PLA and PCL degrade more slowly. Degradation first occurs in the amorphous regions, followed by the crystalline domains. The latter functions to restrict polymer relaxation and, hence, the number of suitable conformations for ester hydrolysis. Therefore, the degree of polymer crystallinity is inversely related to the rate of degradation. While homopolymers of PLA and PCL are commonly used clinically, their mechanical and degradable properties are diversified by copolymerization with various monomers. Thus, differing compositions display altered degradation kinetics based on a hydrophobicity of the monomeric constituents, polymer crystallinity, and bulk surface area. In the body, however, it has yet to be verified whether enzyme-catalyzed processes contribute to polymer degradation. Under certain condition, it is likely that the mere presence of enzymes may influence the rate of chain dissociation.⁴³ This may be related to nonspecific oxidative degradation and/or base-catalyzed chemical hydrolysis. Such nonspecific effects could have been, in part, pertinent to the results obtained by Williams and co-workers.⁴⁴⁻⁴⁶ Regardless of the mode of degradation, biodegradable polymers can be tailored to address a variety of therapeutic objectives. This has been most evident in the area of surgery where the choice of suture takes into consideration the strength of tissue reapproximation, the time required for wound healing, and any clinical features of the patient that may compromise healing. In short, with all the possible permutations, the choice of absorbable material for sustained drug delivery will depend on the route of administration, the physicochemical properties of the therapeutic agents, and the duration of response. However, the advantage for cancer chemotherapy lies in the diversity of materials already generated from years of research in the suture industry and more recently from the area of controlled drug release.

15.3.7 Absorbable Delivery Systems to Manipulate Drug Exposure Duration (DED) "Pegylated" Systems

The FDA had approved polyethylene glycol (PEG) as a vehicle or base in foods, cosmetics and pharmaceuticals, including injectable, topical, rectal, and nasal formulations. PEG shows little toxicity, lacks immunogenicity, and is eliminated by renal excretion (PEG < 30 kDa) or hepatic secretion (PEG > 20 kDa).^{47,48} PEG can be activated through a variety of chemical modifications suitable for coupling to a given target molecule via stable ester linkages. PEG derivatives can also include degradable linkages to release drugs at targeted sites. These hetero-bifunctional PEGs can use para- or ortho-substituted disulfides of benzyl urethane that release the drug under mild reducing conditions.⁴⁹ Pegylation may be an effective method of modifying the pharmacokinetic/pharmacodynamic properties of protein drugs. Pegylation reduces renal clearance and, for some agents, results in a more sustained absorption after subcutaneous administration as well as restricted distribution. These pharmacokinetic changes may result in more constant and sustained plasma concentrations, which can improve clinical effectiveness when

TABLE 15.3

Pharmacokinetic Influence of Pegylated Systems in Terms of Elimination Half-Life

Parent Drug and Pegylated Form	Elimination Half-Life (h)
Interferon- α 2a	3–8
Pegylated — Interferon- α 2a	65
Interleukin-6	0.04
Pegylated — Interleukin-6	3.4
Tumor Necrosis Factor (TNF)	0.05
Pegylated — TNF	2.27
Doxorubicin	20–48
(PEG)-liposomal doxorubicin	45–55
Daunorubicin	0.75–3
(PEG)-liposomal daunorubicin	4

Source: Adapted from Harris, J. M., Martin, N. E. and Modi, M., Pegylation: A novel process for modifying pharmacokinetics, *Clin. Pharmacokinet.*, 40, 539, 2001.

the desired effects are concentration-dependent. Aside from alterations in renal and hepatic elimination, pegylated compounds facilitate solubilization of hydrophobic agents, stabilize the conformation of protein drugs, and minimize enzyme-catalyzed degradation in the blood. To date, the focus of research has been on protein drugs with dramatic changes in kinetics (Table 15.3). The use of pegylated liposomal carriers is one approach for enhancing the delivery of parenteral chemotherapy agents. Polyethylene glycol (PEG)-liposomal doxorubicin (Doxil, ALZA, Palo Alto, CA) is a formulation of the anthracycline doxorubicin in which the drug is encapsulated in PEG-coated liposomes. This alters the pharmacokinetic properties of doxorubicin, prolonging circulation time. Overall response rates of patients with ovarian cancer refractory to platinum- and paclitaxel-based chemotherapy have ranged from 18.3 to 27.6% in noncomparative clinical trials.^{50,51} PEG-liposomal doxorubicin also has antitumor activity in patients with metastatic breast cancer pretreated with other chemotherapeutic agents. Phase III studies with doxorubicin in breast cancer are being carried out, but accrual has not been completed. Activity against breast cancer has been noted from the initial phase I and II trials.^{52–54} Overall response rates were 31% and 32%, respectively, in patients receiving prior chemotherapy. Other pegylated agents that are in clinical trials include PEG-Taxol and PEG-camptothecins.^{55–57}

15.3.8 Site-Specific (Intracranial)

For more than 20 years the mainstay of single-agent chemotherapy for malignant glioma of the brain was intravenous 1,3-bis (2-chloroethyl)-1-

nitrosourea (BCNU, also called carmustine).^{58,59} Unfortunately, the systemic use of BCNU is associated with considerable toxicity, including pulmonary fibrosis, myelosuppression, and hepatic dysfunction. Furthermore, BCNU has a considerably short half-life both in the plasma and brain. Direct injection of BCNU into brain tumors was tried without success as early as 1975.⁶⁰ In an effort to increase the level of active drug at the target site while limiting toxicity, absorbable implants or wafers containing BCNU were prepared from either EVAc (ethylene-vinyl acetate copolymer) or the polyanhydride, PCPP:SA [Poly(carboxyphenoxy-propane/sebacic acid)], commercially known as the GLIADEL[®] Wafer.⁶¹⁻⁶³ The rationale for this approach was based on the finding that 90% of resected malignant gliomas recurred within a 2 cm margin from the original tumor. Brem et al. conducted a Phase I-II study in 21 patients with recurrent malignant glioma.⁶² Up to eight wafers were placed in the resection cavity intraoperatively upon completion of tumor debulking. Three doses of BCNU wafers were studied (1.93%, 3.85%, and 6.37%). Release profiles were expected for up to 3 weeks based on *in vitro* data. There were no adverse reactions to the BCNU wafer and the treatment was well tolerated. The average survival period after reoperation was 65 weeks for the first dose group, 64 weeks for the second dose group, and 32 weeks for the highest dose group. The overall mean survival time was 48 weeks from reoperation and 94 weeks from the original operation. The overall median survival times were 46 weeks postimplant and 87 weeks from initial surgery. Eighteen (86%) of 21 patients lived more than 1 year from the time of their initial diagnosis and 8 (38%) of 21 patients lived more than 1 year after intracranial implantation of the polymer. The results compared favorably with historical controls. Brem et al. subsequently conducted a randomized, placebo-controlled, prospective study to evaluate the effectiveness of the BCNU wafers.⁶⁴ In 27 medical centers, 222 patients with recurrent malignant brain tumors requiring reoperation were randomly assigned to receive surgically implanted absorbable wafers with or without 3.85% BCNU. Median survival of the 110 patients who received BCNU implant was 31 weeks compared with 23 weeks for the 112 patients who received only the placebo. Among patients with glioblastoma, 6-month survival in those treated with the BCNU discs was 50% greater than in those treated with placebo (mortality = 32 of 72 [44%] vs. 47 of 73 [64%], $p = 0.02$).

15.3.9 Site-Specific (Intratumoral)

In theory, the advantage of site-specific drug delivery is to produce high local drug concentrations at the tumor site with limited systemic exposure. It has been proposed in the setting of neoadjuvant treatment to improve tumor resectability and as adjuvant therapy after surgery. Over the last 30 years, however, a number of novel targeting strategies have been evaluated in preclinical models with very limited clinical success. The major obstacle lies with tumor heterogeneity that is difficult to simulate in the laboratory

setting with immortalized cell lines. Tumor heterogeneity takes on different interpretations and evolves as a function of its intrinsic carcinogenesis, macro- and micro-environmental changes due to surgery or blood supply, and exposure to prior cytotoxic agents. While somewhat oversimplified, these factors function in a continuum, limiting the isolation of meaningful tumor-specific cell markers or conditions that can be targeted without undue toxicity to normal tissues. With respect to solid tumors, the anatomical site of implantation and size provides a perfusion-limited constraint which further impairs potential efficacy. One way to minimize some of these clinical hurdles is through intratumoral administration of chemotherapy using drug delivery systems. An exceptional review has been published by Goldberg et al. which provides a detailed account of the history and recent growing interest in this field.⁶⁵

Cisplatin/epinephrine/bovine collagen (CDDP-EPI gel) (IntraDose™ Injectible Gel, Matrix Pharmaceutical, Inc., Fremont, CA) is a novel technology designed for the intratumoral administration of cisplatin. The goal is to achieve a high intratumor cisplatin concentration for extended periods while minimizing its toxicity to normal tissues. The bovine collagen gel provides a stable vehicle for sustained cisplatin release, while tumor localization is promoted by co-release of epinephrine to cause proximal vasoconstriction limiting systemic uptake. Mok et al. recently examined the pharmacokinetics of direct intratumoral injection of CDDP-EPI gel in patients with unresectable hepatocellular carcinoma (HCC) and cirrhosis.⁶⁶ Patients who received < 15 mg of CDDP-EPI gel were classified as the low-dose group whereas those patients who received > 15 mg were classified as the high-dose group. A control group of similar patients was treated with standard intravenous cisplatin (75 mg/m², as a 1-h IV infusion). The time to attain maximum

TABLE 15.4

Pharmacokinetic Parameters after the Intratumoral Injection of Cisplatin/Epinephrine Gel and Intravenous Infusion of Cisplatin

Parameter	Intravenous Cisplatin	Intratumor Cisplatin Gel (Low Dose)	Intratumor Cisplatin Gel (High Dose)
Dose (mg)	77.50–87.50	6.67–14.67	18.67–26.67
C _{max} (μg/mL)	3.13 ± 0.25	0.34 ± 0.09	0.46 ± 0.06
t _{max} (h)	1.25 ± 0.14	2.32 ± 1.96	12.95 ± 6.64
AUC (0–last) (μg/mL/h)	247.62 ± 26.07	21.89 ± 10.06	48.87 ± 9.70
AUC (0–infinity)	338.69 ± 37.0	37.94 ± 11.67	150.01 ± 40.16
MRT (0–last)	138.33 ± 8.51	61.91 ± 18.21	90.70 ± 20.23
MRT (0–infinity)	281.26 ± 13.52	186.08 ± 22.05	428.13 ± 119.87
Initial t _{1/2}	1.36 ± 0.40	9.19 ± 6.95	25.51 ± 9.78
Terminal t _{1/2}	193.87 ± 14.00	132.58 ± 16.57	297.83 ± 82.58
Bioavailability (relative)	1	0.92	1.65

Note: AUC: area under the curve; MRT: mean residence time; t_{1/2}: terminal half-life. The values are presented as the mean ± the standard error.

concentration after intratumor injection was dose-dependent and ranged from 2 to 13 h (Table 15.4). However, the maximum serum concentrations were an order of magnitude lower compared with the I.V. dose. The concentration-time curve was found to be biphasic in nature with increasing initial and terminal half-lives as a function of dose. This corresponded to a dose-dependent increase in the area under the curve (AUC) and mean resident time (MRT) (Table 15.4). Interestingly, the high-dose intratumor delivery system displayed a significant advantage in terms of relative bioavailability.

Leung et al. recently published a phase II study examining the efficacy and safety of the CDDP-EPI gel in patients with localized unresectable hepatocellular carcinoma.⁶⁷ Patients received up to 10 ml CDDP-EPI gel (1 mL contains 4 mg of CDDP and 0.1 mg of EPI) which was administered percutaneously via ultrasound or CT-guidance. A weekly treatment schedule was intended for a total of four treatments over a 6-week period. A second course (four treatments) was also made available to some patients at the discretion of the physician. Of 58 patients, 51 were assessable for efficacy and safety. The median number of treatments was four with an objective response rate of 53% (27/51). This included 16 complete and 11 partial responses. Median survival was 27 months (range, 18.4 to 35.7 months) with 1-, 2-, and 3-year survival rates of 79%, 56%, and 14% respectively. Of the 27 responders, however, 14 (52%) subsequently developed progressive disease due to tumor implantation at untreated liver sites. This occurred in 13 of the 14 patients who progressed. This observation would suggest that a steep concentration gradient exists between the site of injection and surrounding parenchyma which is driven by hepatic perfusion. Thus, the extent of drug penetration is inversely proportional to perfusion. Similar observations were made in an intracranial animal model using the BCNU wafer.⁶⁸ In this case, drug penetration was dependent on the rates of drug diffusion and convection vs. the rate of drug elimination as a function of hydrolytic degradation and transcapillary clearance. However, this model is more complicated since the diffusion coefficient of the drug is not constant and will change over the release duration and with subsequent doses. Thus, the rate of diffusion and elimination will be time-dependent and influenced by changes in tumor porosity and vascularity as well.

Recently, two identical phase III trials were designed to evaluate the role of intratumoral CDDP-EPI gel in the palliative management of advanced squamous cell carcinoma of the head and neck.^{69,70} A total of 179 heavily pretreated patients with recurrent or refractory disease were enrolled in a double-blind, placebo-controlled trial. Objective responses were noted in 35 (29%) of 119 evaluable patients. This included 23 (19%) complete responses as compared to 1 (2%) of 59 patients who received the placebo gel ($P < 0.001$). In this trial, crossover from blinded to open-label phase was permitted for patients with disease progression. The response rate for this group was 27% (11/41). Patient benefit was also evaluated based on independent assessments by patients and physicians in terms of progress toward prospectively selected treatment goals. Tumor response and patient benefit were significantly cor-

related between responders (47%) and nonresponders (15%). The authors concluded that the CDDP-EPI gel provides a new therapeutic option for these patients by reducing tumor burden and ameliorating tumor symptoms.

Intratumoral CDDP-EPI has also been studied for the treatment of patients with cutaneous and soft tissue metastases of malignant melanoma.⁷¹ A total of 28 patients with refractory or recurrent melanoma were enrolled in this open-label, multicenter study. Of these, 25 patients with 244 lesions were evaluable for efficacy. Lesions were injected with 0.5 ml (2 mg cisplatin + 0.05 mg epinephrine) of gel/cm³ of tumor. Patients received up to six weekly treatments within an 8-week period. The objective response rate for all the tumors treated was 53% (114 complete responses and 16 partial responses). The response rate among target tumors, designated by size, aggressive features, or symptoms, was 44%. The median response duration for all tumors was 347 d (range, 30 to 783 d) and median number of treatments per tumor was five (range, 1 to 12). Systemic toxicity was negligible while local adverse reactions (i.e., erythema, necrosis, or pain) were manageable. The investigators found this treatment overall to be well tolerated, easy to administer, and effective in treating metastatic melanoma confined to the skin or soft tissues.

In short, the use of intratumoral drug delivery appears quite promising in the palliative management of unresectable solid tumors. The proof of principal for this approach is the objective responses seen in three entirely different epithelial cancers with reduced systemic toxicity. One limitation is the restricted regional control of disease which is problematic in cases of multiple lesions due to metastasis. Vogl et al. evaluated intratumoral of CDDP-EPI gel in patients with hepatic metastases from colorectal cancer compared with unresectable primary hepatocellular carcinoma.⁷² A total of 8 patients with 17 colorectal liver metastases (mean of 5.1 injections) and 9 patients with 13 hepatocellular carcinoma nodules (mean of 3.1 treatments) were treated by CT-guided biopsies. Tumor volume was significantly decreased in both treatment groups. However, in the 6-month follow-up period, local control was achieved in only 38% of the metastatic disease group and 71% of the primary hepatocellular cancer group.

15.4 Conclusion and Perspective on the Future

Over the last 40 years of cancer treatment, the modest gains in survival observed may be attributed to a combination of better screening practices and, to a lesser degree, cytotoxic chemotherapy. To date, however, the overwhelming consensus favors further drug development despite the plethora of combination, sequential, adjuvant, neo-adjuvant, or consolidated treatment strategies. Interestingly, the surprising efficacy of recent clinical trials exploiting dose-densification suggests that it may not be attributable to the agents but more to the methodology of study and routes of administration.

These shifts in treatment schedules and dosing suggest that we have yet to determine a true therapeutic index for chemotherapy. Thus, it may be postulated that a minimum effective drug concentration over defined durations must be achieved to optimize tumor response with acceptable toxicity. This concept would also be supported by the mathematical modeling data and observed *in vitro* tumor growth. However, from a clinical standpoint, it would require aggressive therapeutic drug monitoring to correlate tumor response with serum drug levels and drug exposure duration. Using conventional routes of administration, numerous clinical trials could be generated, the prospect of which could significantly impair a patient's quality of life, despite optimizing tumor response. The maturation of clinical data using absorbable delivery systems supports an alternative approach to defining a therapeutic index. In this regard, defined drug levels over predicted durations could be obtained after a single administration. The route of administration could be intravenous, subcutaneous, or even organ-specific. While the intent of this review was to illustrate the clinical data, there is a significant amount of preclinical data in animal models supporting this proof of principle. In summary, utilizing absorbable delivery systems to prolong drug exposure duration may offer surprising clinical advantages that could not be obtained using conventional modes of administration.

References

1. Andersen, L. D., Remington, P., Trentham-Dietza, A. and Reeves, M., Assessing a decade of progress in cancer control, *The Oncologist*, 7(3), 200, 2002.
2. Ries, L. A. G., Wingo, P. A., Miller, D. S., Howe, H. L., Weir, H. K., Rosenberg, H. M., Vernon, S. W., Cronin, K. and Edwards, B. K., The annual report to the nation on the status of cancer, 1973–1997, with a special section on colorectal cancer, *Cancer*, 88(10), 2398, 2000.
3. Bailar, J. C. and Gornik, H. L., Cancer undefeated, *N. Engl. J. Med.*, 336, 1569, 1997.
4. Bajzer, Z., Marusic, M. and Vuk-Pavlovic, S., Conceptual frameworks for mathematical modeling of tumor growth dynamics, *Math. Comput. Modelling*, 23(6), 31, 1996.
5. Von Bertalanffy, L., Quantitative laws in metabolism and growth, *Q. Rev. Biol.*, 32, 217, 1957.
6. Kopelman, R., Fractal reactions kinetics, *Science*, 241, 1620, 1988.
7. Marusic, M., Bajzer, Z., Freyer, J. P. and Vuk-Pavlovic, S., Analysis of growth of multicellular tumor spheroids by mathematical models, *Cell Prolif.*, 27, 73, 1994.
8. Marusic, M. and Bajzer, Z., Generalized two-parameter equation of growth, *J. Math. Anal. Appl.*, 179, 446, 1993.
9. Sherratt, J. A. and Chaplain, M. A. J., A new mathematical model for avascular tumor growth, *J. Math. Biol.*, 43, 291, 2001.
10. Byrne, H. M. and Chaplain, M. A. J., Growth of necrotic tumors in the presence and absence of inhibitors, *Math. Biosci.*, 135, 187, 1996.
11. Skipper, H. E., Kinetics of mammary tumor cell growth and implications for therapy, *Cancer*, 28, 1479, 1971.

12. Gurney, H., How to calculate the dose of chemotherapy, *Br. J. Cancer*, 22; 86(8), 1297, 2002.
13. Norton, L., Adjuvant breast cancer therapy: Current status and future strategies — growth kinetics and the improved drug therapy of breast cancer, *Semin. Oncol.*, 26(3), 1, 1999.
14. Norton, L., Theoretical Concepts and the emerging role of taxanes in adjuvant therapy, *The Oncologist*, 6(3), 30, 2001.
15. Citron, M. L., Berry, D. A., Cirincione, C., Hudis, C., Winer, E. P., Gradishar, W. J., Davidson, N. E., Martino, S., Livingston, R., Ingle, J. N., Perez, E. A., Carpenter, J., Hurd, D., Holland, J. F., Smith, B. L., Sartor, C. I., Leung, E. H., Abrams, J., Schilsky, R. L., Muss, H. B. and Norton, L., Randomized trial of dose-dense versus conventionally scheduled and sequential versus concurrent combination chemotherapy as postoperative adjuvant treatment of node-positive primary breast cancer: First report of Intergroup Trial C9741/Cancer and Leukemia Group B Trial 9741, *J. Clin. Oncol.*, 21(8), 1431, 2003.
16. Fornier, M. N., Seidman, A. D., Theodoulou, M., Moynahan, M. E., Currie, V., Moasser, M., Sklarin, N., Gilewski, T., D'Andrea, G., Salvaggio, R., Panageas, K. S., Norton, L. and Hudis, C., Doxorubicin followed by sequential paclitaxel and cyclophosphamide versus concurrent paclitaxel and cyclophosphamide: 5-year results of a phase II randomized trial of adjuvant dose-dense chemotherapy for women with node-positive breast carcinoma, *Clin. Cancer Res.*, 2001(12), 3934, 2001.
17. Klaassen, U., Wilke, H., Strumberg, D., Eberhardt, W., Korn, M. and Seeber, S., Phase I study with a weekly 1 h infusion of paclitaxel in heavily pretreated patients with metastatic breast and ovarian cancer, *Eur. J. Cancer*, 32A(3), 547, 1996.
18. Alvarez, A., Mikciewicz, E., Brosio, C., Giglio, R., Cinat, G. and Suarez, A., Weekly taxol (T) in patients who relapsed or remained stable with taxol on a 21 day schedule, *ASCO*, 15, 383, 1996.
19. Perez, E. A., Vogel, C. L., Irwin, D. H., Kirshner, J. J. and Patel, R., Multicenter phase II trial of weekly paclitaxel in women with metastatic breast cancer, *J. Clin. Oncol.*, 15; 19(22), 4216, 2001.
20. Kaern, J., Tropé, C., Baekelandt, M., Kristensen, G. B. and Gundersen, G., A study of weekly Taxol® in patients with recurrent platinum resistant ovarian cancer, *Ann. Oncol.*, 11(4), 85, 2000.
21. Willner, J., Schmidt, M., Kirschner, J., Lang, S., Borgmeier, A., Huber, R. M. and Flentje, M., Sequential chemo- and radiochemotherapy with weekly paclitaxel (Taxol) and 3D-conformal radiotherapy of stage III inoperable non-small cell lung cancer. Results of a dose escalation study, *Lung Cancer*, 32(2), 163, 2001.
22. Belani, C. P., Interim analysis of a phase II study of induction weekly paclitaxel/ carboplatin regimens followed by maintenance weekly paclitaxel for advanced and metastatic non-small cell lung cancer, *Semin. Oncol.*, 28; 4(4), 14, 2001.
23. Chougule, P. B., Akhtar, M. S., Akerley, W., Ready, N., Safran, H., McRae, R., Nigri, P., Bellino, J., Koness, J., Radie-Keane, K. and Wanebo, H., Chemoradiotherapy for advanced inoperable head and neck cancer: A phase II study, *Semin. Radiat. Oncol.*, 9; 2(1), 58, 1999.
24. Rosenthal, D. I., Lee, J. H., Sinard, R., Yardley, D. A., Machtay, M., Rosen, D. M., Egorin, M. J., Weber, R. S., Weinstein, G. S., Chalian, A. A., Miller, L. K., Frenkel, E. P. and Carbone, D. P., Phase I study of paclitaxel given by seven-week continuous infusion concurrent with radiation therapy for locally advanced squamous cell carcinoma of the head and neck, *J. Clin. Oncol.*, 1; 19(5), 1363, 2001.

25. Zimmerman, T. M., Grinblatt, D. L., Malloy, R. and Williams, S. F., A Phase I dose escalation trial of continuous infusion paclitaxel to augment high dose cyclophosphamide and thiotepea plus stem cell rescue for the treatment of patients with advanced breast carcinoma, *Cancer*, 15; 83(8), 1540, 1998.
26. Skubitz, K. M., A phase I study of ambulatory continuous infusion paclitaxel, *Anticancer Drugs*, 8(9), 823, 1997.
27. Rosenberger, W. and Haines, L. M., Competing designs for phase I clinical trials: review, *Stat. Med.*, 21, 2757, 2002.
28. Gurney, H., Dose calculation of anticancer drugs: a review of the current practice and introduction of an alternative, *J. Clin. Oncol.*, 14, 2590, 1996.
29. Gurney, H. P., Ackland, S., Gebiski, V. and Farrell, G., Factors affecting epirubicin pharmacokinetics and toxicity: evidence against using body-surface area for dose calculation, *J. Clin. Oncol.*, 16, 2299, 1998.
30. Gaemlin, E., Boisdron-Celle, M., Guerin-Meyer, V., Delva, R., Lortholary, A., Genevieve, F., Larra, F., Ifrah, N. and Robert, J., Correlation between uracil and dihydrouracil plasma ratio, fluorouracil (5-FU) pharmacokinetic parameters, and tolerance in patients with advanced colorectal cancer: A potential interest for predicting 5-FU toxicity and determining optimal 5-FU dosage, *J. Clin. Oncol.*, 17, 1105, 1999.
31. Chatelut, E., Canal, P., Brunner, V., Chevreau, C., Pujol, A., Boneu, A., Roche, H., Houin, G. and Bugat, R., Prediction of carboplatin clearance from standard morpho-logical and biological patient characteristics, *J. Natl. Cancer Inst.*, 87(8), 573, 1995.
32. Duffull, S. B. and Robinson, B. A., Clinical pharmacokinetics and dose optimisation of carboplatin, *Clin. Pharmacokinet.*, 33, 161, 1997.
33. Calvert, A. H., Newell, D. R., Gumbrell, L. A., O'Reilly, S., Burnell, M., Boxall, F. E., Siddik, Z. H., Judson, I. R., Gore, M. E. and Wiltshaw, E., Carboplatin dosage: prospective evaluation of a simple formula based on renal function, *J. Clin. Oncol.*, 7(11), 1748, 1989.
34. Cockcroft, D. W. and Gault, M. H., Prediction of creatinine clearance from serum creatinine, *Nephron*, 16(1), 31, 1976.
35. Van Warmerdam, L. J., Rodenhuis, S., ten Bokkel Huinink, W. W., Maes, R. A. and Beijnen, J. H., Evaluation of formulas using the serum creatinine level to calculate the optimal dosage of carboplatin, *Cancer Chemother. Pharmacol.*, 37(3), 266, 1996.
36. Canal, P., Chatelut, E. and Guichard, S., Practical treatment guide for dose individualisation in cancer chemotherapy, *Drugs*, 56(6), 1019, 1998.
37. Gehan, E. A., The determination of the number of patients required in a preliminary and a follow-up trial of a chemotherapeutic agent, *J. Chron. Dis.*, 13, 346, 1961.
38. Gibaldi, M. and Perrier, D., *Pharmacokinetics*, 2nd ed., Marcel Dekker, New York, 1982, 45.
39. Langer, R., Biomaterials and biomedical Engineering, *Chem. Eng. Sci.*, 50(24), 4109, 1995.
40. Griffith, L. G., Polymeric biomaterials, *Acta. Mater.*, 48, 263, 2000.
41. Peppas, N. A., Bures, P., Leobandung, W. and Ichikawa, H., Hydrogels in pharmaceutical formulations, *Eur. J. Pharm. Biopharm.*, 50(1), 27, 2000.
42. Park, K., Shalaby, W. S. W. and Park, H., *Biodegradable Hydrogels for Drug Delivery*, Technomic Publishing, Lancaster, PA, 1993.

43. Shalaby, S. W., *Biomedical Polymers, Designed to Degrade Systems*, Hanser Publishers, New York, 1994.
44. Williams, D. F. and Mort, E., Enzyme-accelerated hydrolysis of polyglycolic acid, *J. Bioeng.*, 1(3), 231, 1977.
45. Williams, D. F., The effect of bacteria on absorbable sutures, *J. Biomed. Mater. Res.*, 14(3), 329, 1980.
46. Williams, D. F., Mechanisms of biodegradation of implantable polymers, *Clin. Mater.*, 10(1-2), 1992.
47. Working, P. K., in *Chemistry and Biological Applications of Polyethylene Glycol* (American Chemical Society Symposium Series 680, 1997, 45.
48. Yamaoka, T., Tabata, Y. and Ikada, Y., Distribution and tissue uptake of polyethylene glycol with different molecular weights after intravenous administration to mice, *J. Pharm. Sci.*, 83, 601, 1994.
49. Yokoyama, M., Okano, T., Sakurai, Y., Kikuchi, A., Ohsako, N., Nagasaki, Y. and Kataoka, K., Synthesis of poly(ethylene oxide) with heterobifunctional reactive groups at its terminals by an anionic initiator, *Bioconjug. Chem.*, 3(4), 275, 1992.
50. Gordon, A. N., Granai, C. O., Rose, P. G., Hainsworth, J., Lopez, A., Weissman, C., Rosales, R. and Sharpington, T., Phase II study of liposomal doxorubicin in platinum- and paclitaxel-refractory epithelial ovarian cancer, *J. Clin. Oncol.*, 18(17), 3093, 2000.
51. Israel, V. P., Garcia, A. A., Roman, L., Muderspach, L., Burnett, A., Jeffers, S. and Muggia, F. M., Phase II study of liposomal doxorubicin in advanced gynecologic cancers, *Gynecol. Oncol.*, 78(2), 143, 2000.
52. Lyass, O., Uziely, B., Ben-Yosef, R., Tzemach, D., Heshing, N. I., Lotem, M., Brufman, G. and Gabizon, A., Correlation of toxicity with pharmacokinetics of pegylated liposomal doxorubicin (Doxil) in metastatic breast carcinoma, *Cancer*, 89(5), 1037, 2000.
53. Ranson, M. R., Carmichael, J., O'Byrne, K., Stewart, S., Smith, D. and Howell, A., Treatment of advanced breast cancer with sterically stabilised liposomal doxorubicin: results of a multicentre phase II trial, *J. Clin. Oncol.*, 15, 3185, 1997.
54. Uziely, B., Jeffers, S., Isacson, R., Kutsch, K., Wei-Tsao, D., Yehoshua, Z., Libson, E., Muggia, F. M. and Gabizon, A., Liposomal doxorubicin, antitumour activity and unique toxicities during two complementary phase I studies, *J. Clin. Oncol.*, 13, 1777, 1995.
55. Greenwald, R. B., Gilbert, C. W., Pendri, A., Conover, C. D., Xia, J. and Martinez, A., Drug delivery systems: water soluble taxol 2'-poly(ethylene glycol) ester prodrugs-design and *in vivo* effectiveness, *J. Med. Chem.*, 39(2), 424, 1996.
56. Pendri, A., Conover, C. D. and Greenwald, R. B., Antitumor activity of paclitaxel-2'-glycinate conjugated to poly(ethylene glycol): a water-soluble prodrug, *Anticancer Drug Des.*, 13(5), 387, 1998.
57. Conover, C. D., Greenwald, R. B., Pendri, A., Gilbert, C. W. and Shum, K.L., Camptothecin delivery systems: enhanced efficacy and tumor accumulation of camptothecin following its conjugation to polyethylene glycol via a glycine linker, *Cancer Chemother. Pharmacol.*, 42(5), 407, 1998.
58. Kornblith, P. L. and Walker, M., Chemotherapy for malignant gliomas, *J. Neurosurg.*, 68, 1, 1988.
59. Engelhard, H. H., The role of interstitial BCNU chemotherapy in the treatment of malignant glioma, *Surg. Neurol.*, 53(5), 458, 2000.

60. Garfield, J., Dayan, A. D. and Weller, R.O., Postoperative intracavitary chemotherapy of malignant supratentorial astrocytomas using BCNU, *Clin. Oncol.*, 1, 213, 1975.
61. Yang, M. B., Tamargo, R. J. and Brem, H., Controlled delivery of 1,3-bis (2-chloroethyl)-1-nitrosourea from ethylene-vinyl acetate copolymer, *Cancer Res.*, 49, 5103, 1989.
62. Brem, H., Mahaley, M. S. and Vick, N. A., Interstitial chemotherapy with drug polymer implants for the treatment of recurrent gliomas, *J. Neurosurg.*, 74, 441, 1991.
63. Wu, W. P., Tamada, J. A., Brem, H. and Langer, R., In vivo versus *in vitro* degradation of controlled release polymers for intracranial surgical therapy, *J. Biomed. Mater. Res.*, 28(3), 387, 1994.
64. Brem, H., Piantadosi, S., Burger, P. C., Walker, M., Selker, R., Vick, N. A., Black, K., Sisti, M., Brem, S. and Mohr, G., Placebo-controlled trial of safety and efficacy of intraoperative controlled delivery by biodegradable polymers of chemotherapy for recurrent gliomas. The Polymer-brain Tumor Treatment Group, *Lancet*, 345(8956), 1008, 1995.
65. Goldberg, E. P., Hadba, A. R., Almond, B. A. and Marotta, J. S., Intratumoral cancer chemotherapy and immunotherapy: opportunities for nonsystemic pre-operative drug delivery, *J. Pharm. Pharmacol.*, 54(2), 159, 2002.
66. Mok, T. S., Kanekal, S., Lin, X. R., Leung, T. W., Chan, A. T., Yeo, W., Yu, S., Chak, K., Leavitt, R. and Johnson, P., Pharmacokinetic study of intralesional cisplatin for the treatment of hepatocellular carcinoma, *Cancer*, 91(12), 2369, 2001.
67. Leung, T. W., Yu, S., Johnson, P. J., Geschwind, J., Vogl, T. J., Engelmann, K., Gores, G. J., Giovannini, M., O'Grady, J., Heneghan, M., Stewart, M., Orenberg, E. K. and Thuluvath, P. J., Phase II study of the efficacy and safety of cisplatin-epinephrine injectable gel administered to patients with unresectable hepatocellular carcinoma, *J. Clin. Oncol.*, 15; 21(4), 652, 2003
68. Fung, L. K., Ewend, M. G., Sills, A., Sipos, E. P., Thompson, R., Watts, M., Colvin, O. M., Brem, H. and Saltzman, W. M., Pharmacokinetics of interstitial delivery of carmustine, 4-hydroperoxycyclophosphamide, and paclitaxel from a biodegradable polymer implant in the monkey brain, *Cancer Res.*, 58(4), 672, 1998.
69. Wenig, B. L., Werner, J. A., Castro, D. J., Sridhar, K. S., Garewal, H. S., Kehrl, W., Pluzanska, A., Arndt, O., Costantino, P. D., Mills, G. M., Dunphy, F. R., II, Orenberg, E. K. and Leavitt, R. D., The role of intratumoral therapy with cisplatin/epinephrine injectable gel in the management of advanced squamous cell carcinoma of the head and neck, *Arch. Otolaryngol. Head Neck Surg.*, 128(8), 80, 2002.
70. Werner, J. A., Kehrl, W., Pluzanska, A., Arndt, O., Lavery, K. M., Glaholm, J., Dietz, A., Dyckhoff, G., Maune, S., Stewart, M. E., Orenberg, E. K. and Leavitt, R. D., A phase III placebo-controlled study in advanced head and neck cancer using intratumoral cisplatin/epinephrine gel, *Br. J. Cancer*, 87(9), 938, 2002.
71. Oratz, R., Hauschild, A., Sebastian, G., Schadendorf, D., Castro, D., Brocker, E. B. and Orenberg, E. K., Intratumoral cisplatin/adrenaline injectable gel for the treatment of patients with cutaneous and soft tissue metastases of malignant melanoma, *Melanoma Res.*, 13(1), 59, 2003

72. Vogl, T. J., Engelmann, K., Mack, M. G., Straub, R., Zangos, S., Eichler, K., Hochmuth, K. and Orenberg, E. K., CT-guided intratumoural administration of cisplatin/epinephrine gel for treatment of malignant liver tumours, *Br. J. Cancer*, 86(4), 524, 2002.
73. Harris, J. M., Martin, N. E. and Modi, M., Pegylation: A novel process for modifying pharmacokinetics, *Clin. Pharmacokinet.*, 40, 539, 2001.

16

Tumor Immunotherapeutic Systems

Waleed S.W. Shalaby and Shalaby W. Shalaby

CONTENTS

16.1 Introduction	257
16.2 Key Aspects of Contemporary Immunotherapy	258
16.2.1 Strategies for Successful Immunotherapy.....	258
16.2.2 Adaptive Tumor Surveillance	258
16.2.3 Costimulation and Immunotherapy	259
16.2.4 Combination Immunotherapy	260
16.3 Polymeric Biomaterials as Carriers of Immunotherapeutic Agents.....	260
16.3.1 Polymeric Biomaterials as Artificial Antigen-Presenting Cells (APCs)	260
16.3.2 Delivery of Cytokines Using Polymeric Carriers	261
16.4 Role of Synthetic Absorbable Polymers in Immunotherapy	263
16.4.1 Key Features of Synthetic Absorbable Polymers as Carriers of Bioactive Agents	263
16.4.2 New Approaches to Using Absorbable Polymers	263
16.5 Conclusion and Persepctive on the Future	271
References	271

16.1 Introduction

Although tumor immunotherapy was first described a century ago by William Coley, Burnet and Thomas coined the term “immunosurveillance” to describe the nature of tumor recognition by the immune system.¹⁻³ While Burnet favored the self–nonself discrimination hypothesis and Thomas described homograft rejection as a primary defense, neither hypothesis gained much support.⁴ However, recent advances identifying immunogenic tumor-associated antigens (TAAs), the critical role of professional antigen-

presenting cells (APCs) and the existence of regulatory T lymphocytes that inhibit responses against self-tissue (including tumors) have renewed interest in tumor immunotherapy.^{5,6} In the last 25 years, a large body of information has emerged showing the potential efficacy of stimulatory molecules and cytokines to elicit immunologic antitumor responses. Furthermore, combination therapies directed at different arms of the immune response may prove even more effective than the individual components.

To date, multiple cell-based strategies have shown promise in the area of peptide-specific vaccines, *ex-vivo* activation/expansion of T cells or tumors, and tumor cell or bystander cell transfections with various expression vectors. However, the time, cost, and patient morbidity involved with tumor/bystander cell procurement, modification, and maintenance could limit the application of immunotherapy to small, select groups of patients. In addition, the lack of immunogenic, tumor-specific antigens and the potential array of cytokines required for adequate responses could also limit broad application of this technology. The use of biomaterials, and particularly absorbable/biodegradable polymers, as carriers for tumor immunotherapy may provide the platform to introduce an array of macromolecules and cytokines necessary to elicit a vigorous immunologic response. This review is intended to examine recent developments in tumor immunotherapy in an effort to highlight current and potential applications with biomaterials.

Prior to discussing the role of polymeric biomaterials, and particularly synthetic, absorbable polymers in immunotherapy, key aspects of contemporary immunotherapy are outlined. This is to develop a better understanding of the fast-growing role of polymers as carriers of immunotherapeutic agents and therefore sometimes as adjuvants.

16.2 Key Aspects of Contemporary Immunotherapy

16.2.1 Strategies for Successful Immunotherapy

The use of biomaterials as carriers for tumor immunotherapy may provide the platform to introduce an array of macromolecules and cytokines necessary to elicit a vigorous immunologic response. The ease of utilizing these systems near or at the time of tumor diagnosis and/or debulking when burden is lowest may improve clinical response and decrease patient morbidity. From a practical standpoint, many of the conventional biomaterials used in the clinics are easy to prepare, modify, and store. Thus, they can be tailored to meet specific requirements based on route of administration and duration of response.

16.2.2 Adaptive Tumor Surveillance

The activation of antigen-presenting dendritic cells (APCs) is central to the initiation of adaptive immunity. It is believed that the immune system has

evolved to detect danger by employing “professional” APCs as sentinels of tissue distress. Thus, cells undergoing damage or necrotic cell death may express cytokines or heat shock proteins (HSP) to activate APCs.⁷⁻⁹ Once activated, APCs initiate and control an adaptive immune response that is directed toward tumor-associated antigens (TAA). Antigen-specific T-cell and B-cell responses are initiated by dendritic cells (DCs) that capture antigens that are secreted or shed by tumor cells or after cell lysis. Processing and presentation of these antigens by major histocompatibility (MHC) class I and class II molecules on a single DC can enable priming and activation of both CD4⁺ and CD8⁺ T cells. Critical to T-cell activation is the presence of costimulatory molecules on APCs such as B7. In conjunction with costimulation (B7-CD28 interaction), activated APCs carry TAA to the lymph nodes where the TAA-derived peptides are presented via MHC class II molecules to CD4⁺ and MHC class I molecules to CD8⁺ T lymphocytes. Stimulated CD4⁺ T cells subsequently express CD40L, which, in turn, further stimulates CD40-expressing APCs. TAA-specific lymphocytes develop into activated effector cells with the ability to migrate into the tissue and mount an attack against the developing tumor. This armament involves CD4⁺ helper T cells, CD8⁺ cytotoxic T lymphocytes (CTLs), and local APCs.¹⁰⁻¹² Although tumor cell lysis is mediated by CTLs, memory CD4⁺ and CD8⁺ T cells also play a critical role in maintaining protective immunity.

16.2.3 Costimulation and Immunotherapy

The danger model presented by Matzinger argues that many cancers do not appear dangerous to the immune system because initially they grow as healthy cells and do not send out distress signals to activate APCs.⁶ It has been proposed that unstimulated APCs constitutively present captured tumor antigens without costimulation leading to tolerance.¹³ T cells that encounter MHC-presented TAA in the absence of costimulation are inactivated either through anergy or apoptotic death. It is presumably because of this lack of danger signaling that the immune system loses its potential to respond to the tumor.^{7,11} The concept of costimulation involves a two-signal model for T-cell activation by APCs. It requires binding of the T-cell receptor and CD28 receptor to a MHC-antigen complex and B7 (B7-1, B7-2) ligand on the APC, respectively.¹⁴ Most human carcinomas fail to express B7; however, it has been detected in several hematopoietic malignancies of B-cell origin.¹⁵⁻¹⁷ Chen postulated that this lack of B7 expression may explain how tumors can evade effective immune responses. The idea that tumor cells could be engineered to express costimulatory molecules was originally studied by Chen et al.¹⁸ The argument was that tumor cells could become better antigen presenting cells to activate T cells. Chen transfected the murine B7-1 gene into the K1735M2 mouse melanoma expressing a tumor rejection antigen encoded by the E7 gene of HPV type 16.¹⁹ The B7-1 transfected cells failed to grow in immunocompetent syngeneic mice. Furthermore, rejection could be inhibited by treating the mice with CTLA4-Ig to block the B7-1

interaction with CD-28. Chen et al. also found that this approach could induce tumor regression using E7C3 melanoma cells.²⁰ The effects were determined to be mediated by cytotoxic CD8⁺ T lymphocytes.

16.2.4 Combination Immunotherapy

Combination therapy directed at different arms of the immune response may prove more efficacious than the individual components alone. Recently, Hurwitz et al. described the rejection of SM1 tumors by using both CTLA-4 blockade and a GM-CSF-expressing tumor vaccine.²¹ They found that this combination resulted in regression of parental SM1 tumors, despite the ineffectiveness of either treatment alone. This synergistic therapy resulted in long-lasting immunity to SM1 which depended on both CD4⁺ and CD8⁺ T cells. Interestingly, coexpression of B7 and IFN-gamma on SM1 tumors was also sufficient to cause regression of SM1 tumors by a CD8⁺ T cell-dependent mechanism. Rejection of the B7/IFN-gamma-expressing SM1 tumor resulted in protection from rechallenge.²¹

16.3 Polymeric Biomaterials as Carriers of Immunotherapeutic Agents

The ability to modulate the composition and physicochemical properties of polymeric biomaterials to meet release and surface requirements of different immunotherapeutic agents makes them quite valuable as carriers of these agents.

16.3.1 Polymeric Biomaterials as Artificial Antigen-Presenting Cells (APCs)

Polymeric systems may be designed to bias the cell-mediated immune response toward a tumor-specific response through local, prolonged delivery of cytokines and stimulatory/costimulatory signals at the tumor site. Conventional approaches for cytokine or costimulation delivery rely on incorporating the agent by encapsulation or dispersion techniques. Localizing the cytokine or signaling molecule on the polymer surface is another strategy by which to achieve delivery.²² This can be achieved by chemical conjugation to an activated surface or by simple adsorption. In the latter case, irreversible adsorption may be exploited for signaling purposes and release mediated by reversible adsorption. Microparticle systems are particularly versatile as artificial APCs since they can be formulated with an array of cytokines or signaling molecules without the added complexities of cell-based strategies. As an injectable formulation, these systems may be studied in various com-

binations and routes of administration. Thus, the potential for rapid and less costly implementation of tumor immunotherapy to a broader range of patients is a distinct possibility. The prospect of using microparticulate carriers as artificial APCs is highlighted in Figure 16.1. Here we see an *in situ* vaccination strategy whereby microparticulates are peripherally injected with a patient's irradiated tumor cells. The stimulatory microparticles carrying anti-CD3 and anti-CD28 antibodies are designed for local activation of T-cells, whereas the granulocyte-macrophages colony stimulating factor (GM-CSF)-releasing microparticles recruit dendritic cells. The latter is critical to the presentation of tumor-specific antigen and eventual clonal expansion of tumor-specific T-cells.

16.3.2 Delivery of Cytokines Using Polymeric Carriers

Cytokine delivery may be achieved through simple reversible adsorption processes. Irreversible vs. reversible protein adsorption occurs at a critical molar mass above which large macromolecules remain immobilized on the polymer surface and below which desorption occurs. The latter may be broadly applied to cytokines. Reversible protein adsorption occurs when the net energy of individual peptides is smaller than the thermal energy. If the energy gained by the peptide is small, local relaxation of the protein structure is relatively fast, leading to rapid equilibration. Most theories underlying reversible adsorption would predict that desorption is a relatively slow process requiring the simultaneous release of all anchored contacts, which is energetically unfavorable. However, adsorption of a relatively small protein likely gives rise to a distribution of reversibly and irreversibly bound conformations on the polymer surface. The net effect is the release of potentially biologically active cytokine from the biomaterial surface via reversible adsorption. Sustained release may also be achieved through degradation of the biomaterial which would allow release of pre-existing irreversibly bound cytokine. The amount of cytokine loaded on the surface may be increased through the choice of biomaterial. Adsorption affinity may be enhanced through electrostatic interactions that favor charge neutralization between the cytokine and the polymeric surface. In this context, the surface charge or zeta potential of the polymer surface can be manipulated relative to the isoelectric point (pI) of the adsorbate.²³⁻²⁶ This approach has recently been exploited to enhance DNA adsorption on microspheres by Singh et al.²⁷

In recent years, the use of biomaterial as vaccine adjuvants has received considerable interest in oral and parenteral vaccine development. They have been formulated to elicit either mucosal or humoral immunity via targeted phagocytosis in the Peyer's patches or as conventional subcutaneous depots.²⁸⁻³⁰ Golembek et al. were one of the first groups to apply microspheres for tumor immunotherapy.³¹ GM-CSF or IFN- γ was encapsulated in gelatin-chondroitin sulfate microspheres and mixed with irradiated B16/F10

murine melanoma cells prior to injection. The GM-CSF releasing microspheres prevented tumor implantation and produced systemic antitumor immunity on rechallenge. No effect was observed using IFN- γ . The authors purported that the level of protection was comparable to GM-CSF transduced tumor vaccines. Interleukin (IL-2)-loaded poly(lactic acid) microspheres were evaluated in a human tumor xenograft/severe combined immunodeficiency (SCID) mouse model.³² Subcutaneous injection of IL-2 microspheres and tumor cells resulted in complete suppression of tumor implantation in 80% of animals. The antitumor effect was mediated by the mouse natural killer cells. Biodegradable microspheres were recently developed to induce antiidiotypic responses against human ovarian cancer antigen CA125.³³ Murine monoclonal antibodies B43.13 were encapsulated in poly(DL-lactic-co-glycolic acid) microspheres which resulted in enhanced humoral and cellular immune responses compared with mAb B43.13 alone or mAb B43.13 mixed with microspheres. The antibody responses could be further enhanced by coencapsulating the mAb with monophosphoryl lipid A, a nontoxic adjuvant.

Interleukin-12 delivered by poly-lactic acid (PLA) microspheres was used to promote antitumor activity in a human head and neck tumor xenograft/SCID mouse model.³⁴ Lymphocyte subset depletion studies established that tumor suppression was dependent on both the CD8⁺ T lymphocytes and the CD56⁺ natural killer cells. Treatment of tumors with a single intralesional injection of IL-12-loaded PLA resulted in complete suppression of tumor engraftment in 50% of the mice. In contrast, treatment of tumors with repeated bolus IL-12 injections suppressed tumor engraftment only transiently and did not result in complete tumor rejection in any of the mice. Similar results were observed using IL-12-loaded PLA microspheres in a murine alveolar lung carcinoma line.³⁵ IL-12 and GM-CSF microspheres were studied in combination with systemic IL-2 using a similar murine tumor model.³⁶ The local intratumor injection of IL-12 and GM-CSF microspheres in the absence or presence of soluble IL-2 provided significant protection in terms of local recurrence and overall survival. The most effective therapy was the GM-CSF microspheres with IL-2 or in combination with IL-12 microspheres.

The size of the microsphere can be manipulated to target macrophages via phagocytosis. Mullerad et al. encapsulated h-IL-1 within poly(lactic/glycolic acid) microspheres ranging in size from 1 to 5 μm .³⁷ The microspheres were efficiently taken up by macrophages in culture and after intraperitoneal injection into mice. In culture, phagocytosis was maximized after 3 h. *In vivo* uptake by macrophages led to cell activation, as evidenced by the enhanced production of murine IL-1, IL-6 and IL-12. Control microspheres containing bovine serum albumin induced only background levels of cytokine. The authors postulated that activating macrophages through microsphere-mediated phagocytosis might be an effective strategy for eliciting an antitumor response.

16.4 Role of Synthetic Absorbable Polymers in Immunotherapy

The attributes of polymeric biomaterials as carriers of immunotherapeutic agents have been outlined in Section 16.3. To further the useful application of polymeric biomaterials in contemporary immunotherapy, recent studies have focused on synthetic, absorbable polymers as carriers of immunotherapeutic agents and potentially as adjuvants. Prior to discussing recent developments in this area, key features of synthetic, absorbable polymers are outlined.

16.4.1 Key Features of Synthetic Absorbable Polymers as Carriers of Bioactive Agents

In addition to the ability of tailor-making absorbable polymers to suit the release requirements of bioactive agents, these materials have the advantage of being transient in nature and having controllable half-lives. This, in turn, allows their use in providing finite bioavailability. Absorbable/biodegradable systems are particularly attractive since their degradation profiles can be manipulated to control the rate of drug release or maintain a desired mechanical integrity depending on the therapeutic goal.^{38–40} They can be designed to release therapeutics over extended periods of time or to act as platforms from which cell interactions may take place. One of their biggest advantages is that they may be formulated in various shapes and sizes ranging from monolithic implants to injectable microspheres.

The use of biodegradable polymeric systems for tumor immunotherapy has received limited study as compared with more conventional cell-based approaches.^{27,31,32,34,35,41} However, the advantage for tumor immunotherapy lies in the diversity of materials already generated from years of research in the suture industry and more recently from the area of controlled drug release.

16.4.2 New Approaches to Using Absorbable Polymers

It is generally agreed that multiple components must coexist to establish an effective, antigen-specific, antitumor immune response. Many agree that appropriate presentation of tumor-specific antigens accompanied by costimulation to cytotoxic (cd8⁺) and helper (cd4⁺) T lymphocytes and antigen presenting cells (APCs) are necessary to promote a long-lived immune response. However, the ability to achieve clonal expansion of tumor-specific T-cell populations with associated memory remains elusive. Presently, it is not clear what factors are critical to overcoming immunologic tolerance vs. ignorance. Shalaby and co-workers postulated that *in situ* delivery of stim-

ulatory, costimulatory, and necessary cytokines to the tumor site can improve T-cell response and promote tumor-specific memory through the recruitment of dendritic cells which function as APCs (Figure 16.1).⁴⁴ The use of biodegradable, polymeric systems for tumor immunotherapy has received limited study as compared to more conventional cell-based approaches.^{27,31,32,34,35} Accordingly, these investigators have developed novel biodegradable, polymeric microparticles as substrates to deliver stimulatory (cd3) and costimulatory (cd28) signals to activate T cells while providing sustained release of granulocyte-macrophage colony stimulating factor (GM-CSF) for dendritic cell recruitment and maturation. It is expected that local T-cell activation and dendritic cell recruitment will support clonal expansion of tumor-specific T cells to induce a cell-mediated antitumor response with associated memory.

The properties of the acid terminated polyglycolide microparticles (PG-MP) are described in Table 16.1. The volume-weighted mean diameter and median diameter were 7.02 and 6.85 microns, respectively. The corresponding size distribution ranged from 2.09 to 14.58 microns. Potentiometric titration of accessible carboxylic acid groups was 0.3 mmole/g with an estimated zeta potential of -21.87 mV in phosphate-buffered saline (PBS, pH-7.2). Selected samples were also assayed for the presence of endotoxin to eliminate

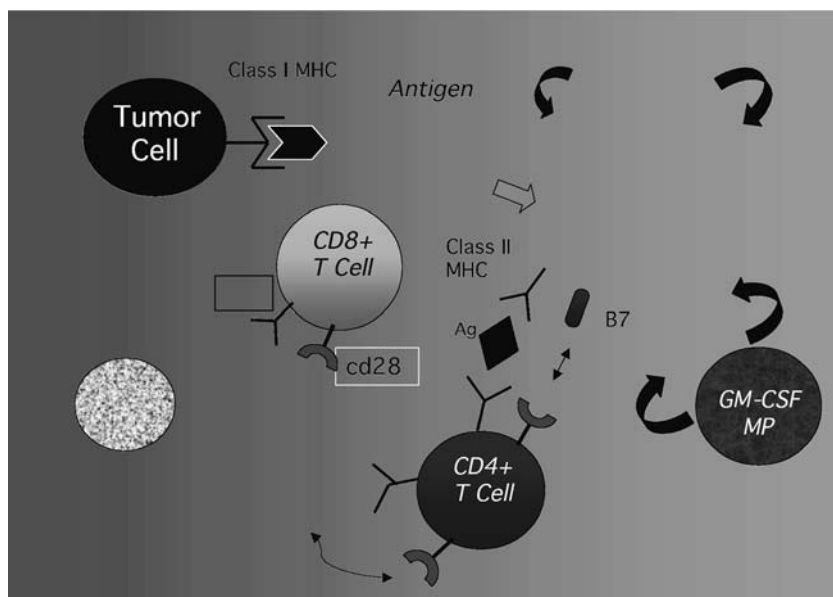


FIGURE 16.1

Proposed mechanism of *in situ* vaccination using microparticulate (MP) carriers as artificial antigen-presenting cells for tumor immunotherapy. The stimulatory microparticles (a-MP) carry anti-cd3 and anti-cd28 to activate T cells (CD8+ and CD 4+). The GM-CSF releasing microparticles (GM-CSF MP) are designed to local recruitment of dendritic cells for the clonal expansion of T cells specific for tumor antigen.

TABLE 16.1

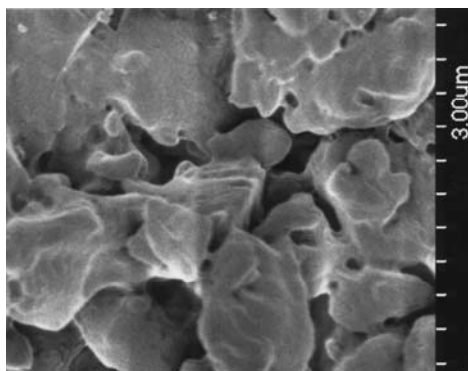
Properties of Acid-Terminated Polyglycolide Microparticulates (PG-MP)

Parameter	Measured value
Volume weighted mean diameter	7.02 μ
Median diameter	6.85 μ
Particle size distribution	2.09 – 14.58 μ
Accessible carboxylic acid groups	0.3 mmoles/g
Zeta potential	-21.87 mV
Endotoxin assay	negative

Note: μ = microns; mV = millivolts; mmoles/g = millimoles/gram.

confounding anti-tumor responses that could be observed in planned animal experiments. The endotoxin assay was negative as determined using a chromogenic limulus amoebocyte lysate test kit. SEM analysis of the PG-MP showed a highly textured surface at low magnification due to the jet milling. However, a significant porous structure was observed at higher magnifications (Figure 16.2). Microparticulate porosity was attributed to the exothermic nature of the polymerization reaction and subsequent removal of acetone-soluble monomeric and oligomeric components. Interpretation of electron spectroscopy for chemical analysis (ESCA) revealed a typical surface composition for polyglycolic acid consisting of an atomic concentration for oxygen and carbon of 42.91% and 57.01%, respectively. ESCA data in Table 16.2 depict the chemical states of the oxygen 1s and carbon 1s level spectrum. Two and three chemical states were identified in the 1s level spectrum, respectively. They corresponded to the characteristic carbon and oxygen bonds associated with this absorbable polyester (Table 16.2).

PG-MP immobilized with either anti-human CD3/CD28 or anti-mouse cd3/cd28 induced significant proliferation of T cells (Figure 16.3). Intracel-

**FIGURE 16.2**

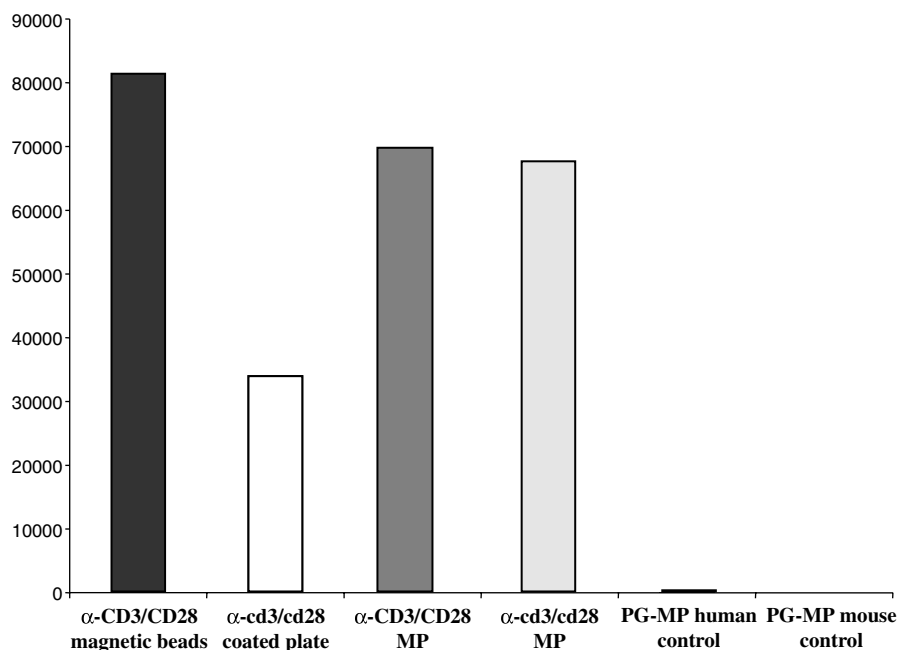
Scanning electron microscopy of acid-terminated polyglycolide microparticulates (PG-MP).

TABLE 16.2

Electron Spectroscopy for Chemical Analysis (ESCA) of Acid-Terminated Polyglycolide Microparticulates (PG-MP).

Peak	Position BE (eV)	Raw Area (cps)	Atomic Mass	Atomic Concentration (%)	Chemical Bonding
O 1s 1	531.400	40047.6	15.999	24.73	C=O, -OH
O 1s 2	529.920	27895.9	15.999	17.21	OH
C 1s 1	287.024	14222.3	12.011	23.27	-C=O, C-OH
C 1s 2	284.628	14678.3	12.011	24.00	C-C in an ester, C-H, C-O
C 1s 3	282.811	6326.2	12.011	10.34	-CH

Note: BE-binding energy; eV-electronvolt; cps-counts per second.

**FIGURE 16.3**

Activation of resting human and mouse t-cells with a-human CD3/CD28-MP and a-mouse cd3/cd28-MP, respectively. a-CD3/CD28 magnetic beads and well plates coated with a-cd3 and a-cd28 were used as positive controls.

lular flow cytometry in activated mouse T cells was significant for IFN- γ , but not IL-4. Stimulation with a-cd3/cd28MP resulted in more than 50% of T cells producing IFN- γ . This was consistent with a cell-mediated or TH-1 response.

Microparticles surface-modified for GM-CSF release were prepared from either untreated PG-MP or PG-MP pretreated with poly-l-lysine (PG/Lys) to manipulate surface charge. As depicted from ESCA (Table 16.3), adsorp-

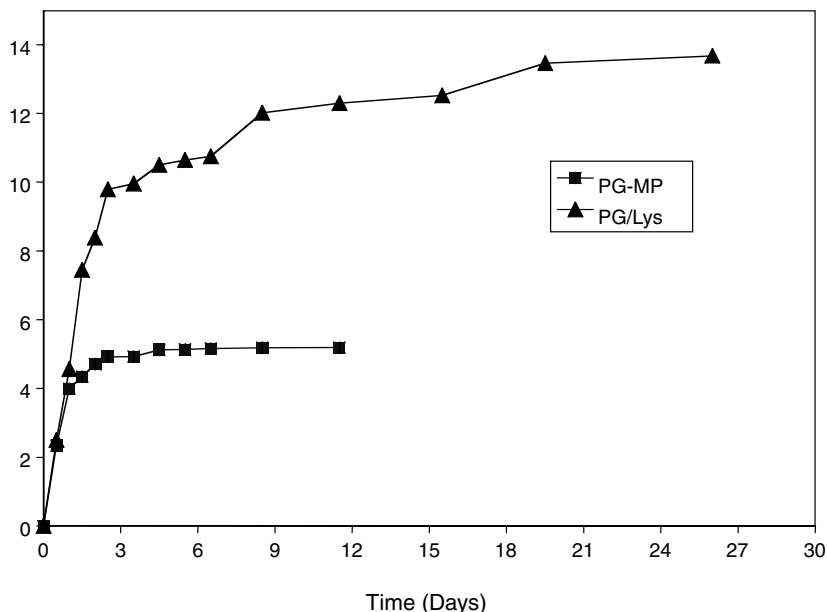
TABLE 16.3

ESCA Data of Surface Treated and Untreated PG-MP

Surface Treatment	O1s 528 eV	O1s 530 eV	O1s 531.5 eV	O1s 533.5 eV	C1s 282 eV	C1s 285 eV	C1s 287 eV	C1s 289 eV	N1s 395.6 eV	N1s 397.7 eV	N1s 399 eV	Cl 2p 196.4 eV	Cl2p 198 eV
PG-MP	—	17.21	24.73	—	10.34	24.00	23.27	—	—	—	—	—	—
PG-GMCSF	0.59	19.40	25.19	0.79	3.27	24.66	24.27	0.79	—	0.77	0.28	—	—
PG/Lys	—	20.83	18.73	1.02	8.42	26.45	22.89	—	—	0.76	0.44	0.22	0.10
PG/Lys-GMCSF	—	19.39	11.93	—	21.04	23.66	18.26	—	—	3.84	0.49	0.32	0.11
PG-GMCSF (PR)	—	21.93	16.16	—	13.36	25.19	21.17	—	0.07	2.12	—	—	—
PG/Lys-GMCSF (PR)	0.83	19.45	13.85	1.33	18.29	22.84	17.29	—	—	1.34	1.05	1.65	0.90

Note: PG-MP: polyglycolic acid microparticulate; PG-GMCSF: surface modification with GM-CSF; PG/Lys: surface modification with poly-L-lysine hydrochloride; PG/Lys-GMCSF: pretreated surface with poly-L-lysine HCl followed by modification with GM-CSF; PG-GMCSF (PR): Post-release surface of PG-GMCSF; PG/Lys-GMCSF (PR): Post-release surface of poly-L-lysine HCl/GMCSF.

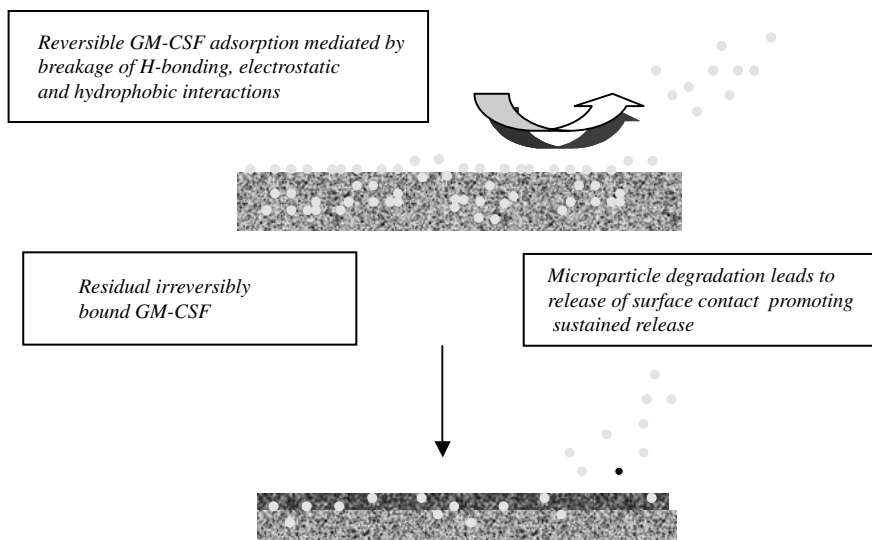
* Surface characterization in terms of bond energies and atomic concentration (%). Bold-faced data reflect values characteristic for selected surface modifications.

**FIGURE 16.4**

Release of GM-CSF from the surfaces of PG-MP and PG/Lys.

tion of GM-CSF on the PG-MP (PG-GMCSF) produced a surface atomic concentration of nitrogen of 0.97%. Treatment of PG-MP with poly-l-lysine hydrochloride (PG/Lys) resulted in only a marginal increase in surface nitrogen to 1.47%. However, pretreating PG-MP with poly-l-lysine hydrochloride followed by the addition of soluble GM-CSF (PG/Lys-GMCSF) produced a nearly threefold increase (4.20%) in the surface atomic concentration of nitrogen. It was postulated that the proposed positive shift in zeta potential produced by the poly-l-lysine HCl promoted adsorption of the negatively charged GM-CSF (pI-5.23). On the three different surfaces, nitrogen peaks were composed of two chemical states for the 1s level spectrum. The oxygen 1s level spectrum due to the PG-GMCSF surface was associated with a unique chemical state at a binding energy of 528 electron volts (eV). This was not observed on either the PG/Lys or PG/Lys-GMCSF surfaces. Despite dramatic differences in GM-CSF adsorption, the release of biologically active cytokine was addressed using a series of *in vitro* experiments. The release of GM-CSF from both the treated and untreated PG-MP is shown in Figure 16.4. GM-CSF released from the untreated PG-MP surface was nearly complete by day 6, whereas release from the PG/Lys surface was observed for up to 26 days. The ratio of released GM-CSF/microparticulate weight was 51.9 ng/mg and 136.7 ng/mg, respectively.

While direct structural analysis is lacking, others have observed that protein adsorption on polycationic supports leads to weak conformational changes since the protein interactions involve only negatively charged resi-

**FIGURE 16.5**

Proposed mechanism of GM-CSF release from PG-MP. GM-CSF adsorption comprises both reversibly bound and irreversibly bound adsorbate clusters. Reversible adsorption (GM-CSF release) is initially mediated by breakage of weaker hydrogen bonding, electrostatic and hydrophobic interactions. However, after an initial release phase, a predominance of irreversibly bound adsorbate clusters remain. Over time, the degradation (by hydrolysis) of PG-MP releases anchored peptides until desorption becomes energetically favorable. Thus, the latter release profile may be attributed to a degradation-controlled mechanism of desorption.

dues located on the periphery of the protein.⁴³ Thus, limited peripheral contacts would favor desorption, while shifts in the internal hydrophobic-domains to the periphery would promote irreversible adsorption. On the PG-MP surface, it was postulated that differences in the conformation of adsorbate clusters depended on the presence or absence of the poly-L-lysine. In its absence or after microparticulate degradation, one observes the oxygen 1s level chemical state at 528 eV, which may represent more irreversibly adsorbed GM-CSF. When poly-L-lysine is present, ESCA is no longer able to detect this chemical state given the predominance of a reversibly bound GM-CSF conformation at the surface. However, the sustained release of GM-CSF suggest that the GM-CSF remaining on the PG/Lys surface after the initial release phase resembles an adsorbate conformation that may be irreversibly bound (Figure 16.5). Over time, the degradation of PG-MP releases anchored peptides until desorption becomes energetically favorable. Thus, the latter release profile may be attributed to a degradation-controlled mechanism of desorption. Furthermore, even after 26 days at 37°C, it appears that protein conformation is stabilized by the microparticulate, as evidenced by enzyme-linked immunosorbent assay (ELISA).

The efficacy of PG-MP as a function of surface manipulation was tested in a flank tumor model using Balb-C mice. The prevention of tumor implan-

TABLE 16.4

Results of Tumor Implantation on the Flanks of Balb-C Mice after Co-Injection of Meth A Fibrosarcoma Cells And PG-MP as a Function of Surface Manipulation.

Treatment Group	Microparticulate	Mice	Mice with Tumor	Tumor Diameter (mm)	SE (+/-)
Tumor only	---	16	6	8.2	0.71
PG-MP control	* α -cd28-PGMP PG/Lys	15	15	8.6	1.10
T-cell stimulatory only	α -cd3/cd28-PGMP PG/Lys	16	5	3.6	0.40
GM-CSF only	* α -cd28-PGMP PG/Lys-GMCSF	8	2	4	---
Combination	α -cd3/cd28-MP PG/Lys-GMCSF	8	0	---	---

* α -cd28-PGMP: T-cell control microparticulates prepared with heat-denatured α -cd28 MoAb

Note: PG/Lys: treatment control for PG/Lys-GMCSF; SE- standard error.

tation after co-injection of PG-MP with Meth A cells is shown in Table 16.4. PG-MP controls displayed no intrinsic ability to impair tumor implantation. Average tumor sizes were 8.6 mm as compared with 8.2 mm for the controls. Co-injection of Meth A fibrosarcoma cells with either α -cd3/cd28-MP or PG/Lys-GMCSF alone resulted in significant prevention of tumor implantation. Only 5/16 and 2/8 mice developed tumors, respectively; however, a nearly 50% reduction in the average tumor diameter was noted. Interestingly, co-injection with the microparticulate combination completely prevented tumor implantation (0/8). A more stringent tumor regression model was then used to validate in vivo biological activity. Mice flanks were first injected with Meth A fibrosarcoma cells (1×10^6 cells). At a diameter between 2 to 4 mm, the tumor was injected with the combination treatment using α -cd3/cd28MP and PG/Lys-GMCSF. After 14 days, average tumor diameter was 13 mm and 15 mm in the tumor only and microparticulate control groups, respectively. However, the treatment group showed complete tumor regression in 4 of 7 animals and stable disease in 3 of 7. Staining of representative sections for the dendritic cell marker cd11c showed a dramatic level of dendritic cell infiltration in the treatment group only. This was consistent with the premise that released GM-CSF mediated dendritic cell recruitment and maturation.

Results of their study allowed Shalaby and co-workers to conclude that a large body of information has emerged supporting the use of various stimulatory molecules and cytokines to elicit antitumor responses.⁴² Multiple cell-based strategies have shown promise; however, the time, cost, and associated patient morbidity could limit the application of this approach to a small, select group of patients. Furthermore, the lack of immunogenic, tumor-specific antigens and the potential array of cytokines required for adequate responses could also limit broad application of such technology.

16.5 Conclusion and Perspective on the Future

It can be concluded that the use of cytokines and stimulatory molecules in conjunction with absorbable/biodegradable carriers for eliciting immunomediated antitumor responses is one of the most promising approaches for cancer immunotherapy. Availability of potent cytokines and signaling molecules, and advances in peptide-specific and DNA vaccines, coupled with recent developments in absorbable, solid, ionic micro- and nano-particles as well as liquid polyelectrolytes are expected to produce an exponential growth in the area of immunotherapy. This projection is in concert with:

- Emerging evidence suggesting that combination modalities may be the most effective clinical approach to immunotherapy
- Recent results showing that acid-terminated polyglycolide micro-particles as carrier substrates offer a potentially versatile means to introduce an array of macromolecules and cytokines to the tumor site that may be critical to eliciting an immunologic response

The use of these biomaterials has additional practical advantages related to ease of preparation, modification, storage, biodegradability, and existing approval by the FDA. In the clinical setting, employing these systems near or at the time of diagnosis and/or debulking when tumor burden is lowest may improve response and decrease patient morbidity. Thus, more rapid, practical, and potentially less costly clinical trials could be offered to a broader range of patients.

References

1. Coley, W. B., The treatment of malignant tumors by repeated inoculations of erysipelas: with a report of ten original cases, *Am. J. Med. Sci.*, 105, 487, 1893.
2. Burnet, F. M., Cancer: a biological approach, *Br. Med. J.*, 1, 779, 1957.
3. Burnet, F. M., Immunological aspects of malignant disease, *Lancet*, 1, 1171, 1967.
4. Ada, G., The coming of age of tumour immunotherapy, *Immunol. Cell Biol.*, 77, 180, 1999.
5. Medzhitov, R. and Janeway, C., Jr., Innate immune recognition: mechanisms and pathways, *Immunol. Rev.*, 173, 89, 2000.
6. Fuchs, E. J. and Matzinger, P., Is cancer dangerous to the immune system? *Semin. Immunol.*, 8, 271, 1996.
7. Gallucci, S., Lolkema, M. and Matzinger, P., Natural adjuvants: endogenous activators of dendritic cells, *Nature Med.*, 5, 1249, 1999.
8. Gallucci, S. and Matzinger, P., Danger signals: SOS to the immune system, *Curr. Opin. Immunol.* 13, 114, 2001.
9. Matzinger, P., Tolerance, danger, and the extended family, *Annu. Rev. Immunol.*, 12, 991, 1994.

10. Bennett, S. R., Carbone, F. R., Karamalis, F., Flavell, R. A., Miller, J. F. and Heath, W. R., Help for cytotoxic-T-cell responses is mediated by CD40 signaling, *Nature*, June 4, 393(6684), 478, 1998.
11. Ridge, J. P., Fuchs, E. J. and Matzinger, P., Neonatal tolerance revisited: turning on newborn T cells with dendritic cells, *Science*, 271, 1723, 1996.
12. Schoenberger, S. P., Toes, R. E., van der Voort, E. I., Offringa, R. and Melief, C. J., T-cell help for cytotoxic T lymphocytes is mediated by CD40-CD40L interactions, *Nature*, 393, 480, 1998.
13. Kurts, C., Heath, W. R., Carbone, F. R., Allison, J., Miller, J. F. and Kosaka, H., Constitutive class I-restricted exogenous presentation of self antigens in vivo, *J. Exp. Med.*, 184(3), 923, 1996.
14. Greenfield, E. A., Nguyen, K. A. and Kuchroo, V. K., CD28/B7 costimulation: a review, *Crit. Rev. Immunol.*, 18(5), 389, 1998.
15. Freeman, G. J., Freedman, A. S., Segil, J. M., Lee, G., Whitman, J. F. and Nadler, L. M., B7, a new member of the Ig superfamily with unique expression on activated and neoplastic B cells, *J. Immunol.*, 143(8), 2714, 1989.
16. Munro, J. M., Freedman, A. S., Aster, J. C., Gribben, J. G., Lee, N. C., Rhyndhart, K. K., Banchereau, J. and Nadler, L. M., In vivo expression of the B7 costimulatory molecule by subsets of antigen-presenting cells and the malignant cells of Hodgkin's disease, *Blood*, 83(3), 793, 1994.
17. Chen, L., McGowan, P., Ashe, S., Johnston, J., Li, Y., Hellstrom, I. and Hellstrom, K. E., Tumor immunogenicity determines the effect of B7 costimulation on T cell-mediated tumor immunity, *J. Exp. Med.*, 179(2), 523, 1994.
18. Chen, L., Ashe, S., Brady, W. A., Hellstrom, I., Hellstrom, K. E., Ledbetter, J. A., McGowan, P. and Linsley, P. S., Costimulation of antitumor immunity by the B7 counterreceptor for the T lymphocyte molecules CD28 and CTLA-4, *Cell*, 71(7), 1093, 1992.
19. Chen, L. P., Thomas, E. K., Hu, S. L., Hellstrom, I. and Hellstrom, K. E., Human papillomavirus type 16 nucleoprotein E7 is a tumor rejection antigen, *Proc. Natl. Acad. Sci. USA*, 88(1), 110, 1991.
20. Chen, L., Mizuno, M. T., Singhal, M. C., Hu, S. L., Galloway, D. A., Hellstrom, I. and Hellstrom, K. E., Induction of cytotoxic T lymphocytes specific for a syngeneic tumor expressing the E6 oncoprotein of human papillomavirus type 16, *J. Immunol.*, 148(8), 2617, 1992.
21. Hurwitz, A. A., Yu, T. F., Leach, D. R. and Allison, J. P., CTLA-4 blockade synergizes with tumor-derived granulocyte-macrophage colony-stimulating factor for treatment of an experimental mammary carcinoma, *PNAS*, 95(17), 10067, 1998.
22. Park, K., Shalaby, W. S. W. and Park, H., *Biodegradable Hydrogels for Drug Delivery*, Technomic Publishing, Lancaster, PA, 1993.
23. Baschnagel, A., Johner, A. and Joanny, J. F. Adsorption kinetics of a bidisperse polymer solution, *Eur. Phys. J.*, 6, 45, 1998.
24. Gotting, N., Fritz, H., Maier, M., von Stamm, J., Schoofs, T. and Bayer, E., Effects of oligonucleotide adsorption on the physicochemical characteristics of a nanoparticle-based model delivery for antisense drugs, *Colloid Polym. Sci.*, 277, 145, 1999.
25. Shubin, V., Samoshina, Y., Menshikova, A. and Evseeva, T., Adsorption of cationic polyelectrolyte onto a model carboxylic latex and the influence of adsorbed polycation on the charge regulation at the latex surface, *Colloid Polym. Sci.*, 275(7), 655, 1997.

26. Nguyen, S. H. and Berek, D., Adsorption and desorption of macromolecules on solid surfaces studied by on-line size exclusion chromatography 2. Preferential adsorption and exchange processes, *Colloid Polym. Sci.*, 277, 1179, 1999.
27. Singh, M., Briones, M., Ott, G. and O'Hagan, D., Cationic microparticles: A potent delivery system for DNA vaccines, *Proc. Natl. Acad. Sci. USA*, 97(2), 811, 2000.
28. Tabata, Y., Inoue, Y. and Ikada, Y., Size effect on systemic and mucosal immune responses induced by oral administration of biodegradable microspheres, *Vaccine*, 14(17-18), 1677, 1996.
29. Dange, C., Aprahamian, M., Marchais, H., Benoit, J. P. and Pinget, M., Intestinal absorption of PLGA microspheres in the rat, *J. Anat.*, 189(Pt 3), 491, 1996.
30. Shalaby, S. W., *Biomedical Polymers, Designed to Degrade Systems*, Hanser Publishers, New York, 1994.
31. Golumbek, P. T., Azhari, R., Jaffee, E. M., Levitsky, H. I., Lazenby, A., Leong, K. and Pardoll, D. M., Controlled release, biodegradable cytokine depots: a new approach in cancer vaccine design, *Cancer Res.*, 53(24), 5841, 1993.
32. Egilmez, N. K., Jong, Y. S., Iwanuma, Y., Jacob, J. S., Santos, C. A., Chen, F. A., Mathiowitz, E. and Bankert, R. B., Cytokine immunotherapy of cancer with controlled release biodegradable microspheres in a human tumor xenograft/SCID mouse model, *Cancer Immunol. Immunother.*, 46(1), 21, 1998.
33. Ma, J., Samuel, J., Kwon, G. S., Noujaim, A. A. and Madiyalakan, R., Induction of anti-idiotypic humoral and cellular immune responses by a murine monoclonal antibody recognizing the ovarian carcinoma antigen CA125 encapsulated in biodegradable microspheres, *Cancer Immunol. Immunother.*, 47(1), 13, 1998.
34. Kuriakose, M. A., Chen, F. A., Egilmez, N. K., Jong, Y. S., Mathiowitz, E., DeLacure, M. D., Hicks, W. L., Jr., Loree, T. L. and Bankert, R. B., Interleukin-12 delivered by biodegradable microspheres promotes the antitumor activity of human peripheral blood lymphocytes in a human head and neck tumor xenograft/SCID mouse model, *Head Neck*, 22(1), 57, 2000.
35. Egilmez, N. K., Jong, Y. S., Sabel, M. S., Jacob, J. S., Mathiowitz, E. and Bankert, R. B., *In situ* tumor vaccination with interleukin-12-encapsulated biodegradable microspheres: induction of tumor regression and potent antitumor immunity, *Cancer Res.*, 60(14), 3832, 2000.
36. Hill, H. C., Sabel, M., Egilmez, N. and Bankert, R. B., An in-situ neoadjuvant vaccination with IL-12 and GM-CSF in biodegradable microspheres with systemic IL-2 provides protection against metastatic disease, *J. Am. Coll. Surg.*, 191, Suppl. 1, S19, 2000.
37. Mullerad, J., Cohen, S., Voronov, E. and Apte, R. N., Macrophage activation for the production of immunostimulatory cytokines by delivering interleukin 1 via biodegradable microspheres, *Cytokine.*, 12(11), 1683, 2000.
38. Peppas, N. A., Bures, P., Leobandung, W. and Ichikawa, H., Hydrogels in pharmaceutical formulations, *Eur. J. Pharm. Biopharm.*, 50(1), 27, 2000.
39. Griffith, L. G., Polymeric Biomaterials, *Acta Mater.*, 48, 263, 2000.
40. Langer, R., Biomaterials and Biomedical Engineering, *Chem. Eng. Sci.*, 50(24), 4109, 1995.

41. Denis-Mize, K. S., Dupuis, M., MacKichan, M. L., Singh, M., Doe, B., O'Hagan, D., Ulmer, J. B., Donnelly, J. J., McDonald, D. M. and Ott, G., Plasmid DNA adsorbed onto cationic microparticles mediates target gene expression and antigen presentation by dendritic cells, *Gene Ther.*, 7(24), 2105, 2000.
42. Shalaby, W. S. W., Yeh, H., Woo, E., Hendron, S., Corbett, J. T., Gray, H., June, C. H. and Shalaby, S. W., *J. Controlled Rel.*, 2003 (in press).
43. Pantazaki, A., Baron, M. H., Revault, M. and Vidal-Madjar, C., Characterization of human serum albumin adsorbed on a porous anion-exchange support, *J. Colloid Interface Sci.*, 207, 324, 1998.

Index

A

- A/BP, *see* Absorbable/biodegradable polymers
- Absorbable/biodegradable devices, toxicity, 151
- Absorbable/biodegradable polymers (A/BP), 4, 5
- Absorbable biomaterial design, order of toxicity testing in, 147
- Absorbable copolymers, block/segmented, 26
- Absorbable implants, 162
- Absorbable medical devices, advances in
 - morphological development to tailor performance of, 113–141
 - advanced methods to accelerate
 - crystallization kinetics of absorbable copolymers, 130–135
 - novel synthetic method using mixed initiators, 132–135
 - stress-induced crystallization, 130–131
 - effect of crystallinity on segmental dynamics, 122–129
 - effect on glass transition temperature, 122–126
 - intra- and inter-spherulitic amorphous phase dynamics, 127–129
 - effect of morphology on polymer
 - absorption profiles, 135–138
 - drug delivery vehicles, 138
 - effect of crystallinity, 136
 - effect of molecular orientation, 135–136
 - hydrolysis profiler, 137–138
 - methods and techniques for monitoring
 - crystallinity, 116–121
 - overall crystallization kinetics, 119–121
 - supramolecular crystal developments, 116–119
 - novel polyesters, 138–139
 - perspective on future, 139
- Absorbable polymers
 - application of in vascular grafts, 187
 - evolution of, 162
- Absorbable synthetic polymers, homochain ester-based, 7
- ACP sponges, 96
- Acquired immunodeficiency syndrome (AIDS), 49
- Acute toxicity, 145
- Adhesion
 - pelvic, 192
 - prevention of postoperative, 53, 93
 - rating criteria, 200
 - reduced incidence of postoperative, 8
 - scores, 201
- Adhesive(s)
 - consumer-type, 60
 - formulations, uncured, 64
 - industrial, 60
 - joint strength, 60, 66
 - strength, tensile strength of, 66
 - tissue
 - comparison of absorbable and nonabsorbable, 74
 - in vivo* performance of, 72
 - model, 68
 - polymerization scheme, 63
 - properties of, 62
 - radiolabeled, 70
 - sutures vs., 61
 - wound healing strength of, 73
- Adrenalitis, 49
- Adriamycin, 243
- Adrucil, 243
- AFM, *see* Atomic force microscopy
- Agar diffusion assay, 149
- AIDS, *see* Acquired immunodeficiency syndrome
- ALCAP, *see* Aluminio–calcium–phosphorous oxide
- Alginate, 152, 161
- All-*trans*-retinoic acid (ATRA), 82
- Altretamine, 243

Alumino–calcium–phosphorous oxide (ALCAP), 220
 American Society for Testing and Materials, 144
Ames salmonella, 146
 Amino acids, RGD sequence of, 168
 Anesthetic agents, 41
 Angiogenesis, 192
 Anterior segment surgery, 92
 Anthrax vaccine, 46
 Antibiotic(s), 41
 carriers of, 8
 chitosan films and, 78
 periodontal application of, 45
 -releasing chitosan bone scaffolds, 81
 vehicles for controlled delivery of, 46
 Antifungals, 41
 Antigen-presenting cells (APCs), 257–258, 260
 Antimicrobial agents, 41
 Antimitotic agents, 93
 Antiplatelet agent, 201
 Antiviral
 intravitreal injections of, 50
 therapy, intravenous, 49
 APCs, *see* Antigen-presenting cells
 Area under the curve (AUC), 238, 248
 Arterial seals, 176
 Arterio-venous shunt systems, 153
 Articular cartilage, wound healing of, 84
 Atomic force microscopy (AFM), 116
 ATRA, *see* All-*trans*-retinoic acid
 AUC, *see* Area under the curve

B

Bacillus anthracis, 46
 Basic fibroblast-derived growth factor (bFGF), 51
 bFGF, *see* Basic fibroblast-derived growth factor
 Biocompatibility
 determination of, 144
 PLA pellets, 212
 testing, 144
 Biodegradable plastics, 94
 Biodegradable polymers, therapeutic objectives, 244
 Biodegradation, definition of, 243
 Biologically friendly implant, 177
 Biomaterials, hemocompatibility requirements of, 175–176
 Biomedical devices, polyaxial polymers and, 36

Biomolecules, as drug delivery system, 217
 Blenoxane, 243
 Bleomycin, 243
 Block copolymer, 108
 PEG, 217
 PLGA, 217
 Body surface area (BSA), 234, 238
 Bone
 imaging, radioisotope-bearing PEG-PCL for, 52
 osteomyelitis-inflicted, 81
 Bowman–Birk inhibitor, 82
 Braid construction, segmented copolylactides used for, 22
 Breaking strength retention (BSR), 15, 16
 data, copolyester compositions of, 33
 hydrolytic stability data of films, 35
 in vitro, 20, 22, 31
 in vivo, 21, 22
 radiochemically sterilized sutures, 32
 Breast cancer, node-positive, 233
 BSA, *see* Body surface area
 BSR, *see* Breaking strength retention
 Burn wounds, healing of, 8
 Burst kinetics, 209

C

Calcium phosphate cement (CPC), 83
 Camptosar, 243
 Cancer, *see also specific types*
 chemotherapy, gold standard for, 239
 mortality, leading causes of, 228
 treatments, chitosan and, 82
 Cancer therapy, absorbable delivery systems for, 227–255
 emerging challenges for cancer chemotherapy, 232–249
 absorbable delivery systems to manipulate drug exposure duration pegylated systems, 244–245
 biodegradable or absorbable polymers for drug delivery, 242–244
 clinical model for dose determination and schedule, 237–239
 defining therapeutic index for chemotherapy agents, 240
 dose-densification using paclitaxel, 234–236
 dose-densification using prolonged infusion of paclitaxel, 236–237
 rationale for sustained drug delivery, 240–242

- site specific (intracranial), 245–246
- site-specific (intratumoral), 246–249
- models of tumor growth, 228–232
- perspective on future, 249–250
- CAP, *see* Chitosan coated with polylysine
- Capecitabine, 243
- ϵ -Caprolactone (CL), 6, 16, 18, 21, 29, 40
 - microporous prostheses made of, 184
 - polyalkylene succinate prepared with, 108
 - polytrimethylene succinate end-grafted with, 109
- Carbon-13 NMR, 135
- Carboplatin, 243
 - clearance, 238
 - dosage, 239
- Carmustine, 246
- Cartilage
 - mechanical properties of, 92
 - repair, 95
 - replacement materials for damaged, 95
- Catecholamines, 222
- CBS, *see* Chitosan-based systems
- CDDP-EPI gel, *see* Cisplatin/epinephrine/bovine collagen
- Cell(s)
 - antigen-presenting, 257–258
 - apoptosis, definition of, 230
 - cycle kinetics, 228
 - death, 230
- Cellular events, regulation of, 41
- Cellular xenotransplantation, 154
- Cervical ripening
 - modulus of elasticity, 48
 - PEG-based controlled release systems for, 47
- Chain molecule, basic design of, 16
- Chemically controlled systems
 - biodegradable, 208
 - pendant chain, 208
- Chemotherapy agents, half-lives of, 243
- Chitosan(s)
 - absorbable/biodegradable polysaccharides and, 4
 - bone scaffolds, antibiotic-releasing, 81
 - calcium phosphate complex, 81
 - challenge in production of, 77
 - coated with polylysine (CAP), 83
 - genipin-treated, 81
 - membrane, neutrons cultured on, 83
 - microcapsules, 219
 - phosphorylated, 83
 - safety, 78
 - toxicity, 152
 - water-soluble, 79
 - xanthan (CH-X), 81
- Chitosan-based systems (CBS), 77–89
 - advances in, 78–80
 - chitosan-based materials and clinical relevance, 78–79
 - processing of chitosan-based systems and clinical relevance, 79–80
 - advances in CBS applications, 80–85
 - biomedical applications, 83–84
 - healthcare applications, 84
 - pharmaceutical applications, 81–83
 - tissue engineering, 84–85
 - perspective on future, 85
- Chronic toxicity, 145
- CH-X, *see* Chitosan-xanthan
- Cidofovir, 49
- CIMS, *see* Crystallization-induced microphase separation
- Cirrhosis, 247
- Cisplatin, 243
- Cisplatin/epinephrine/bovine collagen (CDDP-EPI gel), 247, 248
- CL, *see* ϵ -Caprolactone
- Cleavage-induced crystallization, 136
- Clinical trials, phase I, 240
- Closed vitrectomy, 92
- CMC, *see* Critical micelle concentration
- CMV, *see* Cytomegalovirus
- Coagulation tests, 78
- Cockcroft formula, 238
- Colitis, 49
- Collagen(s)
 - based polymers, 161
 - matrix, surface erosion in, 181
 - synthesis, inhibitors of, 193
 - toxicity, 152
- Compression molded films
 - hydrolytic stability data of, 35
 - thermal properties of, 35
- Consumer-type adhesives, 60
- Controlled drug delivery
 - systems, inadvertent drug overdose, 208
 - vehicles, 114
- Copolyester(s)
 - aliphatic, *see* Crystalline fiber-forming aliphatic copolyesters, new approaches to synthesis
 - gel-forming, 41, 194, 201
 - PEG, 40, 41
 - advantages of, 42
 - leaching process, 42
 - local drug delivery and, 45
 - placebos, 199
 - radiation-sterilizable, 6
- Copolymer(s)

- absorbable, block/segmented, 26
- bioadhesive, 82
- block, 108
 - PEG, 218
 - PLGA, 218
- braided sutures, 19
- caprolactone-glycolide segmented, 104
- clock heterochain, 26
- crystalline, precrystallization viscosity, 27
- ethylene-vinyl acetate, 209
- glycolide
 - /caprolactone segmented, fiber
 - properties of, 107
 - containing, 119
 - microporous prostheses made of, 184
 - polyalkylene succinate, end-grafted, 110
 - properties of, 17, 18
- Copolymerization, one-step, 110
- Corneal perforation, 92
- Coronary artery vascular graft, ideal, 180
- Corticosteroids, 222
- CPC, *see* Calcium phosphate cement
- Critical micelle concentration (CMC), 52, 53
- Crosslinked polyacrylamide systems, 209
- Crystal growth, relaxation, 128
- Crystalline fiber-forming aliphatic
 - copolyesters, new approaches to
 - synthesis of, 103–111
 - copolyesters made by end-grafting cyclic
 - monomers onto polyalkylene
 - succinate and monofilament
 - sutures thereof, 108–110
 - design of polymerization scheme and
 - rationale, 108–109
 - physical and *in vivo* properties of
 - typical monofilament sutures,
 - 109–110
 - properties of typical polymers, 109
 - one-step synthesis of caprolactone-
 - glycolide segmented copolymers
 - and monofilament sutures
 - thereof, 104–107
 - design of polymerization scheme and
 - rationale, 104–105
 - physicochemical and biological
 - properties of typical
 - monofilament sutures, 105–107
 - properties of typical polymers, 105
 - perspective on future, 110
 - Crystallization
 - cleavage-induced, 136
 - induced microphase separation
 - (CIMS), 8
 - isothermal, quantitative measure of, 120
 - kinetics, 119
 - advanced methods to accelerate, 130
 - manipulation of, 130
 - onset of, 124
 - PDS, 129
 - phenomena, 118
 - rate, 121, 131
 - stress-induced, 130
 - temperature, 123
 - C-TA, *see* Cyanoacrylate tissue adhesive
 - Cushing-like syndrome, 234
 - Cyanoacrylate(s)
 - tissue adhesive (C-TA), 200
 - toxicity profiles of, 152
 - Cyanoacrylate-based systems as tissue
 - adhesives, 59–75
 - evolution of evaluation methods for
 - synthetic absorbable tissue
 - adhesives, 64–74
 - effect of pH on molecular weight and
 - thermal properties of absorbable
 - tissue adhesives, 64–65
 - in vitro* evaluation of adhesive joint
 - strength and pertinent data,
 - 66–68
 - in vitro* and *in vivo* absorption profiles
 - and typical results, 69–72
 - in vivo* performance of absorbable
 - tissue adhesives, 72–74
 - uncured adhesive formulations, 64
 - perspective on future, 75
 - rationale for and genesis of synthetic
 - absorbable cyanoacrylate-based
 - systems, 61–62
 - unique properties of absorbable tissue
 - adhesives and evolution of
 - cyanoacrylate-based systems,
 - 62–63
 - Cyclodextrin derivative, carboxyl-bearing, 9
 - Cyclophosphamide, 243
 - Cytokines, 93, 261
 - Cytomegalovirus (CMV), 49
 - Cytotoxicity testing, 148
 - Cytoxan, 243

D

- Dacarbazine, 237, 243
- Dacron grafts, 179
- Daunorubicin, 245
- DCC, *see* Dicyclohexylcarbodiimide
- DD, *see* Dodecanol
- DED, *see* Drug exposure duration
- Deep wounds, treatment of, 85
- DEG, *see* Diethylene glycol

DFS, *see* Disease-free survival

Diabetes mellitus, implantable insulin
 controlled release systems for
 treating, 205–226

 absorbable polymeric delivery systems,
 211–217

 block copolymers/hydrogels, 216–217

 polylactic acid microcapsules, 213–215

 polylactic acid pellets, 212–213

 polylactic-*co*-glycolic acid
 microcapsules, 215–216

 biomolecules as drug delivery systems,
 217–220

 chitosan microcapsules, 219–220

 lipid microparticles, 218

 liposomes, 218

 serum albumin beads, 218–219

 ceramic delivery systems, 220–221

 alumino–calcium–phosphorus oxide
 ceramic systems, 220–221

 hydroxyapatite ceramic
 microspheres, 220

 zinc–calcium–phosphate oxide
 ceramic systems, 221

 early nonabsorbable polymeric insulin
 delivery systems, 209–211

 crosslinked polyacrylamide
 systems, 209

 ethylene–vinyl acetate copolymer
 pellets, 209–211

 genesis and general types of controlled
 drug delivery systems, 207–209

 perspective on future, 221–224

Diabetics, insulin-requiring, 206

Dicyclohexylcarbodiimide (DCC), 52

Dielectric relaxation spectroscopy (DRS), 120

 detection of crystallinity by, 126

 overall crystallization rate from, 121

Diethylene glycol (DEG), 133

Diethylenetriamine pentaacetic acid
 (DTPA), 53

Differential scanning calorimetry (DSC), 28,
 30, 119–120

 determination of polymer thermal
 properties using, 65

 thermal data, annealed polymer, 35

Dimethylsulfoxide (DMSO), 167

p-Dioxanone, 40

1,5 Dioxepan-2-one (DOX), 6

Disease-free survival (DFS), 234

DMSO, *see* Dimethylsulfoxide

DNA

 adsorption, enhanced, 261

 evaluation, 150

 vaccines, 271

Docetaxel, 243

Dodecanol (DD), 133

DOX, *see* 1,5 Dioxepan-2-one

Doxorubicin, 237, 243, 245

Doxycycline, 8, 48

DRS, *see* Dielectric relaxation spectroscopy

Drug

 delivery

 biodegradable polymers for, 242

 cryopreservation, HA as
 adjuvant in, 97

 intraocular, 45

 rate-limiting barrier to, 207

 rationale for sustained, 240

 system, biomolecules as, 217

 exposure duration (DED), 241, 244

 -HA bioconjugates, 98

 overdose, inadvertent, 208

DSC, *see* Differential scanning calorimetry

DTIC-Dome, 243

DTPA, *see* Diethylenetriamine pentaacetic
 acid

E

EDTA, *see* Ethylene-diamine-tetra-acetic acid

EGF, *see* Epidermal growth factor

Electron spectroscopy for chemical analysis
 (ESCA), 265

Elimination kinetics, 232

ELISA, *see* Enzyme-linked immunosorbent
 assay

Ellence, 243

Embryonic extracellular matrix changes,
 mimicking of, 97

Encephalitis, 49

Endosomolytic peptide, 83

End-stage renal disease, 206

Enzymatic degradation, prevention of, 82

Enzyme

 -linked immunosorbent assay
 (ELISA), 269

 stability, 92

EO, *see* Ethylene oxide

Epidermal growth factor (EGF), 5

Epirubicin, 243

ePTFE, *see* Expanded polytetrafluoroethylene

Erythropoietin, 53

ESCA, *see* Electron spectroscopy for chemical
 analysis

Esophagitis, 49

Ester–ester interchange, 30

Ethylene-diamine-tetra-acetic acid (EDTA),
 82, 83

Ethylene oxide (EO), 115
 Ethylene–vinyl acetate copolymer (EVAC),
 209, 210, 211
 Etoposide, 237
 EVAC, *see* Ethylene–vinyl acetate copolymer
 Expanded polytetrafluoroethylene (ePTFE),
 44, 176, 179, 186
 Extract assays, 149

F

Fabric peel test (FPT), 67, 68
 Fatty acids, acylation of insulin with, 222
 Femoral sealing devices, absorbable, 184, 185
 Fertility, impaired, 192
 Fibrinolysis, 192
 Fibronectin, 168
 Filament-wound prostheses, 182
 Fluorouracil, 238
 Formaldehyde, detection of in body
 tissues, 71
 Fosarnet, 49
 FPT, *see* Fabric peel test
 Fracture fixation pin, 152
 Free-radical polymerization, 64, 65

G

GA, *see* Glycolic acid
 GAG, *see* Glycosaminoglycan
 Gamma irradiation, 146
 Ganciclovir, 49, 50
 Gas foaming, 167
 Gel-former (GF), 8, 44, 200
 Gel-forming copolyesters, 41
 Gel-permeation chromatography (GPC),
 28, 29, 199
 Gel–sol transition temperature, 216, 217
 Gemcitabine, 243
 Gemzar, 243
 Genotoxicity, methods to assess, 150
 GF, *see* Gel-former
 GFR, *see* Glomerular filtration rate
 Glass transition temperature, 28, 115, 122, 215
 Glomerular filtration rate (GFR), 238
 Glucagon, 222
 Glucosuria, 210
 Glutaraldehyde, 81
 Glycolic acid (GA), 198
 Glycolide, 6, 40
 /caprolactone segmented copolymers,
 fiber properties of, 107
 polymers, 133

Glycosalicylate (GS), 6
 Glycosaminoglycan (GAG), 84
 GM-CSF, *see* Granulocyte-macrophages
 colony stimulating factor
 Goatskin model, 66
 Gompertz growth equation, 229
 Gompertzian growth kinetics, 233
 Gompertzian tumor model, 232
 Gore-Tex
 grafts, 182
 Surgical Membrane®, 194
 GPC, *see* Gel-permeation chromatography
 Graft(s)
 Dacron, 179
 DS woven, 177
 ePTFE, 179, 186
 Gore-Tex, 182
 sterility, 176
 vascular, 17, 44
 application of absorbable polymers
 in, 178
 coronary artery, 180
 Vicryl, 179
 Granulocyte-macrophages colony
 stimulating factor (GM-CSF),
 261, 264
 Growth hormone, 222
 GS, *see* Glycosalicylate

H

HA, *see* Hyaluronic acid
 HA, *see* Hydroxyapatite
 HA
 covalent modification of, 94
 hydrophilicity of, 96
 receptors, 98
 viscosity, 195
 HA-Na, *see* Sodium hyaluronate
 HCC, *see* Hepatocellular carcinoma
 Head and neck cancer, 235
 Healed incision strength, 73
 Healthcare, chitosan-based systems in, 84
 Heat shock proteins (HSP), 259
 Hemoagglutination tests, 78
 Hepatocellular carcinoma (HCC), 247, 249
 Hernia repair, 16
 Hexalen, 243
 Hot-stage optical microscopy (HSOM), 116,
 118, 134
 HPP, *see* Hydroxyphenylpropionic acid
 HSOM, *see* Hot-stage optical microscopy
 HSP, *see* Heat shock proteins
 Hyaluronic acid (HA), 91

alkyl esters of, 94
 formulations, multivalent ion-modified, 195, 196
 technology, evolution of, 4
 Hyaluronic acid-based systems, 91–100
 advances in application of sodium hyaluronate, 92–93
 key roles of HA and derivatives in therapeutic applications, 97–98
 drug-HA bioconjugates, 98
 HA as adjuvant in drug delivery cryopreservation, 97–98
 modification of HA and advances in application of modified forms, 93–97
 complex formation of HA with other functional polymers, 93–94
 covalent modification of HA, 94–97
 ionic interaction of HA with divalent and trivalent metallic ions, 93
 perspective on future, 98
 Hycamtin, 243
 Hydrolysis profiler, 137
 Hydroxyapatite (HA), 220
 Hydroxyphenylpropionic acid (HPP), 53
 Hyperglycemia, 206, 210
 Hypoinsulinemia, 210

I

Ibuprofen, 78
 IBW, *see* Ideal body weight
 Ideal body weight (IBW), 239
 IFEX, 243
 Ifosfamide, 237, 243
 IL-4, *see* Interleukin-4
 Immunostimulatory agents, 41
 Immunosuppressive agents, 41
 Immunosurveillance, 257
 Immunotherapy
 key aspects of contemporary, 258
 role of synthetic absorbable polymers in, 263
 Implant(s)
 biologically friendly, 177
 porosity of tubular, 177
 tissue-engineered constructs vs., 169
 Implantable insulin controlled release systems, *see* Diabetes mellitus, implantable insulin controlled release systems for treating
 Incert®, 194
 Indomethacin, 51

Industrial adhesives, 60
 Infection, graft sterility and, 176
 Infrared spectroscopy (IR), 28
 Injectable polymers, 169
 Injection molded products, 114
 Insulin
 acylation of with fatty acids, 222
 deactivation of, 216
 deficiency, 206
 delivery
 early nonabsorbable polymeric, 209
 system, EVAC-based, 210
 /dichloromethane dispersion, 215
 glargine, 222
 hydroxyapatite as delivery system for, 220
 lente, 222
 -loaded EVAC pellets, 211
 NPH, 222
 release profile, 213, 222
 resistance, 206
 therapy, shortcomings of, 207
 ultralente, 222
 Interceed®, 194
 Interleukin-4 (IL-4), 196, 197
 International Organization for Standardization (ISO), 143
 Intramuscular drug-delivery agent, 8
 Intraocular drug delivery, 45
 Intraocular pressure, postoperative, 92
In vitro fertilization procedures, improvement of artificial, 98
In vitro toxicity assessment, 148
 IR, *see* Infrared spectroscopy
 Irinotecan, 243
 ISO, *see* International Organization for Standardization
 Isothermal crystallization, quantitative measure of, 120

K

Ketoprofen, *in vitro* release profile of, 80
 Kinetics
 cell-cycle, 228
 elimination, 232
 Gompertzian growth, 233
 Kohlrausch–Williams–Watts (KWW)
 function, 129
 Kruskal–Wallis analysis of variance, 97
 KWW function, *see* Kohlrausch–Williams–Watts function

L

Lactide, 20, 40
 Lactones, polymerization of, 6
 Lanreotide, 201
 Lauritzen and Hoffmann (LH) nucleation theory, 119
 Lente insulin, 222
 LH nucleation theory, *see* Lauritzen and Hoffmann nucleation theory
 Liposomes, definition of, 218
 Litchfield-Wilcoxon method, 51
 Lubricants, viscoelastic, 98
 Lung cancer, 235
 Lymphocyte subset depletion studies, 262

M

Machine direction, molecular orientation and, 115
 MAG3, *see* Mercaptoacetyl glycine glycidyl glycine
 Maximum tolerated dose (MTD), 237
 Maximum tolerated regime (MTR), 240
 MD, *see* Morpholine-2,5-dione
 Mean resident time (MRT), 248
 Medical devices, absorbable, *see* Absorbable medical devices, advances in morphological development to tailor performance of
 Melting temperature, 28
 MEMS, *see* Micro electromechanical systems
 MEP, *see* Middle endothermic peak
 MePEG, *see* Methoxy polyethylene glycol
 MER, *see* Minimum effective regimen
 Mercaptoacetyl glycine glycidyl glycine (MAG3), 53
 Methotrexate, 243
 Methoxy polyethylene glycol (MePEG), 51
 Methoxypropyl cyanoacrylate (MPC), 7, 43, 63
 Micro electromechanical systems (MEMS), 122
 Middle endothermic peak (MEP), 28
 Minimum effective regimen (MER), 240
 Mitomycin C (MMC), 79, 243
 Mitozytrex, 243
 MMC, *see* Mitomycin C
 Model tissue adhesive, 68
 Monofilament(s)
 physical properties of, 19
 sutures
 copolymers for, 18, 103
 in vivo properties of, 109

 properties of, 29, 105, 107
 tensile properties of, 32
 tensile properties of typical oriented, 30
 Monomer(s)
 -to-catalyst ratio, 105, 133
 conversion, 28
 copolymerization with cyclic, 26
 cyanoacrylate, 70
 cyclic, 7, 8, 17
 copolymerization with, 26
 end-grafting, 108, 199
 reacting, 27
 free-radically polymerized, 64
 hard phase-forming, 108
 lactone, 139
 removal of residual, 30, 34
 sequences, distribution of, 135
 soft phase-forming, 108
 tissue response to, 60
 toxic, 152
 unreacted, 18
 vinyl, 60
 Morpholine-2,5-dione (MD), 6
 MPC, *see* Methoxypropyl cyanoacrylate
 MRT, *see* Mean resident time
 MTD, *see* Maximum tolerated dose
 MTR, *see* Maximum tolerated regimen
 MTS MiniBionix Universal Testing Unit, 19, 20, 30, 33, 67
 Multifilament sutures, 114

N

Naproxen sodium (NP), 195, 196
 Natural polymers, 161, 162
 Navelbine, 243
 Neovascularization, 44
 Newtonian viscosity, zero shear rate, 95
 Nexaband®, 74
 NMR, *see* Nuclear magnetic resonance
 Non-small cell lung cancer (NSCLC), 236
 Nonsteroidal antiinflammatory drugs (NSAIDs), 41, 78, 93, 193, 195
 NP, *see* Naproxen sodium
 NPH insulin, 222
 NSAIDs, *see* Nonsteroidal antiinflammatory drugs
 NSCLC, *see* Non-small cell lung cancer
 Nuclear magnetic resonance (NMR), 18, 28, 199
 carbon-13, 135
 polymer composition determined by, 133
 Nucleation
 density, 131

- rates, 130
 - parameters, use of HSOM method to monitor, 118
 - visual characterization method and, 116
- Nylon
 - peel test, 67
 - synthetic polymers based on, 243
- O**
 - Oligopeptides, amine-bearing, 4
 - Oncovin, 243
 - OPN, *see* Osteopontin
 - Orthopedic devices, absorbable polymers used in, 7
 - Orthopedics, use of absorbable systems in, 15
 - Osteomyelitis, 45, 81
 - Osteopontin (OPN), 84
 - Ovarian cancer, platinum-resistant, 235
- P**
 - PAA, *see* Polyacrylamide
 - Paclitaxel, 51, 201, 243
 - dose-densification using, 234, 236
 - infusion, prolonged, 237
 - steady-state drug concentration, 241
 - Panacryl[®], 19
 - Paraplatin, 243
 - Parkinson's disease, 160
 - Particulate leaching technique, 165, 166
 - P-C, *see* Phosphorylated chitosan
 - PCL, *see* Poly- ϵ -caprolactone
 - PDL-LA, *see* Poly D-L lactide
 - PDS, *see* Poly(*p*-dioxanone)
 - PEC, *see* Polyelectrolyte
 - PEG, *see* Polyethylene glycol
 - PELA, *see* Polyethylene oxide and polylactic acid
 - Pelvic adhesions, 192
 - PEO, *see* Polyethylene oxide
 - Periodontal therapy, doxycycline controlled release system for nonsurgical, 48
 - Peripheral nerves, regeneration of, 160
 - Peripheral nervous system, diabetes and, 206
 - PET, *see* Polyethylene terephthalate
 - PGA, *see* Polyglycolide
 - PG-MP, *see* Polyglycolide microparticles
 - PHA, *see* Polyhydroxyalkanoates
 - Phase I clinical trials, 240
 - PHB, *see* Poly(2-hydroxybutyrate)
 - PHEMA, *see* Polyhydroxyethylmethacrylate
 - Phosphorylated chitosan (P-C), 83
 - Photopolymerizable PEG-copolyesters, 53
 - PLA, *see* Polylactic acid
 - Plastics, biodegradable, 94
 - Platelet aggregation, 176
 - Platinol, 243
 - PLGA, *see* Poly-L-lactide-co-glycolide
 - PLLA, *see* Poly-L-lactic acid
 - PMMA, *see* Polymethylmethacrylate
 - PMN, *see* Polymorphonuclear leukocytes
 - P-MPC, *see* Polymethoxypropyl cyanoacrylate
 - PMR, *see* Proton-magnetic resonance
 - Pneumonitis, 49
 - POA, *see* Postoperative adhesion prevention
 - POEs, *see* Polyoxaesters
 - Polyacrylamide (PAA), 209
 - Polyalkylene succinate copolymers, end-grafted, 110
 - Polyamidoesters, 6
 - Polyanhydrides, 6
 - Polyaxial crystalline fiber-forming copolyester, 25–37
 - perspective on future, 36
 - synthesis and properties of typical polyaxial polymers, 26–36
 - conceptual designs of polyaxial chain, 26–28
 - contributions of polyaxial chain configuration and composition of polymeric initiators to thermal and hydrolytic stability, 34–36
 - effect of composition on breaking strength retention of radiochemically sterilized sutures, 32–33
 - examples of polyaxial copolyesters and properties of monofilament sutures therefrom, 29
 - polyaxial copolyesters with different central atoms and monofilaments thereof, 29–31
 - preparation and processing of selected polyaxial copolyesters as synthetic alternatives to surgical gut suture, 31–32
 - Polyaxial initiators (PPIs), 27, 28, 34
 - Polyaxial polymeric initiators, crystalline end-grafted products and, 36
 - Polyaxial polymers
 - biomedical devices and, 36
 - synthesis and properties of, 26
 - Poly- ϵ -caprolactone (PCL), 51
 - Polycationic polypyrrole (PP), 94
 - Polydioxanone, 161

- Poly(*p*-dioxanone) (PDS), 116
 crystallization, 128, 129, 130
 dielectric loss of, 129
 homopolymer, 134
 HSOM images of, 119
 relaxed permittivity of, 121
 spherulite, birth of, 116
 woven grafts, 177
 wrapping, 183
- Polyelectrolyte (PEC), 84
- Polyesters
 deficiency of, 167
 fiber-forming, 25
- Polyethylene glycol (PEG), 6, 8, 40, 161
 -based copolyesters
 advantages of, 42
 leaching process, 42
 local drug delivery and, 45
 block copolymer of, 217
 copolyesters of, 41
 diglycidyl ether, 96
 end-grafting of with cyclic monomers, 199
 FDA approval of, 244
 -liposomal doxorubicin, 245
- Polyethylene glycol-based copolyesters, 39–58
 advances in solid PEG-based
 copolyesters, 50–53
 alternating multiblock copolymers in
 wound healing compositions, 51
 copolyether-ester block copolymers
 for thermo-responsive controlled
 delivery systems, 52
 in situ crosslinkable PEG-based
 copolymers for protein
 controlled delivery, 53
 nanospheres of PEG-polycaprolactone
 A-B block copolymer as novel
 drug carrier, 51–52
 radioisotope-bearing PEG-PCL for
 bone imaging, 52–53
 novel gel-forming liquid PEG-based
 copolyesters, 40–50
 advances in applications of controlled
 delivery systems and clinical
 relevance, 45–50
 advances in biomedical applications
 and clinical relevance, 43–45
 molecular design and attributes of
 tailored properties, 40–43
 perspective on future, 54
 photopolymerizable
 PEG-copolyesters, 53
- Polyethylene oxide (PEO), 51, 161
- Polyethylene oxide and polylactic acid
 (PELA), 181
 elastomer, degradation and dissolution
 of, 181
 graft sealant and, 182
- Polyethylene terephthalate (PET), 176
- Polyglycolide (PGA), 160–161
 Dacron-reinforced, 177, 180
 fiber-based felt, 164
in vivo degradation of, 170
 toxicity, 152
- Polyglycolide microparticles (PG-MP), 264
 acid-terminated, 266
 immobilized, 265
 pretreatment of, 268
 release of GM-CSF from, 268
 SEM analysis, 265
- Polyhydroxyalkanoates (PHA), 5
- Poly(2-hydroxybutyrate) (PHB), 5
- Polyhydroxyethylmethacrylate
 (PHEMA), 161
- Polylactic acid (PLA), 212
 microcapsules, 213, 214
 microspheres, interleukin-12
 delivered by, 262
 pellet, implantable, 212
- Poly-*L*-lactic acid (PLLA), 51, 163
 crystallinity of, 170
 dipole loss data of constrained, 124
 glass transition temperature of, 122
 morphological change in, 125
 SALS scattering patterns on, 126
 supercooled, 124
- Polylactic-*co*-glycolic acid (PLGA), 215
 glass transition temperature, 215
 molecules, annealing of, 215
- Poly lactide(s), 160
 injection molded products of, 114
 toxicity, 152
- Poly D-L lactide (PDL-LA), 84
- Poly-L-lactide-*co*-glycolide (PLGA), 161
- Polymer(s)
 absorbable, 114
 application of in vascular grafts, 187
 /biodegradable, 4
 evolution of, 162
 synthetic, homochain ester-based, 7
 absorption profiles, effect of morphology
 on, 135
 annealed, DSC thermal data of, 35
 biodegradable, therapeutic objectives, 244
 biodegradation of, 243
 blood-contacting, 149
 collagen-based, 161
 composition, 133, 138

- crystalline fiber-forming, 20
 - crystallinity, rate of degradation and, 244
 - crystallization process, characterization of, 116
 - formation of HA with, 93
 - free-radically prepared, 64
 - gamma irradiation and, 146
 - gel-forming liquid, wound healing and, 44
 - glycolide, 133
 - hyaluron-based, 96
 - hydrolysis, monitoring of, 137
 - influence of mechanical stress on crystallizing, 131
 - injectable, 169
 - lactide-based, 20
 - morphology, 114
 - natural, 161, 162
 - polyaxial
 - biomedical devices and, 36
 - synthesis and properties of, 26
 - processing, toxicity and, 145
 - properties, 105, 106, 138
 - semicrystalline, morphological characterization of, 114
 - supramolecular structure of crystallizing, 118
 - synthetic, 160
 - degradation, 170
 - fabrication of, 163
 - tissue adhesive, 61
 - toxicity, forms of, 144
- Polymer biocompatibility and toxicity, 143–156
- critical test methods for implants and drug carriers, 154
 - evolution and status, 144–150
 - forms of polymer toxicity, 144–145
 - methods of toxicity testing, 146–150
 - polymer processing and effect on toxicity, 145–146
 - historical, 143–144
 - perspective on future, 154
 - specific absorbable/biodegradable systems, 151–154
 - devices, 151–153
 - drug carriers, 153–154
- Polymeric initiators, glycolide-containing, 35
- Polymerization
- polyacrylamide, 209
 - ring-opening, 132
 - scheme, design of, 104, 108
- Polymethoxypropyl cyanoacrylate (P-MPC), 70
- absorption of, 70, 72
 - degradation of, 71, 72
- Polymethylmethacrylate (PMMA), 46, 160
- Polymorphonuclear leukocytes (PMN), 84
- Polyorthoesters, 6
- Polyoxaesters (POEs), 138
 - homopolymer, 139
 - hydroxy termination and, 138
- Polyoxymethylene (POM), 213
- Polyphosphazenes, 6
- Polypropylene fumarate (PPF), , 170
- Polysaccharide, natural, 161
- Poly(trioxyethylene glycol oxalate) (PTOX), 43
- Poly(trioxyethylene oxalate) (PTOEO), 63, 66
- Polyurethanes (PU), 149, 176, 184
 - based prostheses, 184
 - /PLLA system, compliance of, 178
- Polyvinyl alcohol (PVA), 213
- POM, *see* Polyoxymethylene
- Postoperative adhesion (POA) prevention, 191–204
- advances in use of absorbable/biodegradable polymers for POA prevention, 194–201
 - absorbable gel-forming liquid copolyesters as transient barriers and multifaceted compositions for POA prevention, 198–201
 - covalently crosslinked HA films, 196
 - effect of pharmacological adjuvants on hyaluronic acid performance, 196–198
 - multivalent ion-modified hyaluronic acid formulations, 195–196
- approaches, 192–194
- adjuvants, 193
 - barrier systems, 194
 - surgery, 192–193
- perspective on future, 202
- Postsurgical adhesion, prevention of, 53
- PP, *see* Polycationic polypyrrole
- PPF, *see* Polypropylene fumarate
- PPIs, *see* Polyaxial initiators
- Precrystallization viscosity, crystalline copolymers, 27
- Prepolymers, end-grafting radiostable aromatic, 6
- Prostate cancer, 235
- Prosthetic tendons, 17
- Protease inhibitors, 82
- Protein(s)
 - adsorption, reversible, 261
 - controlled delivery, *in situ* crosslinkable PEG-based copolymers for, 53
 - heat shock, 259

Proton-magnetic resonance (PMR), 64
 PTOEO, *see* Poly(trioxyethylene oxalate)
 PTOX, *see* Poly(trioxyethylene glycol oxalate)
 PU, *see* Polyurethanes
 PVA, *see* Polyvinyl alcohol

R

Radiation sterilization, 42
 Radiochemical sterilization (RC-S), 9, 31
 Radiochemically sterilized sutures, 32
 RANTES, 53
 RC-S, *see* Radiochemical sterilization
 Recombinant protective antigen (r-PA), 47
 Retinal detachment, 92
 Retinitis, 49
 Ring-opening polymerization (ROP), 132
 ROP, *see* Ring-opening polymerization
 r-PA, *see* Recombinant protective antigen

S

SALS, *see* Small-angle light scattering
 SAXS, *see* Small-angle x-ray scattering
 Scanning electron microscopy (SEM), 94, 116
 Scanning electron microscopy analysis
 PG-MP, 265
 PLGA microcapsules, 215
 SCID, *see* Severe combined
 immunodeficiency
 Sealing devices, absorbable femoral, 184, 185
 Segmented copolyesters with prolonged
 strength retention profiles, 15–24
 composition and properties of typical
 copolymers and sutures thereof,
 17–23
 copolymers for braided sutures, 19–21
 copolymers for monofilament sutures,
 18–19
 effect of composition on properties of
 segmented polymers, 21–23
 molecular chain design for tailored
 properties, 16–17
 perspective on future, 23
 SEM, *see* Scanning electron microscopy
 Septrafil[®], 194
 Serum albumin beads, 218
 Severe combined immunodeficiency
 (SCID), 262
 Silk control, adhesion scores of, 201
 Silk sutures, 197, 198, 200
 Skin wounds
 closure of, 43

 healed, biomechanical strength testing
 data of, 74
 Small-angle light scattering (SALS), 116
 scattering patterns, 126, 127
 transmission measurements, 119
 Small-angle x-ray scattering (SAXS),
 118, 119, 120
 Sodium hyaluronate (HA-Na) 91
 applications of, 92
 viscoelastic properties of, 92
 Solvent casting, 165
 Spherulite
 birth of, 116
 growth rates, 119, 134
 Stagnation point flow systems, 153
 Stent mantle, absorbable, 185
 Sterilization, vacuum post-ethylene
 oxide, 146
 Steroids, 234
 Surgical articles, production of, 94
 Surgical gut suture, synthetic alternatives
 to, 31
 Suture(s)
 absorbable, monomers used in
 production of commercial, 182
 biocompatible, 23
 biodegradable, 161
 braided
 copolymers for, 19
 segmented polymers, 21
 choice of, 244
 collagen-based surgical gut, 3
 coreless, 184, 185
 industry, 152, 263
 monofilament
 copolymers for, 18, 103
 in vivo properties of, 109
 properties of, 29, 32, 105, 107
 multifilament, 114
 pH sensitive, 145
 placement, 193
 radiochemically sterilized, 32
 silk, 197, 198, 200
 sterility, 29
 surgical gut, synthetic alternatives to, 31
 tissue adhesives vs., 61
 Synchrotron radiation
 small-angle x-ray scattering, 119
 wide-angle x-ray diffraction, 120
 Synthetic polymers, 160, 162
 degradation, 170
 fabrication of, 163
 Synthetic vascular constructs, 175–189
 contemporary vascular applications of
 absorbable polymers, 184–186

- absorbable femoral sealing devices, 184–185
 - absorbable sealant/drug carrier for polytetrafluoroethylene grafts, 186
 - absorbable stent mantle, 185–186
 - partially absorbable biocomponent fibers for vascular grafts, 186
 - early development, 176
 - evolution in use of synthetic absorbable polymers for vascular grafts and patches, 176–178
 - new approaches to development of
 - vascular grafts and allied devices, 178–184
 - absorbable grafts, 178
 - general, 178
 - partially absorbable vascular grafts and wraps, 179–183
 - vascular wraps or patches, 183–184
 - perspective on future, 186–187
- T**
- TAA, *see* Tumor-associated antigens
 - Taxol, 243
 - Taxotere, 243
 - TBW, *see* Total body weight
 - T-cell activation, 264
 - TEA, *see* Triethanolamine
 - Technology evolution, absorbable/
 - biodegradable polymers, 3–12
 - evolving applications and pertinent processing methods of absorbable/biodegradable polymers, 7–10
 - enabling of new processing methods, 9–10
 - extrudable gel-forming implants, 8
 - polyester/peptide ionic conjugates, 8–9
 - scaffolds for tissue engineering, 8
 - perspective on future, 10
 - technology evolution of absorbable/
 - biodegradable polymers as materials, 4–7
 - evolution of natural absorbable/
 - biodegradable polymers, 4–5
 - evolution of synthetic absorbable/
 - biodegradable polymers, 5–7
 - TEM, *see* Transmission electron microscopy
 - TGF- β , *see* Transforming growth factor beta
 - Therapeutic index (TI), 240
 - Thermo-responsive controlled delivery systems, copolyester-ester block copolymers for, 52
 - Thrombin formation, 193
 - Thrombogenesis, 44
 - Thrombosis, 176
 - TI, *see* Therapeutic index
 - Tie molecules, 136
 - Tissue
 - adhesive(s), *see also* Cyanoacrylate-based systems as tissue adhesives
 - comparison of absorbable and nonabsorbable, 74
 - effectiveness of, 62
 - formulations, V-200, 72
 - in vitro* absorption, 69, 70
 - in vivo* performance of, 72
 - model, 68
 - peel force data of, 69
 - polymer, 61
 - polymerization scheme, 63
 - properties of, 62
 - radiolabeled, 70
 - strength of, 60
 - sutures vs., 61
 - wound healing strength of, 73
 - barriers, 194
 - application of absorbable scaffolds in, 10
 - chitosan-based systems for, 84
 - coining of term, 160
 - deficiency of polyesters used in, 167
 - definition of, 159
 - scaffolds for, 8
 - injury, 192
 - lubricant, natural, 91
 - necrosis, 146
 - regenerated, cellularity of, 179
- Tissue engineering systems, 159–174
 - clinical relevance, 169–171
 - injectable polymers, 169–170
 - synthetic polymer degradation, 170–171
 - evolution and status, 162–168
 - nonabsorbable and absorbable polymers, 162
 - scaffold design, 164–168
 - synthetic and natural polymers, 162–164
 - historical, 159–162
 - natural polymers, 161–162
 - synthetic polymers, 160–161
 - perspective on future, 171
 - TMC, *see* Trimethylene carbonate
 - TMP, *see* Trimethylolpropane

TNF, *see* Tumor necrosis factor

Tolectic acid, 78

Topotecan, 243

Total body weight (TBW), 239

Toxicity

absorbable/biodegradable devices, 151

acute, 145

assessment, *in vitro*, 148

chronic, 145

testing, 144

in vivo, 150

methods of, 146

order of in absorbable biomaterial

design, 147

TP, *see* Trepidil

Transforming growth factor beta (TGF- β), 60

Transmission electron microscopy (TEM), 116

Trepidil (TP), 196, 201

Triethanolamine (TEA), 29

Trimethylene carbonate (TMC), 18, 29, 40

copolymerization of, 42

polyalkylene succinate prepared
with, 108

polytrimethylene succinate end-grafted
with, 109

Trimethylolpropane (TMP), 29, 34

Triptoreline, 201

Tropocollagen, 80

Tumor(s)

-associated antigens (TAAs), 257, 258

biopsies, 237

clearance, 237

configurations, 230, 231

diameter, reduction in, 270

growth, prediction of, 229

-microenvironment interactions, 228

model, Gompertzian, 232

necrosis factor (TNF), 245

regression, 231

surveillance, adaptive, 258

unresectable solid, 249

vaccine, GM-CSF-expressing, 260

volume, 249

Tumor immunotherapeutic systems, 257–273

key aspects of contemporary

immunotherapy, 258–260

adaptive tumor surveillance, 258–259

combination immunotherapy, 260

costimulation and immunotherapy,
259–260

strategies for successful

immunotherapy, 258

perspective on future, 271

polymeric biomaterials as carriers of
immunotherapeutic agents,
260–262

delivery of cytokines using polymeric
carriers, 261–262

polymeric biomaterials as artificial
antigen-presenting cells, 260–261

role of synthetic absorbable polymers in
immunotherapy, 263–270

key features of synthetic absorbable
polymers as carriers of bioactive
agents, 263

new approaches to using absorbable
polymers, 263–270

Type I diabetes, characteristics of, 206

Type II diabetes, 206

U

Ultralente insulin, 222

Unresectable solid tumors, 249

U.S. Food and Drug Administration, 143–144

V

Vaccine(s)

anthrax, 46

controlled release of, 45

DNA, 271

Vancomycin, 8, 46

Vascular constructs, *see* Synthetic vascular
constructs

Vascular diseases, 175

Vascular endothelial growth factor
(VEGF), 168

Vascular graft(s), 17, 44

application of absorbable polymers
in, 178

compound, 179

coronary artery, 180

development of, 178

material, longevity of potential, 177

partially absorbable biocomponent fibers
for, 186

Vascular wraps, 183

VEGF, *see* Vascular endothelial growth factor

Vein grafts, 184

arterialization of autologous, 183

de-endothelialization of, 184

Velban, 243

Vepesid, 243

Vicryl grafts, 179

Vigilon®, 161

Vinblastine, 243
Vincristine, 243
Vinorelbine, 243

W

WAXD, *see* Wide-angle x-ray diffraction
Wide-angle x-ray diffraction (WAXD), 120
Wound(s)
 deep, treatment of, 85
 dressing hydrogel, 161
 healing
 articular cartilage, 84
 compositions, alternating multiblock
 copolymers in, 51
 gel-forming liquid polymers and, 44
 processes, 192
 strength data, 73

repair, implants for, 7, 10
sites, biomechanics of, 43
skin, closure of, 43

X

Xeloda, 243
X-ray
 diffraction, 139
 photoelectron spectroscopy, 94

Z

ZCAP, *see* Zinc–calcium–phosphate oxide
Zinc–calcium–phosphate oxide (ZCAP), 221

Absorbable and Biodegradable Polymers

Shalaby W. Shalaby • Karen J.L. Burg

Over most of the past two decades, interest in synthetic absorbable polymers diverted attention away from natural, biodegradable polymers. Recently, however, investigators have revived interest in naturally derived polymers. The two technologies have common uses in clinical applications, but they developed independently and the published research results tend to be scattered.

Absorbable and Biodegradable Polymers integrates recent developments in both areas of research to form a coherent source of diverse but interrelated information. After an introduction that sets the stage for the detailed sections that follow, the book describes evolutionary materials development, processing methods, characterization and evaluation techniques, and applications—those available, those emerging, and those being actively pursued.

All of the chapters were contributed by leading polymer scientists, engineers, and clinicians, and together they consolidate the field's activities over the last 10 years. Anyone interested in research or development of absorbable or biodegradable polymers for pharmaceutical or biomedical applications will welcome having this information in a single fully referenced volume.

FEATURES

- Integrates key material and clinical aspects of synthetic absorbable polymers with those of naturally derived polymers
- Illustrates creative approaches to customizing fiber-forming materials for unique applications
- Presents state-of-the-art methods and processes used to characterize polymers and modulate their clinically relevant properties
- Reviews new and emerging compositions and applications for absorbable polymers, including tissue engineering, adhesion, and drug delivery

CRC PRESS
www.crcpress.com

